

# Deliverable 1.15

## D1.15 Final reporting to the EU commission

Deliverable information	
<b>Work package</b>	[WP1: Management]
<b>Lead</b>	[ETH]
<b>Authors</b>	[Stefan Wiemer, Banu Mena Cabrera, Ian Main, Warner Marzocchi, Iunio Iervolino, Remy Bossu, Helen Crowley, Danijel Schorlemmer, Max Werner, Michele Marti, all task leaders and all RISE Consortium]
<b>Reviewers</b>	[Management Board]
<b>Approval</b>	[Stefan Wiemer]
<b>Status</b>	[Final]
<b>Dissemination level</b>	[Public]
<b>Delivery deadline</b>	[30.04.2023]
<b>Intranet path</b>	[Project library/Documents/D. Deliverables]

---

## Table of contents

### Summary 3

<b>1.</b>	<b>Project Overview and Executive Summary</b>	<b>4</b>
1.1	RISE Main Objectives	4
1.2	Executive Summary	5
<b>2.</b>	<b>Work Package Progress</b>	<b>10</b>
1.2.1	Work Package 1	10
1.2.2	Work package 2	13
	Task 2.2 Next generation sensors and hyper-dense networks for use in EEW, OEF and RLA	
	16	
	Hardware - Cost Effective MEMS	16
	Hardware - Short Period Seismometer	17
	Smart Seismic Sensors - Edge Computing	17
	Network Fleet Management	18
1.2.3	Work package 3	44
	References	56
1.2.4	Work package 4	60
1.2.5	Work package 5	92
1.2.6	Work package 6	116
1.2.7	Work package 7	133
1.2.8	Work package 8	154

#### Liability Claim

The European Commission is not responsible for any that may be made of the information contained in this document. Also, responsibility for the information and views expressed in this document lies entirely with the author(s).

## Summary

Deliverable 1.15 refers to the Final Report, which presents the work completed by the beneficiaries for each work package during the period of 01/09/2021 to 31/05/2023. The report also includes an overview of the project's results in line with the Grant Agreement's objectives, a summary of submitted deliverables and milestones, a description of the exploitable results, and an explanation of how they will be exploited.

This deliverable serves as the foundation for the CORE report, which is the technical part of the upcoming periodic report for the second reporting period [M5-M45], due by the end of July 2023. Additionally, it provides crucial information for the Scientific Advisory and International Partner Board (SAIPB) to assess the project's progress and deliver their Final Report (D1.12) evaluating the RISE results.

This deliverable is prepared by the contribution of all RISE Consortium.



Map of RISE beneficiaries that have contributed to the report.

# 1. Project Overview and Executive Summary

## 1.1 RISE Main Objectives

The primary objective of RISE is to revolutionise the way in which earthquake risk is perceived and managed by leveraging scientific and technological advancements. Our vision is to move beyond the traditional static concept of earthquake hazard and risk, to a dynamic and evolving one that is influenced by multiple factors, such as location, soil conditions, topography, structural type, occupancy, and seismic activity. To achieve this, RISE has coordinated a multidisciplinary approach that focuses on Operational Earthquake Forecasting, Earthquake Early Warning, Rapid Loss Assessment and Recovery, and Rebuilding Efforts.

Through our efforts, we have significantly advanced Europe's real-time seismic risk reduction capabilities, and established a new paradigm of dynamic risk. We have developed and validated the next generation of forecasting models, which have improved short-term and operational earthquake forecasting. We have also collaborated with a European effort to ensure the quality of earthquake prediction and forecasting through validation and rigorous testing. Additionally, we have contributed to the establishment of sound and rational risk reduction procedures and have enhanced the preparedness of societies, emergency managers, and long-term recovery management. RISE is a multidisciplinary effort that has brought together earth scientists, engineering scientists, computer scientists, and social scientists. We have 19 partners from eight different European countries and five international partners. Our collective efforts seek to minimize the negative impact of future earthquakes and promote a more resilient Europe.

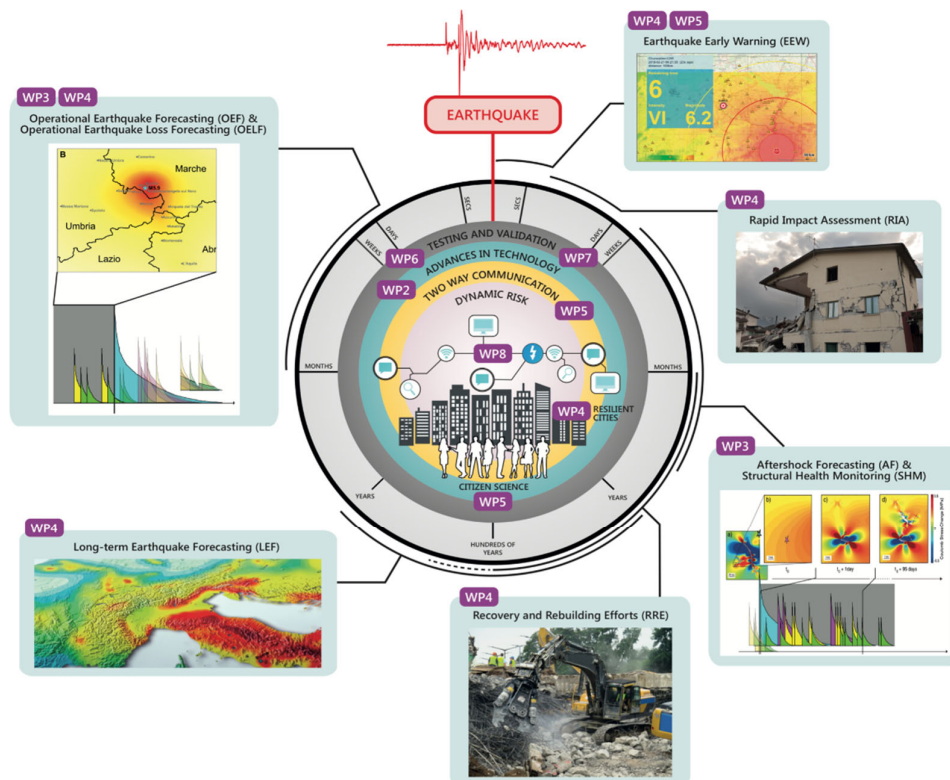


Figure 1. Conceptual view of the RISE work packages relative to the mainshock time.

## 1.2 Executive Summary

This mid-term report summarises the activities within the Horizon 2020 funded project RISE at the end of the project. RISE stands for Real-time earthquake rIsk reduction for a reSilient Europe; it brings together 19 partners from across Europe and five international participants into a multi-disciplinary effort involving earth-scientists, engineering-scientists, computer-scientists, and social-scientists.

In our self-assessment, the RISE project has achieved its ambitious goals. Despite the challenges posed by the Corona pandemic, most of the activities have been on track and some delays did not cause major disruptions.

Coordination and motivation of the team remained high until the end of the project. The RISE project has been strongly engaged in internal and external communication and dissemination activities: We built an attractive and well-visited web site (<http://www.rise-eu.org>) and twitter presence (@research\_rise), we distributed 10 internal and 4 external newsletters and have presented our research on numerous conferences and meetings. Until the day this report was prepared, RISE exceeded 80 peer reviewed publications, openly available via Zenodo (<https://zenodo.org/communities/rise-h2020>).

All RISE activities are supported by an experienced management office centred at ETH, the management board (MB) consists of well engaged and experienced WP leaders, 20 management board meetings have been held. We established a management structure that is in charge of the production of templates, guidelines, internal communication and exchange tools, and the continuous evaluation of project risk and quality. We also established processes for reviewing the deliverables and milestones and for regular consultation with the EC Officer to avoid mistakes and delays.

### WP2:

In the RISE vision, reducing earthquake risk and enhancing resilience requires progress on numerous technological, societal, and methodological frontiers but all targeted towards a common and sustainable framework on dynamic risk that RISE is providing. Within this framework, WP2 has been exploring the use of new technologies. There is a useful summary of our assessment of the technology readiness level and the operational capability of these innovative solutions to improving the inputs to OEF in deliverable 2.14.

Our innovations include:

- *Conducting proof of concept distributed acoustic sensing (DAS) campaigns in challenging environments, including remote fieldwork and in urban environments.*
- *Developing, testing and installing new high-performance low-cost accelerometers (QuakeSaver) for recording strong ground motions using low-cost seismographs.*

- *Characterising the response of buildings to ground motion and impacts.* The excitation sources have been built, deployed and tested successfully on buildings in Istanbul, and are ready for mission testing.
- *Developing new high-resolution earthquake catalogues for Italy using state of the art data processing and automated inversion algorithms.* We have demonstrated and operationalised enhanced observational capabilities of seismic networks, greatly increasing the quality and quantity of earthquake catalogues available for seismicity analysis, forecasting and testing in WP3 and WP7.
- *Exploring the potential of seismic interferometry to estimate changes in the state of stress in the upper crust.* We demonstrated the potential for near real-time monitoring of proxies for the state of stress in the Earth’s crust, notably recording changes in seismic velocity associated with post-seismic transients of larger events.
- *New scalable strategies and services for massive data access and archival,* including cloud-based services, for storing and accessing these large data volumes effectively for community use.

A new open European, building-by-building and dynamic exposure model based on the engineering information from the European Seismic Risk Model and open data from OpenStreetMap. This is already proving to be a highly useful tool for dynamic risk assessment, a core concept developed in the RISE proposal.

WP3 & WP7:

WP3 and WP7 were closely connected. While WP3 investigated various observables for their predictability of earthquakes and developed new methods to advance the state-of-the-art of Operational Earthquake Forecasting (OEF), WP7 applied and extended evaluation methods to test earthquake forecasts, improving the capabilities of the Collaboratory for the Study of Earthquake Predictability (CSEP). Several new insights obtained in WP3 were formulated as a new generation of testable forecasting models and were submitted to WP7’s prospective forecasting experiment for the Italy region. Prospectively testing models and hypotheses is the gold standard of scientific evaluation.

The following points highlight the main efforts and implications of WP3:

- Task 3.1 studied precursor anomalies before large earthquakes in Italy using geophysical and geochemical measurements such as radon emissions and changes in seismic velocity and attenuation; detecting precursors has been challenging in the past, but recent developments in observational capabilities (see WP2) provided new opportunities for continuous monitoring of the Earth’s crust and may improve earthquake forecasting;
- Task 3.2 explored the limits of earthquake predictability by investigating (i) spatiotemporal seismicity patterns before large earthquakes and developing alarm-based forecasts; (ii) the spatiotemporal variation of the magnitude–frequency distribution using high-resolution catalogs; (iii) many explanatory variables that influence triggering/clustering properties of earthquakes. Those discoveries improved the understanding of physical processes related to earthquakes—they led to new OEF models or will potentially be implemented in future OEF models;

- Task 3.3 developed probabilistic forecasting models at regional scales based on new insights and approaches using continuum mechanics, statistical physics, and statistical/stochastic modelling; they were collected in a repository for their prospective test in WP7;
- Task 3.4 studied earthquakes at a small (lab) scale with sensitive monitoring to help understanding physical processes that lead to fracture creation and reactivation; the new datasets will aid in improving OEF models;
- Task 3.5 provided an overview of the best practices and consensuses in OEF in terms of forecast communication, model development, and model testing; the insights were obtained from two surveys and a virtual workshop with experts in the field.

#### WP4 & WP6:

In WP4, RISE engineering teams have been developing the second generation of dynamic risk products for Europe. The following developments have been made in WP4 and demonstrated in WP6 at the local, national (Italy, Switzerland and Iceland) and continental scale:

- A database of building exposure models (time invariant) for 44 European countries has been openly released together with the open source tools for disaggregating the national exposure models to higher levels of resolution, required for scenario modelling.
- Methods to update these exposure models to account for the propagation of damage and the dynamics of populations during sequences of events have been developed and demonstrated.
- A first database of (state-independent) European vulnerability curves for over 200 building classes has been openly released.
- State-dependent fragility models for a number of Italian reinforced concrete and masonry typologies have been developed and implemented in MANTIS 2.0, the upgraded version of the Italian Operational Earthquake Loss Forecasting (OELF) system, thus allowing the forecasts to account for the evolution, over time, of the structural damage conditions.
- A European ShakeMap service prototype (<http://shakemapeu.ingv.it>) using the latest version of ShakeMap has been released, and has been integrated with the aforementioned European exposure and vulnerability models and the OpenQuake engine's 'Scenario from ShakeMap' calculator, to provide a Rapid (earthquake) Loss Assessment (RLA) service for Europe. Case study applications of this system have been provided for Iceland.
- A framework to infer the cost and time required to repair damaged buildings after an earthquake and to dynamically estimate recovery trajectories and thus, resilience, at a regional scale, has been developed and integrated for use with the OpenQuake-engine.
- Structural Health Monitoring (SHM) methods for the automated extraction of damage indicators for building structures, on the basis of monitoring data that is recorded from permanently instrumented buildings during earthquake events, have been developed to allow for a quantitative and near-real-time assessment of the probability of damage of individual buildings.
- An Earthquake Early Warning (EEW) approach for structures that predicts the building's base response from the recordings at early warning ground stations, before seismic waves reach the building, has been developed for a monitored building in Istanbul.

- The many advances described above in the fields of state-dependent fragility, dynamic exposure, OELF (directly using the synthetic catalogues from WP3), RLA and SHM have been combined in the software named Real-Time Loss Tools, developed and released as an open-source tool that the research community can use to continue to explore all the aspects of this integration and develop strategies for future scalability and operationalisation.

In addition to the above, there have been exchanges with EPOS Seismology to ensure that operational services for these dynamic risk products can be made available and sustainable in Europe.

#### WP5:

WP5 is at the interface with the public. It consists of 2 components, one dedicated to the use of crowdsourced data from earthquake early warning and rapid earthquake information to rapid impact assessment, and one dedicated to dynamic crisis communication (for EEW, OEF and RIA). The use of crowdsourced data has been successful, with results well beyond the expected impact. The EQN app was demonstrated as the first smartphone-based EEW system, years before the Google earthquake alert. During the 2019 Albania earthquake, warning times of more than 10 seconds were provided to users with an intensity of 6. The user survey showed that only a fraction (25%) took precautionary measures when receiving the warning. The results for the M7.8 Turkish earthquake are being analysed and it can already be said that significant warning times were provided for higher intensities. The detection capabilities of the system can now be modelled and the number of users is on the increase.

Felt reports collected by the LastQuake system are used to automatically obtain earthquake parameters (magnitude and location) when a seismic location is not available. Methods have also been developed to ingest them into Shakemaps and improve rapid impact assessment (through a prototype application on the USGS PAGER system). A line model of the rupture of the M7.8 Turkish earthquake was computed within 10 min of its occurrence. The performance of this approach, developed with ETHZ, is being analysed. We believe that both the incorporation into ShakeMaps and the line model of seismic rupture will become services in the coming year. The CsLoc method is now fully operational and integrated into the EMSC rapid earthquake parameter service. It jointly analyses crowdsourced and seismic data for rapid determination of felt earthquake parameters, typically available within 100s where seismic data are available. Finally, it has been demonstrated that felt reports collected within the first 10 minutes can discriminate between high and low impact earthquakes independent of any seismic data (such as magnitude or location) and without the need to generate a ShakeMap. This paves the way for a rapid (within minutes) traffic light system to automatically identify damaging, potentially damaging and non-damaging earthquakes.

While developing methods, technologies and tools for OEF, OELF, RLA, RIA; RISE social scientists have been working on dynamic risk communication (WP5); how to cope with the challenges due to high level of uncertainties in earthquake risk and how to best communicate the risk to give all

audiences (including the public, journalists, infrastructure managers and those involved in civil defence) information about the current hazard as perceived by seismological experts. This can lead to better preparedness for an event at both an individual level and at a regional or even national level, such as rehearsing evacuation procedures, ensuring supplies are in hand and all lines of communication are open.

With the support of five scientific collaborations, RISE scientists worked on the demonstration of EQN, the smartphone app turning smartphones into motion detectors, the very first smartphone based EEW system. RISE researchers also work on securing the broad societal, economic, and scientific impact of the project; an impact which is both demonstrable and long-term. This process started on day one of the project, continues throughout, and exposes all activities in RISE to an ongoing dialogue targeting stakeholder and end-user needs.

Working across three countries (Iceland, Italy and Switzerland), RISE researchers working on forecast communication interviewed over 100 members of different potential audiences for OEF and OELF information, as well as seismologists and experts in dynamic risk communication in other fields such as storm and weather forecasting, epidemiology and flood monitoring. They mapped the current lines of communication about seismological information in these three countries, and used user-centred-design to iteratively develop an online dashboard that could be used for public OEF/OELF communication. They then investigated the best ways to communicate the numerical aspects of earthquake forecasts, carrying out controlled studies online involving over 8,000 members of the public in three countries (Italy, Switzerland and USA), providing coverage of different cultures, languages and seismic hazard levels. This is the largest study yet conducted into seismic risk perception and communication. From all of these components, they were able to provide an Open Source working prototype OEF communication platform, available on GitHub and a series of guidelines for those wishing to communicate forecasts.

Additionally, the research group at ETH Zurich co-designed multi-hazard overviews and earthquake notifications which can be integrated on multi-hazard platforms or other applications such as weather apps. Especially in countries where damaging earthquakes occur only rarely and people's earthquake awareness is rather low, multi-hazard platforms allow seismological services to reach a wide audience. To this end, three nation-wide surveys were launched and seven focus groups were conducted in Switzerland to test the multi-hazard communication prototypes. The main recommendations derived from the studies are: i) people want actionable information, thus an indication about what to do is indispensable; ii) people prefer a single map displaying all active hazard notifications; iii) the hazard categories should be defined clearly to minimise the risk of misinterpretations; iv) a timestamp should be added so that people see at first glance that it is real-time information; and v) indicating a trusted source at the top of the hazard notification or multi-hazard overview ensures that people take the information seriously and, consequently, are motivated to take actions.

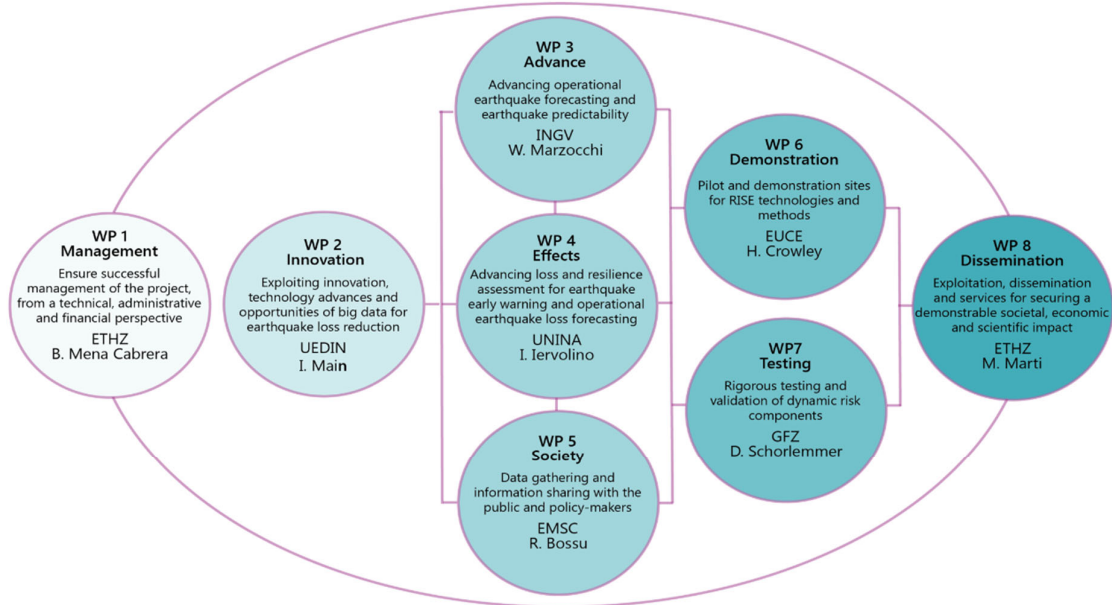


Figure 2. Structure of RISE and responsible WP leaders.

## 2. Work Package Progress

RISE comprises 81 deliverables and 63 milestones over 42 Months, 57 of the deliverables and 31 of the milestones were achieved within the second reporting period.

This section of the report summarises the work carried out in each work package, during the second reporting period. In this section, we include:

- Explanation of the work carried out during the reporting period in line with the Annex 1 to the Grant Agreement.
- An overview of the project results towards the objective of the action in line with the structure of the Annex 1 to the Grant Agreement including summary of deliverables and milestones, and a summary of exploitable results and an explanation about how they can/will be exploited.
- We will report separately for each WP; the overall WP structure is repeated in Figure 1.2.

### 1.2.1 Work Package 1

#### Overview

WP1 is responsible for the project management of RISE from a technical, administrative and financial perspective. The primary focus is to deliver the RISE project within the budget and timeline specified in the proposal. WP1 oversees the project development progress and the overall impact.

## **Summary of achievements in WP1 tasks:**

### **Task 1.1 Financial & Administrative Management**

This task is responsible for managing the financial and administrative aspects of RISE, as well as monitoring and controlling associated risks.

WP1 played a crucial role in RISE by managing reporting and ensuring timely submission of deliverables and milestones. At least one month prior to submission, the responsible parties are reminded of their upcoming tasks. Administrative management involves providing the internal review of the deliverables before submission to the EU. The deliverables were sent for review to either the WP leader or to an experienced scientist before submission to the EU. Once the reviewer's questions and comments are addressed, the revised deliverables are submitted to the EU. The administrative deliverables were reviewed jointly by the Management Board. During each Management Board meeting, WP1 shared the list of recently submitted and upcoming deliverables and milestones.

Within this task, we prepared the template for the joint RISE deliverables, which required a large participation of RISE scientists such as D1.11 and D1.12. The template has been shared via google doc and compiled by WP1.

This task involves monitoring the expenses of RISE beneficiaries. Every year WP1 collects a financial summary from all beneficiaries. WP1 released the Cumulative Expenditure Reports (CER) in December 2020, 2021, 2022 (D 1.17, 1.18, 1.19), which report the cumulative expenditure of each beneficiary for the previous year.

### **Task 1.2 Management of RISE activities**

In the second half of the project, we utilised the established platforms for project management; namely the RISE website (<http://www.rise-eu.org/>), the Alfresco intranet platform (<https://alfresco.ethz.ch/share/page/site/rise/dashboard>), the open access research and data sharing platform Zenodo (<https://zenodo.org/communities/rise-h2020?page=1&size=20>). WP1 has been responsible for the maintenance of these platforms and making sure that these platforms provide the essential communication between beneficiaries.

Due to the broad span of RISE activities in the scientific, technological and social settings, we must ensure the overall integration of all these facets in all activities and Work Packages. This integration is achieved by designated activity coordinators in all these domains and WP leaders working together and communicating their activities regularly. WP leaders from the Management Board (MB) met every two months to monitor RISE activities and coordinate cross WP tasks. We held 20 MB meetings, all well documented with meeting minutes that are submitted as deliverables (D1.5, 1.6, 1.7, 1.8, 1.9, 1.10).

The management of RISE activities are detailed in annual Project Management Plans (D1.1, D1.2, D1.3, D1.4). The PMP serves as a detailed roadmap for the project, outlining tasks and subtasks, tracking the people involved and Person Months (PMs) spent on each task, and providing information on deliverables and milestones. The PMP also includes a Risk Register section, which identifies potential risks and advises on necessary actions. The Risk Register is regularly updated and shared with the Management Board (MB) in MB meetings, and an updated version is added to the PMP every year.

### **Task 1.3 Legal issues (ETH)**

Managing and preparing the consortium agreement (CA), including annexes and any amendments to the Grant Agreement (GA) that may be needed during the project is under the responsibility of this task. CA manages the intellectual property rights of the foreground. Negotiations between participants regarding stipulations in the consortium agreement are well managed by the ETH team and the RISE CA is signed by all RISE beneficiaries in September 2019. The Consortium requested an amendment package from the EC, which included a number of changes to the original GA. The amendment package was approved by the EC in September 2020. The changes included a 6 months' non-paid extension to the project due to delays in some activities during Covid lock-downs and execution of a beneficiary.

Task 1.3 ensures the implementation and fulfilment of the GA and CA by all consortium participants and actively seeks advice from the Project Officer for requests/questions from beneficiaries, when needed. WP1 is now working towards another amendment to the GA which is related to the parenting request of a RISE beneficiary.

### **Task 1.4 Strategic integration with related projects and platforms**

Task 1.4 supervises activities aimed at guaranteeing integration of RISE project achievements with current European platforms (e.g. EPOS, CSEP, EUROVOLC, COPERNIUCUS and ARISTOTLE). RISE teams work in close collaboration with CSEP, and RISE forecasting models are being implemented in the CSEP2 platform. RISE has been in close contact with EPOS and ARISTOTLE representatives. Task 1.4 guides and monitors the proper integration.

### **Task 1.5 Project internal communication**

The objective of this task is to ensure effective internal communication and interactions within the RISE consortium (beyond project meetings). The following actions have been implemented:

In the second half of the project, we utilised the established platforms for project management; namely the RISE website (<http://www.rise-eu.org/>), the Alfresco intranet platform (<https://alfresco.ethz.ch/share/page/site/rise/dashboard>), the open access research and data sharing platform Zenodo (<https://zenodo.org/communities/rise-h2020?page=1&size=20>). WP1 has been responsible for the maintenance of these platforms and making sure that these platforms provide the essential communication between beneficiaries. In addition, dedicated email distribution lists created for the whole consortium, each WP and specific sub-groups have been used for internal communication. The main communication is done through emails and enhanced by using Alfresco Platform as the project's intranet. Together with WP8, 10 internal newsletters have been released.

### **Task 1.6 Meetings and workshops**

WP1 has been responsible for organising Management Board (MB) meetings every two months to ensure effective communication across different work packages, monitor progress, and assess risks adequately. Throughout the project, we held 20 MB meetings, which were highly successful in bringing together dedicated WP leaders who reported progress on each task. Minutes of all MB meetings are available on Alfresco and have been submitted as deliverables (D1.5, 1.6, 1.7, 1.8, 1.9, 1.10) to ensure transparency and accountability.

WP1 had established a series of scientific focus-meetings in September 2020 called “ZOOMing into RISE”. We had 20 ZOOMing into RISE meetings throughout the project. Meetings lasted 1-2 hours and enhanced the cross-institute and cross-work package collaboration.

### **Task 1.7 General assembly meetings**

General Assembly meetings are organised with a frequency in coherence with the conferences. During the General Assembly meetings, the progress of the project will be discussed with the General Assembly member of each Party and necessary decisions will be taken. In the first reporting period, we conducted a Kick-off meeting in September 2019 in Zurich and an online Mid-Term Conference in May 2021. In the second half of the project, we held an annual project meeting in May 2022 in Florence and have scheduled the RISE Final meeting to take place in May 2023 in Lugano. WP1 has been responsible for the organisation and agenda of these key project meetings, ensuring that they strengthen team connections, foster scientific discussions and collaborations, and facilitate timely achievement of RISE objectives. In addition, we organised conference dinners during these meetings to provide an opportunity for team bonding and additional scientific discussions. We keep the meeting minutes for the RISE GA Meetings and share them with the Consortium through Alfresco.

### **List of submitted deliverables**

- D1.1 Project management plan updated
- D1.2 Project management plan updated
- D1.3 Project management plan updated
- D1.4 Project management plan updated
- D1.5 Minutes of Meeting of the RISE management board conducted
- D1.6 Minutes of Meeting of the RISE management board conducted
- D1.7 Minutes of Meeting of the RISE management board conducted
- D1.8 Minutes of Meeting of the RISE management board conducted
- D1.9 Minutes of Meeting of the RISE management board conducted
- D1.10 Minutes of Meeting of the RISE management board conducted
- D1.11 Mid-term report of the scientific advisory board
- D1.12 Final report of the Scientific Advisory Board
- D1.13 Strategic integration of RISE activities with EPOS-IP
- D1.14 Mid-term report, including impact assessment and updated risk register
- D1.15 Final reporting to the EU commission
- D1.16 Data Management Plan
- D1.17 Cumulative Expenditure Report 1
- D1.18 Cumulative Expenditure Report 2
- D1.19 Cumulative Expenditure Report 3

### **1.2.2 Work package 2**

#### **Overview**

WP2 deals with innovation, specifically addressing the question: How can we improve the

technologies, methods, services and capabilities to improve the forecasting of dynamic risk?

In terms of *new technology and capability* we developed new equipment for (a) recording strong ground motions using low-cost seismographs (Task 2.2) and (b) characterising the response of buildings to ground motion and impacts (Task 2.3). We also tested and proved the operational capability of field deployments of relatively recently developed distributed acoustic sensors as a complementary method of recording ground motion in challenging environments (Task 2.1).

In terms of *improved data analysis*, we have developed a suite of new-generation high-resolution earthquake catalogues using a range of state of the art full waveform techniques to provide much more information particularly on smaller, previously undetected earthquakes (WP4). We have also provided near real time monitoring of the state of stress in the Earth's crust, notably recording the proxy of changes in seismic velocity associated with post-seismic transients of larger events (Task 2.5).

In providing *new services* we explored and delivered prototyped strategies for massive data access and archival beyond existing seismological waveform services, including cloud-based services (Task 2.6), and created an open European, building-by-building and dynamic exposure model based on the engineering information from the European Seismic Risk Model and open data from OpenStreetMap (Task 2.7).

There is a useful summary of our assessment of the technology readiness level and the operational capability of these innovative solutions to improving the inputs to OEF in deliverable 2.14.

## **Summary of achievements in WP2 tasks**

### **Task 2.1 Utility and value of high-density DAS**

Distributed Acoustic Sensing (DAS) is an emerging technology for the measurement of deformation using conventional fibre-optic cables. The outstanding potential of DAS mostly derives from the high spatial resolution at metre scale and the co-use of existing telecommunication cables, especially in densely-populated urban areas where conventional seismic station deployments are challenging. In task 2.1, we investigated the utility of DAS for high-resolution seismic tomography and earthquake source inversion.

Within the RISE project, we performed a series of DAS experiments that roughly fall into three categories: (i) urban, (ii) volcano-glacial, and (iii) submarine environments. These five diverse experiments are briefly listed and summaries below:

1. Bern pilot experiment: Urban DAS experiment using a 3 km telecom cable. Confirmation that noise interferometry with urban DAS data can produce subsurface images at 10 m resolution. Development of processing schemes specifically for urban data with anthropogenic signal pollution. First indication that urban experiments are easily feasible.
2. Athens experiment: Large-scale urban DAS experiment using a 23 km telecom cable. Recording of urban seismicity and comparison to newly-developed integrated sensing systems. Extension of processing and imaging methods developed in Bern to large experiments producing 10 of TB of data.
3. Mt. Meager experiment: Deployment of 3 km fibre-optic cable on Canada's most active volcano. Discovery of previously unknown levels of seismicity and continuous volcanic tremor. Proof of logistic feasibility in challenging environments. Development of an autonomous recording system that operates for >1 month under harsh conditions.

4. Grimsvötn experiment: Deployment of 12 km fibre-optic cable on Iceland's most active volcano, fully covered by the Vatnajökull ice cap. Detection of 100 times more earthquakes than in the regional catalog. Discovery of tremor-induced ice sheet resonance. Development of a system to rapidly trench and couple a cable of >10 km length on glaciers and ice sheets.
5. Santorini experiment: Co-use of telecom cable connecting the islands of Santorini and Ios. Detection of seismicity and tremor related to Kolumbo submarine volcano. Development of modelling methods for complex geographic settings with water, islands, soft sediments and rough topography.

A visual summary of the Bern, Mt. Meager and Grimsvötn experiments is provided in Figure 2.1.1.



Figure 2.1.1: Top left: Telecom cable layout used for a DAS experiment in Bern (upper right). Anthropogenic noise correlations (lower left) can be used to constrain structure at 10 m scale. Top right: Deployment of a DAS cable on a ridge of Mount Meager, and active volcano in British Columbia (left). The DAS array recorded a previously unknown level of seismic activity, including numerous repeating events (right). Bottom left: In April 2021, we deployed a 12 km long cable around Grimsvötn, Iceland's most active volcano (upper left). The DAS array records numerous low-magnitude volcanic earthquakes that are not seen on the regional seismic network stations.

Two major conclusions can be drawn from this series of DAS experiments:

1. Logistic feasibility: All experiments were logistically feasible, regardless of the environment. On volcanoes and glaciers, equipment could be transported with helicopters, and trenching the cable was doable with reasonable effort. In urban and submarine environments, we used pre-installed telecommunication cables. Attaching the DAS interrogator to these cables was nearly effortless, and support from local authorities and telecom companies was generally great.
2. Seismicity: In all experiments we discovered previously unknown types and levels of seismic activity. On Grimsvötn, for example, we detected nearly 2 orders of magnitude more events than the regional seismometer network. On both Grimsvötn and Mt. Meager we found new forms of seismic tremor, partly related to geothermal activity. In Athens we were able to detect low-magnitude urban seismicity, and in Bern the anthropogenic noise data provide a subsurface model with metre-scale resolution.

### **Task 2.2 Next generation sensors and hyper-dense networks for use in EEW, OEF and RLA**

Marius Paul Isken, Marius Kriegerowski - QuakeSaver GmbH The motivation behind building smart seismic sensors is to enhance earthquake monitoring and preparedness. Smart seismic sensors provide real-time data on seismic activity, which can help detect earthquakes early, assess their impact, and enable rapid response and recovery. By leveraging cost-effective MEMS sensor technology and short-period coil seismometers, sophisticated algorithms, and edge computing, smart seismic sensors can continuously monitor seismic activity, even in remote and resource-constrained areas. The development of open-source firmware and network fleet management technologies also ensures scalability, flexibility, and continuous improvement, making smart seismic sensors a powerful tool for earthquake monitoring and preparedness. In addition to detecting and characterising seismic activity, the motivation to build smart seismic sensors is to provide accurate and reliable data to stakeholders for various purposes. This includes the mitigation of risks associated with earthquakes by providing information on ground motion, shaking intensities, and site responses of buildings and infrastructure. The data collected by these sensors can be used to create exposure and hazard models, which are critical for emergency preparedness and response. Furthermore, the data can be integrated into rapid loss assessment models to quickly estimate potential losses and allocate resources accordingly.

#### **Hardware - Cost Effective MEMS**

The MEMS sensor development of QuakeSaver is a cost effective and open smart seismic sensor solution. QuakeSaver's MEMS sensor is a high-performance sensor that provides accurate and reliable seismic data. It features a low noise, 3-axial 20-bit MEMS accelerometer with a variable sampling rate of up to 200 Hz and a configurable range of 2 g and 4 g. The sensor is designed to be deployed both indoors and in harsh outdoor environments. It also includes a temperature sensor for continuous system and instrument health monitoring. The USB power supply and power-over-ethernet (PoE) option allows for operation in different environments. The powerful compute platform features a quad-core with 512 MB RAM and enables real-time analysis using on-device algorithms for real-time signal analysis and data processing. This allows the sensor to

provide meaningful data products downstream for exposure and hazard modelling, including shaking intensities and seismic site responses of the underground and buildings.



### **Hardware - Short Period Seismometer**

The QuakeSaver HiDRA sensor is a smart short-period seismometer that has been developed to provide high-quality seismic data for earthquake monitoring and structural health monitoring applications. The sensor features a 3-component short-period seismometer with a cut-off frequency of 0.5 Hz, which makes it suitable for detecting seismic signals in the frequency range of interest for earthquake monitoring. The HiDRA sensor features an ultra-low-noise 24-bit ADC that has an RMS of

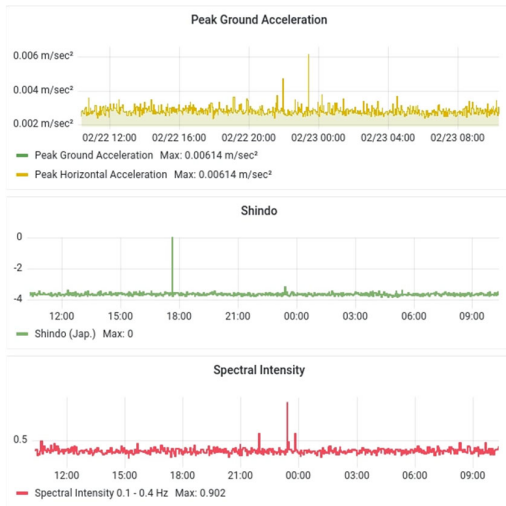
approximately 4 counts and a dynamic range of 139 dB, allowing for high-precision measurements of seismic signals.

The HiDRA sensor has a variable sampling rate of 50 Hz, 100 Hz, and 200 Hz, and analog pre-amplification options of 1x, 2x, and 4x. The sensor also includes a low-noise 3-component 20-bit MEMS accelerometer with a configurable acceleration range of 2 g and 4 g (optional), allowing for accurate measurements of strong ground motion. The HiDRA sensor is designed to operate in harsh environments, and it has a flexible power supply that can range from 9 to 36 V. Additionally, the sensor includes a hygrometer, barometer for atmospheric pressure, and a temperature sensor that provide continuous system and instrument health monitoring.



### **Smart Seismic Sensors - Edge Computing**

QuakeSaver's smart edge computing open firmware is a crucial component of its sensor system. It processes and analyses seismic data in real-time, providing valuable insights into seismic activity and ground motion. The software features a range of ground motion analysis parameters such as peak ground acceleration (PGA), peak ground velocity (PGV), and peak horizontal acceleration (PHA), which can help assess potential damage and hazards caused by earthquakes. In addition, the software provides instrument intensities such as Japanese Shindo and spectral intensity, which give critical insight into local ground shaking.



Another significant feature of the software is its ability to continuously calculate horizontal over vertical (H/V) spectra, which is an important parameter for assessing the potential damage, site conditions and hazards that can be caused by an earthquake. Furthermore, it can calculate continuous station autocorrelation, which is useful in structural health monitoring (SHM) and rapid loss assessment (RLA). The real-time neural network P- and S-wave phase detection featured by the open-source SeisBench package, is another valuable feature that enables accurate detection of earthquake onset times and phases. A first step towards autonomous

earthquake early warning (EEW).

The extensible firmware is designed for edge computing, which means that it can process data on the sensor itself, reducing the need for large-scale data transmission and enabling the system to function in remote and resource-constrained areas. This makes it a highly scalable solution for continuous monitoring of medium-scale building structures and obtaining classical seismological data outdoors. Moreover, the software's open-source nature facilitates continuous improvement and scalability, making it an effective tool for earthquake preparedness and response.

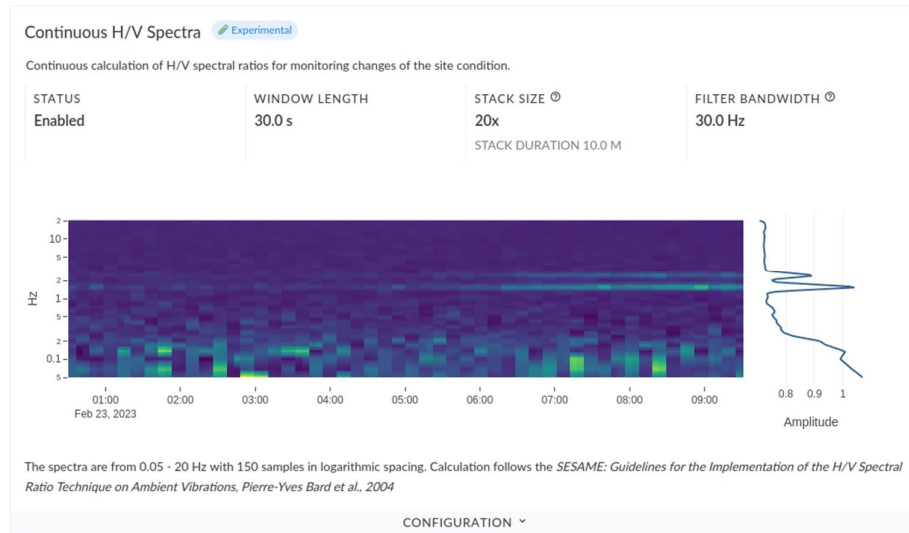


Figure 2.2.1: Continuous records of H/V spectra from a QuakeSaver MEMS sensor installed in a high-rise building in Montenegro.

### Network Fleet Management

The QuakeSaver smart seismic sensors come with a remote network fleet management system that allows for remote configuration and monitoring. The system enables data aggregation and storage through existing protocols such as SeedLink and FDSNWS. It also provides real-time instrument health monitoring, ensuring that any issues can be quickly addressed. The fleet

management system allows for easy and efficient management of a large network of sensors, providing the ability to remotely update firmware and adjust settings.

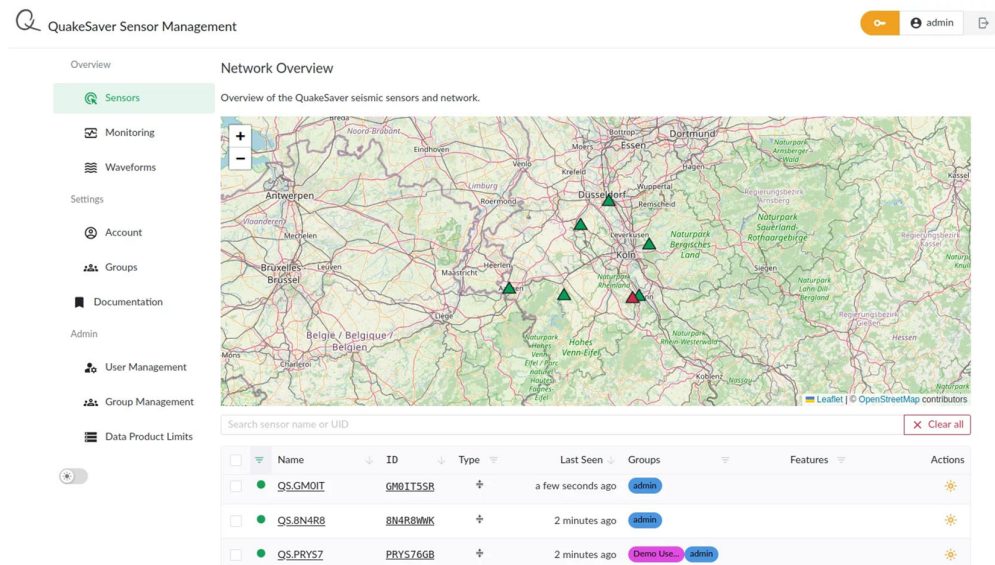


Figure 2.2.2: Developed remote network management console for QuakeSaver smart seismic networks.

The QuakeSaver smart seismic sensors have been field-tested in various locations, including indoor and outdoor environments, to ensure their reliability and accuracy. The sensors have been deployed in buildings of varying heights, from low-rise to high-rise, and in different regions of interest to monitor ground motion and gain insights into building responses. The field testing has allowed for the identification of any issues and improvements that need to be made, ensuring that the sensors meet the requirements of seismic monitoring and preparedness.

### Task 2.3. Innovative portable excitation sources for field testing of existing and densely instrumented structures

Two portable test equipment for dynamic testing of structures were designed and built: an Impact Hammer (IH) and an Eccentric Mass Shaker (EMS). Each piece of equipment is small and portable enough to be disassembled and moved to any floor of a multi-story building via elevators. This section presents the technical specifications of IH and EMS, and their utilization in testing structures. We present examples of data collected and information that can be extracted from the data.

#### Impact Hammer (IH)

The objective in developing an impact hammer is to give an impulsive force to a multi-story building and measure the propagation (i.e., the arrival times) of the impulse along the height of the building. The impulsive forces can be given from any floor by moving the Impact Hammer. These data are used to identify each story as if it were a one-story structure and to determine wave propagation characteristics of seismic waves in multi-story buildings. The response is measured by acceleration sensors. The measurements are used to identify the natural frequency and damping ratio of each story, as well as the wave travel times in the building, wave reflection and transmission coefficients at floor levels, and story damping. It is shown that such information

provides a better insight into the dynamic characteristics of the building than the modal properties alone.

The impact hammer is designed to be small and light enough such that it can be disassembled and moved to any floor of the building, including the roof, via elevators and does not require electrical power. The design sketch of the Impact Hammer and its specifications are given in Fig.2.3.1 below.

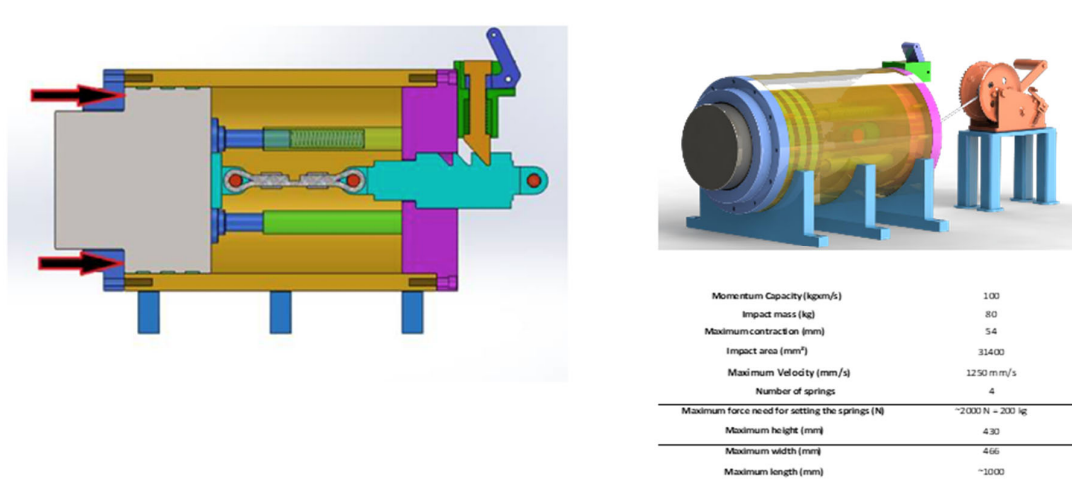


Figure 2.3.1. Specifications and cross-section of the Impact Hammer.

The IM can transfer the impulsive force to the building via floor slab by attaching it to the floor, or via a wall or column by placing it against them, as in Fig. 2.3.2.

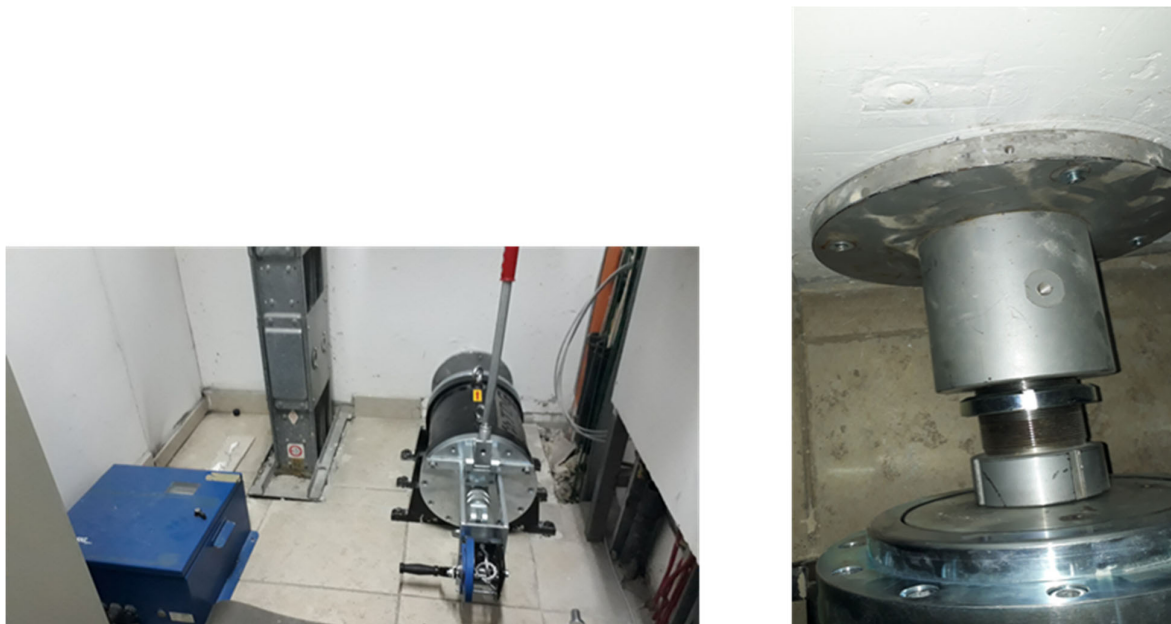


Figure 2.3.2. Use of Impact Hammer: (a) Attached to the floor, (b) Placed against a column.

When selecting the location for the Impact Hammer on a floor, it is important that the impulsive force given by the IH should mobilize the entire structure, not just the local element that the force is applied to. In a typical multi-story apartment building, an appropriate place would be against one of the shear walls surrounding the elevator shaft, generally placed near the centre of the cross-section. An alternative location would be a beam-column connection near the centre and the IH is typically placed to impact the column bottom near the floor slab. Alternatively, the IH can be attached to the floor slab by the base plate and six connecting bolts, as shown in Fig. 2a, above. The connecting bolts of IH and the in-plane stiffness of the floor slab should be strong enough such that the impact force is transmitted to the structural system via the floor slab without any slippage or loss of force at the installation. Again, the location of IH should be close to the centre, preferable near a major vertical component of the building, such as a shear wall or a column.

The direction of IH force should be in the direction of one of the two major structural axes of the building. Generally, two applications of IH force are required, one for each structural axis. If the building is not symmetric, such that significant torsional motions are expected, additional tests should be performed by placing the IH near the edges of the cross-section. The details of the formulation and the system identification algorithm can be found in the paper by Cetin and Safak (2021), prepared within the RISE project and published recently in *Earthquake Spectra*.

More detail on its design and technical specifications of IH, the properties of the instrumented buildings and the test details are given in RISE Deliverable D2.7.

### **Eccentric Mass Shaker - EMS**

The objective in developing an EMS (Eccentric Mass Shaker) is to identify the resonant frequencies of buildings and surrounding soil, as well as to identify the presence of soil-structure interaction. The EMS designed to have two sets of four discs each rotating in opposite directions and generating a uni-directional sinusoidal horizontal force acting on the structure or soil surface at selected frequencies between 1 to 25 Hz. The amplitude of the sinusoidal force can be adjusted by adding or removing the masses in the shaker.

The key technical specifications of the Eccentric Mass Shaker are given in Fig. 2.3.3 below.

ECCENTRIC MASS SHAKER TECHNICAL SPECIFICATIONS	
<b>ACTUATOR TYPE:</b> <u>Schneider Servo Motor</u> BMH100 Series Maximum Revolution: 3000 rpm	
	
TECHNICAL PROPERTIES	
<b>Eccentricity Per Disc</b>	0,181 kgm
<b>Number of Discs</b>	4 on each shaft, 8 in total
<b>Mass Per Disc</b>	4,2 kg
<b>Maximum Force</b>	1575 kgf
<b>Axis of Force</b>	Horizontal: X or Y (Depending on initial disc position)
<b>Maximum Frequency</b>	25 Hz
<b>General Dimensions</b>	Height: 440 mm Length: 250 mm Width: 470 mm
<b>Total Weight</b>	105 kg
<b>Power Requirements</b>	6 kW Single Phase 220 V AC

Figure 2.3.3. Mechanical properties of EMS and belt-pulley mechanism

In order to utilize EMS for possible SSI (Soil-Structure Interaction) tests, we supplemented EMS with a thick base plate and metal stakes as schematically shown in Figure 2.3.4. The base plate is anchored to the soil near the building with eight thick and long metal stakes. The EMS is firmly attached to the base plate such that the horizontal force from the shaker is transferred to the soil to excite the soil near the building, and the building itself, so that we can see the characteristics of wave transmission from the soil to the building.

EMS is very useful to identify the natural frequencies of short and stocky buildings, as well as the dominant frequencies of the soil surrounding the foundation. For buildings 7-10 stories and higher, ambient vibration data taken from the top are normally sufficient to identify dominant frequencies. For short buildings, or buildings where the data are available only from the lower floors, and for the ground, the ambient vibrations do not show the dominant frequencies because of very low signal-to-noise ratios.

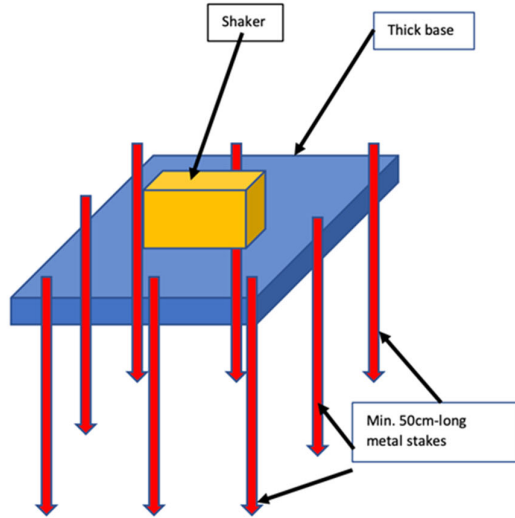


Figure 2.3.4. Sketch and application of base plate to EMS for SSI testing.

As an example, Fig. 2.3.5 shows the time-history and the corresponding FAS (Fourier Amplitudes Spectra) of a 2-story short and stocky building. The EMS is used to apply a sine-sweep excitation to the building from 1.0 Hz to 25 Hz. The corresponding FAS clearly shows the dominant frequencies.

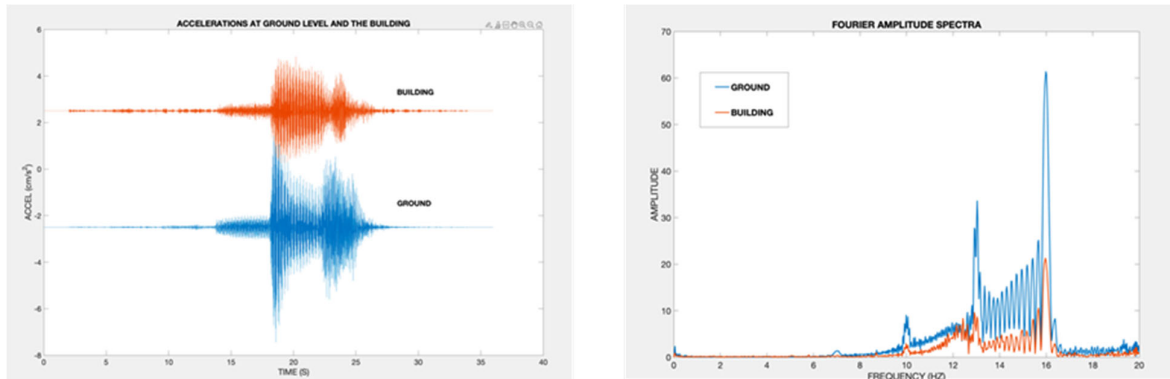


Figure 2.3.5. For a 2-story building, recorded accelerations on the ground surface near the building and the building's second story, and the corresponding Fourier Amplitude Spectra.

It is important that the base plate of the EMS and the ground surface are fully coupled, i.e., no slippage or deformation of soil around the stakes. This will ensure that the force from the EMS is completely transferred to soil. For soft soil, soil deformations may be unavoidable. This can be minimized by using more and longer stakes. More detail on its design and technical specifications of EMS, the test details are given in RISE Deliverable D2.7.

### **Task 2.4 Advancing observational capabilities**

This task was devoted to the improvement of the observational capabilities mainly in terms of enhanced earthquakes catalogues provision, as a key ingredient to improve OEF and RLA tools. The completeness, homogeneity and accuracy of the earthquake catalogues, including earthquake hypocentral locations and magnitudes, are fundamental characteristics to evaluate the needs to improve earthquake predictability.

#### **Catalogue of Relative Seismic locations (CARS)**

We generated high-resolution and more consistent earthquake catalogues for the Italian peninsula (CSEP testing region), including homogeneous local and moment magnitudes (ML and MW respectively). The new Catalog of Relative Seismic locations (CARS) consists of about 320,000 events that occurred in Italy in the period 1981-2018. We started from the CLASS catalogue (Latorre et al., 2023), consisting of homogeneous earthquake absolute locations constrained within a regional 3D velocity model and relocated those events.

The relative locations are obtained by inverting for P- and S- waves arrival times derived from data collected by National Seismic Network (RSN) plus permanent Regional Networks for the period 1981-2008 and only by RSN for 2009-2018. For this latter period, we also integrated the absolute travel times with relative ones obtained by waveforms similarities analysis grounded in cross-correlations measurements and performed on pairs of similar events. The time domain cross-correlation method proposed by Schaff et al. (2004) and Schaff & Waldhauser (2005) was applied to seismograms of all pairs of events separated by 10 km or less and recorded at common stations. Seismograms were filtered in the 1–15 Hz frequency range using a four-pole, zero-phase band-pass Butterworth filter. The correlation measurements were performed on a 1.0 s long window for P- and S-waves. We retain all measurements with correlation coefficients greater than 0.7, resulting in a total of ~17 million P- and ~23 million S-wave delay times. The resulting cross-correlation delay time measurements have been combined with delay times computed from picks for event pairs.

We then used the outcome as input for the HypoDD code (Waldhauser and Ellsworth, 2000), that being based on the double-difference algorithm, can ingest differential arrival times. For locating the events we used 1D velocity models characterising 18 different (geologically, seismically and tectonically homogeneous) Italian macro-areas (orange dashed lines in Fig. 2.4.1 after Pastori et al. B2-2019-2021, Wp1-task4).

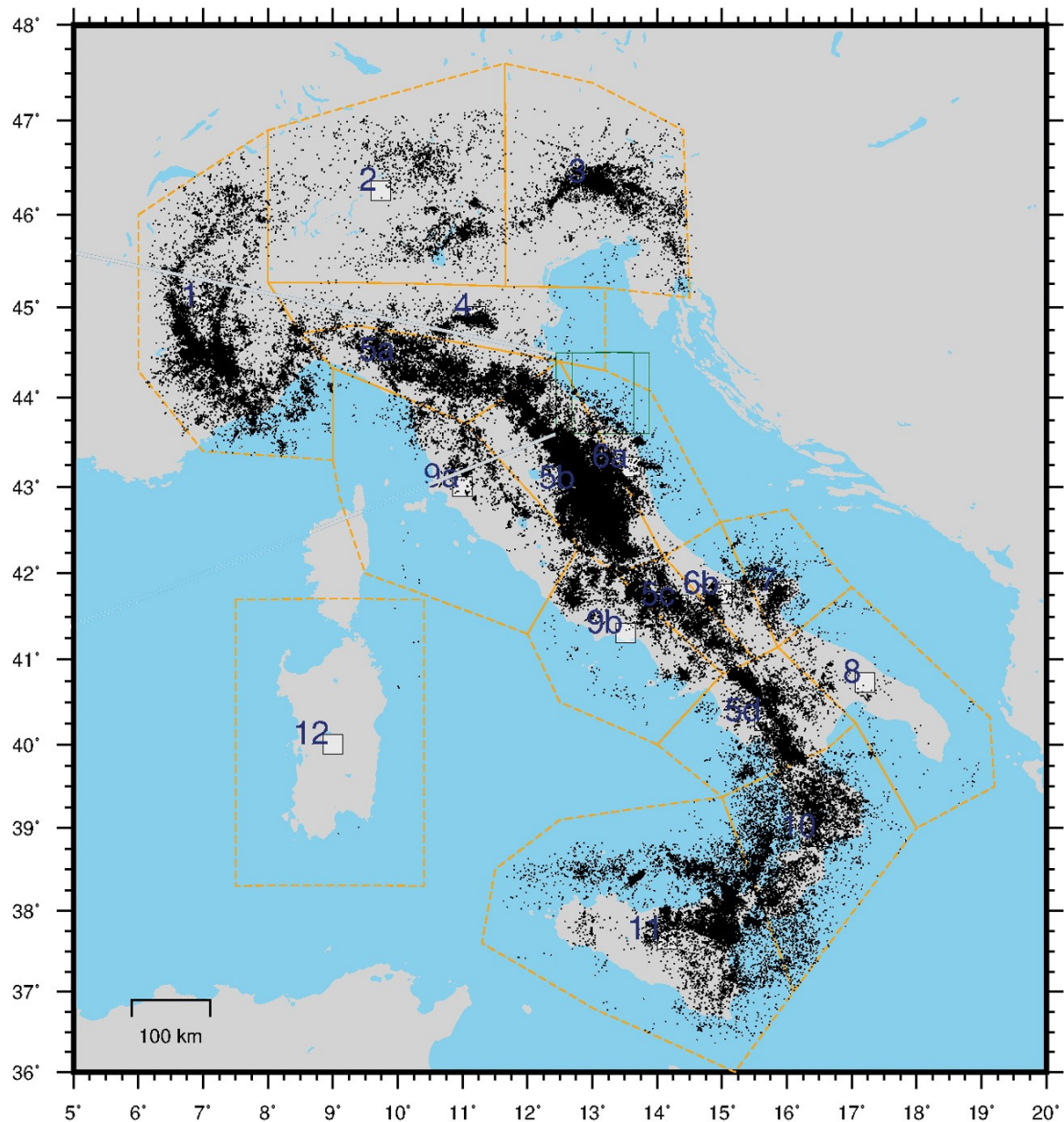


Figure 2.4.1 - Map of epicentral locations for the CARS Catalog. Orange dashed lines show macro-areas defining 18 different 1D velocity models (Pastori et al. B2-2019-2021, Wp1-task4) used for event location.

In Figure 2.4.2 we show a map view and cross section of the Calabrian slab as an example of the improvements in earthquake location.

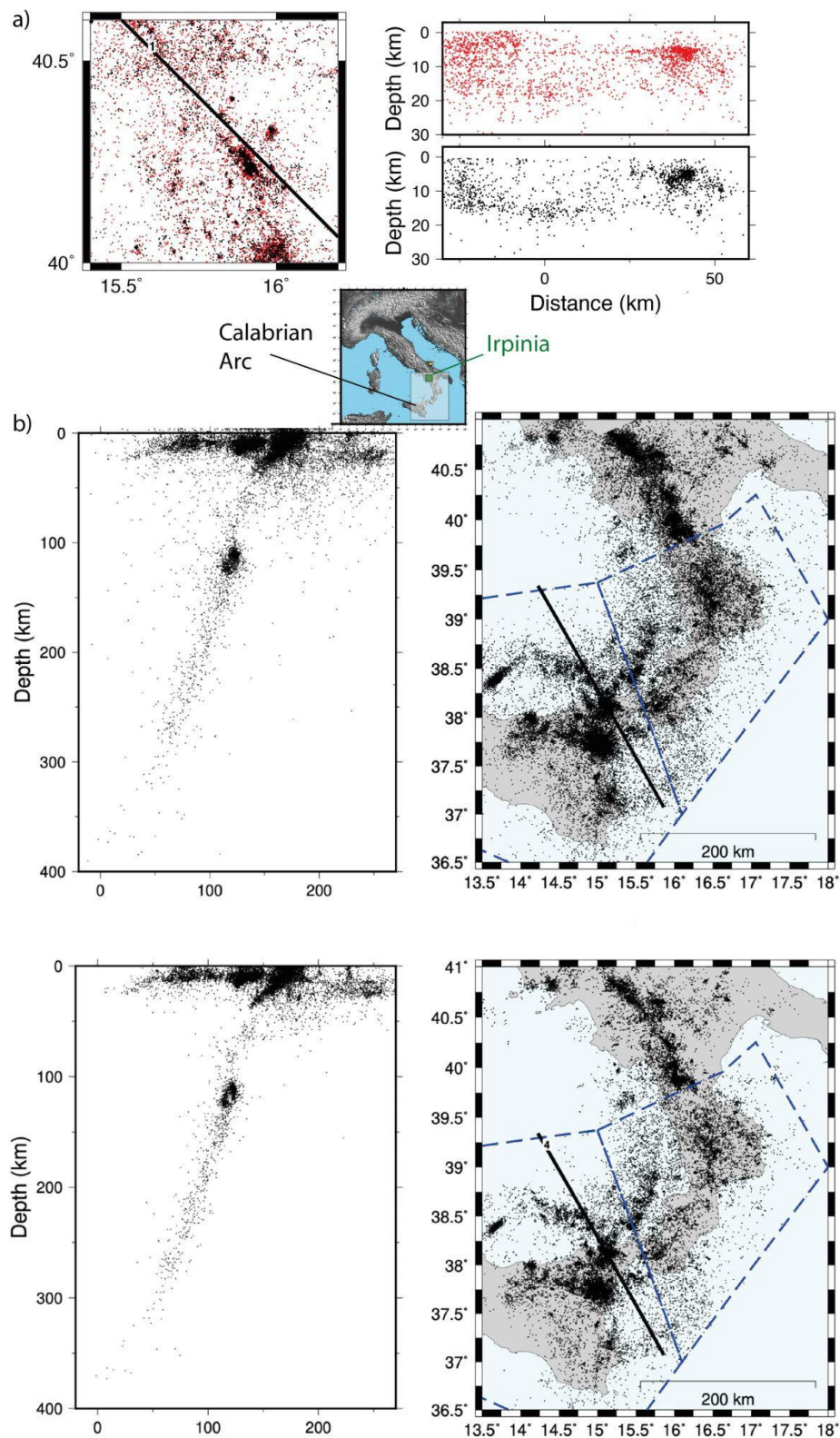


Figure 2.4.2. CLASS and CARS locations in between Sicily and Calabria (white box in the inset); right: map view of CLASS (top) and CARS (bottom) locations; left: CLASS (top) and CARS (bottom) locations within +/-50 km from the trace represented in the map-view; blue lines correspond to the two different 1D velocity models zones from Pastori et al. B2-2019-2021, Wp1-task4.

### Catalogues of Local and Moment Magnitude for the 2009-2018 Italian seismicity

We produced two catalogues respectively for local (ML) and moment (Mw) magnitudes for about 250,000 earthquakes that occurred in Italy from 2009 to 2018, extracted from the CLASS catalogue. These events are represented in Figure C as single event solutions (grey circles) and bin-averaged estimates (red circles with bin-size = 0.2 Mw). The red bars are associated weighted standard deviations while the black dashed line represents a 1:1 scaling.

The ML catalogue represents the first homogenous local magnitude catalogue for the Italian National Seismic Network (RSN) covering a 10-year time interval, since during the years RSN used different methods of peak-to-peak maximum elongation measurement and ML event calculations, producing inhomogeneity within the ML catalogue.

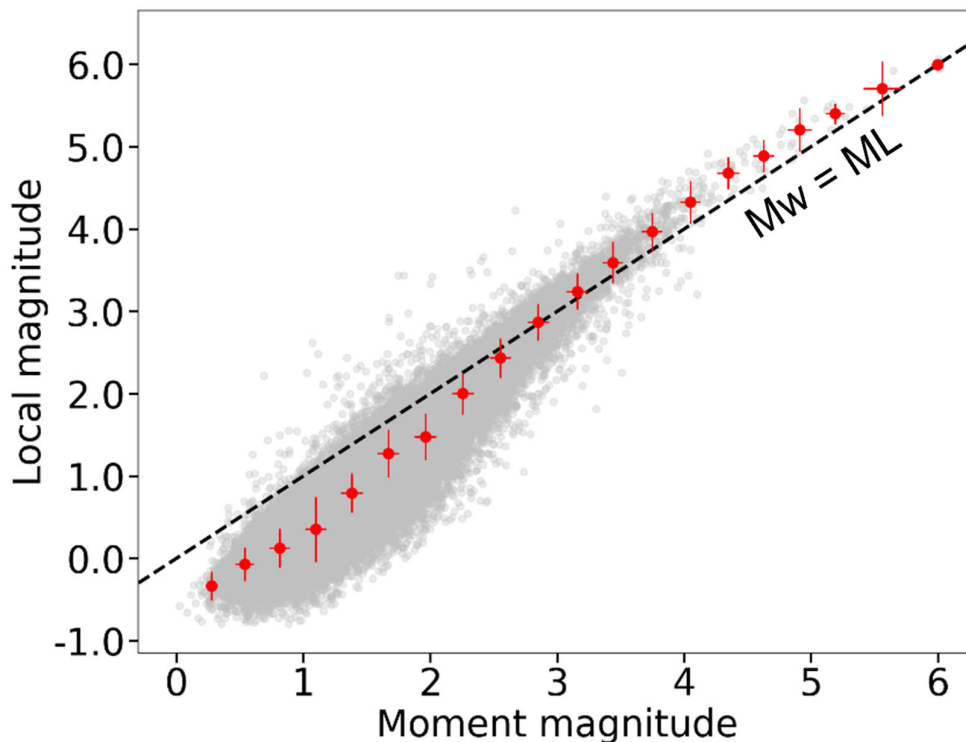


Figure 2.4.3 – ML and Mw catalogues. Grey circles are single event solutions, red circles are bin-averaged estimates (bin-size = 0.2 Mw) and red bars are associated weighted standard deviations. The black dashed line represents a 1:1 scaling.

To perform these tasks automatically and homogeneously, we developed two new python codes (PyAmp and PyML) designed on purpose to:

- Apply an adaptive band-pass filter to the waveforms, based on the results of a signal to noise analysis.
- Convert the signal to the equivalent signal recorded on a Wood-Anderson (WA) seismometer.

- Define the maximum peak-to-peak elongation search window.
- Find the maximum peak-to-peak elongation.
- Solve issues: automatically identify and remove saturated waveforms from ML analysis for  $M \geq 4$  events, and prevent amplitude's misidentification due to close events overlapping
- Apply an attenuation law specific for the Italian region, Di Bona et al. (2016), for channel ML calculation.
- Calculate the event's ML with a unique different statistical method (Huber Weighted Mean).

All the analysis, including the amplitude re-estimation, has been performed on the new seismic waveforms database we built during the first part of the project (see D2.8). The  $M_w$  catalogue is also novel, in the sense that it is the first moment magnitude catalogue systematically obtained for events with  $M_w < 3.5$ . This is because  $M_w$  are usually evaluated from moment tensor inversions, which can be routinely performed only for large earthquakes.

We use the probabilistic method of Supino et al. (2019, 2020) to invert the displacement spectra of more than 2,000,000 manually picked S-waves, estimating the a-posteriori joint probability density function (PDF) of the source parameters seismic moment  $M_0$  and corner frequency  $f_c$  (Fig 2.4.4, where  $M_0$  has been converted to moment magnitude ( $M_w$ ) using the Kanamori, 1977, equation).

The produced ML and  $M_w$  catalogues are characterised by:

- Homogeneity. For ML, the same peak-to-peak search method has been applied to all the recordings and the same attenuation law to all the stations' ML. For  $M_w$ , the same probabilistic approach has been applied to all the inverted S-waves.
- Quality. For ML, the amplitudes are searched for when a P-pick is present, and the pre-filtering method is adaptive, preserving the seismic signal. For  $M_w$ , only manually picked S-waves have been used, the inverted frequency band is defined event by event and station by station only where the signal is actually larger than the noise, the uncertainty is evaluated from a joint PDF and accounts for parameter correlation.

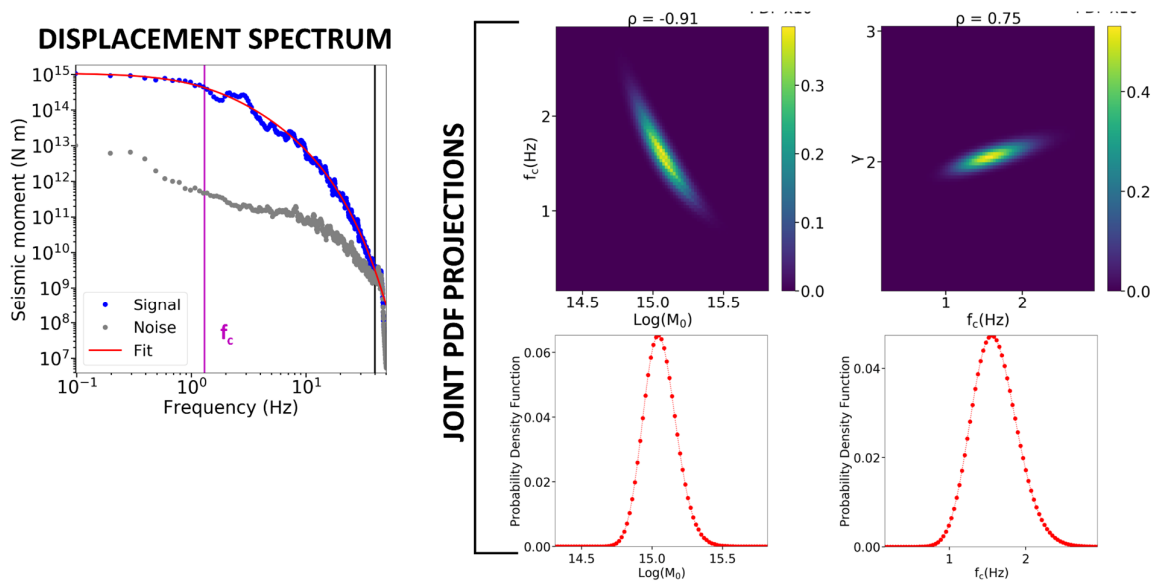


Figure 2.4.4 – Example of  $M_0$  and  $f_c$  joint PDF estimation from spectral inversion (Supino et al., 2019, 2020).

The comparison of our  $M_w$  and  $M_L$  catalogues shows the systematic underestimation of  $M_L$  with respect to  $M_w$  for small magnitude events (Figure C). The deviation from a 1:1 scaling relationship overlaps the magnitude range where a constant apparent corner frequency arises in the  $M_w$ - $f_c$  scaling ( $M_L < \sim 2.5$ ), as expected from theory (Deichmann, 2017).

### Template Matching

We used parts of these improved catalogues to perform network-wide cross-correlation analyses to the continuous waveform archives in our test region. We focused on the seismicity in central Italy before the 2016 seismic sequence to perform a detailed analysis of the seismic activity that occurred between the 2009 L'Aquila and the 2016 seismic sequence, to investigate this preparatory phase and the impact of the availability of the improved catalogue on OEF analysis during an ongoing seismic sequence. We started from approximately 23,000 well-located earthquakes that occurred between 2009 to 2016, to recover, by applying a template matching approach, the seismic activity preceding the 2016 Central Italy seismic sequence. Newly retrieved 91,000 events have been analysed in space and time to characterise the earthquake preparatory phase leading to the first mainshock of the sequence.

### Enhanced earthquake catalogues and OEF models

The newly-generated enhanced catalogues were used to quantify the advantages and limitations of using them for earthquake forecasting (see details in D2.9). The three employed catalogues were the ones describing the 2016-17 Central Italy earthquake sequence (Chiaraluce et al., 2022) that were used to inform physical Coulomb Rate-and-State and empirical ETAS forecast models (details in Mancini et al., 2022). The suite of relocated and dramatically richer catalogues were compared to the real-time one allowing to design an experiment to: (i) investigate if incorporating information from high-resolution catalogues boosts the predictive skills of current state-of-art

modelling strategies; (ii) clarify which serial components of enhanced catalogues are the most beneficial or detrimental for forecast performance; (iii) quantify the benefits of considering the triggering effects from the smaller events revealed by enhanced catalogues.

### **Task 2.5 Explore the use of ambient noise correlations to systematically monitor the temporal evolution of active faults**

The long-term objective of Task 2.5 is to assess the spatio-temporal evolution of the state of the Earth's crust related to tectonic processes, and to investigate possible changes in the crust prior to large-magnitude earthquakes. We focused on Italy and Greece, which are among the most seismically active regions in Europe, while building a large database of continuous seismic noise records recordings covering a large part of Europe for the time period 2010-2020 so that the approach developed in this task can be easily used in different European regions. Indeed, earthquakes occur on fault systems as a consequence of long-term strain accumulation and transient triggering mechanisms. However, our current understanding of the preparation, nucleation of earthquakes and their consequences on the crustal properties are still limited. The use of seismic ambient noise correlations has opened up a new way to monitor seismic wave velocity changes associated with earthquakes and the hydrological cycle, which may shed light on the seismic cycle. The method consists in repeatedly extracting the Green's function of the medium by correlating the ambient noise records. Seismic wave velocity and attenuation changes within the medium can be monitored by analysing the coda part of the correlation.

#### **Seismic velocity variations in the 1-3s period band in Greece and Italy**

To look for possible crustal changes associated with large magnitude earthquakes ( $M_w > 5$ ), we analysed 10 years of continuous seismic noise records using all broadband seismological stations in Greece and Italy. For each station, we computed the evolution of the seismic wave velocity  $dv/v$  over time with a sliding window of 2 months in the 1-3s period band.

In Greece and Italy, we found that in the upper crust, in specific regions close to aquifers, the dominant signal is a seasonal change in velocity, sometimes associated with a multi-year linear trend that indicates an increase or decrease in the amount of groundwater resources. Measuring velocity variations can therefore be useful for monitoring water resources at a large spatial scale. This could be of great interest since water stress is increasingly important in many European countries. In the case where aquifer charge and discharge is controlled by rainfall and not by anthropic pumping, we have shown that with a simple hydrological model and precipitation records, it is possible to predict velocity changes due to changes in the amount of groundwater. By subtracting this signal, this makes it possible to highlight velocity changes related to tectonic processes.

In order to look for possible precursor changes in the medium prior to large magnitude earthquakes in Italy, we mapped the evolution of seismic wave velocity over the period 2015-2017, which includes the Amatrice-Visso-Norcia earthquake sequence (Figure 2.5.1). The results show that the seismic wave velocity in the upper crust is not stable in time, but evolves on the scale of several weeks, with variations of the order of 0.1%, which is extremely low but

nevertheless resolvable using time-lapse interferometry. The accuracy of the measurements depends on the time window used and the density of seismological stations. We are able to capture these variations with a temporal resolution of about 2 months. Some of these variations are clearly related to the Amatrice-Visso-Norcia sequence: this is the case of the co-seismic velocity drops followed by a co-seismic recovery visible in Central Italy. We were able to highlight that the Amatrice earthquake is associated with a small velocity drop locally around the epicentre, while the Visso-Norcia is associated with a larger velocity drop extending to the Po plain.

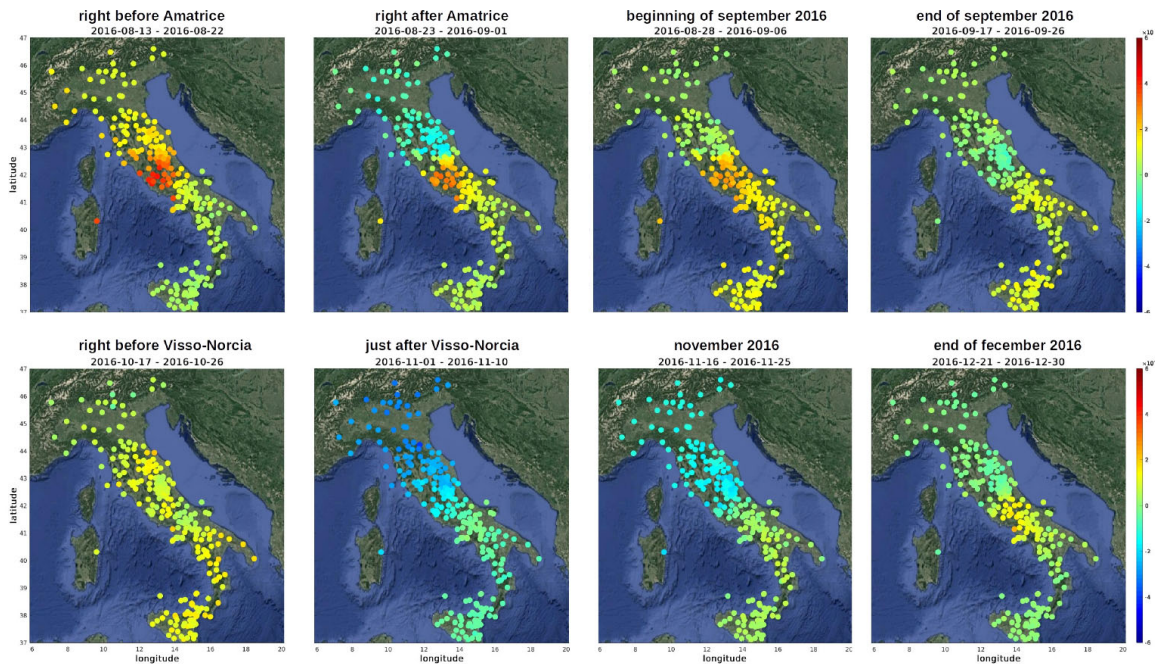


Figure 2.5.1.  $dv/v$  measured with a sliding window of 10 days around each station within a radius ranging from 50 to 200 km chosen to get at least 200 measurements. The upper panels present the velocity change measured just before and after the Amatrice earthquake. The lower panels present the velocity change measured just before and after the Visso-Norcia events.

### Monitoring seismic velocity variations deeper in the crust

Theoretically, by analysing noise correlations at longer periods, we could track velocity changes in the middle and lower crust. However, we found that at periods greater than 3s, the measurements are dominated by changes in the noise source rather than changes related to tectonic processes. Therefore, we explored the possibility of detecting structural changes deeper in the crust by analysing different noise coda waves time windows. Indeed, the ratio of surface to body waves, and thus the depth sensitivity of coda waves, depends on the lapse time (the coda window analysed). By measuring velocity variations at different lapse times, we found that at several stations seasonal changes in  $dv/v$  increases with the lapse time, which could indicate that changes occurred in the mid or lower crust. This observation is still being investigated.

### Towards monitoring attenuation changes from noise correlations in Greece

In addition to measuring velocity changes over time in the crust, we attempted to measure changes in seismic wave attenuation. We proceeded in two steps. The first step consisted in

constructing attenuation maps in Greece in the upper and middle crust (2-20s period band), by measuring the quality factor of coda waves ( $Q_c$ ) reconstructed by noise correlations. To that end, we developed a robust algorithm that allows us to estimate  $Q_c$  such that the measurements are independent of the lapse time or the length of the coda window that is analysed. Major areas with low  $Q_c$  (high attenuation) are observed in the gulf of Corinth, in Cyclades and the Marmara Sea, which can be explained by fluid activity related with the high rate of rifting, volcanic activity and metamorphic core complex distribution, and the westward extent of the North Anatolian Fault respectively. Good correlation of  $Q_c$  anomalies with broad geological structures in all period bands shows the potential of ambient noise cross-correlations for monitoring and explaining the spatial variability in attenuation in the crust, and hence local impacts on ground motion.

The second step was to measure the evolution of coda wave attenuation over time. For this purpose, we computed coda  $Q$  measurements with a sliding window of 3 months at each Greek station. We found that the velocity and coda  $Q$  variations are positively correlated at most sites, and in rare cases negatively correlated. Both types of measurements show a similar seasonal pattern to that in the temporal variations in velocity, implying both are controlled by the hydrological cycle. This confirms that it is possible to measure the temporal evolution of seismic wave attenuation reliably. We are currently investigating whether the large magnitude earthquakes in Greece and Italy are associated with a change in attenuation that could be a signature of crustal damage and/or fluid pressure changes for instance.

### **Task 2.6 Strategies for scalability, high-volume data access and archival beyond existing waveform services, exploiting cloud-based services**

Task 2.6 was devoted to exploring and prototyping strategies for massive data access and archival beyond existing waveform services, including cloud-based services. This Task was motivated by the fact that current emerging techniques, methods and technologies in seismic monitoring, data acquisition and processing have started to pose new, significant technical and organisational challenges to the seismological data centres in terms of a) data collection and storage, b) providing services for transparent and rapid access, c) efficient processing of huge amounts of data and d) quality assurance of data and services. A detailed discussion of the aforementioned challenges can be found in the international study led by Quinteros et al. (2021a). Task 2.6 produced two project Deliverables. In Deliverable 2.11 (Sleeman et al., 2011) we selectively described current state-of-the-art technical solutions to rapidly serve, access and process massive seismic datasets, including the current strategies provided by the European Integrated Data Archive (EIDA; <http://www.orfeus-eu.org/data/eida/>), the recommendations compiled by the EPOS-ORFEUS Competence Center (CC) within project EOSC-Hub (<https://www.eosc-hub.eu/>), emerging challenges to handle new exotic datasets like those generated by distributed acoustic sensing (DAS) systems, and initial experiences gained into Cloud services and distributed computing environments for data processing and interactive exploration at ORFEUS associated data centres. All strategies and experiences documented in D2.11 are representative of the state-of-the-art and possibly the avant-garde on the topic at hand. Clearly pointed out in D2.11 is also the need to promote coordination with several additional data centres worldwide, within the framework of the Federation of Digital Seismograph Networks (FDSN; <https://www.fdsn.org/>), as well as the

encouragement of international collaborations among scientists, datacenter operators and managers for successful future standardised developments and implementations. In Deliverable 2.12 (Danecek et al., 2012) we demonstrated the technical implementation of selected strategies, namely:

(i) **SeiSpark**, that allows access and processing of massive datasets by creating a "computational archive" where storage resources and computational resources converge; the proposed processing framework leverages on existing solutions from the Big Data ecosystem and combines them with the popular open-source scientific Python framework which is well established in seismological research (Figure 2.6.1).

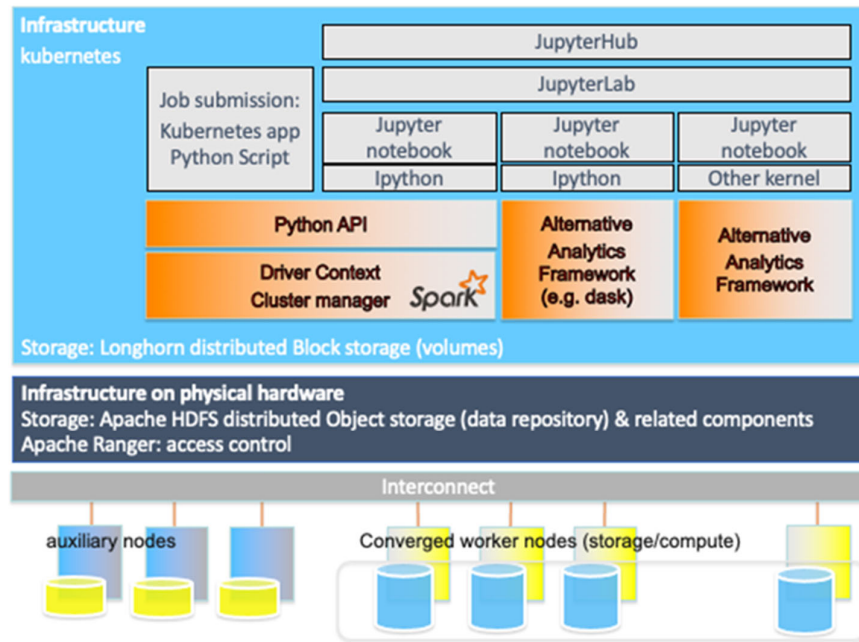


Figure 2.6.1: A schematic simplified setup of SeiSpark.

(ii) **Dastools** (Quinteros et al., 2021b), that allows converting DAS data into standardised seismological data formats hence making the waveform data and metadata easily available in current seismological archives and in turn to users; the software is available and documented on GitLab at <https://git.gfz-potsdam.de/javier/dastools>. An example of its application is given in Figure 2.6.2.

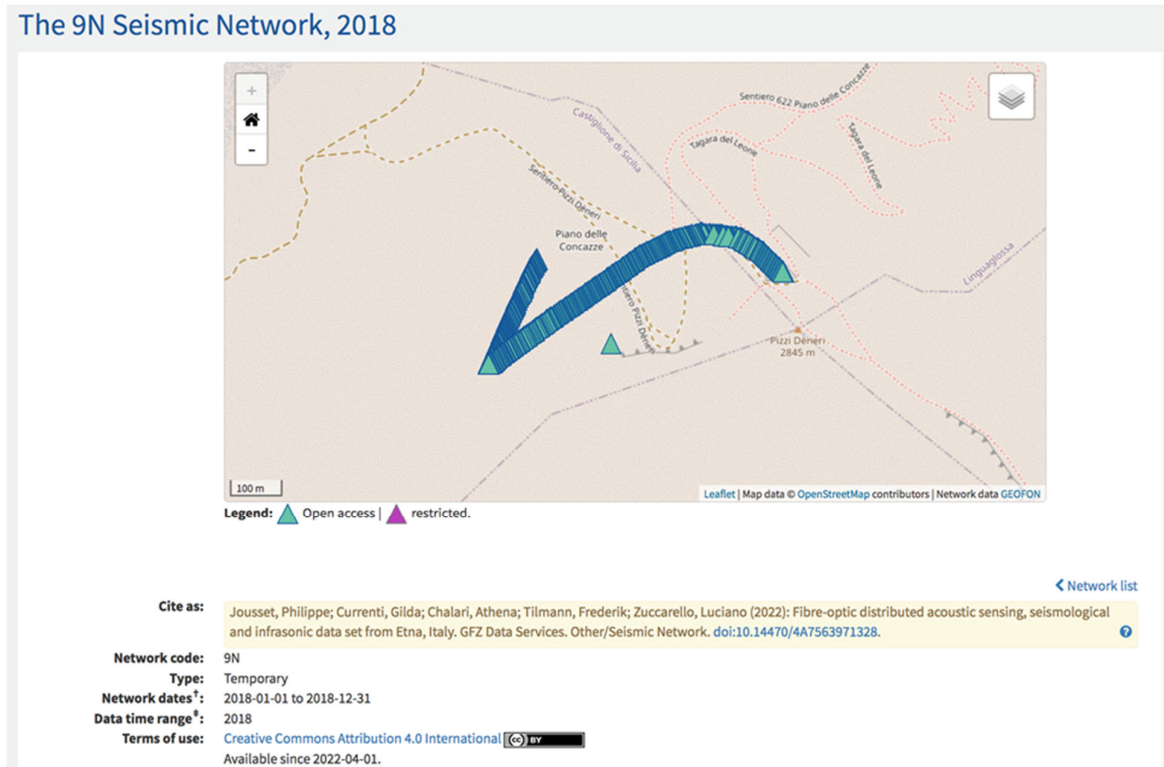


Figure 2.6.2: 9N seismic network, integrated in the GEOFON archive using dastools

(iii) **the cloud strategy implemented by the ORFEUS Data Center at KNMI**, that allows operating more efficiently than maintaining an in-house infrastructure; all seismological waveform data at ODC c/o KNMI are stored in the Amazon Simple Storage Service (S3) as objects in so-called buckets. A bucket is a container for objects, while an object is a file and any metadata that describes that file. Amazon's S3 is able to efficiently handle very large volumes of data, and its API is a widely adopted standard for object storage APIs. Applications run by ODC c/o KNMI are progressively being migrated to AWS, while new products are developed primarily within AWS from their start. Among recent developments is the calculation and storage of Power Spectral Densities (<http://www.orfeus-eu.org/data/odc/quality/ppsd/>; Koymans et al., 2021), for supporting e.g. data quality clients, that runs completely on AWS.

### **Task 2.7 Develop an open, dynamic and high-resolution exposure model for EEW, OEF and RLA based on crowdsourced big data**

We created an open European, building-by-building and dynamic exposure model based on the engineering information from the European Seismic Risk Model (Crowley et al., 2020) and open data from OpenStreetMap. This European model is part of the Global Dynamic Exposure (GDE) Model that aims at providing building-specific exposure data globally. This model combines engineering knowledge from existing classical exposure models with open data and predominantly OpenStreetMap to characterise every building as precisely as possible. It provides these exposure data in a fully open fashion, including the software system to generate it. To keep the model and

its output open, only open input data is considered. The model is discretized to approx. 100m x 100m tiles of a global grid while still preserving the information for each building separately. The tiles are used to approximate building counts in cases where OpenStreetMap data is incomplete. To preserve privacy, the publicly available data is aggregated to these tiles such that information about single buildings cannot be derived. However, the model input data and codes are openly available and users can create these data themselves. To create building-wise damage and loss assessments, we also provide a loss-calculator that aggregates losses by buildings or tiles.

The model is fully dynamic which means that it pulls new building data from OpenStreetMap every minute. These data are immediately processed and the exposure at the building locations is updated. The GDE model consists of six parts:

1. Generation of approx. 100m x 100m tiles and their properties related to the built environment as provided by the Global Human Settlement Layer.
2. Building processing to understand all available properties from OpenStreetMap.
3. Completeness estimation of the OpenStreetMap buildings as compared to the GHSL built area per tile.
4. Spatial disaggregation of classical exposure models over the tiles.
5. Combination of spatially-distributed classical exposure models with building data.
6. The full dynamic chain to keep the tile, building, and exposure data up-to-date.
7. Export of static data excerpts.

In this model processing chain (Figure 2.7.1), every building is enriched with exposure indicators that can be derived from the open data. Also, for every tile that contains a changed or added building, its building completeness is assessed and the exposure of the tiles is computed based on the input of the classical exposure models and detailed building data available. Each building is represented by one or more assets describing in a probabilistic way what is known about this building. The model currently contains all European countries considered in the European Seismic Risk Model, most countries of South America, all African countries, Syria, Vietnam and Japan (Figure 2.7.2). Within RISE, the European part of the model was planned to be finalised. More countries around the world will be included soon as open classical exposure models are available. The model data is available as country-excerpts in SpatiaLite databases for easy handling in QGIS or similar software. We also provide an API for damage and loss assessments based on the model data.

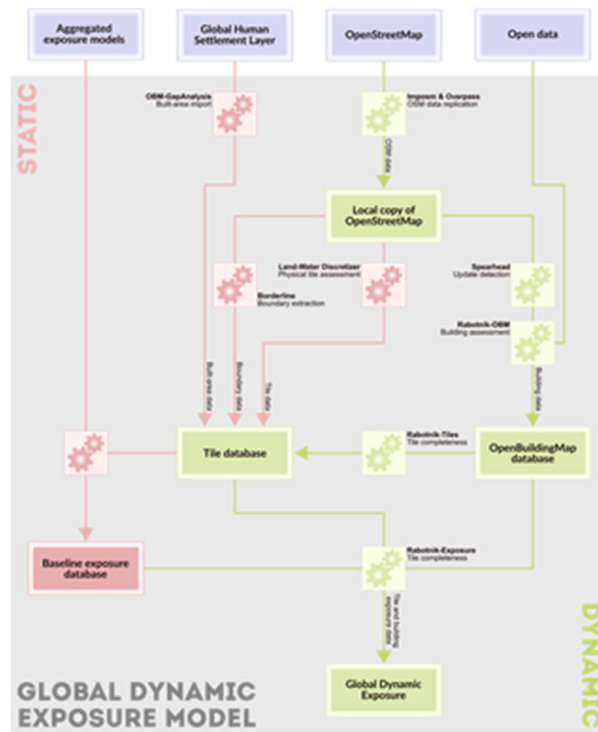


Figure 2.7.1: Schema of the Global Dynamic Exposure model. Static elements and processes (run once) are displayed in red, dynamic ones running with every change in OpenStreetMap are shown in green.

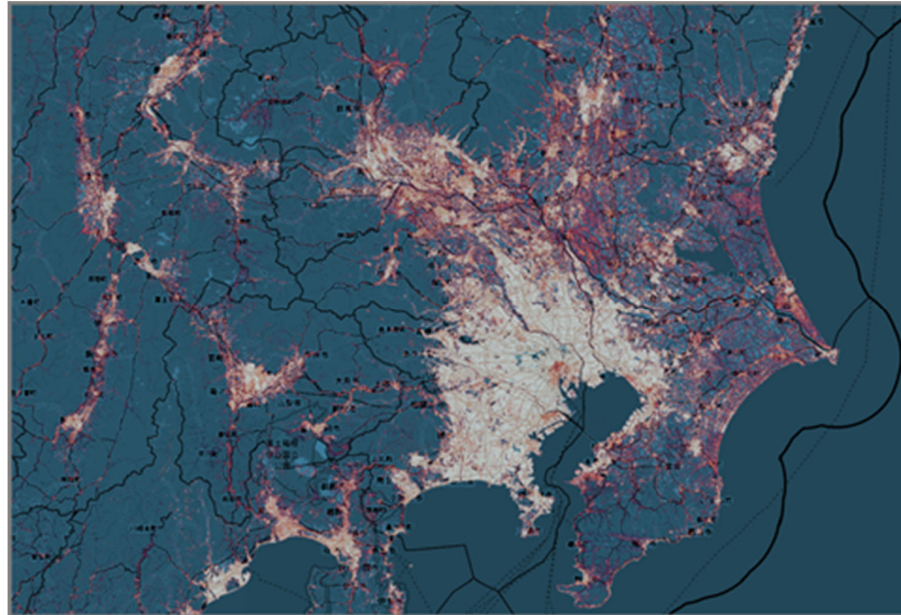
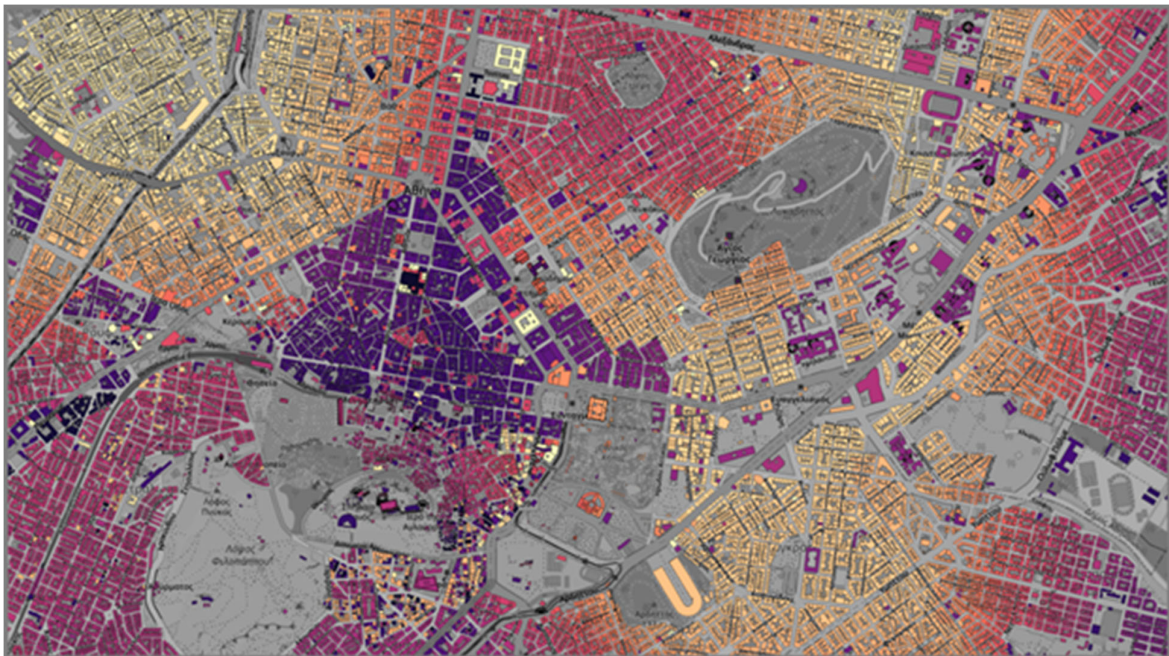


Figure 2.7.2: Exposure model for Japan. The number of buildings per tile in the Kanto region is displayed in color. The lighter the color, the more buildings are located in the tile. Background map: copyright OpenStreetMap contributors.

OpenStreetMap is changing constantly with approx. 2 buildings being added per second on average, while others are modified. To keep up with these changes, we developed our processing

engine Robotnik. This engine is rule-based and distributes and processes tile and building assessments dynamically. The rules describe how to compute tile or building properties. The rule-processes are executed in parallel, depending on the computational resources available. This processing engine allows us to keep the tile, exposure and building databases up-to-date and have the latest information at hand for each tile and building globally.

To enable the user of our model to run damage and loss assessments with the model, we developed the Loss-Calculator and additionally an API that can be used for smaller-scale assessments. The API takes the basic parameters of an earthquake and uses the ShakeMAPI to compute a ground-motion field for the earthquake. Depending on the extent of the ground-motion field, a suitable exposure model is retrieved from the main database and stored as data excerpted in a SpatialLite database. The user can choose the level of aggregation for this excerpt. The more tiles are aggregated into parent tiles, the faster the loss assessment will be computed; likewise, the full resolution is possible and all buildings will be used separately for any damage or loss assessment. The Loss-Calculator computes the estimated damage probabilities and losses using the fragility and vulnerability functions that the user provides (discrete or continuous fragility functions). The results are aggregated to each building and tile so that various visualisations are possible. The damage and loss values are also stored in the same SpatialLite database that contains the exposure data. This database is augmented with special database views about various results and data properties that makes it easy for the user to visualise them in QGIS, see Fig. 2.7.3.



*Figure 2.7.3: Damage assessment in the city of Athens for an earthquake northwest of the city. Buildings are coloured by their probability for experiencing slight damage. The brighter the color, the higher the probability. Both, the spatially varying ground-motion levels and the*

*specific building characteristics influence the expected damage grade probabilities. Background map: copyright OpenStreetMap contributors.*

### **References not cited in project publications**

Crowley H, Despotaki V, Rodrigues D, et al. (2020) Exposure model for European seismic risk assessment. *Earthquake Spectra* 36(1\_suppl):252-273, 10.1177/8755293020919429

Deichmann, (2017). Theoretical basis for the observed break in ML/Mw scaling between small and large earthquakes. *Bulletin of the Seismological Society of America*, 107(2), 505-520. doi: 10.1785/0120160318.

Di Bona M., (2016). A Local Magnitude Scale for Crustal Earthquakes in Italy. *Bull. Seismol. Soc. Am.*, 106 (1), pp. 242–258. doi: 10.1785/0120150155.

Di Stefano R. and M. G. Ciaccio (2020). Seismic Velocity Model of P- and S-waves for the Italian Lithosphere (Version 1.0) [Data set]. <http://doi.org/10.13127/tomorama.1>.

Kaya, Y ., S. Kocakaplan, and E. Şafak (2015). System identification and model calibration of multi-story buildings through estimation of vibration time histories at non- instrumented floors. *Bulletin of Earthquake Engineering* 13(11), 3301–3323.

Lomax, A., J. Virieux, P. Volant, and C. Berge-Thierry (2000). Probabilistic earthquake location in 3D and layered models: introduction of a Metropolis–Gibbs method and comparison with linear locations. In: *Advances in seismic event location*, ed. C. H. Thurber and N. Rabinowitz, 101–134. Dordrecht and Boston: Kluwer Academic Publishers.

Magnoni, F., Casarotti, E., Komatitsch, D., Di Stefano, R., Ciaccio, M.G., Tape, C., Melini, D., Michelini, A., Piersanti, A., Tromp, J. Adjoint Tomography of the Italian Lithosphere. 2021, submitted.

Mele F.M. e Quintiliani M., (2020). Correzioni di stazione per il calcolo della Magnitudo Lo-cale in Italia (aggiornate alla configurazione della Rete Sismica Nazionale di giugno 2018). *Rapp. Tec. INGV*, 412: 1-60.

Michele, M., Latorre, D., Emolo, A. (2019). An Empirical Formula to Classify the Quality of Earthquake Locations. *Bulletin of the Seismological Society of America*. Vol. 109, No. 6, pp. 2755–2761, December 2019, doi: 10.1785/0120190144.

Şafak,E.(1995). Detection and identification of soil-structure interaction in buildings from vibration recordings, *Journal of Structural Engineering*, ASCE, Vol.121, No.5, May 1995, pp.899-906.

Safak, E. (1999). Wave propagation formulation of seismic response of multi-story buildings, *Journal of Structural Engineering, ASCE*, Vol. 125, No. 4, pp.426-437.

Supino, M., Festa, G., & Zollo, A. (2019). A probabilistic method for the estimation of earthquake source parameters from spectral inversion: application to the 2016–2017 Central Italy seismic sequence. *Geophysical Journal International*, 218(2), 988-1007. doi:10.1093/gji/ggz206.

Supino, M., Poiata, N., Festa, G., Vilotte, J. P., Satriano, C., & Obara, K. (2020). Self-similarity of low-frequency earthquakes. *Scientific reports*, 10(1), 1-9. doi: 10.1038/s41598-020-63584-6.

Vuan, A., Sukan, M., Chiaraluce, L., & Di Stefano, R. (2017). Loading rate variations along a midcrustal shear zone preceding the Mw6.0 earthquake of 24 August 2016 in Central Italy. *Geophysical Research Letters*, 44, 12,170– 12,180. <https://doi.org/10.1002/2017GL076223>.

### **List of submitted deliverables for WP2:**

- D2.1 Large-scale DAS logistic feasibility study on new applications
- D2.2 Deployment of Prototype DAS Array
- D2.3 Report on all DAS field deployments
- D2.4 Field ready internal next generation sensors
- D2.5 Functional next generation sensors and hyper-dense networks
- D2.6 Portable excitation sources for field testing
- D2.7 Results of excitation sources and recommendations
- D2.8 Progress of new generation catalogues for public dissemination.
- D2.9: Accuracy and precision of earthquake forecasts using the new generation catalogues for open dissemination.
- D2.10: Report on the temporal change of the upper crust properties using ambient noise techniques
- D2.11: Technical solutions on open, dynamic, high volume, cloud-based services
- D2.12: Technical development of prototype big data solutions
- D2.13: An open, dynamic, high-resolution exposure model for Europe
- D2.14: Technology Readiness Assessment

### **Summary of Exploitable Results in WP2:**

#### *New technology*

- Quakesaver cost effective MEMS sensors
- Quakesaver Short Period seismometers
- QuakeSaver's smart edge computing open firmware
- Quakesaver remote network fleet management system for remote configuration and monitoring

- Impact hammer
- Eccentric mass shaker

#### *New Capability*

- Field expertise for logistically efficient DAS experiments in urban, volcanic and glacial environments
- Major result that DAS arrays may record up to 2 orders of magnitude more local events than existing seismometer networks
- Technology for rapid deployment of >10 km long DAS cables in glaciers and ice sheets (Klaasen et al., 2022)

#### *Improved data analysis and data products*

- More specific tools and codes for urban DAS data processing, cleaning, noise interferometry and local imaging
- Image-processing based method for event detection in DAS data (Thrustarson et al., 2022)
- Theory for phase transmission fibre-optic sensing, modelling and inversion (Fichtner et al., 2022a,b)
- Forward modelling tools for DAS acquisition in submarine environments in the presence of islands, rough topography and soft sediments
- A suite of new-generation high-resolution earthquake catalogues for 1981-2018 Italian Seismicity, using a range of state of the art full waveform techniques, including
  - (a) relative and absolute locations
  - (b) Both local magnitude (ML) and seismic moment magnitude (Mw)
- Near real time monitoring of proxies for the state of stress in the Earth's crust (velocity transients)

#### *New services*

- Prototypes of technical solutions for open, dynamic, high volume, scaleable, cloud-based European data archiving and provision services in anticipation of the explosion of data from existing and new technologies
- Software dastools: Quinteros, J. (2021b). dastools - Tools to work with data generated by DAS systems, Potsdam: GFZ Data Services. doi:10.5880/GFZ.2.4.2021.001.
- Seismological services in the cloud, e.g., Koymans, M. R., Domingo Ballesta, J., Ruigrok, E., Sleeman, R., Trani, L., & Evers, L. G. (2021). Performance assessment of geophysical instrumentation through the automated analysis of power spectral density estimates. *Earth and Space Science*, 8, e2021EA001675. <https://doi.org/10.1029/2021EA001675>
- An open European, building-by-building and dynamic exposure model based on the engineering information from the European Seismic Risk Model and open data from OpenStreetMap.
- A repository for the global dynamic exposure model codes: (<https://git.gfz-potsdam.de/dynamicexposure>)

**Peer reviewed publications**

Bowden, D., Fichtner, A., Nikas, T., Bogris, A., Simos, C., Smolinski, K., Koroni, M., Lentas, K., Simos, I., Melis, N. S (2022). Linking distributed and integrated fibre-optic sensing. *Geophysical Research Letters*, 49, doi:10.1029/2022GL098727.

Bogris, A., Nikas, T., Simos, C., Simos, I., Lentas, K., Melis, N. S., Fichtner, A., Bowden, D., Smolinski, K., Mesaritakis, C., Chochliouros, I. (2022). Sensitive seismic sensors based on microwave frequency fiber interferometry in commercially deployed cables. *Scientific Reports*, 12, doi:10.1038/s41598-022-18130-x.

Caglar, N.M. and E. Safak (2022). Estimation of the response of non-instrumented floors using the Timoshenko and Bernoulli-Euler Beam Theories, *Earthquake Engineering & Structural Dynamics*, 2022, Vol.1, No.3, DOI: 10.1002/eqe.3636

Cetin M, and E. Safak (2021) . An algorithm to calibrate analytical models of multi-story buildings from vibration records, *Earthquake Spectra*, 1–17, DOI: 10.1177/87552930211046969.

Chiaraluce L., M. Michele, F. Waldhauser, Y. J. Tan, M. Herrmann, D. Spallarossa, G. C. Beroza, M. Cattaneo, C. Chiarabba, P. De Gori, R. Di Stefano, W. Ellsworth, I. Main, S. Mancini, L. Margheriti, W. Marzocchi, M-A. Meier, D. Scafidi, D. Schaff and M. Segou (2022). A comprehensive suite of earthquake catalogues for the 2016-2017 Central Italy seismic sequence. *Scientific Data*, 9:710, <https://doi.org/10.1038/s41597-022-01827-z>.

Fichtner, A., Bogris, A., Nikas, T., Bowden, D., Lentas, K., Melis, N. S., Simos, C., Simos, I., Smolinski, K. (2022a). Sensitivity kernels for transmission fiber optics. *Geophysical Journal International*, 231, 1040-1044, doi:10.1093/gji/ggac238.

Fichtner, A., Bogris, A., Nikas, T., Bowden, D., Lentas, K., Melis, N. S., Simos, C., Simos, I., Smolinski, K. (2022b). Theory of phase transmission fibre-optic sensing. *Geophysical Journal International*, 231, 1031-1039, doi:10.1093/gji/ggac237.

Fichtner, A., Klaasen, S., Thrastarson, S., Cubuk-Sabuncu, Y., Paitz, P., Jonsdottir, K. (2022c). Fiber-optic observation of volcanic tremor through floating ice sheet resonance. *The Seismic Record*, 2, 148-155, doi:10.1785/0320220010.

Klaasen, S., Paitz, P., Lindner, N., Dettmer, J., Fichtner, A. (2021). Distributed Acoustic Sensing in volcano-glacial environments – Mount Meager, British Columbia. *Journal of Geophysical Research*, 126, doi:10.1029/2021JB022358.

Klaasen, S., Thrastarson, S., Fichtner, A., Cubuk-Sabuncu, Y., Jonsdottir, K. (2022). Sensing Iceland’s most active volcano with a «buried hair». *EOS*, 103, doi:10.1029/2022EO220007.

Latorre D., R. Di Stefano, B. Castello, M. Michele, L. Chiaraluca (2023). An updated view of the Italian seismicity from probabilistic location in 3D velocity models: The 1981–2018 Italian catalog of absolute earthquake locations (CLASS). *Tectonophysics*, 846, 229664, <https://doi.org/10.1016/j.tecto.2022.229664>.

Mancini, S., Segou, M., Werner, M. J., Parsons, T., Beroza, G., & Chiaraluca, L. (2022). On the use of high-resolution and deep-learning seismic catalogs for short-term earthquake forecasts: Potential benefits and current limitations. *Journal of Geophysical Research: Solid Earth*, 127, e2022JB025202. <https://doi.org/10.1029/2022JB025202>.

Quinteros, J., J. A. Carter, J. Schaeffer, C. Trabant, and H. A. Pedersen (2021a). Exploring Approaches for Large Data in Seismology: User and Data Repository Perspectives, *Seismol. Res. Lett.* 92, 1531–1540, doi: 10.1785/0220200390.

Sugan M., S. Campanella, L. Chiaraluca, M. Michele and A. Vuan (2023). The unlocking process leading to the 2016 Central Italy seismic sequence. *Geophys. Res. Letters*, doi: 10.1029/2022GL101838.

Thrustarson, S., Torfason, R., Klaasen, S., Paitz, P., Cubuk-Sabuncu, Y., Jonsdottir, K., Fichtner, A. (2022). Detecting seismic events with computer vision: Applications for fiber-optic sensing. *Earth and Space Science Open Archive*, doi:10.1002/essoar.10509693.1.

### **Conference publications**

Moment vs local magnitude scaling of small-to-moderate earthquakes from seismic moment estimation of 10 years (2009-2018) of Italian seismicity. Supino M., L. Chiaraluca, R. Di Stefano, B. Castello, and M. Michele. EGU2023- 11928

CARS - Catalog of Relative Seismic Locations of 1981-2018 Italian Seismicity. Michele M., R: Di Stefano, L. Chiaraluca, D. Latorre, and B. Castello. EGU2023-14033.

Exploring the feasibility of seismic monitoring using ambient noise coda Q : experiments in the Aegean (Greece), Ranjan P., L. Stehly and E. Delouche. EGU2023-10372

Seasonal velocity variations in Greece associated with aquifers, Delouche E. and L. Stehly. EGU2023-13055

Seasonal variations of seismic velocities in Greece measured from seismic noise cross-correlations, Delouche E., L. Stehly and M. Campillo, EGU 2022-12347

Temporal evolution of mechanical properties of the crust in Greece. Delouche E, and L. Stehly, AGU 2021-S35B-0221

Temporal evolution of seismic velocity in the Gulf of Corinth (Greece), Delouche E., and L. Stehly  
EGU2021-15222

Distributed Acoustic Sensing for the Exploration of the Mount Meager Volcanic Complex, British Columbia, Canada, Sara Klaasen, Andreas Fichtner, Patrick Paitz, Jan Dettmer, 2020, AGU

Combining Distributed Acoustic Sensing and Beamforming in a Volcanic Environment on Mount Meager, British Columbia, Sara Klaasen, Patrick Paitz, Jan Dettmer, Andreas Fichtner, 2021, EGU

Combining Distributed Acoustic Sensing (DAS) and Beamforming in a Volcanic Environment on Mount Meager, British Columbia, Sara Klaasen, Patrick Paitz, Jan Dettmer, Andreas Fichtner, 2021, SSA

Earthquake Monitoring in Glacial and Volcanic Environments with Distributed Acoustic Sensing (DAS), Sara Klaasen, Jan Dettmer, Kristín Jónsdóttir, Andreas Fichtner, 2021, Mid-Term RISE

Distributed Acoustic Sensing on Volcanoes: Grimsvotn and Fagradalsfjall, Iceland, Sara Klaasen, Solvi Thrastarson, Kristin Jonsdottir, Yeşim Çubuk-Sabuncu, Patrick Paitz, Andreas Fichtner, 2021, AGU

Distributed Acoustic Sensing on Volcanoes, Sara Klaasen, Solvi Thrastarson, Kristín Jónsdóttir, Yeşim Çubuk-Sabuncu, Jan Dettmer, Paraskevi Nomikou, Patrick Paitz, Andreas Fichtner, 2021, AGU DAS workshop

Fibre-Optic Sensing for Volcano Monitoring on Grímsvötn, Iceland, Sara Klaasen, Solvi Thrastarson, Yeşim Çubuk-Sabuncu, Kristín Jónsdóttir, Lars Gebraad, Andreas Fichtner, 2022, EGU

Volcanic Event Characterization with Fiber-Optic Sensing, Sara Klaasen, Solvi Thrastarson, Yeşim Çubuk-Sabuncu, Kristin Jonsdottir, Lars Gebraad, Andreas Fichtner, 2022, AGU

Monitoring glacially covered volcanoes with Fibre-Optic Sensing, Sara Klaasen, Solvi Thrastarson, Yeşim Çubuk-Sabuncu, Kristín Jónsdóttir, Lars Gebraad, Andreas Fichtner, 2023, IAVCEI

Analysis of Shallow Wave Propagation Using Distributed Acoustic Sensing Beneath Bern, Switzerland; Krystyna T. Smolinski, Patrick Paitz, Daniel Bowden, Pascal Edme, Felix Kugler and Andreas Fichtner; 2020; AGU

Urban Distributed Acoustic Sensing Using In-Situ Fibre Beneath Bern, Switzerland; Krystyna Smolinski, Patrick Paitz, Daniel Bowden, Pascal Edme, Felix Kugler and Andreas Fichtner; 2020; EGU

Urban Distributed Acoustic Sensing in Bern, Switzerland: Observations and Modelling; Krystyna T. Smolinski, Daniel Bowden, Patrick Paitz, Pascal Edme, Brian L.N. Kennett, Felix Kugler and Andreas Fichtner; 2021; AGU

Utility and Value of High Density DAS; Krystyna Smolinski, Sara Klaasen, Sölvi Thrastarson, Daniel Bowden, Patrick Paitz, Pascal Edme, Andreas Fichtner; 2022; RISE Annual Meeting

Introduction to Fibre-Optic Sensing; Krystyna Smolinski and Philippe Jousset; 2022; SPIN Short Course

Distributed Acoustic Sensing in the Athens Metropolitan Area: Preliminary Results; Krystyna T. Smolinski, Daniel C. Bowden, Konstantinos Lentas, Nikolaos S. Melis, Christos Simos, Adonis Bogris, Iraklis Simos, Thomas Nikas, and Andreas Fichtner; 2022; EGU

Exploring DAS as a Tool for Earthquake Monitoring in Urban Environments; Krystyna T. Smolinski, Daniel C. Bowden, Konstantinos Lentas, Nikolaos S. Melis, Christos Simos, Adonis Bogris, Iraklis Simos, Thomas Nikas, and Andreas Fichtner; 2022; AGU

### **1.2.3 Work package 3**

#### **Overview**

WP3 dealt with advancing operational earthquake forecasting (OEF) capabilities at different spatial scales by (i) improving our understanding of the earthquake generation process and (ii) developing various forecasting models to translate new-gained insights into improved forecasts.

#### **Summary of achievements in WP3 tasks: (2-3 pages for each task)**

##### **Task 3.1 Exploring seismic and non-seismic precursory signals**

Task 3.1 provides an overview of seismic and non-seismic precursor anomalies of recent large earthquakes in Italy and discusses the importance of precursor candidates in predicting strong earthquakes. Precursor candidates are defined as geophysical or geochemical anomalies linked to potentially destructive earthquakes. Recognizing precursors before an earthquake occurs has been challenging, but recent developments in observational capabilities have provided new opportunities for continuous monitoring of the Earth's crust, which may lead to improved earthquake prediction. The RISE project aims to cover all of Europe, but the task primarily focuses on Italy due to its history of being hit by violent earthquakes and its dense monitoring networks. The sustained background seismicity in the central Apennines region of Italy allows for testing and implementing old and new precursor candidates in a time-varying risk analysis approach.

**Geochemical measurements:** Terrestrial gases in groundwater and soil air have been extensively studied in seismically active areas to search for premonitory changes useful for earthquake prediction. High concentrations of various volatiles have been found along active faults, suggesting that faults may provide paths of least resistance for gases to escape. Changes in gas concentrations have been observed before large earthquakes at "sensitive" stations located along active faults, but environmental factors can also significantly affect gas measurements. These studies have mainly been conducted in ex-USSR, China, Japan, and the United States. The Italian Radon mOnitoring Network (IRON) is a permanent network of 26 stations in Italy designed to monitor radon emissions in seismically active areas and explore the potential physical link between seismogenic processes and temporal variability in radon emissions. An empirical correction procedure has been developed to account for the effect of meteorological parameters on the measured radon concentration. Data recorded by two stations close to the epicenter of the Amatrice-Visso-Norcia seismic sequence in central Italy from August 2016 to October 2016 is analyzed, and an increase in radon emanation is observed about 2 weeks before the Mw 6.5 earthquake occurred. This suggests that radon could be a powerful tracer for fluid movements in the crust and a potentially effective marker to study processes connected with earthquakes preparatory phase. However, the recognition as such of emanation peaks preceding earthquakes is complicated by environmental effects and the sometimes significant delay between the peak(s) and the rupture leading to numerous false detections. In addition to Radon monitoring, various local initiatives exist in Italy to monitor water concentrations of different elements, including CO<sub>2</sub>, and their link to the desorption of Arsenic and Vanadium. The Tyrrhenian plate allows for free degassing of deep CO<sub>2</sub> up to the surface, while the Adriatic plate holds traps for deep CO<sub>2</sub> where pressure could build up. The seismicity in the region concentrates along the boundary between these two provinces, and continuous monitoring of the quality of thermal waters and springs is necessary to understand the destabilization of the faults in the area. A positive anomaly in the concentration of Arsenic and Vanadium started nearly five months before the occurrence of the Amatrice earthquake, and this sustained high concentration increases the confidence in the possibility of an earthquake preparation process at work.

**Observations of the seismic activity:** A classical framework for earthquakes to occur is that they are the result of long-term strain accumulation on active faults and complex transient triggering mechanisms. The 2016 Amatrice-Visso-Norcia earthquake sequence in central Italy provided a unique opportunity to image the preparatory phase of a large earthquake. Seismic tomography was used to reveal precursory changes in elastic wave speed, indicating the final locked state of the fault and rapid fault-stiffness alterations near the hypocentre a few weeks before the event. The study confirms laboratory observations of precursory velocity changes before fault failure in nature and provides new perspectives for understanding earthquake nucleation mechanisms. Systematic documentation of these changes and their statistical significance over long time frames is essential for improving earthquake forecasts, but the significance of the results depends on the density and location of seismicity. Changes in the size distribution of background seismicity (b-value, average magnitude) over space and time are not discussed here.

**Continuous velocity changes measurements from seismic noise:** Ambient seismic noise interferometry is used to derive the crustal velocity changes from correlations of seismic noise recordings. The velocity changes are related to mechanical changes at depth. It was used to investigate the 2009 L'Aquila earthquake case. The results suggest that the velocity variations measured before the earthquake are probably due to environmental disturbances such as changes in water table level. The limited time resolution required to obtain this result implies that the velocity changes measurement remains unable to track the fast changes related to the preparation of the earthquake indicated by the numerous foreshocks that preceded the rupture. The velocity changes are related to mechanical changes at depth.

**Continuous attenuation changes measurements:** Measuring the attenuation of seismic waves before earthquakes has become possible using ambient seismic noise. This method allows for the measurement of attenuation through correlated waveform changes induced by fluid movements. The application of this method to recent earthquakes that occurred in Italy (L'Aquila, Amatrice, and Visso-Norcia) shows that the crustal volume hosting the normal faults of the Central Apennines underwent a non-seismic anomaly for several months before the ruptures, over a distance larger than 100 km. This anomaly consists of a series of increasingly pronounced and frequent disturbances that progressively focus on the future rupture zone. These disturbances persist after the rupture, although less powerful and frequent, and broaden the understanding of the phenomena that precede and follow a major earthquake. The most interesting case concerns the Amatrice earthquake. The beginning of the non-seismic anomaly coincides with the beginning of the geochemical anomaly in arsenic (As) and vanadium (V) induced by intrusions of deep CO<sub>2</sub>.

**Enhancing forecasting:** Because of its properties the nonseismic precursor is a good candidate to be a predictor of an impending earthquake. Issuing a prediction requires a geographical location; a time window; a range of magnitude; and the level of confidence in the prediction. In space, it spreads over a distance of 100km of radius and progressively focuses towards the future epicentre. In time, the rate of the successive perturbations can be modelled with a very simple mathematical description (either polynomial or exponential), which allows for the definition of a time window of prediction related to the rate of divergence of the model. Concerning the range of magnitude of the impending event, it is hard to relate the duration of the precursor to the size of the event to come. Based on seldom observations, we introduce a concept of a minimum magnitude; set to 6 for the Central Apennines. Further directions concern the window of observations. Predicting the past is easier because we know where and when the rupture occurred. Our precursor is easy to be detected because we can see it as a whole over the period of observation. Using the modelling of the precursor of Amatrice, we have derived the minimum period of observation to issue a correct time window for the prediction: it ranges between 25 and 30 days, to be compared to the 5 months' duration of the precursor. Finally, the use of supervised classification on the measurement also allows for a rapid and efficient characterization of the state of the crust in the vicinity of a fault on a daily basis.

### **Task 3.2. Enhancing earthquake predictability**

This task was planned to explore the limits of earthquake predictability. It is subdivided into three subtasks.

In subtask1, forecasting methods taken from the literature and newly developed were applied to Italy by the retrospective testing using the HOMogenized InstrUMENTal Seismic Catalog (HORUS) of Italy from 1960 to present partially developed also in Task 2.4 of RISE. In particular, Gasperini et al. (2021) developed an alarm-based forecasting method based on the occurrence of strong foreshocks. This was tested using the Molchan diagrams and the Area Skill score approaches. Considering an alarm duration of three months, the algorithm retrospectively forecast more than 70 percent of all shocks (mainshocks+aftershocks) with  $M_w \geq 5.5$  occurred in Italy from 1960 to 2019 with a total space–time fraction covered by the alarms of the order of 2 per cent. Considering the same space–time coverage, the algorithm is also able to retrospectively forecast more than 40 per cent of the mainshocks only with  $M_w \geq 5.5$  of the seismic sequences occurring in the same time interval.

Biondini et al. (2022) applied to Italy the EEPAS (Every Earthquake a Precursor According to Scale) forecasting model. EEPAS is a pace–time point–process model based on the precursory scale increase phenomenon and associated predictive scaling relations. It has been previously applied to New Zealand, California and Japan earthquakes with target magnitude thresholds varying from about 5 to 7. In all previous applications, computations were done using the computer code implemented in Fortran language by the model authors. Biondini et al. (2022) developed a suite of computing codes completely rewritten in Matlab and Python. They first compared the two software codes to ensure the convergence and adequate coincidence between the estimated model parameters for a simple region capable of being analysed by both software codes, then using the rewritten codes they optimised the parameters for a different and more complex polygon of analysis using the catalogue data from 1990 to 2011. Finally, they performed a retrospective (pseudo-prospective) forecasting experiment of Italian earthquakes from 2012 to 2021 with  $M_w \geq 5.0$  and compares the forecasting skill of EEPAS with other forecasting models using the standard test developed in the ambit of the Collaboratory for the Study of Earthquake Predictability (CSEP). The EEPAS approach was demonstrated to be slightly worse than ETAS for short forecasting windows (3 months) and better for longer windows (up to 10 years).

Another forecasting approach is that followed by Gulia et. al. (2020, 2021) for the application of the Traffic Light System (TLS) to the pseudo-prospective forecasting of Ridgecrest  $M_w 7.1$  earthquake of July 2021, based on the temporal variation of the b-value of the frequency–magnitude (Gutenberg–Richter) relation. In normally decaying aftershock sequences, the b-value of the aftershocks was found, on average, to be 10%–30% higher than the background b-value. A drop of 10% or more in “aftershock” b-values was postulated to indicate that the region is still highly stressed and that a subsequent larger event is likely. In this Ridgecrest case study, after analysing the magnitude of completeness of the sequences, they were able to determine reliable b-values over a large range of magnitudes within hours of the two mainshocks. They then find that in the hours after the first  $M_w 6.4$  Ridgecrest event, the b-value drops by 23% on average, compared to the background value, triggering a red foreshock traffic light. Spatially mapping the changes in b values, they identify an area to the north of the rupture plane as the most likely location of a subsequent event. After the second magnitude 7.1 mainshock, which did occur in

that location as anticipated, the b-value increased by 26% over the background value, triggering a green traffic light. Finally, comparing the 2019 sequence with the Mw 5.8 sequence in 1995, in which no mainshock followed, they find a b-value increase of 29% after the mainshock. Their results suggest that the real-time monitoring of b-values is feasible in California and may add important information for aftershock hazard assessment.

Gulia and Gasperini (2021) observed that artefacts often affect seismic catalogues. Among them, the presence of man-made contaminations such as quarry blasts and explosions is a well-known problem. Using a contaminated dataset reduces the statistical significance of results and can lead to erroneous conclusions, thus the removal of such nonnatural events should be the first step for a data analyst. Blasts misclassified as natural earthquakes, indeed, may artificially alter the seismicity rates and then the b-value of the Gutenberg and Richter relationship, an essential ingredient of several forecasting models.

At present, datasets collect useful information beyond the parameters to locate the earthquakes in space and time, allowing the users to discriminate between natural and nonnatural events. However, selecting them from webservices queries is neither easy nor clear, and part of such supplementary but fundamental information can be lost during downloading. As a consequence, most statistical seismologists ignore the presence in seismic catalogue of explosions and quarry blasts and assume that they were not located by seismic networks or in case they were eliminated. They show the example of the Italian Seismological Instrumental and Parametric Database. What happens when artificial seismicity is mixed with natural one?

In subtask2, Spassiani & Marzocchi (2021) proposed to model the MFD of seismic events that nucleate in a confined area with an energy dependent tapered Gutenberg–Richter (GR) relation, (TGRE). TGRE acknowledges the elastic rebound theory in the sense that the probability for another large event to nucleate in the same area within a short time interval has to be lower than according to the (tapered) GR relation. The validity and applicability of the TGRE model is demonstrated for the 1992 M7.3 Landers sequence, California. As expected by TGRE, it was shown that the on-fault MFD differs from the off-fault MFD (lower corner magnitude), evidencing the magnitude independence assumption. The TGRE fits the magnitude–frequency distribution (MFD) of on-fault seismicity better than the tapered GR model. An ETAS model with TGRE could improve OEF, i.e., finding the highest probability for a large earthquake not where the previous large earthquake occurred.

Herrmann & Marzocchi (2021) inspected the magnitude–frequency distribution (MFD) of high-resolution catalogues at the example of the 2019 M7.1 Ridgecrest sequence, 2009 M6.3 L’Aquila Sequence, and of whole Southern California. They found that the MFD of small earthquakes in these catalogues does usually not comply with the exponential Gutenberg–Richter (GR) relation. In fact, when using this relation rigorously, high-resolution catalogues do not seem to offer a crucial benefit over ordinary catalogues. This impediment is mostly due to an improper mixing of different magnitude types, spatiotemporally varying detection capabilities, or distorted data processing. Common methods to apply the GR relation do not detect these discrepancies. These findings are relevant for both producers of high-resolution catalogues and modellers that use MFDs of such catalogues.

Herrmann et al. (2022) reanalyzed the 2016–2017 central Italy sequence using a high-resolution catalogue and introduced an alternative perspective for studying MFD variability—using a

spatiotemporal scale that considers the 3-D distribution of recorded seismicity. This approach is based on Piegari et al. (2022) of the same group: using a cluster analysis of a sequence using density-based algorithms to spatially isolate the most seismogenic zones; temporal periods are defined by the occurrence time of the largest events. They demonstrate that this approach proves beneficial in resolving the spatiotemporal variation of the MFD and b-value. For instance, they resolved what happened in the days before the largest event (Norcia) in its associated seismogenic zone. Rather than solely focusing on b-value estimates, they exploited more information from the MFD, e.g., by assessing and comparing its exponential-like part and reporting the b-value stability as a function of  $M_c$ . They showed that the MFD behaves in a complex manner among the spatially isolated clusters throughout the sequence. Their findings reflect on the appropriate spatiotemporal scale to resolve the b-value and challenge existing approaches.

Manganiello et al. (2022) re-examined foreshock activity in southern California to investigate the existence and main characteristics of foreshock sequences that cannot be explained by ETAS, i.e., anomalous foreshock sequences. In other words, they looked for new insights on the evidence against the cascade model. They performed different statistical tests and considered the potential influence of subjective choices, such as the method to identify mainshocks and their foreshocks. They found anomalous foreshock sequences mostly for mainshock magnitudes below 5.5. These anomalies preferentially occurred in zones of high heat flow, which were already known to host swarm-like seismicity. Outside these regions, the foreshocks generally behave as expected by ETAS. These findings will contribute to an improving earthquake forecasting (e.g., by stimulating the discrimination of swarm-like from ETAS-like sequences) and the understanding of earthquake nucleation processes (e.g., anomalous foreshock sequences are not indicating a pre-slip nucleation process, but swarm-like behaviour driven by heat flow).

In subtask3, systematic empirical studies to search for additional explanatory variables in the triggering properties of earthquakes were conducted. Obvious candidates include (i) surface heat flow, (ii) geodetic strain-rate, (iii) thickness of the seismogenic zone, (iv) lithology (inferred rigidity, rheology if available), (v) plate tectonic setting, (vi) inferred regional stress field, (vii) triggering susceptibility, (viii) time since last major earthquake (on well-characterised faults), and some variables that can be measured during a seismic sequence such as (i) source focal mechanism, (ii) aseismic afterslip moment, (iii) stress drop, and (iv) ShakeMap footprint. Specifically, we will search for dependencies between these variables and various clustering properties including (i) size/timing/location of largest triggered event, (ii) triggering productivity, (iii) foreshock statistics, (iv) swarm-like behaviour. The research will benefit from advances in observational capabilities (-> 2.4) and exploit computational statistics to uncover hidden relationships.

In this regard, Bayliss et al. (2020) has developed a Bayesian framework to make inferences of the effect of the explanatory variables listed above on the Epidemic-Type Aftershock Sequence (ETAS) model parameters. This allows them to have a comprehensive representation of the uncertainty by calculating a full posterior distribution for each quantity of interest. The novelty of their approach is to represent the ETAS model as a Latent Gaussian model (LGM). This allows them to use the Integrated Nested Laplace Approximation (INLA) methodology to obtain the posterior distribution of the parameters. The INLA methodology is an alternative to MCMC techniques designed to handle large LGM's having parameters with complex covariance

structures, specifically, it has been used extensively to study the effect of spatially or temporally (or both) varying covariates on a phenomenon of interest. Applications of the INLA methodologies range from finance to biostatistics. This creates a theoretical framework to include covariates in the ETAS model and to compare models based on different combinations of those. Moreover, the INLA algorithm is deterministic which makes the result more reproducible than simulation based techniques such as MCMC. Finally, this theoretical framework is easily extensible to consider the parameters as spatially and/or temporally variable, by using Gaussian Markov Random Fields with the parameters of the covariance function determined by the data.

Probabilistic earthquake forecasts estimate the likelihood of future earthquakes within a specified time-space-magnitude window and are important because they inform planning of hazard mitigation activities on different timescales. The spatial component of such forecasts, expressed as seismicity models, generally rely upon some combination of past event locations and underlying factors which might affect spatial intensity, such as strain rate, fault location and slip rate or past seismicity. Bayliss et al. (2022) for the first time, extend previously reported spatial seismicity models, generated using the open source `inlabru` package, to time-independent earthquake forecasts using California as a case study. The `inlabru` approach allows the rapid evaluation of point process models which integrate different spatial datasets. They explore how well various candidate forecasts perform compared to observed activity over three contiguous five year time periods using the same training window for the seismicity data. In each case they compare models constructed from both full and declustered earthquake catalogues. In doing this, they compare the use of synthetic catalogue forecasts to the more widely used grid-based approach of previous forecast testing experiments. The simulated-catalogue approach uses the full model posteriors to create Bayesian earthquake forecasts. They show that simulated-catalogue based forecasts perform better than the grid-based equivalents due to (a) their ability to capture more uncertainty in the model components and (b) the associated relaxation of the Poisson assumption in testing. They demonstrate that the `inlabru` models perform well overall over various time periods, and hence that independent data such as fault slip rates can improve forecasting power on the time scales examined. Together, these findings represent a significant improvement in earthquake forecasting, though this has yet to be tested and proven in true perspective mode.

Aseismic afterslip is postseismic fault sliding that may significantly redistribute crustal stresses and drive aftershock sequences. Afterslip is typically modelled through geodetic observations of surface deformation on a case-by-case basis, thus questions of how and why the afterslip moment varies between earthquakes remain largely unaddressed. Churchill et al. (2022) compiled 148 afterslip studies following 53 M 6.0–9.1 earthquakes, and formally analysed a subset of 88 well-constrained kinematic models. Afterslip and coseismic moments scale near-linearly, with a median Spearman's rank correlation coefficient (CC) of 0.91 after bootstrapping (95% range: 0.89–0.93). They inferred that afterslip area and average slip scale with coseismic moment as  $M_0^{2/3}$  and  $M_0^{1/3}$ , respectively. The ratio of afterslip to coseismic moment ( $M_{rel}$ ) varies from <1% to >300% (interquartile range: 9%–32%).  $M_{rel}$  weakly correlates with  $M_0$  (CC: –0.21, attributed to a publication bias), rupture aspect ratio (CC: –0.31), and fault slip rate (CC: 0.26, treated as a proxy for fault maturity), indicating that these factors affect afterslip.  $M_{rel}$  does not correlate with mainshock dip, rake, or depth. Given the power-law decay of afterslip, studies that started earlier and spanned longer timescales to capture more afterslip are expected, but  $M_{rel}$  does not correlate

with observation start time or duration. Because  $M_{rel}$  estimates for a single earthquake can vary by an order of magnitude, it is proposed that modelling uncertainty currently presents a challenge for systematic afterslip analysis. Standardising modelling practices may improve model comparability, and eventually allow for predictive afterslip models that account for mainshock and fault zone factors to be incorporated into aftershock hazard models.

Strong earthquakes cause aftershock sequences that are clustered in time according to a power decay law, and in space along their extended rupture, shaping a typically elongated pattern of aftershock locations. A widely used approach to model earthquake clustering, the Epidemic Type Aftershock Sequence (ETAS) model, shows three major biases. First, the conventional ETAS approach assumes isotropic spatial triggering, which stands in conflict with observations and geophysical arguments for strong earthquakes. Second, the spatial kernel has unlimited extent, allowing smaller events to exert disproportionate trigger potential over an unrealistically large area. Third, the ETAS model assumes complete event records and neglects inevitable short-term aftershock incompleteness as a consequence of overlapping coda waves. These three aspects can substantially bias the parameter estimation and lead to underestimated cluster sizes. Grimm et al. (2022) combine the approach of Grimm et al. (Bull. Seismol. Soc. Am. 112, 474–493, doi: 10.1785/0120210097), who introduced a generalised anisotropic and locally restricted spatial kernel, with the ETAS-Incomplete (ETASI) time model of Hainzl (Bull. Seismol. Soc. Am. 112, 494–507, doi: 10.1785/0120210146), to define an ETASI space-time model with a flexible spatial kernel that solves the above mentioned shortcomings. We apply different model versions to a triad of forecasting experiments of the 2019 Ridgecrest sequence and evaluate the prediction quality with respect to cluster size, largest aftershock magnitude and spatial distribution. The new model provides the potential of more realistic simulations of ongoing aftershock activity, e.g. allowing better predictions of the probability and location of a strong, damaging aftershock, which might be beneficial for short term

### **Task 3.3. A new generation of OEF models**

This task developed forecast models that go beyond the state of the art by incorporating novel insights and approaches based on continuum mechanics, statistical physics, and statistical/stochastic modelling. To test them independently in WP7, this task set up a repository that contains both the source codes and a detailed description of each model. The following is an outline of the repository and different classes of models it contains. So far, eight models have been submitted; some additional models are almost finished but not yet ready for the testing phase. We will invite more modelers of the scientific community to increase the diversity of the forecasts.

#### The repository

The models in the repository were developed within WP3 and will be tested in WP7 in different phases. The most important phase is the prospective test for the Italian region, which will be carried out in collaboration with the Collaboratory for the Study of Earthquake Predictability (CSEP).

To efficiently interact between WP3 and WP7, we take advantage of version control, open-source software, and open-access repositories. Version control allows us to clearly document the model implementation process, quickly inspect code errors, and understand algorithms. The models,

experiment setup, and deployment architecture are set up in a GitLab version control server hosted at GFZ: [https://git.gfz-potsdam.de/csep-group/rise\\_italy\\_experiment](https://git.gfz-potsdam.de/csep-group/rise_italy_experiment). As long as modelers have not finalized their corresponding scientific publications, the corresponding source code is kept private (i.e., closed to the general public, but a specific request to the WP leader is possible).

Testers and modelers act collaboratively as model maintainers, with rapid communication about the underlying codes. The open-source software pyCSEP (Savran et al. 2021, see Deliverable D7.1) acts as a wrapper for the forecasts, authoritative data sets, and testing methods, to which modelers had full access; their use was explained during workshops. To ensure reproducibility, the whole repository will eventually be uploaded to Zenodo for public access, and updated once a new model is compatible with the experiment infrastructure.

The testing experiment architecture contained in the repository has access to the latest version of the models' codes. The modelers have access to the experiment rules and authoritative data, along with guidelines to make their codes fully compatible with the experiment. The modelers prescribe the software/libraries required to create their forecasts. Accordingly, a virtual environment (Docker containers) is automatically created to set up their model's computational architecture, which will be continuously integrated to ensure code integrity as the model undergoes any technical modification prior to the start of the prospective experiment. Docker containers freeze the code library dependencies and requirements, so that models' outputs can be reproduced even if a model-incompatible version of external software/libraries is released later on.

#### A brief description of the OEF models

During the RISE project, modelers have explored a wide range of possible OEF forecasting improvements. Only some of these improvements have been committed in the repository because preliminary tests showed that some models do not perform better than already existing models. For example, one important achievement of the project is also that some more complex models, such as the ETAS (Epidemic-type aftershock sequence) model with spatially varying b-value does not bring any improvements in earthquake forecasting skill.

The models in the repository can be grouped into different classes summarized as follows:

- tweaking existing best-performing models, resulting in different flavors of the ETAS model: *ETES*, *fIETAS*;
- refining ETAS to include temporal memory: *TimeMemory-ETAS*;
- simplifying ETAS to capture the essence of earthquake clustering but remain flexible enough to be applied in regions where earthquake catalogs have limited quality (e.g., poor quality, short instrumental observation, or inhomogeneous coverage like Europe): *SimplETAS*. It may also represent a suitable (homogeneous) reference model for any CSEP experiment;
- utilizing INLABRU, a spatiotemporal Bayesian model that is non-parametric and data-driven: *INLABRU time-independent*, *INLABRU time-independent*;
- considering temporal variability of the completeness magnitude (especially after a large earthquake, when a forecast is especially useful, the magnitude of completeness markedly increases): *PETAI*;

- considering continuum mechanics, i.e., the physics of rate-and-state friction, Coulomb failure function, and the slip distribution on the source fault to describe nearby stress heterogeneities: *CRS*;
- ensembling all contributing forecast models by choosing model weights, using logistic regression, that maximize the forecasting skill of the ensemble model itself: *weighted-average ensemble, logistic model ensemble*.

A more detailed summary of the models' main features can be found in Deliverable 3.3, or for the ensemble models in Task/Deliverable 7.3. Full descriptions can be found in the repository and the corresponding publications.

### **Task 3.4 Knowledge transfer from and to other scales**

Experiments conducted at the cm to decametre/hectometre scale provide a fundamental understanding of physical processes leading to fracture creation and reactivation. The current development of monitoring techniques, including very sensitive earthquakes sensors as well as deformation monitoring will allow to significantly lower the completeness magnitude and hence bring the OEF models to a new level. In this task, we present two datasets at different scale and pave the way to the development of new OEF models that account for a more advanced physical understanding of the earthquakes processes.

### **Task 3.5. Eliciting expert views on earthquake forecasting: Model development, testing, and forecast communication**

Deliverable 3.5 offers a comprehensive overview of the current status of Operational Earthquake Forecasting (OEF) systems in Italy, New Zealand, and the United States, along with progress updates on OEF system development for Switzerland and Europe. The discussion of each OEF system is divided into three parts: forecast communication, model development, and model testing and vision. This status summary of the existing OEF systems highlights the heterogeneity of the systems in all three parts. From this starting point, our objective for the second part of Deliverable 3.5 was to establish a consensus among a panel of international experts on best practices pertaining to these subjects, for which we employed the Delphi methodology.

A Delphi study is an iterative process that involves a curated group of experts who participate in successive survey rounds, followed by group discussions of survey results. This continues until a consensus is achieved. The survey typically consists of statements that experts can either agree or disagree with on a seven-point scale. A consensus is considered reached when at least 70% of participants either agree to a statement (agreement level 6 or 7), disagree to a statement (agreement level 1 or 2), or are undecided about a statement (agreement levels 3, 4, or 5). In the latter case, the consensus is that a decision on the statement cannot be made at the current state of research.

In our study, an initial group of 20 experts completed the first survey, which was divided into three sections: "Model Development," "Model Testing," and "Forecast Communication." Following the survey, we held an online workshop on April 5th, 2023, where the results were discussed among 18 participants. The workshop primarily focused on statements that did not achieve a consensus in the initial survey, allowing experts to exchange ideas, deliberate on differing

perspectives, and identify common ground. Subsequently, a revised version of the survey was distributed to the expert group with adjusted and new statements.

Below we describe the consensus that was reached after the first survey, and we describe the points raised in the workshop discussing the results of this first survey. The second survey round, for which more consensus is expected because it was adapted based on the inputs from the panel of experts, will be concluded by the end of April 2023. The results thereof will be reflected in deliverable 3.5, but cannot be discussed in this document as of now.

### **Model Development**

After the first survey, *Model Development* was the part in which the least consensus could be reached among the panel of earthquake forecasting experts. The statements with early consensus are the following:

- It is unclear if the Reasenberg & Jones model (Reasenberg and Jones, 1989) is suited for earthquake forecasting.
- It is unclear if the EEPAS model (Rhoades and Evison, 2004) is suited for earthquake forecasting.
- [almost] The ETAS model (Ogata, 1988) is suited for earthquake forecasting.
- Ensembles of the above are suited for earthquake forecasting.
- [almost] Earthquake forecasting models should account for catalog incompleteness.

The statements annotated with “[almost]” did not reach consensus according to the 70% definition given above, but there was a tendency towards reaching consensus.

The statements that were presented to the experts in the first survey were designed to identify specific models and model features that experts agree on being suited/necessary for earthquake forecasting. The workshop discussion revealed however that no such explicit recommendations could be given because the development of earthquake forecasting models depends on a variety of factors. Above all, the end-users’ needs and preferences determine how models should be developed, tested, and how forecasts are communicated. This issue therefore will reoccur in the following two sections.

### **Model Testing**

As in the *Model Development* part, the first survey and workshop discussion revealed that specific recommendations on which tests to use to test a forecasting model can not be given. Again, the end-users’ needs and preferences play an important role in the decision of whether a model is ‘ready to be used’ or not. There was however a large consensus that forecasting models *should* be tested, that models and archived forecasts should transparently be made available to the community, and the experts agreed on ideal modes of testing. There is consensus on the following statements:

- Source code of forecasting models should be publicly available.
- Operationally issued forecasts should be archived for retrospective analysis.
- Archived forecasts should be publicly available for retrospective analysis by the community.

- A model that is already used for earthquake forecasting should continue to be tested.
- it is necessary to test the model pseudo-prospectively (i.e., excluding testing data when training the model).
- [almost] it is necessary to test the model truly prospectively (i.e., the testing data may not exist yet when the model is developed).
- A forecasting model is ready to be used if it has been tested by a third party (e.g., in a CSEP experiment).
- [almost] A forecasting model is *not* ready to be used because the model developers trust the model.

The expert discussion further revealed that the most universally accepted mechanism for deciding whether a model is ready to be used operationally may be for it to be described and published in a peer-reviewed journal. The second survey aims at reaching consensus on recommended tests that would be useful to an expert when peer-reviewing such a paper, and more consensus is expected to be reached on this topic.

### **Forecast communication**

As with the previous two topics, the ideal way to communicate earthquake forecasts depends on the end-users' needs. Who these end-users could be, and which pieces of information they might be interested in was discussed in this last section of the survey. The experts reached consensus on the following statements:

- Earthquake forecasts are relevant for [sorted by % of experts agreeing]
  - o Civil protection
  - o Critical infrastructure providers
  - o Emergency managers and responders
  - o Search and rescue organizations
  - o National and cantonal authorities
  - o Communication experts
  - o Seismologists
  - o Policymakers
  - o Structural engineers
  - o Insurances
  - o General public
  - o [almost] geotechnical engineers
  - o [almost] construction managers
  - o [almost] business owners
- Earthquake forecasts should contain the following information [sorted by % of experts agreeing]:
  - o Earthquake probabilities
  - o Earthquake hazard/expected ground motion
  - o Spatial distribution of earthquake probabilities/rates
  - o Temporal evolution of earthquake probabilities/rates
  - o Earthquake risk
  - o Uncertainties in probabilities/rates

- Earthquake probabilities should be translated into recommended actions target audiences can/should take.
- Earthquake forecasts should be provided together with an explanation on how to interpret the numbers.
- [almost] Earthquake forecasts should be part of rapid impact assessment reports after an event (e.g., integrate it on rapid impact assessment leaflets such as PAGER).
- Scenarios should be used to communicate earthquake forecasts (e.g., most likely and least likely scenario).
- The way earthquake forecasts are communicated to the society should be
  - o tested and co-designed with the end-users (e.g., civil protection, infrastructure owners, public), using surveys, workshops or other activities.
  - o regularly evaluated to check if the end-users' needs are still fulfilled.
  - o discussed informally with the end-users.
- [almost] It is unclear if the way earthquake forecasts are communicated to the society should be defined by the model developers.
- The following challenges are relevant when communicating earthquake forecasts:
  - o The government/politicians does/do not want that earthquake forecasts are publicly available.
  - o [almost] Civil protection does not want that earthquake forecasts are publicly available.
  - o [almost] The legal basis to publish earthquake forecasts publicly does not exist.
- It is unclear if the following challenge is relevant when communicating earthquake forecasts:
  - o It is difficult to combine earthquake forecasts with other available communication products (e.g., earthquake notifications, rapid impact assessments).

## References

Reasenber, P. A., & Jones, L. M. (1989). Earthquake hazard after a mainshock in California. *Science*, 243(4895), 1173-1176.

Rhoades, D. A., & Evison, F. F. (2004). Long-range earthquake forecasting with every earthquake a precursor according to scale. *Pure and applied geophysics*, 161, 47-72.

Ogata, Y. (1988). Statistical models for earthquake occurrences and residual analysis for point processes. *Journal of the American Statistical association*, 83(401), 9-27.

## List of submitted deliverables and achieved milestones in WP3

D3.1 New perspective in OEF models through the analysis of candidate precursory signals

D3.2 Exploring the limits of earthquake predictability

D3.3 A new generation of OEF models

D3.4 Scalability of new OEF techniques from the field to the laboratory and Bedretto URL

D3.5 Guideless for experts' judgments in OEF

MS23 Scheme of OEF model to include anomalies

MS24 Defining testing experiments

MS25 Prototype of OEF model "experts'-based"

MS26 OEF codes for testing in WP6 & 7

### Summary of Exploitable Results in WP3

#### 1) Peer reviewed publications

- Bayliss, K., Naylor, M., Illian, J., & Main, I. G. (2020). Data-driven optimization of seismicity models using diverse data sets: Generation, evaluation, and ranking using inlabru. *Journal of Geophysical Research: Solid Earth*, 125(11). <https://doi.org/10.1029/2020JB020226>
- Bayliss, K., Naylor, M., Kamranzad, F., & Main, I. (2022). Pseudo-prospective testing of 5-year earthquake forecasts for California using inlabru. *Natural Hazards and Earth System Sciences*, 22(10), 3231–3246. <https://doi.org/10.5194/nhess-22-3231-2022>
- Biondini, E., Rhoades, D. A. and Gasperini, P. (2023). Application of the EEPAS earthquake forecasting model to Italy, *Geophys. J. Int.* (accepted manuscript), <https://doi.org/10.1093/gji/ggad123>
- Churchill, R. M., Werner, M. J., Biggs, J., & Fagereng, Å. (2022a). Afterslip Moment Scaling and Variability from a Global Compilation of Estimates, *Journal of Geophysical Research: Solid Earth*, e2021JB023897. <https://doi.org/10.1029/2021JB023897>
- Churchill, R. M., Werner, M. J., Biggs, J., & Fagereng, Å. (2022b). Relative afterslip moment does not correlate with aftershock productivity: Implications for the relationship between afterslip and aftershocks. *Geophysical Research Letters*, 49(24). <https://doi.org/10.1029/2022GL101165>
- Falcone, G., Spassiani, I., Ashkenazy, Y., Shapira, A., Hofstetter, R., Havlin, S., & Marzocchi, W. (2021). An operational earthquake forecasting experiment for Israel: Preliminary results. *Frontiers in Earth Science*, 9, 729282. <https://doi.org/10.3389/feart.2021.729282>
- Gasperini, P., Biondini, E., Lolli, B., Petruccelli, A., & Vannucci, G. (2021). Retrospective short-term forecasting experiment in Italy based on the occurrence of strong (Fore)shocks. *Geophysical Journal International*, 225(2), 1192–1206. <https://doi.org/10.1093/gji/gqaa592>
- Grimm, C., Hainzl, S., Käser, M., & Küchenhoff, H. (2022). Solving three major biases of the ETAS model to improve forecasts of the 2019 Ridgecrest sequence. *Stochastic Environmental Research and Risk Assessment*, 36(8), 2133–2152. <https://doi.org/10.1007/s00477-022-02221-2>
- Gulia, L., & Gasperini, P. (2021). Contamination of frequency–magnitude slope (b-value) by quarry blasts: An example for Italy. *Seismological Research Letters*, 92(6), 3538–3551. <https://doi.org/10.1785/0220210080>
- Gulia, L., Gasperini, P., & Wiemer, S. (2022). Comment on “High-definition mapping of the gutenbergrichter b-value and its relevance: A case study in Italy” by m. Taroni, j. Zhuang, and w. Marzocchi. *Seismological Research Letters*, 93(2A), 1089–1094. <https://doi.org/10.1785/0220210159>
- Gulia, L., Wiemer, S., & Vannucci, G. (2020). Pseudoprospective evaluation of the foreshock traffic-light system in Ridgecrest and implications for aftershock hazard assessment. *Seismological Research Letters*, 91(5), 2828–2842. <https://doi.org/10.1785/0220190307>

- Herrmann, M., & Marzocchi, W. (2021). Inconsistencies and lurking pitfalls in the magnitude–frequency distribution of high-resolution earthquake catalogs. *Seismological Research Letters*, 92(2A), 909–922. <https://doi.org/10.1785/0220200337>
- Herrmann, M., Piegari, E., & Marzocchi, W. (2022). Revealing the spatiotemporal complexity of the magnitude distribution and b-value during an earthquake sequence. *Nature Communications*, 13(1), 5087. <https://doi.org/10.1038/s41467-022-32755-6>
- Mancini, S., Segou, M., Werner, M. J., & Parsons, T. (2020). The predictive skills of elastic Coulomb rate-and-state aftershock forecasts during the 2019 Ridgecrest, California, earthquake sequence. *Bulletin of the Seismological Society of America*, 110(4), 1736–1751. <https://doi.org/10.1785/0120200028>
- Mancini, S., Segou, M., Werner, M. J., Parsons, T., Beroza, G., & Chiaraluce, L. (2022). On the use of high-resolution and deep-learning seismic catalogs for short-term earthquake forecasts: Potential benefits and current limitations. *Journal of Geophysical Research: Solid Earth*, 127(11), e2022JB025202. <https://doi.org/10.1029/2022JB025202>
- Mancini, S., Werner, M. J., Segou, M., & Baptie, B. (2021). Probabilistic forecasting of hydraulic fracturing-induced seismicity using an injection-rate driven ETAS model. *Seismological Research Letters*, 92(6), 3471–3481. <https://doi.org/10.1785/0220200454>
- Manganiello, E., Herrmann, M., & Marzocchi, W. (2023). New physical implications from revisiting foreshock activity in southern California. *Geophysical Research Letters*, 50(1). <https://doi.org/10.1029/2022GL098737>
- Mizrahi, L., Nandan, S., Savran, W., Wiemer, S., & Ben-Zion, Y. (2023). Question-driven ensembles of flexible ETAS models. *Seismological Research Letters*, 94(2A), 829–843. <https://doi.org/10.1785/0220220230>
- Mizrahi, L., Nandan, S., & Wiemer, S. (2021a). The effect of declustering on the size distribution of mainshocks. *Seismological Research Letters*, 92(4), 2333–2342. <https://doi.org/10.1785/0220200231>
- Mizrahi, L., Nandan, S., & Wiemer, S. (2021b). Embracing data incompleteness for better earthquake forecasting. *Journal of Geophysical Research: Solid Earth*, 126(12). <https://doi.org/10.1029/2021JB022379>
- Piegari, E., Herrmann, M., & Marzocchi, W. (2022). 3-D spatial cluster analysis of seismic sequences through density-based algorithms. *Geophysical Journal International*, 230(3), 2073–2088. <https://doi.org/10.1093/gji/ggac160>
- Rinaldi, A. P., Improta, L., Hainzl, S., Catalli, F., Urpi, L., & Wiemer, S. (2020). Combined approach of poroelastic and earthquake nucleation applied to the reservoir-induced seismic activity in the Val d’Agri area, Italy. *Journal of Rock Mechanics and Geotechnical Engineering*, 12(4), 802–810. <https://doi.org/10.1016/j.jrmqge.2020.04.003>
- Serafini, F., Lindgren, F., & Naylor, M. (2023). Approximation of Bayesian Hawkes process with inlabru. *Environmetrics*. <https://doi.org/10.1002/env.2798>
- Spassiani, I., & Marzocchi, W. (2021). An energy-dependent earthquake moment–frequency distribution. *Bulletin of the Seismological Society of America*, 111(2), 762–774. <https://doi.org/10.1785/012020190>

- Taroni, M., Zhuang, J., & Marzocchi, W. (2021). High-definition mapping of the Gutenberg–Richter b-value and its relevance: A case study in Italy. *Seismological Research Letters*, 92(6), 3778–3784. <https://doi.org/10.1785/0220210017>
- Zhang, L., Werner, M. J., & Goda, K. (2020). Variability of etas parameters in global subduction zones and applications to mainshock–aftershock hazard assessment. *Bulletin of the Seismological Society of America*, 110(1), 191–212. <https://doi.org/10.1785/0120190121>
- Zhang, Y., Ashkenazy, Y., & Havlin, S. (2021). Asymmetry in earthquake interevent time intervals. *Journal of Geophysical Research: Solid Earth*, 126(9). <https://doi.org/10.1029/2021JB022454>
- Zhang, Y., Fan, J., Marzocchi, W., Shapira, A., Hofstetter, R., Havlin, S., & Ashkenazy, Y. (2020). Scaling laws in earthquake memory for interevent times and distances. *Physical Review Research*, 2(1), 013264. <https://doi.org/10.1103/PhysRevResearch.2.013264>
- Zhang, Y., Zhou, D., Fan, J., Marzocchi, W., Ashkenazy, Y., & Havlin, S. (2021). Improved earthquake aftershocks forecasting model based on long-term memory. *New Journal of Physics*, 23(4), 042001. <https://doi.org/10.1088/1367-2630/abeb46>

## 2) Other exploitable results/data/reports

- Bayliss, K. (2022). California inlabru forecasts. [Earthquake forecasts and R source code for generating forecasts with inlabru and testing resulting forecasts]. url: <https://github.com/kirstybayliss/california-inlabru-forecasts>; doi: [10.5281/zenodo.6534724](https://doi.org/10.5281/zenodo.6534724)
- Herrmann M., W. Marzocchi (2021). Mc-Lilliefors: a completeness magnitude that complies with the exponential-like Gutenberg–Richter relation. [Python source code]. url: <https://gitlab.com/marcus.herrmann/mc-lilliefors>; doi: [10.5281/zenodo.4162496](https://doi.org/10.5281/zenodo.4162496)
- Manganiello, E., Herrmann, M., & Marzocchi, W. (2023). Foreshock analyses. [Matlab source code]. url: <https://gitlab.com/ester.manganiello/foreshock-analyses>; doi: [10.5281/zenodo.7438161](https://doi.org/10.5281/zenodo.7438161)

## 1.2.4 Work package 4

### Overview

WP4 deals with loss and resilience assessment for earthquake early warning (EEW) and operational earthquake loss forecasting (OELF). The main objectives of the work package are summarised in the following:

- develop a 2nd generation real-time seismic structural assessment and rapid loss assessment tools for Europe;
- operationalize earthquake loss forecasting for Europe and, eventually including time-variant hazard and fragility, accounting for accumulating damage;
- develop near real-time recovery forecasting, rebuilding management and resilience assessment for infrastructures;
- advance technologies for data-driven structural health monitoring and damage detection in structural systems in the context of EEW and OELF during seismic sequences;
- improve structure-specific early warning algorithms for real buildings;
- develop a user-ready risk-cost-benefit analysis framework for quantifying socio-economic costs.

Each of these issues is specifically addressed by a task, which has been working from the beginning of the project. In the following, the main achievements of each task (i.e., from task 4.1 to 4.6) are summarised.

### Summary of achievements in WP4 tasks: (2-3 pages for each task)

#### Task 4.1 Exposure, Vulnerability and ShakeMaps for OELF and RLA

##### 4.1.1 Introduction

This task provides data, models and scripts/software related to European exposure, vulnerability and ShakeMaps to other tasks and applications within RISE.

##### 4.1.2 Exposure Models

Both time invariant and time variant exposure models are being developed and tested in the RISE project, as documented in Deliverables D4.1 and D4.2. For time invariant exposure models, the following activities have been undertaken:

- The database of building exposure models for 44 European countries initiated in the SERA project has continued to be developed and reviewed and has now been publicly released on both GitLab and Zenodo (Crowley et al., 2021a; 10.5281/zenodo.4062044). These exposure models cover the number and economic value of residential, commercial and industrial buildings, as well as their occupants. These models have been used in the development of the European Seismic Risk Model (ESRM20; Crowley et al., 2021b)
- Open source tools for disaggregating the aforementioned national exposure models to a higher level of resolution (necessary for scenario assessment) have been developed in collaboration with the Global Earthquake Model: <https://github.com/GEMScienceTools/spatial-disaggregation>.
- The exposure models for 44 countries have been disaggregated to a 30-arc second resolution using WorldPop data (<https://www.worldpop.org/>) and these have been openly

released on the aforementioned repository. Figure 4.1.1 shows the change in resolution from the original exposure models to the disaggregated exposure models. The final exposure models have been formatted in the OpenQuake-engine NRML format for Rapid Loss Assessment and they can be accessed here: [https://gitlab.seismo.ethz.ch/efehr/esrm20/-/tree/main/Exposure\\_30arcsec](https://gitlab.seismo.ethz.ch/efehr/esrm20/-/tree/main/Exposure_30arcsec)

- A paper on the impact of exposure model resolution on European seismic risk modelling has been published in the Bulletin of Earthquake Engineering (Dabbeek et al., 2021).
- Improvements to the spatial and temporal distribution of population using open data from the ENACT project (<https://ghsl.jrc.ec.europa.eu/enact.php>) have been made. These improvements have allowed the variation of population during day/night and different seasons to be incorporated in the aforementioned exposure models.
- Task 2.7 is developing a Dynamic Exposure Model that is frequently updated using OpenStreetMap/OpenBuildingMap data. Collaboration with this task was undertaken to ensure that this individual building data would be combined with the statistical building data from the time invariant exposure models for 44 European countries (described above).

For time variant exposure models, we have worked with the demonstration activity of Task 6.1 to produce models of the dynamic variation of occupants following a damaging earthquake (or sequence of earthquakes), such that a more realistic representation of the occupants can be represented in Rapid Loss Assessment and Operational Earthquake Loss Forecasting estimates. Both the probability of damage of the building as well as the probable injury states of the occupants are taken into account when assessing the likely occupancy rates of the building over time.

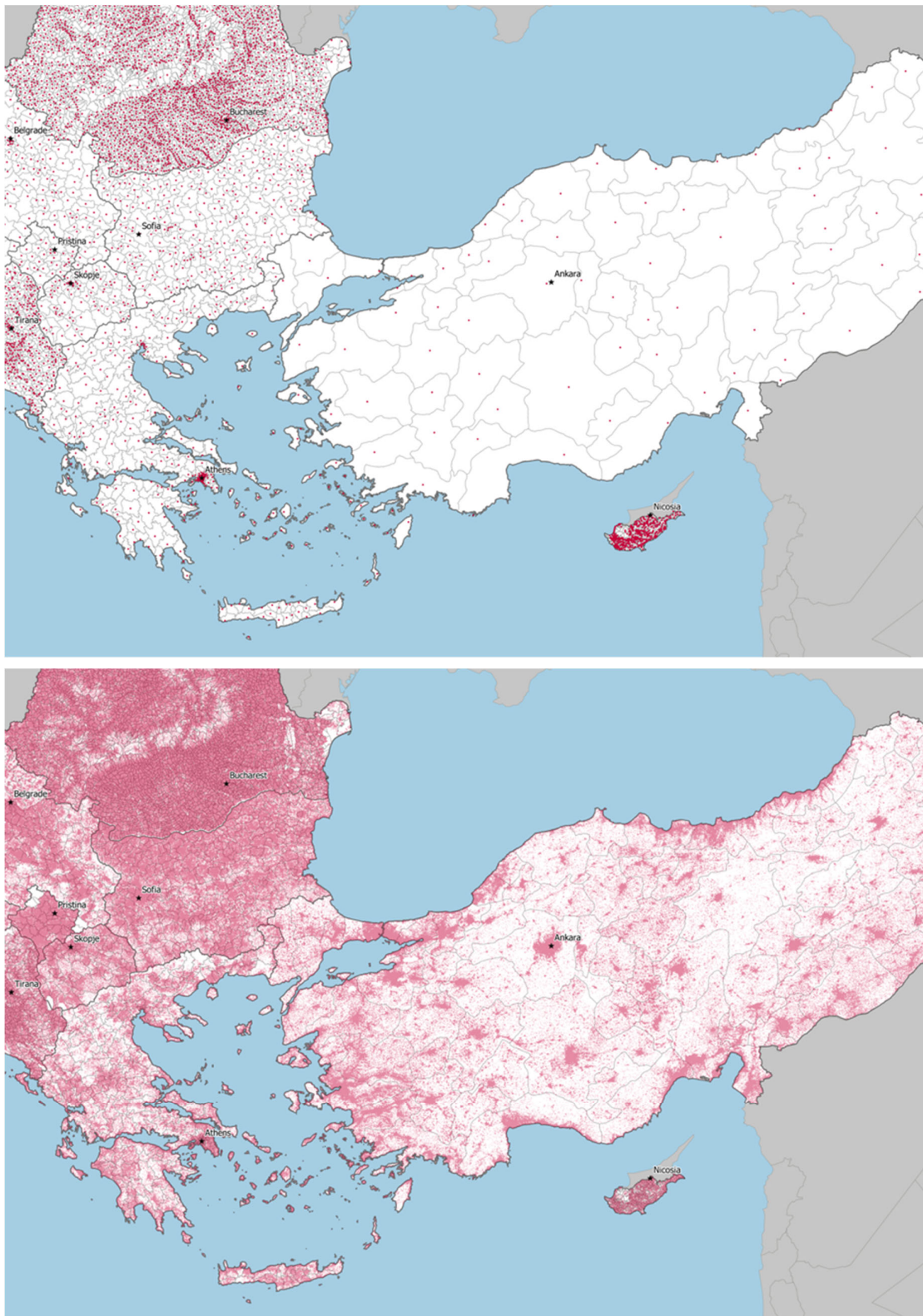


Figure 4.1.1 Original (top) versus 30 arc second (bottom) resolution of the residential building stock exposure models in south-eastern Europe

### 4.1.3 Vulnerability Models

As part of the European Seismic Risk Model (ESRM20: Crowley et al., 2021b), initiated in the SERA project and completed in the RISE project, vulnerability models for 511 building classes have been developed (as documented further in Deliverables D4.1 and D4.2). Capacity curves for a large range of building classes are needed to cover the varying construction types in Europe present in the exposure models described above. The GEM Building Taxonomy v3.1 (Silva et al., 2022: [https://github.com/gem/gem\\_taxonomy](https://github.com/gem/gem_taxonomy)) has been used to define the vulnerability classes of European buildings. The GEM Foundation has released a global database of capacity curves (Martins and Silva, 2020) as part of their Global Seismic Risk Map. These curves have been derived through the compilation of data coming from research studies and experimental campaigns. In ESRM20 these capacity curves have been used to represent the European CR\_LDUAL, CR\_LWAL, MCF, MR, MUR, S and W typologies with different heights and ductility levels, for a total of 248 vulnerability classes.

As part of the European SERA project ([www.sera-eu.org](http://www.sera-eu.org)), a detailed set of capacity curves for European reinforced concrete infilled frames (CR\_LFINF) and moment frames (CR\_LFM) were developed (Romão et al., 2019). A total of 264 reinforced concrete classes were identified by combining different numbers of storeys (1 to 6), seismic design code levels (no code: CDN, low code: CDL, moderate code: CDM, high code: CDH) and lateral force coefficient levels (0, 5, 10, 15, 20, 25, 30 % of the weight of the structure). The capacity curves for these 264 vulnerability classes were developed through simulated design of prototype frames and then nonlinear analysis has been undertaken to obtain the backbone capacity curves of these frames.

The fragility functions of the European vulnerability classes have been computed using the Vulnerability Modeller’s Toolkit (VMTK), a resource that has been developed and released by the GEM Foundation in collaboration with RISE partners (Martins et al., 2021). This toolkit is a set of Python scripts that read the capacity curves, produce SDOF hysteretic models (based on standard hysteretic models), launch OpenSeesPy (<https://openseespydoc.readthedocs.io/en/latest/>) to run nonlinear dynamic analysis, apply linear censored regression to the cloud of nonlinear responses, and compute fragility functions for different damage states, based on the user-defined damage state thresholds. The complete toolkit, including source code and GUI, is currently hosted in a publicly available GitHub repository <https://github.com/GEMScienceTools/VMTK-Vulnerability-Modellers-ToolKit>. All of the details of how GEM’s Vulnerability Modeller’s Toolkit (VMTK) has been applied in the development of fragility models in Europe are provided in Crowley et al. (2021b).

Damage-loss models have been applied to the fragility functions (which are provided for slight, moderate, extensive and complete damage) leading to two types of vulnerability models:

- economic loss due to direct costs to repair/replace buildings;
- loss of life of occupants due to damage/collapse of buildings.

These vulnerability models are publicly available at [https://gitlab.seismo.ethz.ch/efehr/esrm20\\_vulnerability](https://gitlab.seismo.ethz.ch/efehr/esrm20_vulnerability) (Romão et al., 2021, released on Zenodo with DOI 10.5281/zenodo.5639318), and have been formatted in the OpenQuake-engine NRML format for Rapid Loss Assessment and can be accessed here: <https://gitlab.seismo.ethz.ch/efehr/esrm20/-/tree/main/Vulnerability>. For RLA and OELF, other risk metrics can be important for stakeholders, such as displaced people and injured people. A first set of vulnerability functions for injured people, based on the 4 injury severity levels of HAZUS have been produced, based on assumptions developed as part of the activities in Task 6.1, and made publicly available at the aforementioned GitLab repository.

#### **4.1.4 European ShakeMap Development**

A European ShakeMap service prototype (<http://shakemapeu.ingv.it>) using the latest version of ShakeMap (v4, Worden et al., 2020) has been consolidated under the management and maintenance of both ETH Zurich and the National Institute for Geophysics and Volcanology in Italy (INGV). The service adopts the publicly available ShakeMap (v4) web portal development to display all the Shake-Maps and makes available the resulting metadata. A number of web services produced by EMSC (the European-Mediterranean Seismological Centre: <https://www.emsc-csem.org>) and ORFEUS (Observatories and Research Facilities for European Seismology: <https://www.orfeus-eu.org/>) are used by the European ShakeMap system to automatically register when an earthquake above magnitude 3.5 occurs within Europe, and to receive any recorded strong motion data.

The European ShakeMap system is fully consistent with the data and modelling protocols used in the national services for Italy, Greece and Switzerland (and also therefore could serve as a backup for these national installations), and there are plans to expand this harmonisation to other European countries in the GeoINQUIRE project (<https://www.geo-inquire.eu/>).



Figure 4.1.2 European ShakeMap Service: <http://shakemap.eu.ingv.it/>. The source code for this web portal is publicly available at: <https://github.com/INGV/shakemap4-web> The image shows the ShakeMap (macroseismic intensity) for the 6th February 2023 mainshock in eastern Turkey.

### References cited above

Crowley H., V. Despotaki, D. Rodrigues, V. Silva, C. Costa, D. Toma-Danila, E. Riga, A. Karatzetzou, S. Fotopoulou, L. Sousa, S. Ozcebe, P. Gamba, J. Dabbeek, X. Romão, N. Pereira, J.M. Castro, J. Daniell, E. Veliu, H. Bilgin, ... U. Hancilar. (2021a). European Exposure Model Data Repository (v1.0) [Data set]. Zenodo. <https://doi.org/10.5281/zenodo.5730071>

Crowley H., Dabbeek J., Despotaki V., Rodrigues D., Martins L., Silva V., Romão, X., Pereira N., Weatherill G. and Danciu L. (2021b) European Seismic Risk Model (ESRM20), EFEHR Technical Report 002, V1.0.1, 84 pp, <https://doi.org/10.7414/EUC-EFEHR-TR002-ESRM20>

Dabbeek J., Crowley H., Silva V., Weatherill G., Paul N., Nievas C. (2021) "Impact of exposure spatial resolution on seismic loss estimates in regional portfolios," Bulletin of Earthquake Engineering, <https://doi.org/10.1007/s10518-021-01194-x>

Martins L. and Silva V. (2020) "Development of a fragility and vulnerability model for global seismic risk analyses," Bulletin of Earthquake Engineering, <https://doi.org/10.1007/s10518-020-00885-1>

Martins L., Silva V., Crowley H. and Cavalieri F. (2021) "Vulnerability Modeller's Toolkit, an Open-Source Platform for Vulnerability Analysis," Bulletin of Earthquake Engineering, <https://doi.org/10.21203/rs.3.rs-458348/v1>

Romão X., Castro J.M., Pereira N., Crowley H., Silva V., Martins L. and Rodrigues D. (2019) European physical vulnerability models, SERA Deliverable D26.5, Available at: [http://static.seismo.ethz.ch/SERA/JRA/SERA\\_D26.5\\_Physical\\_Vulnerability.pdf](http://static.seismo.ethz.ch/SERA/JRA/SERA_D26.5_Physical_Vulnerability.pdf).

Romão X., N. Pereira, J.M. Castro, H. Crowley, V. Silva, L. Martins, & F. De Maio. (2021). European Building Vulnerability Data Repository (v2.1) [Data set]. Zenodo. <https://doi.org/10.5281/zenodo.5639318>

Silva V., Brzev S., Scawthorn C., Yepes-Estrada C., Dabbeek J. and Crowley H. (2022) "A Building Classification System for Multi-Hazard Risk Assessment," International Journal of Disaster Risk Science, 13, 161–177 DOI: <https://doi.org/10.1007/s13753-022-00400-x>

Worden C.B., Thompson E. M., Hearne M. and Wald D.J. (2020) ShakeMap Manual Online: Technical Manual, User's Guide, and Software Guide, <https://doi.org/10.5066/F7D21VPQ>. <http://usgs.github.io/shakemap/>.

#### **Task 4.2 Improve and operationalize earthquake loss forecasting (OELF)**

In Italy a system of operational earthquake loss forecasted, named MANTIS-K, was developed in 2015 (Iervolino et al., 2015). Because MANTIS-K was not able to account for the possible structural damage accumulation during seismic swarms, the aim of this task was to define a methodology to improve the Italian OELF systems and to provide all the models and data to implement such a methodology at national scale. Thus, the upgraded version of the OELF system, named MANTIS v2.0, developed during the RISE project, was formulated to account for the evolution, over time, of the structural damage conditions. This implies that loss forecasting must account for the possible structural damage accumulation due to the occurrence of more than one earthquake in the forecasting period. Moreover, the upgraded system has to estimate the possible damage due to the occurred earthquakes (RLA) and, consequently, forecast the performance level of buildings that, at the time of computation, are already at an intermediate performance level.

The detailed description of the analytical procedure at the base of MANTIS v2.0 is provided in Chioccarelli et al. (2022) and is not reported here for the sake of brevity. However, it should be recalled that a fundamental model for the operationalization of MANTIS v2.0 is represented by the state-dependent fragility functions for the Italian structural typologies identified in Task 4.1. Thus, a significant computational effort was addressed to the development of such state-dependent fragility functions for both reinforced-concrete and masonry Italian structural typologies.

The Italian reinforced-concrete existing residential buildings are represented by eighteen structural typologies, whereas the Italian masonry structures portfolio is represented by a set of fifteen wall masonry structures. For each of them, after defining the backbone of the equivalent SDoF and the hysteretic behaviour in accordance with the SERA project, a proper intensity measure was identified and the fragility functions (i.e., for the undamaged structure) and state-dependent fragility functions were evaluated using incremental dynamic analyses (IDA) and back-to-back IDA, respectively. For a selected set of records, IDA collects the response of a non-linear undamaged structure to the records that are progressively scaled in amplitude to represent increasing levels of seismic intensity. Back-to-back IDA is an extension of IDA, in which the

structural model, representing the structure at its intact state, is first subjected to a set of records, each of them scaled in amplitude to the lowest intensity measure value that causes the structure to reach the engineering demand parameter threshold for a first considered damage state,  $DS_i$ . Each record produces a different realisation of the now-damaged structural model, which can be considered to have made the transition to  $DS_i$ . Thus, each damaged incarnation of the structural model is subjected to a second set of accelerograms, that are representative of a second earthquake. Each record of the second set is applied to each damaged model and is progressively scaled in amplitude until the damaged structure reaches a more severe damage threshold, say  $DS_j$ , where  $j > i$ . The realisations of the seismic intensity leading the structure to equal a certain damage state threshold are adopted to describe the distribution of the random variable representing the structural capacity with respect to the considered damage state and, in turn, to derive the state-dependent fragility functions. The whole procedure is repeated for all the couples of damage state,  $DS_i$  and  $DS_j$  with  $j > i$  and for all the Italian structural typologies. All the results are reported in Orlacchio et al. (2021) and Chioccarelli et al. (2022).

### References cited above

Iervolino, I. *et al.* Operational (short-term) earthquake loss forecasting in Italy. *Bulletin of the Seismological Society of America* 105, 2286–2298 (2015).

Orlacchio, M., Chioccarelli, E., Baltzopoulos, G., & Iervolino, I. (2021). State-Dependent Seismic Fragility Functions for Italian Reinforced Concrete Structures: Preliminary Results. *31th European Safety and Reliability Conference*, 19-23 September 2021, Angers, France, 1591–1598. [https://doi.org/10.3850/978-981-18-2016-8\\_660-cd](https://doi.org/10.3850/978-981-18-2016-8_660-cd)

Chioccarelli, E., Pacifico, A., & Iervolino, I. (2023). Operational earthquake loss forecasting for Europe, RISE Project Deliverable 4.3.

## Task 4.3 Develop near real-time recovery forecasting for infrastructures

### 4.3.1 Introduction

This task provides a framework to infer the cost and time required to repair damaged buildings after an earthquake and to dynamically estimate recovery trajectories and thus, resilience, at a regional scale. The findings are reported in RISE Deliverable 4.4 (Reuland, et.al, 2022).

Considering the time dimension of earthquake losses, this task complements and extends the loss estimates of task 4.1 and complements the state-dependent fragility functions of task 4.2 by offering dynamic estimates of repair time using the available data. The process is illustrated in Figure 1.

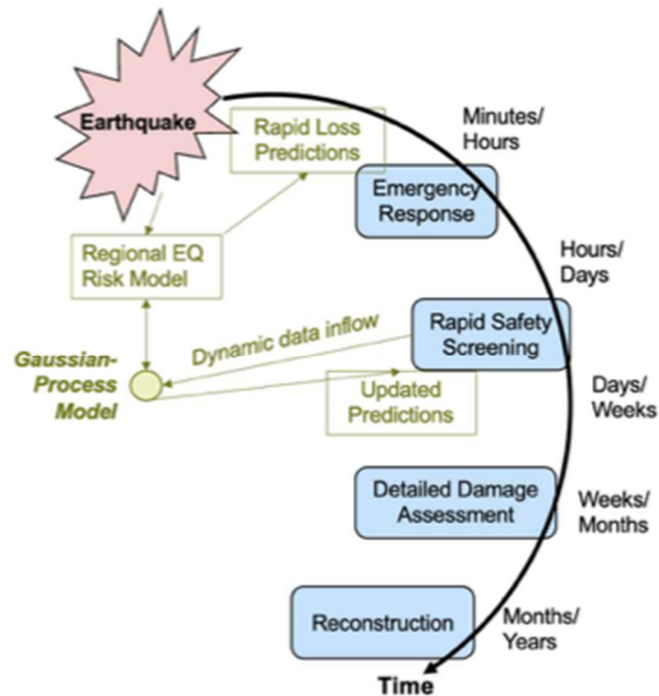


Figure 4.3.1 Use of Gaussian-Process models to infer updated damage predictions by fusing early inspection outcomes with underlying risk-model predictions to reduce the uncertainty of latent functions, such as the ground-motion field.

#### 4.3.2 Repair sequences for damaged buildings

Recovery of a building can be simulated as a sequence of events, occurring in serial or in parallel, such as inspection, permitting and repair, where for each a duration, demand and preceding activities must be defined. For instance, inspection service demand is needed to inspect a building, while workers are needed to start building's repair (Blagojevic et al., 2021a). However, repair works can only start if the demand for all impeding recovery factors, such as inspection, repair time, financing, and contracting, are met. Thus, while the repair time of a building depends on the building-specific excitation, vulnerability, and geometry (allowing for the derivation of consequence functions, such as shown in Figure 2 for a typical Swiss masonry building), the recovery time of a building depends on community-level preparedness and the availability of recovery resources, such as materials, machinery and workers.

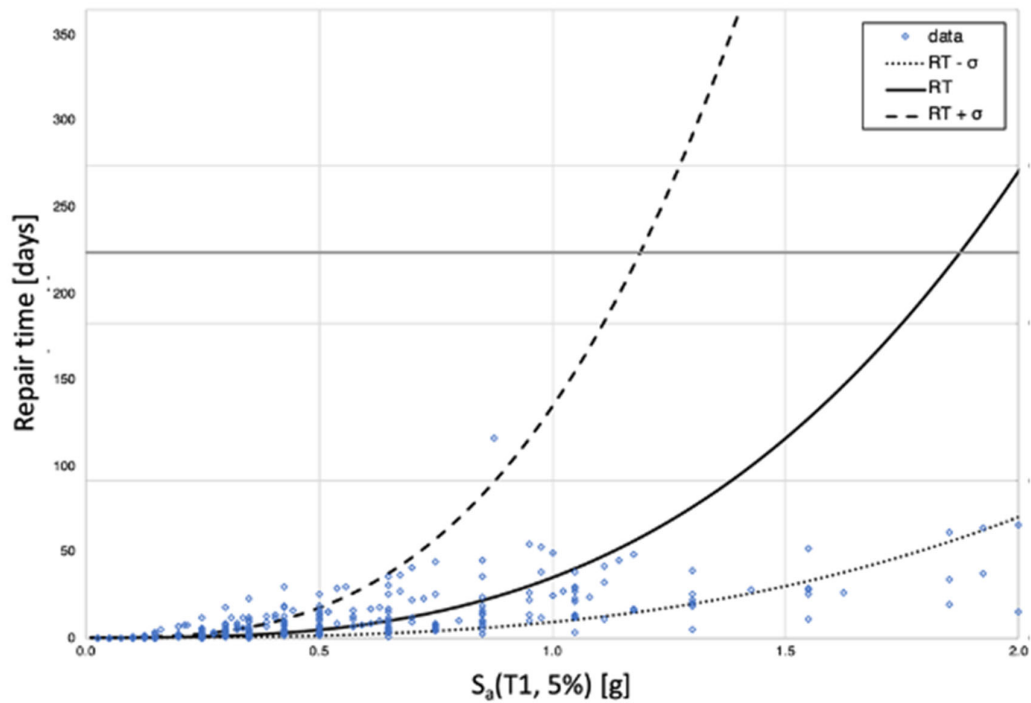


Figure 4.3.2 Consequence function providing estimates of repair time as a function of spectral acceleration for a typical 4-story Swiss unreinforced masonry building.

#### 4.3.2 Regional repair and recovery estimates

Repair and recovery predictions start where the traditional loss assessment stops. By evaluation the evolution of the level of functionality of buildings (or other infrastructure systems), recovery models add the dimension of time to loss assessment, enabling a dynamic prediction of direct losses incurred through building repairs as well as indirect losses incurred due to the loss of building functionality. While several models exist to predict recovery, we chose a bottom-up modelling iRe-CoDeS framework that is based dynamically evaluating the demand and supply of recovery services and resources (Blagojevic et al., 2021a; Didier et al., 2018). Each damaged building has a recovery demand, that can depend on its properties (e.g., number of floors, occupancy type, socio-economic characteristics) and state of damage.

During the recovery simulation, available R/Ss are distributed among damaged buildings and only the buildings whose recovery demand is met are recovered. Such an approach is also capable of capturing components' functional interdependency and quantifying disaster resilience (Blagojevic et al., 2021c).

Social communities have a persistent demand for services, such as housing. A lack of resilience (LoR) is therefore observed when this service demand cannot be fully supplied, for instance, because a damaged building cannot provide housing services. The total LoR is the sum of un-supplied service over time, until recovery is reached. Thus, the LoR is a resilience metric that informs and supports post-earthquake decision-making (Blagojevic et al., 2022).

### 4.3.3 Integration within the OpenQuake regional risk assessment tool

Within task 4.3, a plug-in code has been developed to extend the OQ damage scenario capabilities towards RRE predictions. The structure of the OQ-RRE is shown in Figure 3. The plug-in takes as input the outcome of a damage scenario calculation, exported as a csv-file, and the exposure file, such as available from the ESRM2020 (Crowley et al 2021). In addition, the information required to perform a compositional demand/supply resilience quantification following the iRe-CoDeS framework, such as the community housing or repair services supply levels, are required. The OQ-RRE plug-in has been applied to a fictitious earthquake event in Switzerland, highlighting the capabilities for simulating recovery scenarios, as illustrated in Figure 4.

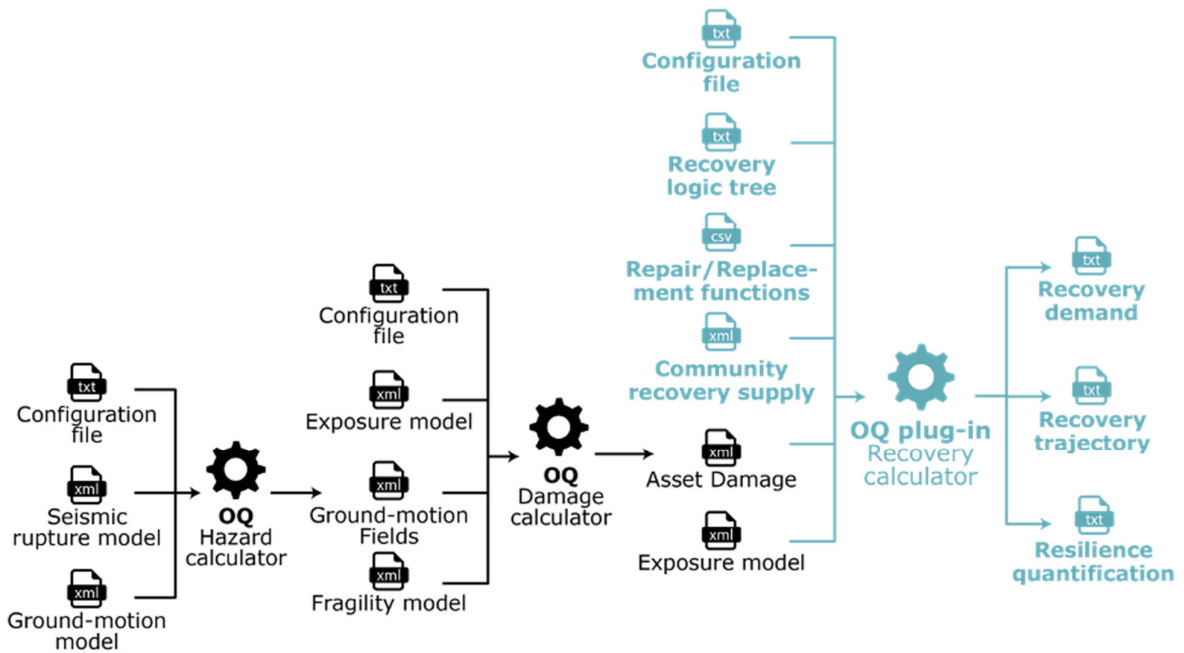


Figure 4.3.3 Inclusion of the recovery plug-in (coloured) into the OpenQuake calculation flow (black) for a scenario damage evaluation.

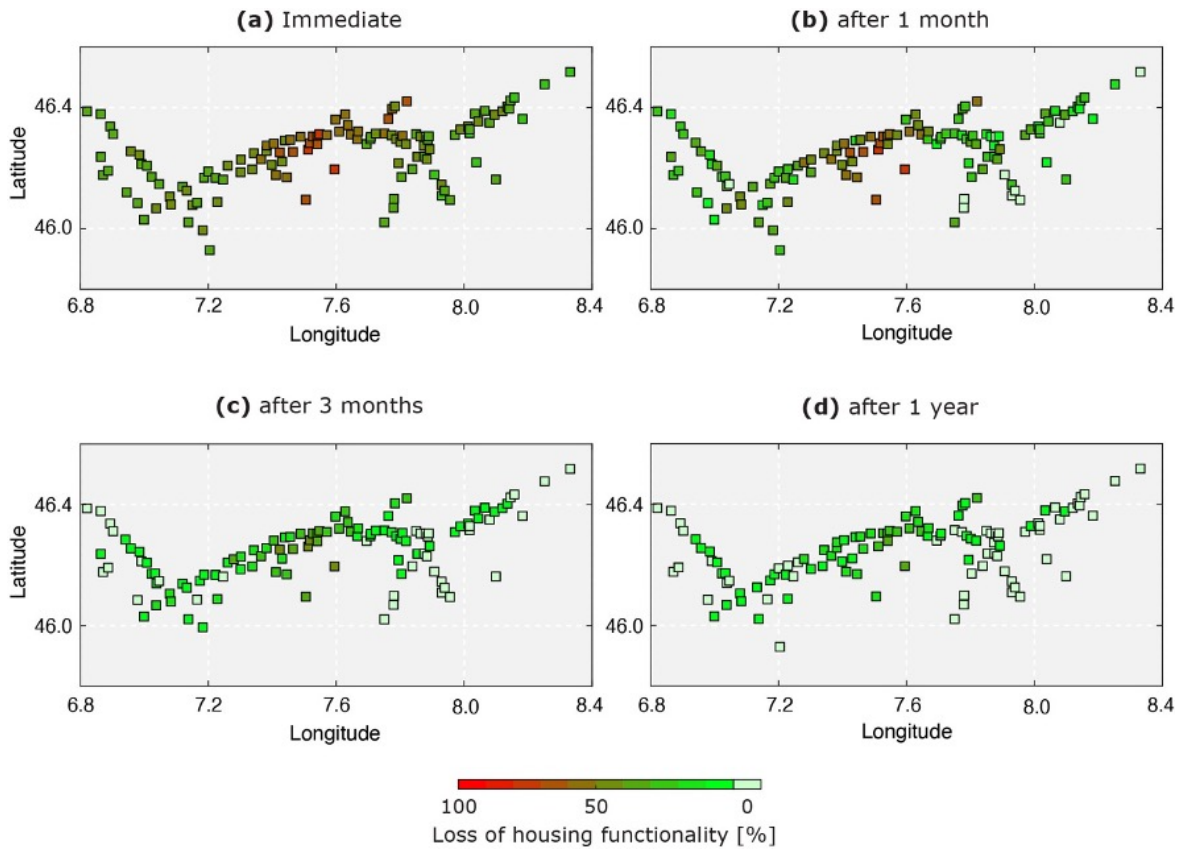


Figure 4.3.4 Recovery trajectory for unreinforced masonry buildings without seismic design (MUR-CDN) after a scenario M5.9 earthquake in the canton of Wallis (Switzerland). Several buildings are lumped into each square and the loss of housing functionality is proportional to the number of buildings being re-occupiable. Geographic location of the squares is presented using degrees of longitude and latitude.

#### 4.3.4 Validating recovery models

In an attempt to validate the iRe-CoDeS framework, the recovery after the 2010 Mw=5.4 Kraljevo earthquake has been simulated (Blagojevic et al., 2023). Early loss assessment is often incomplete and imprecise, which leads to large uncertainties in repair and recovery predictions, in addition to undermining efficiency and speed of public and private stakeholder responses. To reduce the uncertainties pertaining to early loss assessment, we proposed to dynamically update regional post-earthquake damage estimates. Gaussian Process inference models are used to fuse available early inspection data, or a limited subset of information about regional damage and loss, with a pre-existing earthquake risk model (Bodenmann et al., 2023), as shown in Figure 1.

Combining regional recovery and resilience assessment tools with a framework to reduce the uncertainties of regional loss assessment allows for a reduction of the uncertainty in recovery trajectories. Uncertainties stem from stochastic earthquake simulations, numerous assumptions related to the seismic performance of structures and the state of the community at the time of the event, as well as the assumptions related to the post-earthquake repair, institutional recovery strategy and the behavior of the people residing in the community. Thus, what-if analyses can be

conducted in real-time to inform decision-makers on the state of the community during its recovery and on the optimal deployment of community resources for the remaining of the recovery efforts to ensure a swift community recovery, minimizing the post-earthquake unmet demand of community inhabitants for resources they need in their everyday lives.

As shown in Figure 5c, the predicted recovery of all buildings that were in DS2 matches well with the observed data, while the validation set was too small to draw conclusions about intermediate recovery steps. In addition, comparing subplots (a) and (b) of Figure 5, the significant improvement in the precision of the recovery predictions highlights the need for updating frameworks to reduce the uncertainties stemming from regional risk models.

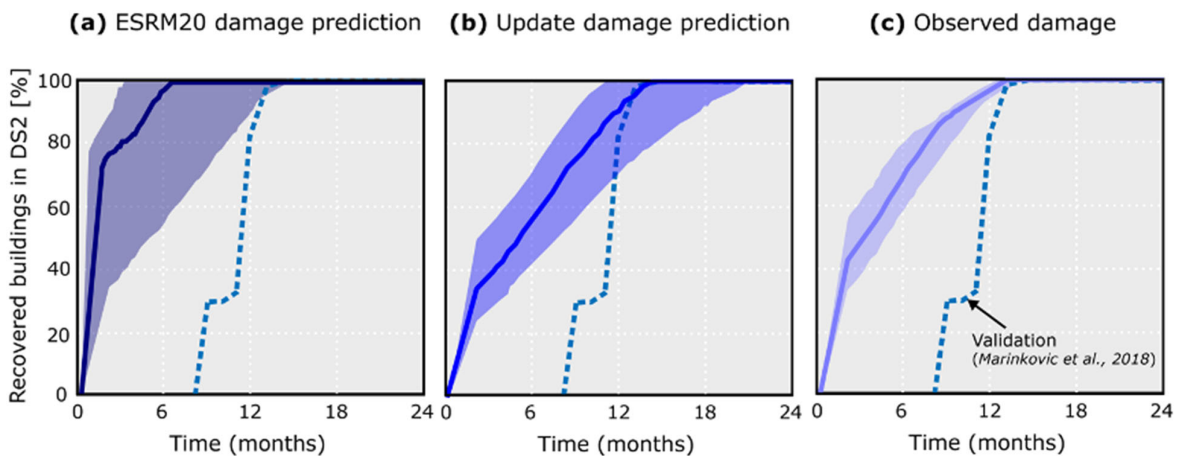


Figure 4.3.5 Damage recovery trajectories for slightly damaged buildings (DS2) after the 2010 Kraljevo earthquake and the reduction of uncertainty using damage data updating. Comparison of recovery predictions based on the ESRM20 damage assessment (a), the ESRM20 assessment after dynamic updating of shake map and fragility (b), and the observed damage states (c).

### References cited above

Blagojevic, N., Didier, M., & Stojadinovic, B. (2021a). Quantifying Component Importance for Disaster Resilience of Communities with Interdependent Civil Infrastructure Systems. *Reliability Engineering and System Safety*, vol. 228, no. 108747, December 2022, on-line: 05.09.2022, <https://doi.org/10.1016/j.ress.2022.108747>

Blagojevic, N., Didier, M., & Stojadinovic, B. (2021b, December 14). Simulating the role of transportation infrastructure for community disaster recovery. *Proceedings of the Institution of Civil Engineers - Bridge Engineering*.

Blagojević, N., Bodenmann, L., Reuland, Y., & Stojadinovic, B. (2022). Improving community disaster resilience by providing adequate supply of recovery resources and services. In *Proceedings of the Third European Conference on Earthquake Engineering and Seismology-3ECEES*, September 4-9, Bucharest, Romania.

Blagojevic, N., Bodenmann, L., Reuland, Y., & Stojadinovic, B. (2023). The case of 2010 Kraljevo

earthquake: Validating a regional recovery model and investigating measures to increase disaster preparedness. *ASCE Journal of Structural Engineering*, submitted.

Bodenmann, L., Reuland, Y., & Stojadinovic, B. (2023). Dynamic Post-Earthquake updating of Regional Damage Estimates using Gaussian Processes, *Reliability Engineering and System Safety*, 234,109201. <https://doi.org/10.1016/j.ress.2023.109201>

Didier, M., Broccardo, M., Esposito, S., & Stojadinovic, B. (2018). A compositional demand/supply framework to quantify the resilience of civil infrastructure systems (Re-CoDeS). *Sustainable and Resilient Infrastructure*, 3(2), 86–102. <http://dx.doi.org/10.1080/23789689.2017.1364560>

Reuland, Y., L. Bodenmann, N. Blagojevic and B. Stojadinovic, (2022) “Development of RRE forecasting services in OpenQuake”, RISE D4.4 report.

## **Task 4.4 Advance technologies for data-driven SHM and damage detection**

### **4.4.1 Introduction**

This task develops methods for automated extraction of damage indicators for building structures, on the basis of monitoring data that is recorded from permanently instrumented buildings during earthquake events. Combined with engineering model predictions, such indicators provide a quantitative and near-real-time assessment of single buildings and thus, contribute towards rapid loss assessment (RLA) and automated post-earthquake building tagging.

### **4.4.2 Damage-sensitive features**

Damage-sensitive features (DSFs) form metrics that can be extracted from monitoring data and that provide information on the presence, location, and severity of damage. Typically, acceleration-based features are used to extract information about the building behaviour, since accelerometers form easy to deploy and low-cost solutions, which ensure economically sustainable regional-scale measurements.

DSFs can indicate the occurrence and severity of damage sustained by the building. As part of this task we overview a series of DSFs (Reuland et al., 2023) and indicate the suitability (or not) of different metrics in terms of identification of both i) occurrence of transient nonlinearity in the global building response and ii) estimation of residual (permanent) damage sustained by the building. In the first case, it is found that changes in the transmissibility between two sensors, one at the ground and one at the top floor level, encoded by the transmissibility assurance criterion (TAC) are sufficient to detect the occurrence of transient nonlinearity. In the second case, it is shown that comparing modal properties, derived from ambient vibrations before and after damaging earthquakes, are useful indicators. Distinguishing between transient and residual damage effects allows for a quantification of the absolute and relative damage increment sustained by a building (see Figures 1 and 2); this is particularly helpful during seismic sequences.

In addition, DSFs can offer information on the likely location of damage (Reuland et al., 2023), as well as on those sub-structures that did not sustain structural damage - and which may thus be

flagged as healthy. This information paves the way towards data-based estimation of repair and recovery of instrumented buildings, using the methodologies proposed in RISE task 4.3.

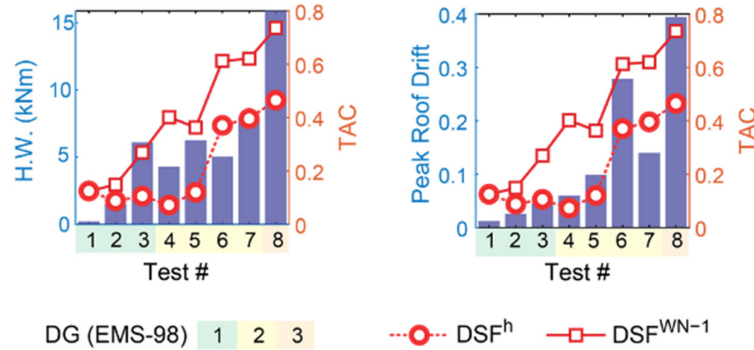


Figure 4.4.1 Correlation of a DSF (TAC) derived from a pair of acceleration sensors with the hysteretic work (H.W.) and peak roof drift ratio measured on a large-scale shake table test by Beyer et al. (2015). Results reported in Reuland et al. (2023a).

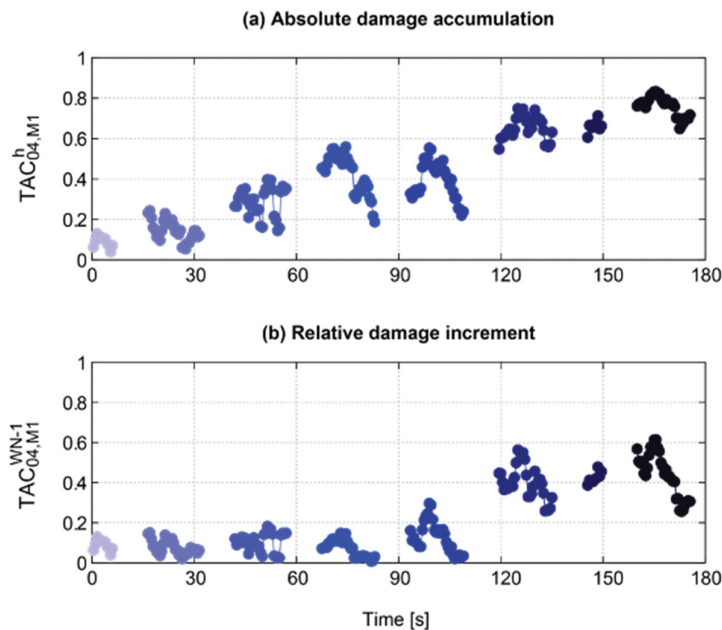


Figure 4.4.2 Validation of the capacity of a DSF (TAC) to track the evolution of absolute damage (a) and relative damage increment (b) of a large-scale structure tested on a shake-table by Beyer et al. (2015). Results reported in Reuland et al. (2023a).

#### 4.4.3 SHM-based fragility functions

Starting from three DSFs that have been found to be efficient indicators of earthquake-induced damage, SHM-based fragility functions can be formulated in a similar manner to traditional fragility models. Based on non-linear time-history analysis, a link between an engineering demand parameter and a DSF can be established (see Figure 3). Based on this relationship, (cumulative) probabilities of exceeding damage-states can be expressed as log-normal distributions with respect to DSFs instead of intensity measures (see Figure 4). Such a tool, expressed in the commonly adopted form of fragility functions, offers an actionable metric that can effectuate SHM-based rapid post-earthquake assessment and smart building tagging. In collaboration with task

6.1, the implementation of SHM-based fragility functions has been tested at regional scale.

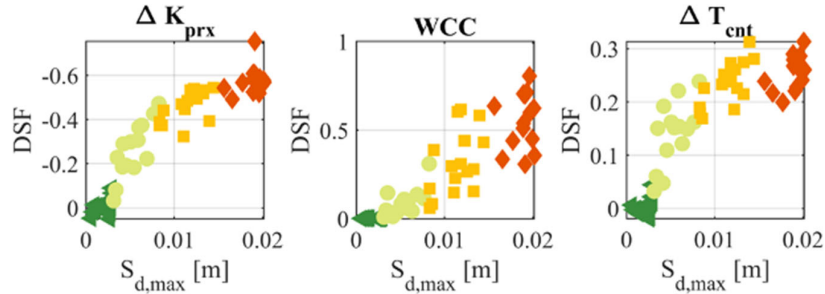


Figure 4.4.3 Model-based relationship between an engineering demand parameter (maximum transient roof displacement) with three damage-sensitive features (change of stiffness proxy, left; wavelet-based correlation coefficient, middle; and change in transmissibility centroid, right). Results reported in Reuland et al. (2023b).

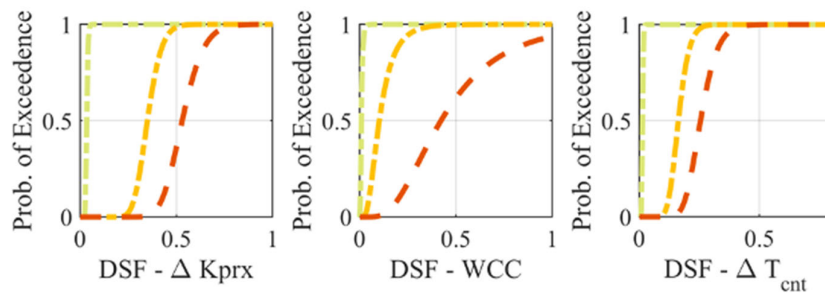


Figure 4.4.4 SHM-based fragility models based on model simulations. Results reported in Reuland et al. (2023b).

#### 4.4.4 Robust fusion of damage-sensitive features

When combining a large ensemble of DSFs in a robust manner, the predictive performance of damage states can be further improved. As part of this work, we propose training a classifier on an extensive dataset of nonlinear simulations of frame structures with varying geometrical and material configurations, and deploying convolutional neural networks to fuse the information from multiple DSFs, thus improving predictive accuracy against use of individual DSFs or further competing schemes (Martakis et al., 2023).

Furthermore, a Domain Adversarial Neural Network (DANN) architecture enables the transfer of knowledge obtained from numerical simulations, affected by inevitable model uncertainties and bias, to data from actual buildings. This capacity is tested and validated on a large-scale shaketable experiment. After exposure to a limited amount of data, pertaining exclusively to ambient vibrations measured in the healthy pre-earthquake building state, the DANN framework succeeds in predicting unseen damage states from monitoring data. The results demonstrate the potential of DANN in transferring knowledge from simulations to real-world monitoring applications, where only limited data on typically healthy structural state is available (Martakis et al., 2023).

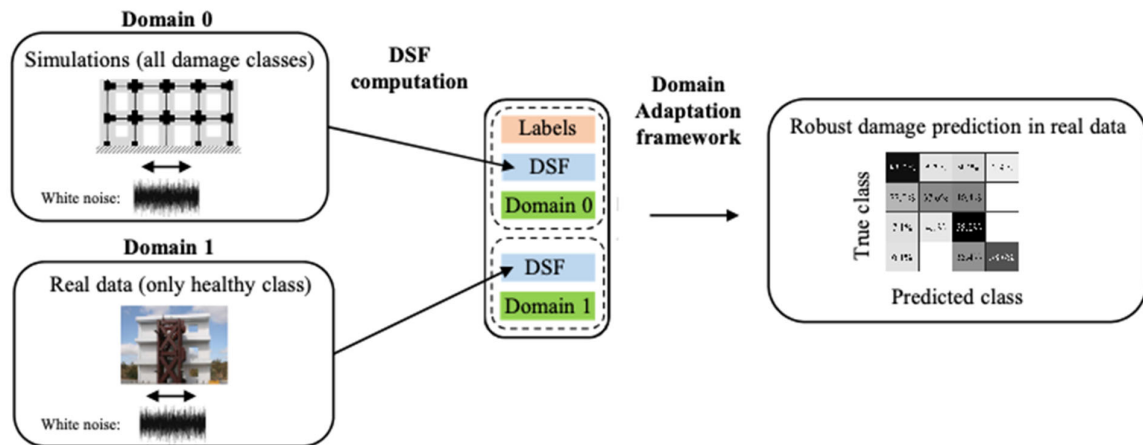


Figure 4.4.5 DANN framework for transferring model-based damage classifiers from model-based training data to real-world structures. Results reported in Martakis et al. (2022).

### References cited above

Beyer, K., Tondelli, M., Petry, S., & Peloso, S. (2015). Dynamic testing of a four-storey building with reinforced concrete and unreinforced masonry walls: prediction, test results and data set. *Bulletin of Earthquake Engineering*, 13, 3015-3064.

Martakis, P., Reuland, Y., Stavridis, A., & Chatzi, E. (2023). Fusing damage-sensitive features and domain adaptation towards robust damage classification in real buildings. *Soil Dynamics and Earthquake Engineering*, 166, 107739.

Reuland, Y., Martakis, P., & Chatzi, E. (2023a). A Comparative Study of Damage-Sensitive Features for Rapid Data-Driven Seismic Structural Health Monitoring. *Applied Sciences*, 13(4), 2708.

Reuland, Y., Khodaverdian, A., Crowley, H., Nieves, C., Martakis, P., & Chatzi, E. (2023b) Monitoring-driven post-earthquake building damage tagging. *10th International Conference on Experimental Vibration Analysis for Civil Engineering Structures (EVACES)*, Milano, Italy, August 30 - September 1, 2023.

## Task 4.5 Development of location- and structure-specific Earthquake Early Warning algorithm for buildings.

### 4.5.1 Introduction

Records from building monitoring systems can be used for earthquake early warning. In its simplest form, the records in the building are analysed in real-time; when a critical response parameter (e.g., base acceleration, top displacement, inter-story drift, base shear, etc.) is exceeded, some of the systems in the building can be automatically stopped, such as the elevators or gas lines. This is an early warning that does not have any lead time and should be done automatically without any human interference.

However, when there are ground stations for early warning in the area, it is possible to develop early warnings for buildings by incorporating the data from those stations. We present an EEW approach for structures by using vibration records from structures and ground motion data from

EEW networks. The methodology basically involves predicting the building's base response from the recordings at early warning ground stations before seismic waves reach the building. The first step is to identify the attenuation of ground motions from each early warning station to the base of the building. Next step involves identifying the base motion of the building that will cause a response critical for building's safety. By knowing the critical base motion and the threshold response values of the building, we can then identify the corresponding ground motions at each early warning station. We present an application of the methodology for a tall building in Istanbul where there is a 10-station early warning seismic network.

#### **4.5.2 Methodology**

To present the methodology for developing location- and structure-specific Earthquake Early Warning (EEW) algorithms, we use an instrumented tall building, the Sapphire Building, in Istanbul, where there is also a 10-station early warning seismic network. First, by using available earthquake records from the EEW stations and the building monitoring system, we develop equations for the attenuation of critical shaking parameters from each EEW station to the building's base. We identify the critical threshold response parameters for the performance of the building and the corresponding critical foundation motions. By using the attenuation equations developed, we then identify the ground motion at each EEW station that will cause the critical foundation motion at the building. The identified EEW values are used to issue an early warning for the building before seismic waves reach to the building. This would give about 5 to 7 seconds early warning time.

#### **4.5.3 Istanbul Earthquake Early Warning network**

The stations of Istanbul EEW network are shown in Figure 4.5.1 below, along with the known faults in Marmara Sea. There are 15 stations, 10 on land along the shores of Marmara Sea and 5 at the bottom of the sea.

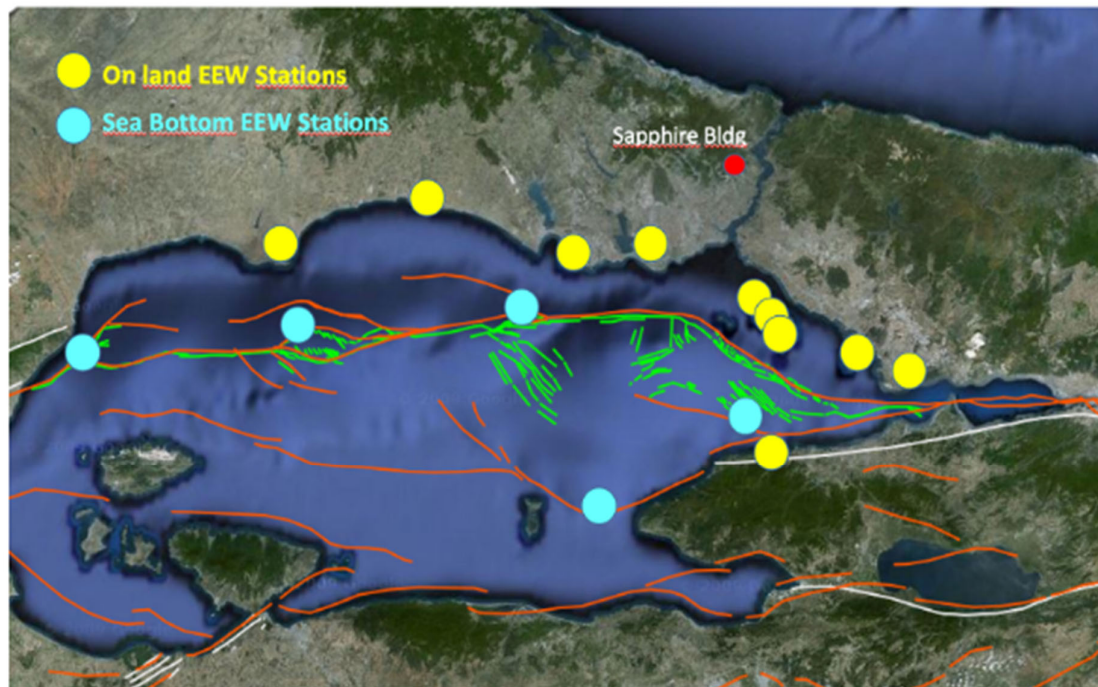


Figure 4.5.1. Earthquake Early Warning (EEW) network in Istanbul.

We compiled the records from the eight EEW stations and the Sapphire Building from 35 earthquakes with  $M_L > 4.0$  during the last 10-years and processed them. The locations of the EEW stations and the Sapphire building are shown in the figure below. Due to irregularities and breaks on the sea-bottom stations, only the data from the EEW stations on land were considered in the study. More on the earthquakes used in the study can be found in RISE Deliverable D4.6.

#### 4.5.4 Sapphire Building

The Sapphire Building is a 261m high, 62 story tall building in Istanbul with a rectangular cross-section and a flat roof. Figure 4.5.2 shows the building and its surroundings. It has 6 stories below ground, and 56 stories above ground. The soil condition is stiff soil; the foundation type is a mat foundation. The structural system is a reinforced-concrete shear wall and frames. It was instrumented with 30 channels of acceleration sensor, operating in real-time at 200 sps. The Guralp 5TC sensors are used in the instrumentation (see: <https://www.guralp.com/documents/DAS-050-0004.pdf>).

The sensor layout in the building and more on the earthquake data recorded from the building is given in RISE Deliverable D4.6.

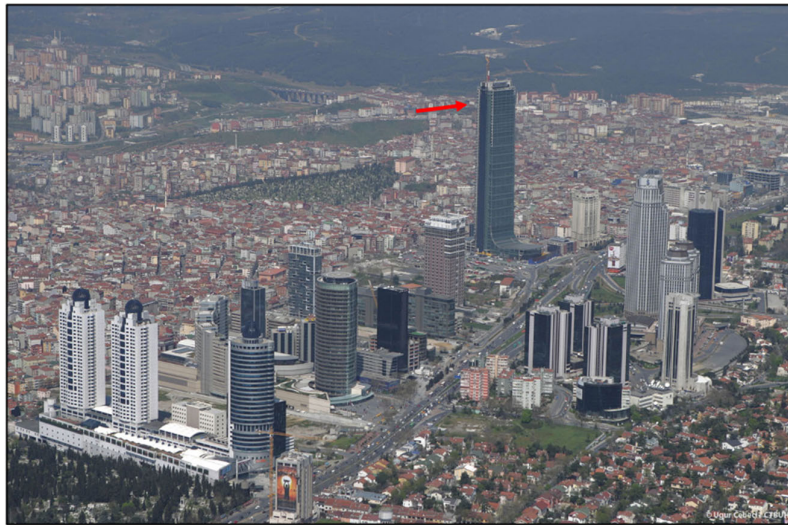


Figure 4.5.2. Sapphire Building in Istanbul.

#### 4.5.5 Attenuation of shaking parameters

We have used the records from the land stations only of the EEW network in Istanbul to calculate the attenuation of various shaking parameters from each EEW station to Sapphire Building. The map in Figure 4.5.3 shows the on-land EEW stations and the building location.



Figure 4.5.3. On-land EEW stations and the location of Sapphire Building.

The following shaking parameters, which are commonly assumed to control damage in structures, are used for the attenuations:

- PGA - Peak Ground Acceleration

- PGV- Peak Ground Velocity
- SA02 – Spectral Acceleration at 0.2 second period.
- SA1– Spectral Acceleration at 1.0 second period.
- CAV – Cumulative Absolute Velocity
- Ia – Arias’s Intensity
- SI \_ Spectral (i.e., Housner’s) Intensity

We have calculated the attenuation of each shaking parameter from each EEW station to Sapphire Building for the 35 earthquakes with  $M_L > 4.0$ . As an example, we show the attenuations of PGA and PGV from Burgaz EEW to Sapphire Building in Figure 4.5.4 below. The blue circles correspond to the earthquakes whose epicentral distance to the building is smaller than the epicentral distance to the EEW station, and the blue circles represent the opposite. The results for the remaining ground motion parameters and the EEW stations are presented in Appendix I of RISE Deliverable D4.6.

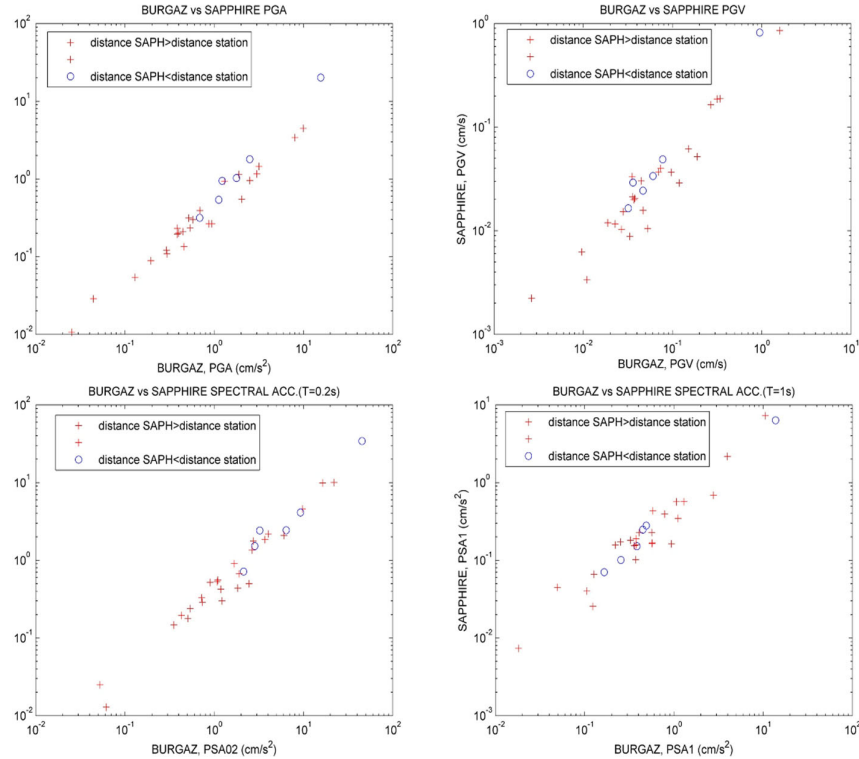


Figure 4.5.4. Attenuation from Burgaz EEW station to Sapphire Bldg. for PGA, PGV, SA(0.2) and SA(1.0).

#### 4.5.6 System Identification of Sapphire Building from the recorded response

We were not able to obtain the structural design drawings and calculations from the building's

owner due to the confidentiality of the information. Therefore, we were forced to use the monitoring data from five different earthquakes to identify the structural properties of the Sapphire Building. We have used advanced tools and techniques for the identification.

Since some of the techniques required that we have the records of every floor, we first had to estimate the accelerations at the non-instrumented floors from those of the instrumented floors. For this, we have used a modified version of the MSBE (Mode-Shape Based Estimation) approach introduced by Kaya, et. al. (2015). The modified approach, abbreviated as MMSBE, is based on the Timoshenko and Bernoulli-Euler beam theories, and approximates the response not only at modal frequencies but at all the frequencies (Çağlar and Şafak, 2022). The tests and confirmation of the MMSBE method, and the estimated records at non-instrumented floors are presented in Appendix II of RISE Deliverable D4.6.

For system identification, we use the transfer matrix formulation of the response, introduced in Cetin and Safak (2021). In this approach, a multi-story building is modelled as a superposition of one-story structures, one put on top of the other. System identification involves finding the natural frequencies and damping of each story, as if it were a single-story building. Moreover, the shear wave and phase velocities of each story are also identified.

Knowing such properties of each story, we can reconstruct a much more accurate analytical model of the building than a standard model identification would permit. Comparisons of the measured responses from five earthquakes with those calculated using the analytical model gives a very good match. The details of the system identification, the analytical model development, and the confirmation of the model accuracy are all presented in Appendix II of RISE Deliverable D4.6.

#### **4.5.7 Critical response parameters and base motions for safety**

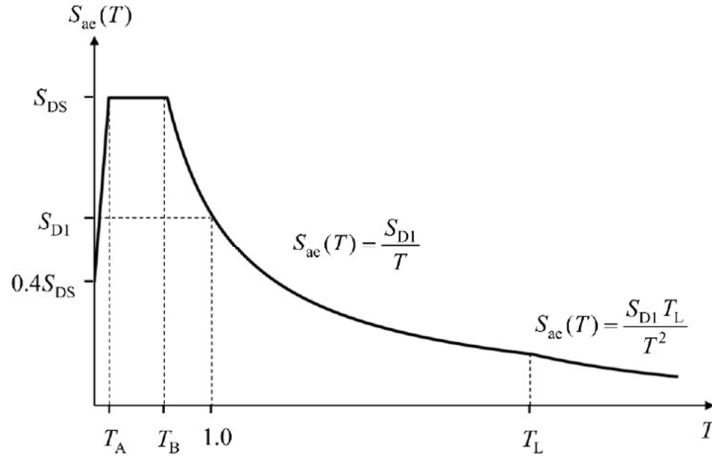
After developing a calibrated analytical model of the building from five earthquakes, we identified the parameters of the base accelerations that will cause response components critical for the building's safety. For the base ground motions, we used the parameters PGA (Peak Ground Acceleration) and PGV (Peak Ground Velocity), and the values of Spectral Acceleration (PSA), Spectral Velocity (PSV), and Spectral Displacement (SV) at the first modal frequency of the building. For the critical response parameters, we used the allowed top-story displacement and inter-story drift values as specified in the latest Turkish seismic design code.

The code considers four different levels of earthquakes:

- DD1: 2% probability of exceeding in 50 years, corresponding to a return period of 2475 years.
- DD2: 10% probability of exceeding in 50 years, corresponding to a return period of 475 years.
- DD3: 50% probability of exceeding in 50 years, corresponding to a return period of 72 years.
- DD4: 50% probability of exceeding in 30 years, corresponding to a return period of 43

years.

The design spectra, in terms of PSA, for each earthquake level is generated based on the latest Turkish Seismic Design Code, as shown in Figure 4.5.5 and Table 4.5.I below.



F

4.5.5. Design spectra as specified in Turkish Seismic Design Co

Table 4.5.I Parameters of design spectra for four different levels of earthquake.

	<b>S<sub>s</sub></b>	<b>S<sub>1</sub></b>	<b>S<sub>DS</sub></b>	<b>S<sub>DS1</sub></b>	<b>PGA</b>	<b>PGV</b>
<b>DD1</b>	1.335	0.372	1.602	0.558	0.543	33.360
<b>DD2</b>	0.752	0.216	0.902	0.324	0.312	19.517
<b>DD3</b>	0.296	0.089	0.385	0.134	0.129	8.248
<b>DD4</b>	0.193	0.058	0.251	0.087	0.084	5.439

Based on the above parameters, the design spectra for four different earthquake levels are presented in Figure 4.5.6 below.

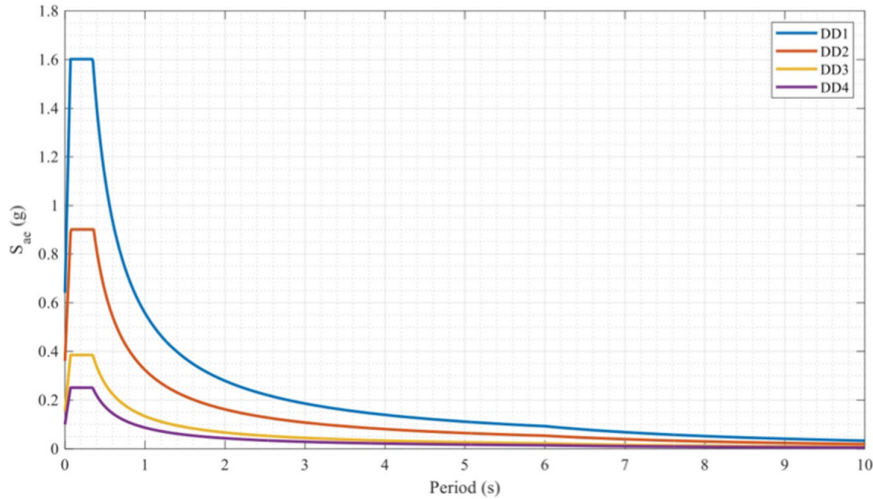


Figure 4.5.6. Design spectra for four different levels of earthquakes.

To evaluate the performance of the building, and using the analytical model developed, the probability of exceeding the code-specified 2% Spectral Acceleration, Spectral Velocity, and Spectral Displacement associated with the first modal frequency and 5% damping is calculated based on the drift at the top of the building. Since five earthquakes are not enough to develop the probability curves, we selected 178 more earthquakes from the PEER Ground Motion Database ([https://ngawest2.berkeley.edu/users/sign\\_in?unauthenticated=true](https://ngawest2.berkeley.edu/users/sign_in?unauthenticated=true)). The selection is based on the magnitudes ( $M > 5$ ) and the similarity of the fault rupture mechanisms for Istanbul (strike-slip).

The list of earthquakes selected is given in Appendix II of RISE Deliverable D4.6. As an example, Figure 4.5.7 shows below the probability of exceedance curve of the code drift limit with PSA in the E-W direction. The probability of exceedance curves for the other ground motion parameters (PSA, PSV, SA, SV, SD) at first modal frequency in the E-W and N-S directions are presented in Appendix II of RISE Deliverable D4.6.

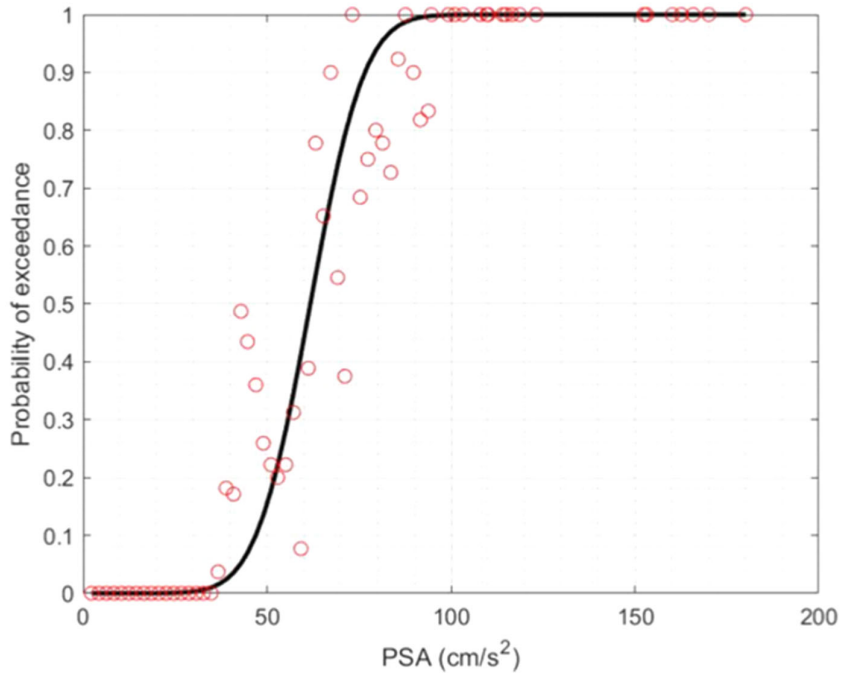


Figure 4.5.7. Probability of exceedance of 2% code drift limit with PSA at the first modal frequency in the E-W direction.

#### 4.5.8 Selection of threshold ground motion values at the EEW stations

The selection of threshold ground motion values at the EEW stations requires the following steps:

1. Select the design earthquake that will be considered for the building's safety (e.g., D1,D2,D3,or D4 level earthquake). This selection is based on the performance criteria (i.e., acceptable damage level for a specified return period of earthquake, importance of the building, etc.), and decided by the design engineer.
2. By using the attenuation of ground motions from the EEW stations and the building, select the ground motion parameter for each EEW station that gives the best correlation between the corresponding values at EEW stations and the building's base (note that the best correlating parameter may be different for different EEW stations).
3. Select the acceptable probability of exceedance levels for the selected parameters. This is also decided by the design engineer depending on the importance of the building, acceptable damage level, and the selected return period of the earthquake.
4. Read the corresponding ground motion values from the probability curves for each parameter.
5. Read the values of the corresponding parameters at EEW stations from the attenuation plots.

#### References cited above

1. Şafak,E.(1995).Detection and identification of soil-structure interaction in buildings from vibration recordings, Journal of Structural Engineering, ASCE, Vol.121, No.5, May 1995, pp.899-906.
2. Safak, E. (1999). Wave propagation formulation of seismic response of multi-

- storybuildings, *Journal of Structural Engineering*, ASCE, Vol. 125, No. 4, pp.426-437.
3. Kaya, Y ., S. Kocakaplan, and E. Şafak (2015). System identification and model calibration of multi-story buildings through estimation of vibration time histories at non- instrumented floors. *Bulletin of Earthquake Engineering* 13(11), 3301–3323.
  4. Cetin M, and E. Safak (2021) . An algorithm to calibrate analytical models of multi-story buildings from vibration records, *Earthquake Spectra*, 1–17, DOI: 10.1177/87552930211046969.
  5. Caglar, N.M. and Safak, E. (2021). Predicting Seismic Response of a Tall Building to a Large Earthquake Using Recorded Waveforms from Small Earthquakes, accepted for presentation and will appear in the proceedings of the European Safety and Reliability Conference, 19-23 September 2021, Angers, France
  6. Caglar, N.M. and E. Safak (2022). Estimation of the response of non-instrumented floors using the Timoshenko and Bernoulli-Euler Beam Theories, *Earthquake Engineering & Structural Dynamics*, 2022, Vol.1, No.3, DOI: 10.1002/eqe.3636
  7. RISE Deliverable D4.6.

#### **Task 4.6 A user-ready risk-cost-benefit analysis framework for quantifying socio-economic impact**

The earthquake risk cost-benefit framework is used to evaluate the benefits and costs of investing in earthquake risk reduction measures. The framework involves identifying risks, assessing damage costs, identifying risk reduction measures, and evaluating costs and benefits. A positive risk-cost-benefit balance is important to secure future investments in earthquake risk mitigation. The benefits of disaster risk reduction interventions can be quantitative or qualitative, and traditional cost-benefit analysis may not easily monetize all benefits. Alternative methods are needed that can account for all possible benefits and be flexible enough to incorporate surveys and expert opinions in decision-making. Cost Benefit Analysis (CBA) compares the total costs of an intervention against the total benefits it provides, while multi criteria decision analysis (MCDA) evaluates and compares different options based on multiple criteria or objectives, considering factors such as cost, effectiveness, and community acceptance. While CBA requires monetization of benefits and may exclude indirect and intangible benefits, it can be a powerful tool for prioritising DRM measures. In contrast, MCDA offers several methods for aggregating data on individual criteria to generate composite indicators of the overall performance of each option, and is not limited to monetary units for its comparisons.

In the first half of the project, we focused on the use of traditional CBA and applied it to EEW. As this deliverable focuses on the second half of the project, we will not detail the EEW and CBA. The details of this work can be found in Deliverable 4.7. In this report we will focus on the work carried out using MCDA only. Below we summarise RISE dynamic risk products being evaluated using MCDA. The focus is on dynamic risk products that represent significant improvements in methodology or procedure throughout the project.

#### **Dynamic Risk Products of RISE**

##### **i) Rapid Loss Assessment (Task 4.1)**

Rapid Loss Assessment (RLA) supports civil protection agencies and emergency services to rapidly

gain an overview of expected building damages, fatalities, injuries, displaced persons, and economic losses after a severe earthquake. The European ShakeMap system is now online, and a new prototype scientific service that allows the damage and losses to be assessed for any ShakeMap in the European ShakeMap system (the ESRM20 Rapid Earthquake Loss Assessment code) has been made available. The ESRM20 Rapid Earthquake Loss Assessment (ReLA) code has been applied to all events in the European ShakeMap archive since it was launched in 2020.

### **ii) Operational Earthquake Loss Forecasting (Task 4.2)**

INGV has developed an operational earthquake forecasting system, OEF-Italy, which probabilistically forecasts the expected number and locations of earthquakes with a magnitude above a threshold occurring in the monitored area. To extend the results of OEF-Italy into the risk domain, a system for operational earthquake loss forecasting (OELF), named MANTIS-K, was developed. It combines the weekly seismicity rates with vulnerability and inventory models for the Italian building stock to obtain weekly forecasts of seismic risk metrics, such as the expected number of collapsed buildings, fatalities, injuries, and displaced residents. However, MANTIS-K has some limitations that may affect the accuracy of the loss forecasting, especially during seismic crises when the structures in the area may have already been damaged by previous seismic events.

### **iii) State dependent fragility functions (Task 4.2)**

MANTIS v2.0 is the upgraded version of the MANTIS-K system, developed in the context of RISE. MANTIS v2.0 addresses the limitations of the previous version by accounting for the evolution of structural damage conditions over time, estimating possible damage due to earthquakes, and forecasting the performance level of buildings that are already at an intermediate performance level. The large-scale vulnerability model used in MANTIS-K is substituted with state-dependent fragility functions developed through an extended version of incremental dynamic analysis. Additionally, an automatic procedure is implemented to update the structural damage condition after each earthquake. The retrospective analysis of the 2009 L'Aquila seismic swarm shows that neglecting the possibility of damage accumulation and updating the building portfolio leads to an underestimation of forecasted losses, especially in areas close to the epicentres of the sequence.

### **Implementation of Multi Criteria Decision Analysis in a Case Study**

MCDA is used to evaluate and compare the different dynamic risk products developed within the RISE project, considering a number of established criteria. The aim is to provide a comprehensive evaluation of the RISE dynamic products against a set of criteria, rather than a simplistic comparison. Below we list the typical steps taken in a typical MCDA, which we followed in our analysis:

- 1) Setting the objectives
- 2) Determining the decision alternatives
- 3) Identifying the criteria
- 4) Criteria weighting
- 5) Scoring
- 6) Building the decision matrix & ranking

7) Examining results, re-score, discuss

The framework involves setting objectives, determining decision alternatives, and identifying criteria for evaluating those alternatives. The objectives in this particular exercise are to evaluate the newly developed dynamic RISE products listed above and their use in RLA based on a set of criteria. The decision alternatives being considered are four different approaches to fragility models with and without updates to the exposure of occupants. The criteria being evaluated include model simplicity, model run time, model uncertainty, realistic estimation of human losses, and realistic estimation of economic losses. The step of examining results, re-scoring, and discussing involves comparing the scores of each alternative and exploring options if no clear winner emerges. If an alternative consistently receives low ratings from all board members, it can be removed from consideration. The board can also examine alternatives with similar scores and adjust their weights or criteria to gain insights and reach a decision. This step may involve conducting sensitivity analysis to explore the impact of different weighting strategies on the ranking of alternatives. Ultimately, the board discusses the results of their analysis to reach a final decision.

We conducted three separate multi-criteria decision analyses (MCDAs) using four alternative case studies developed jointly with Task 6.1, which represent different stakeholder preferences for ranking the alternatives. The four alternatives considered are summarised herein:

- Alternative 1: state-independent fragility models, no updating of occupants
- Alternative 2: state-dependent fragility models, no updating of occupants
- Alternative 3: state-independent fragility models, with updating of occupants
- Alternative 4: state-dependent fragility models, with updating of occupants

A series of rapid loss assessments were run for the four alternatives considering seven different locations, using the open-source Real-Time Loss Tools software developed as part of Task 6.1. An example output of the analysis in terms of percentage of census occupants that are injured with severity 4 (instantaneously killed or mortally injured, as per the HAZUS scale) for location 01 under the 2016–2017 Central Italy sequence and the four alternatives considered is presented (Figure x). The results for various other cases for both Central Italy and L’Aquila were consistent with the analysis in MCDA (can be found in Deliverable 4.7).

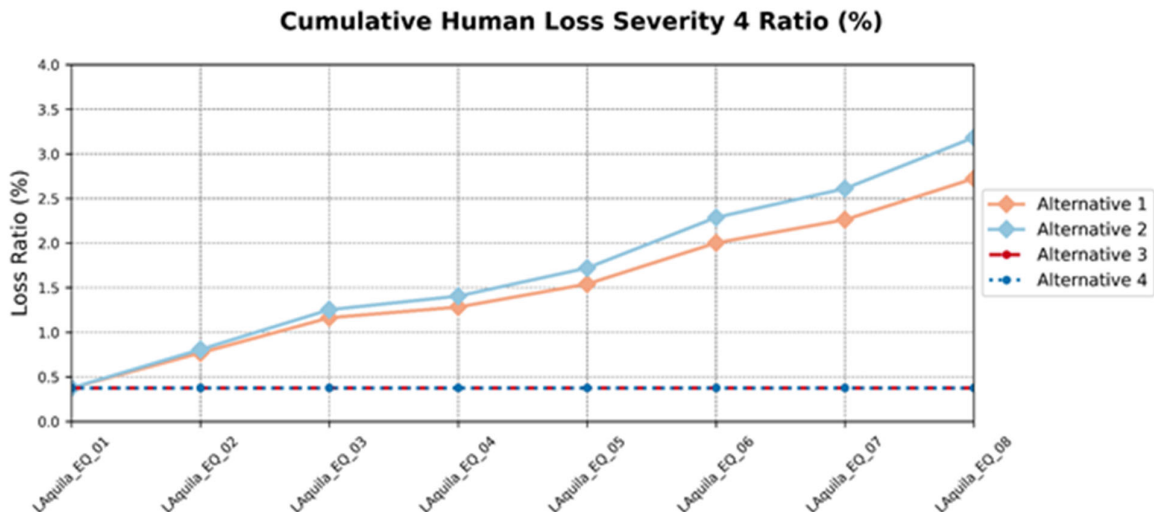


*Figure 4.6.1. Cumulative ratios of deaths (injuries of severity 4) to total number of census occupants for the four alternatives for location 01 of L'Aquila.*

Table 4.6.1. Decision Matrix

DECISION MATRIX WEIGHTED SCORING & RANKING						
	C1	C2	C3	C4	SUM	RANKING
A1	0.53	0.26	0.42	0.42	1.63	4
A2	0.43	0.16	0.42	2.10	3.11	2
A3	0.32	0.21	2.10	0.42	3.05	3
A4	0.21	0.10	2.10	2.10	4.53	1

Table 4.6.1 illustrates how a decision matrix looks like, with the final ranking (for details on how to calculate the decision matrix, please see Deliverable 4,7). The process of examining results, re-scoring, and discussing is an important final step in the multi-criteria decision analysis (MCDA) process. It involves conducting a sensitivity analysis to evaluate the impact of changing criteria weights on the overall ranking of alternatives. The decision-maker must then adjust the criteria weights and re-score the alternatives based on the revised weights to see how changes affect the overall ranking. Finally, the results of the MCDA analysis should be discussed with stakeholders and other decision-makers to ensure that the decision-making process is transparent, robust, and reliable. These steps are crucial to identify any limitations or uncertainties and determine if additional information or analysis is needed to make a final decision.

### **Results and Discussions**

The classic and widely used CBA method is explored at the initial stage of this task, and it is shown that it can effectively be applied to early earthquake warning systems. However, some challenges were encountered in applying CBA to certain risk products, leading to the consideration of MCDA as an alternative approach for decision support. CBA focuses on the economic costs and benefits of different alternatives, while MCDA takes into consideration a broader range of criteria, including non-economic factors such as model bias, model simplicity or social and environmental impacts. The flexibility and transparency of MCDA makes it a valuable tool in decision-making processes, and the results of both CBA and MCDA support a dialogue with end-users such as decision makers and the public.

### **List of submitted deliverables and achieved milestones in WP4**

D4.1 Second generation of models for RLA service demonstration for Europe

D4.2 Second generation of models for RLA service report for Europe

D4.3 Operational earthquake loss forecasting for Europe

D4.4 Development of RRE forecasting services in OpenQuake

D4.5 The use of structural health monitoring for rapid loss assessment

D4.6 Advances in performance-based earthquake early warning in Europe

D4.7 Good-practise report on risk-cost-benefit in terms of socio-economic impact

MS27 RLA service for Europe transferred to WP6

MS28 OELF service for Europe transferred to WP6

MS29 Risk-cost benefit framework applied to test site Switzerland

MS32 Real time data exchange between EMSC and Bergamo

MS33 Implementation of the AIDR platform for landslides and fire detection

MS34 Development of a new version of Boxer code particularly suited for web questionnaires

## Summary of Exploitable Results in WP4

### 1) Peer reviewed publications

- Astorga A, Guéguen P (2020) Influence of seismic strain rates on the co□and post□ seismic response of civil engineering buildings. *Earthquake Engineering & Structural Dynamics* 49(15): 1758-1764.
- Astorga A, Guéguen P (2023) On the value of weak-to-moderate earthquake data recorded in build-ings. Submitted to *Bull. Seism. Soc. Am.*
- Chioccarelli E, Iervolino I. (2021). Comparing Short-Term Seismic and COVID-19 Fatality Risks in Italy. *Seismol Res Lett*,. doi:10.1785/0220200368.
- Crowley H., Despotaki V., Silva V., Dabbeek J., Romão X., Pereira N., Castro J.M., Daniell J., Veliu E., Bilgin H., Adam C., Deyanova M., Ademović N., Atalic J., Riga E., Karatzetzou A., Besson B., Shendova V., Tiganescu A., Toma-Danila D., Zugic Z., Akkar S., Hancilar U. (2021) "Model of Seismic Design Lateral Force Levels for the Existing Reinforced Concrete European Building Stock," *Bulletin of Earthquake Engineering*, DOI: <https://doi.org/10.1007/s10518-021-01083-3> (Task 4.1)
- Dabbeek J., Crowley H., Silva V., Weatherill G., Paul N., Nievas C. (2021) "Impact of exposure spatial resolution on seismic loss estimates in regional portfolios," *Bulletin of Earthquake Engineering*, <https://doi.org/10.1007/s10518-021-01194-x> (Task 4.1)
- Ghimire S, Guéguen P, Astorga A (2021) Analysis of the efficiency of intensity measures from real earthquake data recorded in buildings. *Soil Dynamics and Earthquake Engineering* 147:106751.
- Guéguen P, Astorga A (2021) The torsional response of civil engineering structures during earthquake from an observational point of view. *Sensors* 21(2):342.
- Guéguen P, Guattari F, Aubert C, Laudat T (2020) Comparing direct observation of torsion with array-derived rotation in civil engineering structures. *Sensors* 21(1):142. <https://doi.org/10.3390/s21010142>
- Guéguen P, Astorga A, Langlais M (2023). Amplitude-frequency noise models for seismic building monitoring in a weak-to-moderate seismic region. Submitted to *Seism. Res. Letters*.

- Iaccarino AG, Guéguen P, Picozzi M, Ghimire S (2021) Earthquake early warning system for structural drift prediction using machine learning and linear regressors. *Frontiers in Earth Science* 9:666444. <https://doi.org/10.3389/feart.2021.666444>.
- Martakis, P., Reuland, Y., Stavridis, A., & Chatzi, E. (2023). Fusing damage-sensitive features and domain adaptation towards robust damage classification in real buildings. *Soil Dynamics and Earthquake Engineering*, 166, 107739. <https://doi.org/10.1016/j.soildyn.2022.107739>
- Martakis, P., Reuland, Y., Imesch, M., & Chatzi, E. (2022). Reducing uncertainty in seismic assessment of multiple masonry buildings based on monitored demolitions. *Bulletin of Earthquake Engineering*, 20(9), 4441-4482. <https://doi.org/10.1007/s10518-022-01369-0>
- Martakis, P., Movsessian, A., Reuland, Y., Pai, S. G., Quqa, S., Garcia Cava, D., Tcherniak, D., & Chatzi, E. (2022). A semi-supervised interpretable machine learning framework for sensor fault detection. *Smart Struct. Syst. Int. J*, 29, 251-266. <https://doi.org/10.12989/sss.2022.29.1.251>
- Martakis, P., Reuland, Y., & Chatzi, E. (2021). Amplitude-dependent model updating of masonry buildings undergoing demolition. *Smart Structures and Systems*, 27(2), 157–172. <https://doi.org/10.12989/SSS.2021.27.2.157>
- Martins L., Silva V., Crowley H. and Cavalieri F. (2021) “Vulnerability Modeller’s Toolkit, an Open-Source Platform for Vulnerability Analysis,” *Bulletin of Earthquake Engineering*, <https://doi.org/10.21203/rs.3.rs-458348/v1> (Task 4.1)
- Reuland, Y., Martakis, P., & Chatzi, E. (2023a). A Comparative Study of Damage-Sensitive Features for Rapid Data-Driven Seismic Structural Health Monitoring. *Applied Sciences*, 13(4), 2708. <https://doi.org/10.3390/app13042708>
- Skłodowska AM, Holden C, Guéguen P, Finnegan J, Sidwell G (2021) Structural change detection applying long-term seismic interferometry by deconvolution method to a modern civil engineering structure (New Zealand). *Bulletin of Earthquake Engineering* 19(9):3551-3569.
- Wang, S., Werner, M. J., & Yu, R. (2022). How well does Poissonian probabilistic seismic hazard assessment (PSHA) approximate the simulated hazard of epidemic type earthquake sequences?. *Bulletin of the Seismological Society of America*, 112(1), 508-526.
- Bodenmann, L., Reuland, Y., & Stojadinovic, B. (2023). Dynamic Post-Earthquake updating of Regional Damage Estimates using Gaussian Processes, *Reliability Engineering and System Safety*, 234,109201. <https://doi.org/10.1016/j.ress.2023.109201>
- Blagojevic, N., Bodenmann, L., Reuland, Y., & Stojadinovic, B. (2023). The case of 2010 Kraljevo earthquake: Validating a regional recovery model and investigating measures to increase disaster preparedness. *ASCE Journal of Structural Engineering*, submitted.

## 2) Conference publications

- Crowley H, Silva V, Kalakonas P, Martins L, Weatherill G, Pitilakis K, Riga E, Borzi B, Faravelli M (2020) “Verification of the European Seismic Risk Model (ESRM20),”

Proceedings of the 17th World Conference on Earthquake Engineering, Japan

<https://doi.org/10.5281/zenodo.4045883> (Task 4.1)

- Martakis, P., Reuland, Y., & Chatzi, E. (2021) "Data-driven model updating for seismic assessment of existing buildings", Proceedings of the 10th International Conference on Structural Health Monitoring of Intelligent Infrastructure, 30 June - 2 July 2021, Porto, Portugal.
- Orlacchio, M., Chioccarelli, E., Baltzopoulos, G., & Iervolino, I. (2021). State-Dependent Seismic Fragility Functions for Italian Reinforced Concrete Structures: Preliminary Results. *31th European Safety and Reliability Conference, 19-23 September 2021, Angers, France*, 1591–1598. [https://doi.org/10.3850/978-981-18-2016-8\\_660-cd](https://doi.org/10.3850/978-981-18-2016-8_660-cd) (Task 4.2)
- Reuland, Y., Martakis, P., & Chatzi, E. (2021) "Damage-sensitive features for rapid damage assessment in a seismic context", Proceedings of the 10th International Conference on Structural Health Monitoring of Intelligent Infrastructure, 30 June - 2 July 2021, Porto, Portugal.
- Reuland, Y., Khodaverdian, A., Crowley, H., Nievas, C., Martakis, P., & Chatzi, E. (2023) Monitoring-driven post-earthquake building damage tagging. 10th International Conference on Experimental Vibration Analysis for Civil Engineering Structures (EVACES), Milano, Italy, August 30 - September 1, 2023. (Accepted)
- Blagojević, N., Bodenmann, L., Reuland, Y., & Stojadinovic, B. (2022). Improving community disaster resilience by providing adequate supply of recovery resources and services. In Proceedings of the Third European Conference on Earthquake Engineering and Seismology–3ECEES, September 4-9, Bucharest, Romania.
- Blagojević, N., Bodenmann, L., Reuland, Y., & Stojadinovic, B. (2022). Validating a resilience quantification framework: The Case of 2010 Kraljevo Earthquake. In Proceedings of the Third European Conference on Earthquake Engineering and Seismology–3ECEES, September 4-9, Bucharest, Romania.
- Bodenmann, L., Reuland, Y., & Stojadinovic, B. (2021). Dynamic Updating of Building Loss Predictions Using Regional Risk Models and Conventional Post-Earthquake Data Sources. *31th European Safety and Reliability Conference, 19-23 September 2021, Angers, France*.
- Bodenmann, L., Reuland, Y., & Stojadinovic, B. (2021). Using regional earthquake risk models as priors to dynamically assess the impact on residential buildings after an event. Published Papers of 1st Croatian Conference on Earthquake Engineering, 1CroCEE, Zagreb, Croatia, March 22-24, 2021, 71.

### 3) Other exploitable results/data

- Crowley H., V. Despotaki, D. Rodrigues, V. Silva, C. Costa, D. Toma-Danila, E. Riga, A. Karatzetzou, S. Fotopoulou, L. Sousa, S. Ozcebe, P. Gamba, J. Dabbeek, X. Romão, N. Pereira, J.M. Castro, J. Daniell, E. Veliu, H. Bilgin, ... U. Hancilar. (2021a). European Exposure Model Data Repository (v1.0) [Data set]. Zenodo. <https://doi.org/10.5281/zenodo.5730071> (Task 4.1)
- Crowley H., Dabbeek J., Despotaki V., Rodrigues D., Martins L., Silva V., Romão, X., Pereira N., Weatherill G. and Danciu L. (2021b) European Seismic Risk Model (ESRM20), EFEHR Technical Report 002, V1.0.1, 84 pp, <https://doi.org/10.7414/EUC-EFEHR-TR002-ESRM20> (Task 4.1)

- Martins Luis, Vitor Silva, Helen Crowley, & Francesco Cavalieri. (2021). GEMScienceTools/VMTK-Vulnerability-Modellers-ToolKit (V2021.0). Zenodo. <https://doi.org/10.5281/zenodo.5019331> (Task 4.1)
- Romão X., N. Pereira, J.M. Castro, H. Crowley, V. Silva, L. Martins, & F. De Maio. (2021). European Building Vulnerability Data Repository (v2.1) [Data set]. Zenodo. <https://doi.org/10.5281/zenodo.5639318> (Task 4.1)
- Open source tools for disaggregating exposure models to higher resolution (in collaboration with the Global Earthquake Model), (Task 4.1):
- <https://github.com/GEMScienceTools/spatial-disaggregation>
- European ShakeMap system(Task 4.1): <http://shakemap.eu.ingv.it/>
- ShakeMap web portal source code (Task 4.1): <https://github.com/INGV/shakemap4-web>
- The upgraded Italian system for operational earthquake loss forecast MANTIS v2.0.
- Demonstrator for seismic SHM: [https://yreuland.github.io/SHM\\_Demonstrator/SHM\\_Demonstration\\_RISE.html](https://yreuland.github.io/SHM_Demonstrator/SHM_Demonstration_RISE.html)

### 1.2.5 Work package 5

#### Overview

The aims of work package 5 are:

- (1) to provide clear and accurate information to policy-makers and the public to enable strategic planning and appropriate preparation for seismic events and;
- (2) to offer timely, appropriate information to a geographical area when the seismic risk rises and explore crowdsourced EEWS for global earthquakes; and
- (3) to collect large numbers of eyewitness observations, both direct and indirect, about the degree of shaking being felt and possibly the damage incurred. This, in turn, will improve rapid situation awareness and augment data at a relatively low cost.

The specific objectives of work package 5 are:

- To discuss the needs and understand the existing decision-making environments and usual routes of communication for each of the different audiences for risk messages (long-term decision-makers, government and organizational leaders, emergency services, public) in different countries.
- Review best practices in risk communication, focusing on dynamic information communication in a range of fields, including medical, economic/financial, natural hazards, engineering, and environmental.
- Undertake an iterated user-centred design process to develop a method of communication, with user-testing across different countries involved to integrate the design process. This will culminate in a formal controlled evaluation of the communications.
- Improve procedures for using internet-based intensity questionnaires for two-way communication and deriving useful scientific information on earthquakes (e.g., fast characterization of seismogenic faults).
- Exploit the LastQuake\* (1.4M users), Earthquake Network† (2.5M users) and MeteoSuisse Apps (2 Million Users) for their synergies for crowdsourced EEWS and RIA.

## **Task 5.1 Dynamic Risk Communication**

Communicating the knowledge that seismologists and other experts have to decision-makers (whether those be policy decisions that affect a large number of people or individual decisions that may only affect one or a few) is a difficult and complex task. This is especially true of a situation where the knowledge is constantly changing.

During the RISE project, we sought to answer the questions:

What information do people want? What information do people need?

How can we best communicate that information?

To do that we had to understand the many different audiences for seismic risk information, where they get information from currently and where they might get it from in the future, how they used such information, and how they might understand or misunderstand different formats.

To do this as thoroughly as possible, we carried out a review of best practice in communicating dynamic risks in other domains, involving both academic and grey literature, and interviews with experts ([deliverable D5.1](#)). We then undertook a series of interviews and focus groups with over 100 people including members of the public in different countries, seismologists, first responders, journalists, civil protection etc, including views on draft OEF communications ([deliverables D5.2, D5.3](#)). Finally we carried out quantitative studies using 8,196 members of the public across three countries (the U.S. - specifically California, Italy & Switzerland) ([deliverable D5.4](#)) in order to evaluate different formats for communicating quantitative risk information. Carrying out the same experiments across these three different countries allows us to be more confident in generalisability across cultures and languages. These quantitative studies, the largest and only cross-cultural studies ever carried out in seismic risk communication, are currently being submitted for publication.

All these aspects of the work culminated in a series of guidance points, each of which was based on evidence that is cited in our final deliverable ([deliverable D5.5](#)):

Before you start communicating OEF:

### ***1) Be clear about the difference between a forecast and a warning; between information and advice.***

This is about understanding the aims of your communication, because you can't achieve your aims unless you are clear about them in your own mind. A warning aims to change people's behaviour, through clear advice and messaging – a forecast aims only to give people information which they can use in their own decision-making: there is no advice or message. The two require different communication techniques and would be evaluated very differently.

### ***2) Build relationships with those who might use your forecasts, and those who might help disseminate them.***

This will help you understand the needs of your audiences so that you can provide them with the information that they want and need, and not just the information that you want to give them or assume that they want. Different audiences might want different things, so you may have to prepare different outputs for them. You may also want to work with audiences to help them know how to respond to the forecast – what actions they may consider. This is particularly advised in schools, but also with others, such as infrastructure managers. When communicating

to the public, use the channels that they are already used to using for similar information rather than trying to invent your own: work with journalists in all media, weather forecasters etc. They will also likely know their audiences well and be able to help. Regular meetings with those who are going to try to interpret and disseminate forecasts can also help ensure that any new people are familiar with the format and ready to help their audiences.

When communicating OEF:

**3) Make the purpose of the forecast, and its limitations, clear to the audience**

Just as you as a communicator had to decide what the aim of your communication is, so your audience also needs to know this aim. If the audience are expecting a warning with a clear behaviour message, they will be confused and unhappy with a forecast that doesn't give them that. Forecast information can help people make all sorts of decisions, depending on their own circumstances – it is useful even when absolute probabilities are low and there is no official 'advice'. For example, people might choose to practice an evacuation drill, test shut down procedures for power stations, identify diversion routes that avoid tunnels or bridges – all depending on their responsibilities. You're not advising people to do any of those things as part of the forecast, but you can give people a sense of decisions that they or others might make. Making it clear why the forecast is being made public and how it might be of use to some people will help the audience know how to respond to it.

**4) Minimise the number of variables that you allow the audience to change**

It is tempting to avoid making decisions on behalf of your audiences, and instead to allow every variable to be customised (e.g. the geographical area and time frame of the forecast, the threshold of event size being considered, metrics such as intensity or magnitude). However, if communicating with the public, this is not helpful for most and instead makes the forecast more complex and difficult to understand. Add as little customisation as possible to the main interface: if possible, allow the audience to vary only one thing - the location for which the forecast applies. For more experienced audiences you can allow more customisation via a 'settings' option, but work with these audiences to identify the variables they need to change and keep the customisation via settings only to those.

**5) Ensure that the forecast is given out regularly & frequently, in the same consistent format, to allow the audience to become familiar with it during quiescent times**

People find it increasingly easy to interpret formats as they become familiar with them, so it is useful to expose people to a format frequently. Additionally, familiarity with what 'normal' looks like in terms of the likelihood of a seismic event will help people interpret the likelihoods displayed in times where the risk level is higher and so make sense of it (which it is important that they are able to do).

**6) Don't try to communicate forecast information to individuals via a geographical map representation. Only use a geographical map to illustrate the area over which the forecast is valid.**

Geographical maps are formats that are very familiar to most audiences, and so they frequently express a liking for information presented in that way. A geographical map can be useful to help them know the area over which a forecast is calculated and valid, but for individuals only interested in the forecast at one particular location, reading absolute risks off a map (illustrated as isolines) seems to be harder than simply displaying the absolute risk probability to them. It

may also confuse people into thinking that the isolines on the map represent something other than the likelihood of an event of a set magnitude (e.g. the geographical distribution of intensity of, or damage caused by, a forecasted earthquake, since such maps are often used after an event to illustrate exactly that).

**7) Communicate information about what impact people might expect, as well as the likelihood/probability**

It's easy to concentrate on communicating the difficult aspect of the numbers involved in the likelihood, but forget that the numbers involved in the impact (e.g. magnitude or intensity) also need to be given a context for people to know what this might mean for them. Although an earthquake of the same magnitude or even intensity can have very different effects depending on the types of buildings in an area, just giving people a sense of what sort of effects different levels of earthquake might have, and in a way that references their experience (e.g. giving examples of earthquakes that they might remember reports from) rather than theoretical (e.g. not through a description like 'light damage likely', which people found unhelpful in our interviews).

**8) Present probabilities of events occurring as both percentages (e.g. 'X% chance of an earthquake') and expected frequencies (e.g. 'out of 100,000 towns with exactly the same chance of an earthquake as this one, we would expect an earthquake to happen in X of them.')**

People shown a probability as a more solid and imaginable expected frequency perceive that probability to present a higher chance of happening than when shown a percentage. However, such expected frequencies also help people discriminate between low probabilities, which would have several decimal points if shown as a percentage (and where changes of whole orders of magnitude are difficult for people to discriminate). A percentage, though, even with decimal places, is seen as clearer and easier to read, so presenting the absolute risk as a percentage in a big, bold font as the main output seems sensible, whilst also showing the interpretation underneath as an expected frequency. Graphics such as bar charts or icons are not helpful for the low probabilities most often applicable to seismic events.

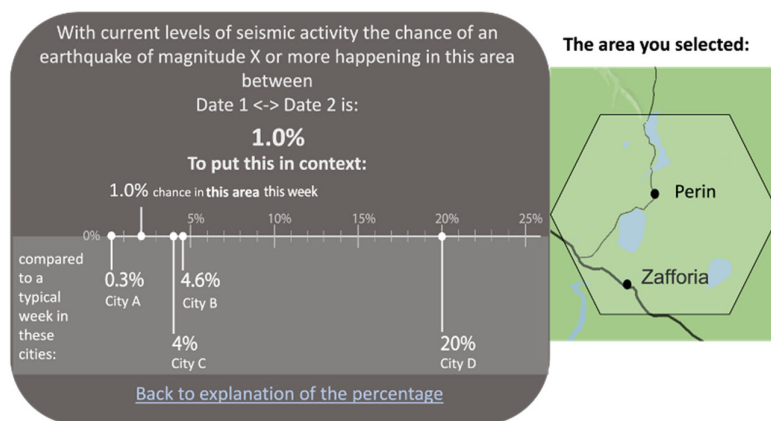
**9) Don't give the baseline risk (the average percentage chance of an event occurring) or a relative risk (how many times higher than average the current risk is) in an attempt to help people understand their current risk level.**

Giving context to the absolute risk of a seismic event is important to help people interpret the (otherwise fairly meaningless) probability of such an event. If they have become used to seeing the forecast regularly (see point 5 above) then they may already have an idea of what 'normal' (baseline) is, but the format should not rely on that knowledge. Experiments where people were given the baseline risk in an area as a piece of context to a forecast gave inconsistent results. Where people were given the relative risk between the current and baseline probabilities (e.g. 'twice as high as average') people had a higher perception of the risk (if it was elevated above baseline), but it also seemed to inhibit discrimination between different probabilities. We therefore don't recommend using either a baseline or relative risk as a way to add context to an absolute forecast probability.

**10) Allow those who want further context to view a graphic which illustrates the current probability of an event happening in the selected geographical area on a risk ladder,**

**compared with the average probability of the same event happening in a few familiar cities that illustrate a broad range of high to low risk levels.**

What does seem to give people useful context to interpret the current probability of a seismic event however, is a graphical comparison of this probability against the average probability in other cities with which they are likely already to have some sense of the likelihood of an earthquake. These cities are likely to be within their country, but may be international in the case of some famously high hazard locations (e.g. Tokyo or Los Angeles). The scale on the risk ladder should be linear, not logarithmic (it can be cut off just above the highest baseline risk). We acknowledge that calculating these comparator risks is complex. Some members of the audience are likely to find the risk ladder ‘too much information’ – especially alongside both the percentage and expected frequency formats described in point 7 - so it is probably better as optional additional information.



Example of a ‘risk ladder’ which could be used to give comparison of the risk in one location with that in familiar cities. The labels ‘City A’ etc would be replaced with cities familiar to the specific audience in mind (e.g. either national cities or international cities well-known for their seismicity).

**11) Allow those who want it to find information about how long events might last for if they happen, and what people might expect in terms of emergency support or communication**

Even if you don’t communicate this information as part of your forecast service, work with others who can provide this information to the relevant audiences. People want to know what to expect if an event occurs – how long an aftershock sequence might last, what sort of effects an earthquake might have, how long before things are likely to return to normal, and who has responsibility for different actions.

**12) Provide some explanation in normal language, and a personal interpretation service for those who want to be able to talk to a ‘real person’ about the forecast and how to interpret it**

Although an automated forecast service might be cost-effective, in order to really support your audiences, you should also provide alongside it a short (1-2 sentences) written explanation for the forecast, and a continually-available personal service for those who need to ring to have an explanation of the forecast. It may be worried members of the public, journalists, or key infrastructure managers or political decision-makers – all will need to be supported by a one-

to-one service, staffed by people who understand the technicalities of the forecast but are able to communicate about it at any level required. This is no small undertaking, but an important one.

**13) Consider 'prebunking' misinformation or common misunderstandings without patronising the audience or showing lack of cultural sensitivity**

It is helpful to be able to pre-empt potential misunderstandings (such as the difference between a forecast and a prediction, or that large seismic events can happen without warning at any time even in 'low hazard' areas). However, it is important to approach this task with humility. Recognise that there is a great deal not known within the geosciences, and that a lot of information is not 'true' or 'false' but a matter of degree, interpretation or debate. Also recognise that many different cultures have different views on the role of aspects such as fate and that insensitivity to this can easily create barriers between groups and foster mistrust – which can undermine all attempts at communication.

The screenshot shows the 'Earthquake Forecast' website. It features a navigation bar with 'Home', 'Countries', 'Regions', 'Communities', 'Presets', and 'Language'. The main content area is divided into three sections:

- Map Section:** A map of a region with a blue triangle indicating a selected area. Text above the map says: "Use the map to select the area you want a forecast for:". Below the map is a link: "How to survive an earthquake" with the text "Click here for useful tips on what to do before, during, and after an earthquake."
- Forecast Section:** A dark blue box titled "Current forecast for a Magnitude 4 or above earthquake in the area you have selected:". It contains the following text:
  - "With current levels of seismic activity the chance of an earthquake of magnitude 4 or more happening in this area between [Date 1] <-> [Date 2] is: [1.0%]"
  - "Imagine 100,000 areas with exactly the same chance of an earthquake as this one."
  - "Within the week of [Date 1] <-> [Date 2] with a [1.0%] chance we would expect: An earthquake of magnitude 4+ to happen in [1000] of them No earthquake of magnitude 4+ to happen in [99,000] of them"
  - Buttons for "Last updated" (00:00 6th July 2021) and "Next update due" (00:00 7th July 2021).
  - A link: "Show me this number in context"
  - A box titled "Explanation for this forecast:" containing text: "Norcia-NW is seeing higher chances than normal because of increased seismic activity around the Mount Vettore fault system. Click here to find out more..."
- Magnitude Scale Section:** A vertical scale of magnitudes from 1 to 9. Magnitudes 4, 5, 6, and 7 are highlighted in purple. Arrows point to specific events:
  - Magnitude 6: "Norcia 2016 Mw6.5"
  - Magnitude 5: "L'Aquila 2009 Mw6.3"
  - Magnitude 5: "Eureka 2012 Mw5.9"
  - Magnitude 4: "Campione 2017 Mw4.2"
  - Magnitudes 1-3 are labeled "Not included in forecast"
- Information Section:** A box titled "What can I do with this information?" with text: "Earthquake forecasts are much less certain than weather forecasts as we cannot see what is happening underground, but they can give useful information to those making decisions. Click here to find out more..."

<http://earthquake-forecast.wintoncentre.uk/> - an Open Source demonstration OEF site designed to include many of the recommendations from the RISE project

During our work we heard many seismologists and other domain experts express concerns about the uncertainties and potential liabilities involved in forecasting. The guidelines above should help reduce these concerns as it is important to ensure that the audience understands that what is being communicated is *information*, not a *warning*. The communicator is not making a decision on behalf of the audience (they cannot, since they do not have all the information that the audience has about their own particular circumstances and options open to them). They are providing the piece of information that they possess (the likelihood of an earthquake of a certain magnitude occurring in a certain location within a certain timeframe) so that the audience can weigh that in their decision-making.

As part of RISE, we created an Open Source code base (<https://github.com/WintonCentre/riose->

[dashboard](#)) for a test OEF website demonstrating these guidelines (as well as other findings from user-testing) <http://earthquake-forecast.wintoncentre.uk>. This is available for others to use and adapt as they wish.

## **Task 5.2 From crowdsourced EEWs to RIA**

This task deals with crowdsourced early warning and rapid impact assessment

- The Earthquake Network citizen science initiative

Since 2012, the Earthquake Network (EQN) citizen science initiative implements a global smartphone-based earthquake early warning system fed by the smartphones voluntarily made available by the citizens who install the EQN smartphone app. More than 12 million people took part in the initiative and the system issued more than 6,000 real-time alerts in at least 20 seismic countries.

Within the RISE project, detection capability and performance of the EQN system have been assessed, while novel statistical techniques for improving the robustness of the system have been developed.

More in detail, Bossu et al. (2021) showed that EQN provided early warnings during at least 50 seismic events with magnitude between 4.5 and 8.0. During the M6.4 Albanian event of November 26, 2019 that killed 51 people, EQN provided a 6.9 seconds forewarning to citizens exposed to intensity 6 shaking of the Modified Mercalli Intensity (MMI) scale.

Fallou et al. (2021), on the other hand, have assessed the efficacy and usefulness of the EQN alerting service through a survey that covered 2,625 Peruvian users of the EQN app who were exposed to a M8.0 earthquake. Survey results showed that only 25% of the users performed a “drop, cover and hold” action when the alert was received on their smartphone, suggesting that the alert alone is not enough for earthquake impact mitigation, and that future works on the EEW topic should also focus on sociological and psychological aspects.

The reliability of the EQN system has been assessed in Finazzi et al. (2022), where a statistical model has been trained to estimate the probability of an earthquake detection by the smartphone network given the characteristic of the earthquake, the geometry of the network and the interaction between the earthquake and the network. As expected, it was discovered that the number of smartphones in the network have a significant role in the earthquake detectability. Nonetheless, when the earthquake is strong and the epicentral area is covered by the smartphone network, the probability of detection tends to be close to one starting from 10 monitoring smartphones in a radius of 30 km. This implies that EQN is suitable for EEW, where the focus is on strong and dangerous earthquakes. In Finazzi and Massoda (2023), a simulation study has been carried out to study the expected EQN performance in Haiti under different scenarios. The scenarios reflect the M7.0 event of January 12, 2010 and the M7.2 event of August 14, 2021, while simulations are based on the true EQN smartphone network in Haiti.

From the development point of view, Massoda and Finazzi (2023) implemented a statistical methodology for minimising the probability of false alarm of the EQN system while controlling the probability to miss a real earthquake. On the other hand, Aiello et al. (2023) implemented a statistical methodology based on survival analysis for improving the EQN estimates of the earthquake parameters when a detection by the smartphone network occurs. The methodology

has been applied to the 2023 Turkish-Syrian earthquake that was detected by the EQN smartphone network with a delay of 11 seconds from origin time. This allowed EQN users exposed to high MMIs (i.e.,  $\text{MMI} > \text{VII}$ ) to receive on their smartphones early warnings up to 20 seconds.

- Rapid earthquake information and impact assessment

The CsLoc (Crowdseeded Seismic Location) method, where seismic and crowdsourced data are jointly analysed for rapid location of felt earthquakes, has been fully integrated into EMSC operations and is a fully operational service since July 2022. From July to December 2022, there were 367 locations (2/day) with a median location accuracy of 11 km and a median publication time of 88 seconds. For 279 of these earthquakes, a magnitude estimate was computed with an accuracy of 0.2 and a publication delay of 176 seconds. We have completed the attempt to integrate the RaspberryShake stations. It proved to be a failure explained by the level of noise. CsLoc performs locations on a limited number of observations by selecting stations and time windows. It implicitly assumes a low noise level, which is not the case with RaspberryShake.

In terms of rapid impact assessment, the crowdsourcing of felt reports continues to grow, with 5,000 reports collected within the first 30 minutes of the M7.8 Turkish earthquake. The methodology for incorporating them into shakemaps is now published (Quitoriano and Wald 2022) and real-time sharing tools are being tested with a likely service with USGS and some national institutes by the end of the year. The use of felt reports for the rapid determination of finite fractures has been in operation for over a year in collaboration with ETHZ and the results are very promising. For example, the rupture geometry of the M7.8 earthquakes in Turkey was correctly determined within 10 minutes of its occurrence. We are currently recruiting to properly evaluate its performance. Again, if validated, it will be put into operational service.

The latest development in the field of felt reports is a statistical method, developed in collaboration with the GFZ, for distinguishing between high and low impact earthquakes worldwide within 10 minutes of an event (Lilienkamp et al., 2023). Notably, such an approach does not require the location or magnitude of the earthquake and is able to detect cases of damaging earthquakes such as the 2022 Afghanistan earthquake, which despite killing 1,100 people, remained under the radar for hours.

Finally, our work on triggered landslide detection on Twitter with QCRI (Qatar) and BGS has expanded far beyond initial expectations. We have now developed the Global Landslide Detector (GLD) as a prototype service (<https://landslide-aidr.qcri.org/>). Exploratory proposals with NASA and USGS are under way to combine GLD with satellite imagery for a multi-disciplinary, multi-technology tool. Finally, a spin-off project has been submitted by EMSC to improve tweets location through direct and automatic response to the author of the identified landslide tweets. However, all these developments will depend on the evolution of Twitter itself, the access policy to its API which at the time of writing remain fuzzy.

- Earthquake parameters derived from crowdsourced data

We computed macroseismic parameters (location and magnitude) using the citizen testimonies, i.e. individual intensity data (IDP) collected since 2012 (Bossu et al., 2017, 2018) and made available by the Lastquake system of the European-Mediterranean Seismological Centre (EMSC,

<https://emsc.csem.org/>).

IDPs available for earthquakes are first selected to eliminate intensities that are geographically inconsistent with most data, then the BOXER code (Gasperini et al., 2010) is used to derive macroseismic earthquake parameters (location and magnitude). However, BOXER cannot be used to assess macroseismic parameters using directly the available IDPs, therefore the IDPs should be grouped into macroseismic data points (MDPs) that correspond to assessing intensity over an area, similar to what is done for localities in macroseismic surveys. This approach is structured in three steps (Fig. 5.2.1):

- A) definition of spatial areas or clusters where grouping IDPs;
- B) evaluation of the occurrence of IDPs in each spatial area or cluster;
- C) assessment of MDPs.

In details, the clusters are based on radius (RA), square grid (SQ), hexagonal grid (HE), radius and grid combinations (RS, i.e. RA+SQ; RH, i.e. RA+HE) and DBSCAN (DB) model (Ester et al., 1996). For each cluster, an intensity value (MDP) equivalent to the assessment for localities in classical macroseismic studies, is computed by statistical methods (STETs: average, median, trimmed average of IDPs, Fig. 5.2.1). According to DYFI (Wald et al., 2011) the areas/clusters with a number of IDPs lower than 3 are not evaluated and MDPs are not assessed. Moreover we performed two separate analysis for raw (original intensities from citizens) and corrected (Bossu et al., 2018) intensities of IDPs.



*not (numbers in red colours). Column C: IDPs are used to compute a combined intensity (MDPs), indicated in different colours and symbols, for selected area/clusters (in white colours) and by using different statistical estimators (STETs).*

We compared the macroseismic parameters computed from different MGROUP-STET-BOXER combinations with the instrumental ones obtaining a retrospective statistical evaluation of their reliability. In total we elaborated 22,671 earthquakes from 2012 to February 2023 with at least 3 IDPs. For each earthquake and for raw and corrected intensities, we apply 132 different MGROUP-STET-BOXER combinations. About 7,000 earthquakes do not have enough IDPs to be grouped together and provide at least one MDP. On a global scale, it is possible to provide a macroseismic location for about 15,000 earthquakes and a magnitude for about 6,000.

In general, macroseismic parameters are more reliable when the instrumental epicentre is located in land than offshore, and the agreement with instrumental data improves by increasing the number of MDPs and/or decreasing the azimuthal gap between MDPs and instrumental epicentre (i.e. when MDPs are well distributed around the instrumental epicentre). There is no MGROUP-STET-BOXER combination that minimises distance and magnitude difference, but we have nevertheless developed an approach to choose between the various MGROUP-STET-BOXER combinations synthesising the processed parameters, useful for future applications of the methodology in near-real time. The main dependency of the results is geographical, i.e. not all parts of the earth have the same reliability of the parameters. In fact, geomorphological factors (sea, lakes, mountains), epicentres located offshore or near the coast, coastal morphology, proximity to desert areas or cities, different population density and Internet coverage or freedom of use influence the collection of IDPs or their geographical distribution. The increase in the collection of IDPs over time, as a consequence of the increased use of the Lastquake system, produces improvements in the number of earthquakes whose parameters can be estimated and in the quality of the results (e.g. Fig. 5.2.2).

Figure 5.2.2 shows for the European area (Lat range 20°-60°N Lon range -20°/60°E) the number of earthquakes available and the comparison of the distance between macroseismic and instrumental epicentres: the smaller the distance, the greater the agreement between macroseismic and instrumental data. A total of 9,339 events are located in this area, i.e. about 2/3 of the processed earthquakes globally. The events are grouped with a different colour scale according to their distance range. By filtering out earthquakes with at least 3 MDPs, there are 4,232 localised events in total. For both the upper and lower graphs in the figure, two columns of data are shown for each year: the one on the left shows all earthquake data, while the one on the right shows earthquakes with at least 3 MDPs. The total number of localised macroseismic earthquakes increases over time, except in 2018 and 2022 where there is a small decrease in the number of events compared to the previous year (Fig. 5.2.2, top). Only two months are available for 2023. In general, 50% of macroseismic earthquakes are located within 20 km of the instrumental epicentre, 66% within 30 km (Fig. 5.2.2, bottom). For about 10% of earthquakes, there are significant differences between macroseismic and instrumental epicentres with distances greater than 100 km. For events with  $MDPs \geq 3$  the percentage of events located within 20 and 30 km increases (54% and 70% respectively), while the percentage of events with distances > 100 km decreases (8%). However, the percentage of agreement tends to increase over time as

the number of IDPs collected increases. For the year 2023, a change is evident with markedly different percentages. Most of 2023 earthquakes are related to the aftershocks of the Turkey earthquake (6 February 2023, M 7.8) and it is possible to assume that doughnut effects in the distribution of IDPs or incorrect associations between IDPs and epicentres during the sequence are related to the statistical worsening of the distance between macroseismic and instrumental epicentres.

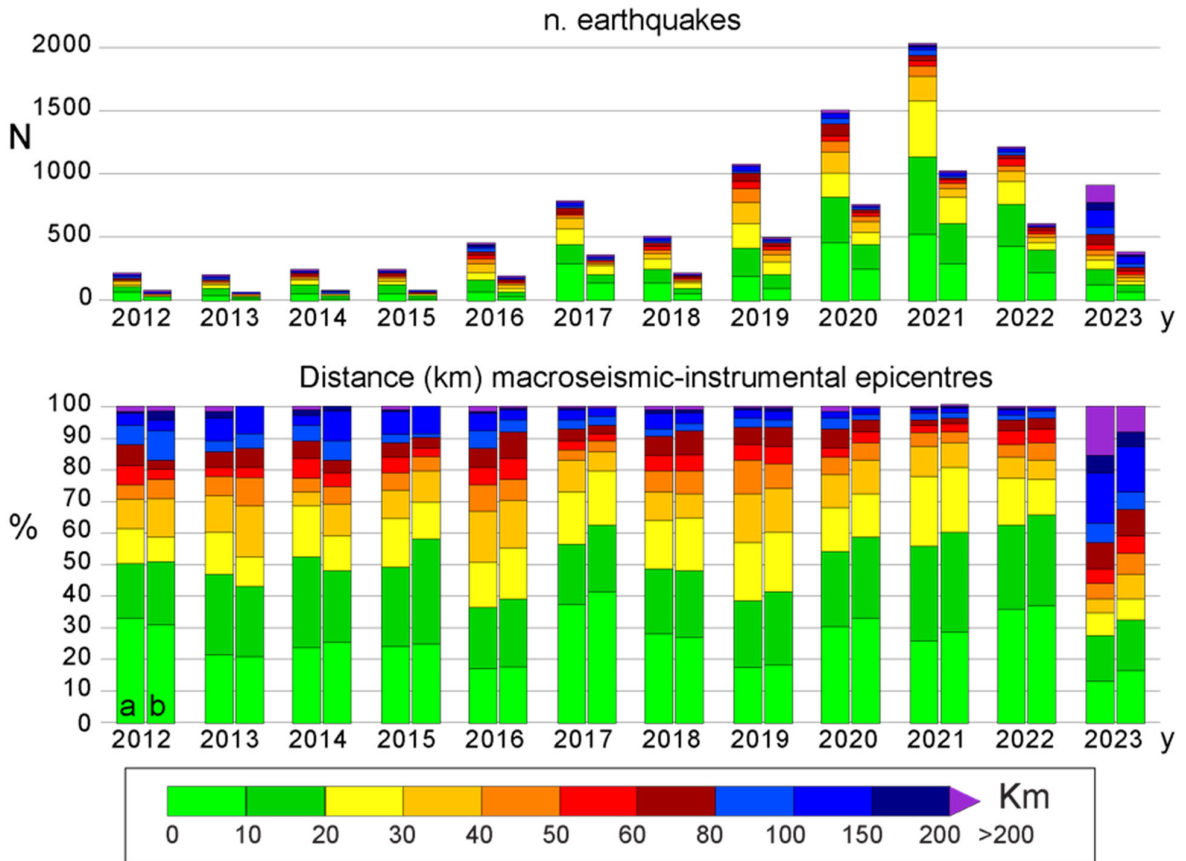
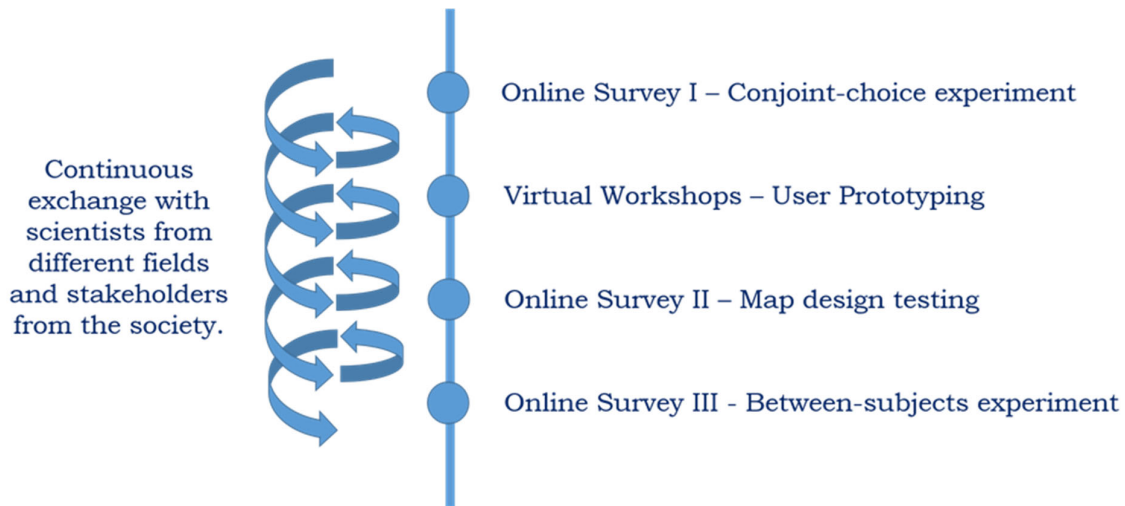


Figure 5.2.2: number of available earthquakes (top) and distance between macroseismic and instrumental epicentres (bottom). The available earthquakes are grouped in different colours by distance interval according to legend. Two columns are shown for each year of analysis: the left column (indicated as "a" in the example for 2012) refers to all earthquakes, the right column to earthquakes with at least 3 MDP ("b").

### Task 5.3 Improving earthquake information in a multi-hazard context

A relatively new approach to increase society’s resilience towards earthquakes is the communication of event-related earthquake information in a multi-hazard context; which is supported by international initiatives such as the Sendai Framework for Disaster Risk Reduction 2015-2030. With resilience we refer to societies’ ability to handle an emergency by taking protective actions before, during, and after an event. In Task 5.3, we analysed in detail how to communicate event-related earthquake information to the public in an understandable, user-oriented, and actionable way to support people in taking informed decisions after an event.

To this end, we conducted a case study in Switzerland with a total of four studies (See Figure 5.3.1). We argue that the results, we present below, can be transferred to any other region when considering the contextual characteristics. More precisely, we apply a user-centred systemic and mixed methods approach, with a major emphasis on user requirements driving technological developments. Throughout the project, we continuously collaborate with scientists from different fields and stakeholders from the society, thus following a transdisciplinarity (td) research approach. The transdisciplinary approach allowed us to co-produce communication products that fulfil the needs of the end users and comply with the latest scientific findings.



**Figure 5.3.1: Overview of the four studies** [adapted from D5.10].

In the following, we summarise the main results of the four studies and provide some general recommendations for the design of earthquake notifications and hazard overviews on multi-hazard platforms. The detailed results are summarised in D5.10, published in three peer-reviewed scientific publications, discussed as part of a doctoral thesis, presented at conferences, and reported to relevant, societal stakeholders. See the collection of these outputs at the end of the WP5 reporting.

### **Study I: What defines the success of maps and additional information on multi-hazard platforms?**

Dallo, I., Stauffacher, M., & Marti, M. (2020). What defines the success of maps and additional information on a multi-hazard platform? *International Journal of Disaster Risk Reduction*, 49, 101761. <https://doi.org/10.1016/j.ijdrr.2020.101761>

In Study I, we conducted a survey with a conjoint-choice experiment (N=810) to assess the public's preferences for information on multi-hazard overviews and hazard notifications.

The **main results** are that the public prefers...

- ... a single map on which all current hazards are displayed.
- ... textual information about the current hazards below the map.
- ... hazard classifications with four or five categories.

... a combination of pictured and textual behavioural instructions for unpredictable hazards such as earthquake. For predictable hazards such as storms, they prefer written behavioral recommendations.

... hazard messages with a sharing function.

Regarding the **personal and social factors**, ...

... people who trust in actors involved in the communication process are more motivated to seek for further information and to take (precautionary) actions.

... people with high numeracy skills answer more map interpretation questions correctly.

... people who have never experienced any hazard yet struggle more to understand the provided information.

... people's risk perception influences their design preferences, i.e. people with a high risk perception perceive single maps as more useful and the hazard categories "alert, warning, information and clear".

... people with high levels of trust and risk perception rate the hazard messages overall better.

### **Study II: Why should I use a multi-hazard app? Assessing the public's information needs and app feature preferences in a participatory process.**

Dallo, I., & Marti, M. (2021). Why should I use a multi-hazard app? Assessing the public's information needs and app feature preferences in a participatory process. *International Journal of Disaster Risk Reduction*, 57, 102197. <https://doi.org/10.1016/j.ijdrr.2021.102197>

In Study II, we conducted seven focus groups à four to five participants in order to better understand which hazards, information, and features people prefer to have on a multi-hazard app.

The **main results** are that the public prefers...

... the combination of multiple hazards on an app. To this end, not only combining natural hazards but also anthropogenic and socio-natural hazards.

... only the most relevant information should be provided on the app and a forwarding function forwards the users to the official website to access more detailed information.

People define the following as relevant information: location, time, hazard severity, behavioural recommendations and the contact details of emergency services.

... short-term & real-time information (containing behavioural recommendations & contact numbers)

... features such as push notifications, buttons to ask for help, sharing feature, chat forum, 'I am Safe' button, report button.

... interlinking/using existing apps, such as sending push notifications via general-purpose apps (e.g., weather apps) and communicating specific information on disaster apps.

### **Study III: An analysis of the earthquake map on the MeteoSwiss app with regard to comprehensibility and its potential for improvement**

Valenzuela Rodríguez, N. (2021). Die aktuelle Erdbebensituation der Schweiz visualisieren—Eine Analyse der Erdbebenkarte der MeteoSchweiz-App hinsichtlich ihrer Verständlichkeit und ihres Verbesserungspotenzials [Master Thesis, Zurich University of Applied Sciences (ZHAW)]. <https://www.polybox.ethz.ch/index.php/s/vaBmjfUr0AgaVtS>

In Study III, we conducted four interviews with the public and a survey (N=356) to assess how to improve the current event-related earthquake notifications on the Swiss Meteo app.

The **main results** are that ...

... when communicating earthquake information together with other natural hazards on one platform, especially the time-related aspects are misleading. For the weather-related hazards (e.g., storms, heatwaves, floods), warnings are mainly provided before an event. This in contrast to earthquakes, where post-event information is presented. Many people currently do not understand this and think the earthquake information is a forecast too. A time slider allowing people to go backwards and forwards or with a text element highlighting that the information provided on the map shows earthquakes that occurred in the past may minimize this misunderstanding.

... when the authorities decide to have consistent danger levels they have to make sure that the names of the levels are clear and do not imply that the event will happen in the future. For example, the hazard level “moderate danger” is ambiguous for people as they are not sure whether this is a hazard assessment of an ongoing/past event or an estimation of the impact of a future event.

... one has to clearly differentiate between the icon of the epicenter and the person’s location. We recommend using a blue circle for the user location that is used by google maps, and not a red circle, for example.

... in times with no recently felt earthquakes, a map with a gray background is misinterpreted. People think that the seismic stations are not working or that they do not have to worry about earthquakes. A neutral map (e.g., basic map with hill shades) with no borders or the regional borders is a much better solution.

... the complementary textual information should contain the location and time of the earthquake, its expected impact, behavioral recommendations for during and after the shaking, the possibility to report an earthquake, and the source of the information.

### **Study IV: Actionable and understandable? Evidence-based recommendations for the design of (multi-)hazard overviews and messages**

Dallo, I., Stauffacher, M., & Marti, M. (2022). Actionable and understandable? Evidence-based recommendations for the design of (multi-)hazard warning messages. *International Journal of Disaster Risk Reduction*, 74, 102917. <https://doi.org/10.1016/j.ijdrr.2022.102917>

In Study IV, we conducted five virtual workshops with scientists and practitioners from different fields to co-produce hazard overviews and hazard messages (N=15), which we then tested with a public survey using a between-subjects experiment (N=601).

The **main results** with respect to the *multi-hazard overviews* are the following:

... Providing a time indication (before, during or after) and an action keyword (inform, prepare, act) for each hazard on the overview ensures that people understand which hazards are urgent and ask for immediate action. Further it triggers people to access further information and minimises their misconception that the earthquake post-event messages are forecasts as most of the weather-related hazard messages are.

... If clearly defined, the choice of the hazard categorization has no effect on people's understanding and perception of the information and their intention to take action.

... Information presented in a list is better understood, perceived as better structured and clearer than the same information presented on a map. However, participants liked the map better than the list.

... A map supported with textual information is perceived as most useful and trust-worthy.

The **main results** with respect to the hazard messages are:

... We identified two misconceptions. First, people think that the most important recommended action is the one at the top of the list. Second, people struggle to understand whether the potential impacts listed in the forecast messages will actually occur or not. Further research thus is needed to explore how to best communicate the corresponding uncertainties and probabilities.

... We confirm the importance of the information elements: hazard type and level, affected areas, time, behavioural recommendations, possible impacts and source. In addition, we recommend adding a time- and action-related icon as our study showed that such an icon motivates people to take action and ensures that they understand whether it is information before, during or after an event.

## Overall recommendations

Dallo, I. (2022). Understanding the communication of event-related earthquake information in a multi-hazard context to improve society's resilience [Doctoral dissertation]. ETH Zurich. <https://doi.org/10.3929/ethz-b-000535657>

These four studies allowed us to derive specific recommendations on how to best present event-related earthquake information on multi-hazard platforms (Figure 5.3.2) and on how to design understandable and actionable earthquake notifications (Figure 5.3.3).

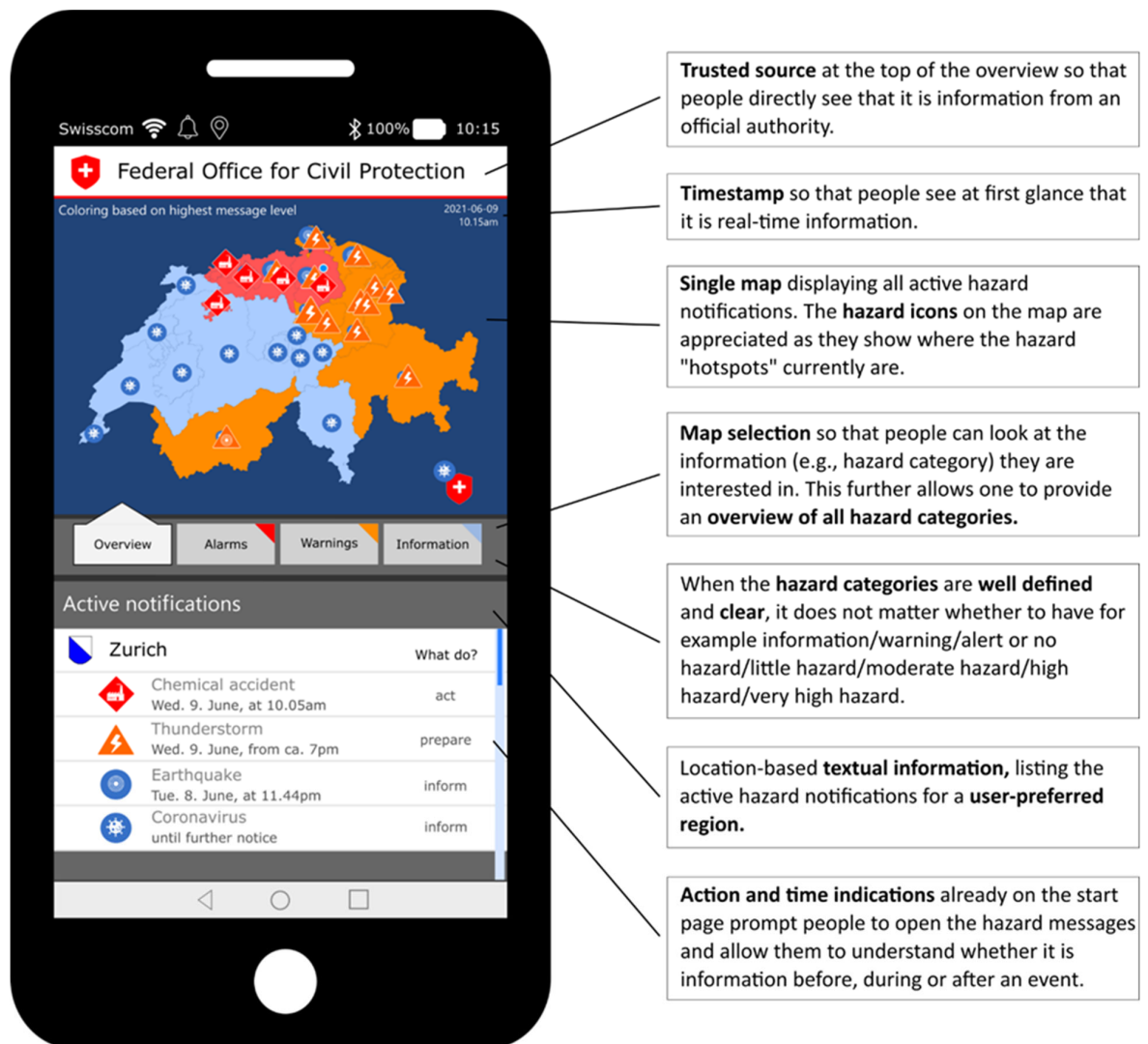


Figure 5.3.2: Recommendations on how to include event-related earthquake information on multi-hazard platforms [from (Dallo, 2022)].



**Forwarding feature** as the first thing that many people want to do is to inform their relatives and friends.

**Trusted source** at the top of the message so that people directly see that it is information from an official authority.

Information about the **hazard type, hazard level and affected areas**.

**Action- and time-related icon**, highlighting which action people should take (prepare, inform, act) and whether it is information before, during or after an event.

**General description** of the event (e.g., time of occurrence, specific characteristics of the hazard) and the **possible impacts** (that may be) caused by the event.

**Interactive features** such a report button, an "I am safe" button or "I need help" button.

**Behavioral recommendations** trigger people to take action. One must be aware that people tend to believe that the most important action is the one at the top of the list. Additionally, a combination of visual and textual behavioral recommendations is wished by the public and allows people not speaking the language in which the message is provided to understand what they can/should do.

**Link** which allows people to **access further information** on the official websites of the responsible authorities.

**Contact details of the responsible authorities** in case people have specific questions. For severe events, also **emergency numbers** should be listed.

**Publication date** so that people know whether the information is still relevant or not and when the message was disseminated.

Figure 5.3.3: Recommendations on how to compile actionable and understandable earthquake notifications for immediately after an event [from (Dallo, 2022)].

## Earthquake early warning - the societal perspective

Dallo, I., Marti, M., Clinton, J., Böse, M., Massin, F., & Zaugg, S. (2022). Earthquake early warning in countries where damaging earthquakes only occur every 50 to 150 years – The societal perspective. *International Journal of Disaster Risk Reduction*, 83, 103441. <https://doi.org/10.1016/j.ijdrr.2022.103441>

In addition to our efforts in Task 5.3 where we assessed which information people prefer to receive immediately after an event, we also analysed how to design earthquake early warnings people, in the optimal way, receive a few seconds before shaking starts (or during shaking). The challenge here is that people should directly grasp what they should do without losing any time.

We conducted again a survey with a between-subjects experiment (N=596) in Switzerland to assess public EEW system preferences and test different versions of EEW messages to identify elements which trigger people to take protective actions on the spot. The questions were adapted from other surveys that were already conducted in Japan, New Zealand, and the US. This allowed us to compare the Swiss public preferences with those in other countries. After the Swiss survey, we also conducted a similar survey in four countries in Central America (Nicaragua, Costa Rica, Guatemala, El Salvador)<sup>1</sup>, which allowed us to do further cross-cultural comparisons.

The **main insights** from the Swiss survey are:

- The public attitudes in countries with moderate seismic hazard are similar to attitudes in countries with high seismic hazard; i.e. Switzerland, New Zealand, the US, and Japan.
- Pictograms trigger people to protect themselves on the spot.
- Maps prompt the public to look for further information or warn others.
- Designs generally preferred by the public are not always those that actually trigger them to take action.
- People would like to receive a second message with more detailed information.
- People tend to react proportionally to the hazard level indicated in the EEW message. Thus, high alert levels motivate people to take protective actions on the spot.
- People prefer to receive EEW alerts for earthquakes that may be felt or are certainly felt.
- People think that they would need 20 or more seconds between receiving the message and the beginning of the shaking to be able to take protective actions.
- People prefer to receive EEW alerts as push notifications
- Misconceptions exist that need to be addressed in education campaigns: i) alerts are sent a couple of minutes to hours before the earthquake strikes; ii) earthquakes are predicted; and iii) foreshocks are registered and a warning is issued for an expected strong earthquake. These exemplary misconceptions can lead to delayed and inaccurate actions.

### WP5 - Joint efforts

Developing and implementing effective communication products, as described in Task 5.1 and Task 5.3, is challenged by the potential spread of misinformation, disinformation, and/or

<sup>1</sup> [https://papers.ssrn.com/sol3/papers.cfm?abstract\\_id=4348227](https://papers.ssrn.com/sol3/papers.cfm?abstract_id=4348227) [preprint]

conspiracy theories. On social media, misinformation can spread rapidly around the world and lead to behaviors that worsen an emergency. Especially after an event, misinformation about predictions and the causes of the earthquake circulate, which has been again observed in the 2023 Türkiye–Syria earthquake sequence.<sup>2</sup> Thus, resources are needed to counteract the spread and provide accurate information.

Therefore, a joint effort between WP5 in RISE and researchers of the Horizon-2020 project [TURNkey](#) was initiated with the primary aims i) to develop recommendations on how to fight earthquake misinformation, and ii) to conduct an expert elicitation. During the process, also communication experts from the US and New Zealand joined our team. In detail, we first did a proper literature review, conducted expert interviews to assess the current status of common communication products, and exchanged our experiences with communicating with the general public. Second, we organised a virtual workshop with representatives of the earth science community to collect a list of the most common earthquake myths. Third, we ran an online survey to let experts elicit the correctness of these common earthquake myths. The results were then presented at a virtual workshop and again discussed with the representatives of the earth science community. An overview of all activities is visible in Figure 5.3.4.

A key output of these efforts is a communication guide<sup>3</sup> that provides general recommendations on how to prevent and fight misinformation about earthquakes, an overview of when different types of earthquake information are available and a timeline that allows strategic planning of the communication during all phases of the seismic cycle. Further, it contains advice on how to deal with misinformation around commonly debated topics: how earthquakes are generated (“Creating earthquakes”), whether earthquakes can be predicted (“Predicting earthquakes”), and whether there is a link between earthquakes and climate (“Earthquakes and Climate”). The communication guide is intended to support institutions, scientists and practitioners who are communicating earthquake information to the public.

A further output is a peer-reviewed publication that presents the insights from the online survey and provides the first elicitation of the opinions of 164 earth scientists on the degree of verity of common public earthquake myths. The results provide important insights for the state of knowledge in the field, helping identify those areas where consensus messaging may aid in the fight against earthquake related misinformation and areas where there is currently lack of consensus opinion.

---

<sup>2</sup> <https://www.theguardian.com/commentisfree/2023/feb/14/turkey-syria-earthquake-misinformation-relief-efforts-turkey>  
[10.03.2023]

<sup>3</sup> The communication guides are available in English (<https://doi.org/10.3929/ethz-b-000530319>) and Spanish (<https://doi.org/10.3929/ethz-b-000559288>).

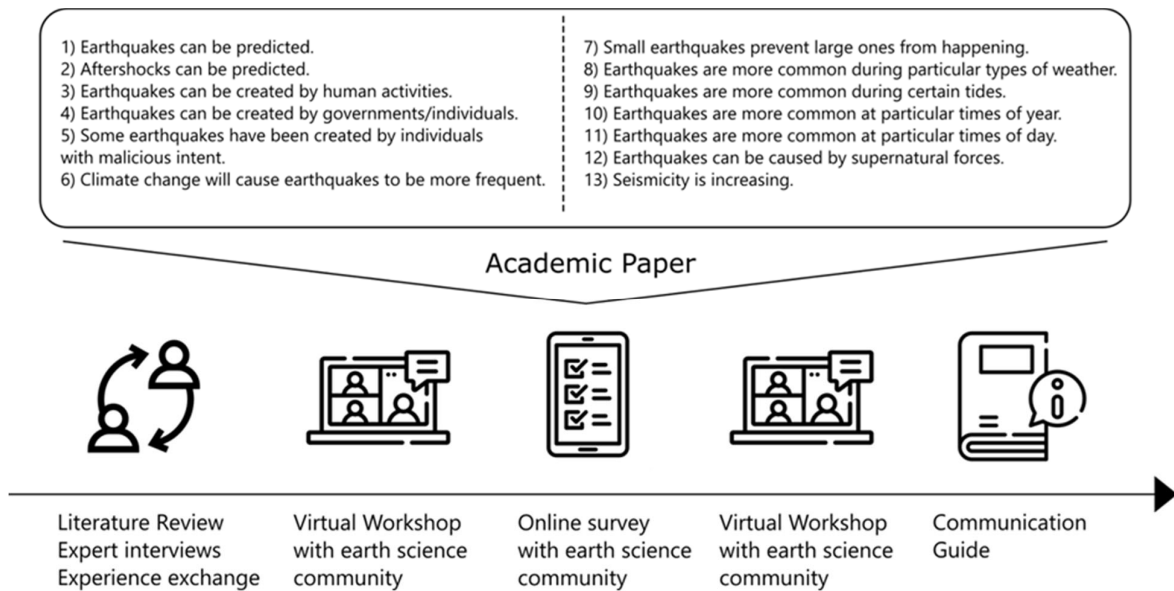


Figure 5.3.4: Overview of the activities of the joint effort regarding earthquake misinformation

The research efforts on earthquake misinformation (on social media) of the EMSC and ETH Zurich group continue as part of the Horizon-2020 project 'sCience and human factOr for Resilient sociEty' ([CORE](#)).

### List of submitted deliverables and achieved milestones in WP5

D5.1: Review of best practice in communication of dynamic risk in all fields

D5.10: Improving earthquake information in a multi-hazard context

MS30: First draft of communication measures

MS36: Concept for multi-hazard warning app completed

### Summary of Exploitable Results in WP5

#### 1) Peer reviewed publications

- Aiello, L., Argiento, R., Finazzi, F., & Paci, L. (2023). Survival modelling of smartphone trigger data for earthquake parameter estimation in early warning. With applications to 2023 Turkish-Syrian and 2019 Ridgecrest events. Under review at: Journal of the Royal Statistical Society. Series A.
- Lilienkamp, H., Bossu, R., Cotton, F., Finazzi, F., Landès, M., Weatherill, G., & von Specht, S. (2023). Utilization of Crowdsourced Felt Reports to Distinguish High Impact from Low Impact Earthquakes Globally within Minutes of an Event. The Seismic Record, 3(1), 29-36.
- Pennington, C. V., Bossu, R., Ofli, F., Imran, M., Qazi, U. W., Roch, J., & Banks, V. J. (2022). A near-real-time global landslide incident reporting tool demonstrator using social media and artificial intelligence. International Journal of Disaster Risk Reduction, 103089.
- Ofli, F. Qazi U., Imran M., Roch J., Pennington C., Banks V. & Bossu R. (2022). A Real-Time System for Detecting Landslide Reports on Social Media Using Artificial Intelligence. Web Engineering. ICWE 2022., vol 13362. Springer, Cham. [https://doi.org/10.1007/978-3-031-09917-5\\_4](https://doi.org/10.1007/978-3-031-09917-5_4)

- Fallou, L. Finazzi F., and Bossu R. "Efficacy and Usefulness of an Independent Public Earthquake Early Warning System: A Case Study—The Earthquake Network Initiative in Peru." *Seismological Research Letters* (2022).
- Finazzi, F., Bondár, I., Bossu, R. & Steed, R. (2022). A Probabilistic Framework for Modeling the Detection Capability of Smartphone Networks in Earthquake Early Warning. *Seismological Research Letters*, 93, 3291–3307.
- Finazzi, F. & Tchoussi, F.Y.M. (2023). A simulation framework for statistical inference on the alerting capabilities of smartphone-based earthquake early warning systems. With a case study on the Earthquake Network system in Haiti. Under review at: *Stochastic Environmental Research and Risk Assessment*.
- Bossu, R., Finazzi, F., Steed, R., Fallou, L., & Bondár, I. (2021). "Shaking in 5 Seconds!"—Performance and User Appreciation Assessment of the Earthquake Network Smartphone-Based Public Earthquake Early Warning System. *Seismological Society of America*, 93(1), 137-148.
- Dallo, I., & Marti, M. (2021). Why should I use a multi-hazard app? Assessing the public's information needs and app feature preferences in a participatory process. *International Journal of Disaster Risk Reduction*, 57, 102197. <https://doi.org/10.1016/j.ijdr.2021.102197>
- Dallo, I., Marti, M., Clinton, J., Böse, M., Massin, F., & Zaugg, S. (2022). Earthquake early warning in countries where damaging earthquakes only occur every 50 to 150 years – The societal perspective. *International Journal of Disaster Risk Reduction*, 83, 103441. <https://doi.org/10.1016/j.ijdr.2022.103441>
- Dallo, I., Stauffacher, M., & Marti, M. (2020). What defines the success of maps and additional information on a multi-hazard platform? *International Journal of Disaster Risk Reduction*, 49, 101761. <https://doi.org/10.1016/j.ijdr.2020.101761>
- Dallo, I., Stauffacher, M., & Marti, M. (2022). Actionable and understandable? Evidence-based recommendations for the design of (multi-)hazard warning messages. *International Journal of Disaster Risk Reduction*, 74, 102917. <https://doi.org/10.1016/j.ijdr.2022.102917>
- Dryhurst, S., Mulder, F., Dallo, I., Kerr, J. R., McBride, S. K., Fallou, L., & Becker, J. S. (2022). Fighting misinformation in seismology: Expert opinion on earthquake facts vs. fiction. *Frontiers in Earth Science*, 10. <https://www.frontiersin.org/articles/10.3389/feart.2022.937055>
- Fallou, L., Marti, M., Dallo, I., & Corradini, M. (2022). How to fight earthquake misinformation: A communication guide. *Seismological Research Letters*. <https://doi.org/10.1785/0220220086>
- Marti, M., Dallo, I., Roth, P., Papadopoulos, A. N., & Zaugg, S. (2022). Illustrating the impact of earthquakes: Evidence-based and user-centred recommendations on how to design earthquake scenarios and rapid impact assessments. Submitted to *International Journal of Disaster Risk Reduction*.
- Massoda Tchoussi, F.Y., & Finazzi, F. (2023). A statistical methodology for classifying earthquake detections and for earthquake parameter estimation in smartphone-based

earthquake early warning systems. *Frontiers in Applied Mathematics and Statistics*, 9:1107243.

- Vannucci G., Gasperini P., Gulia L. & Lolli B. (*next submission*) Earthquakes parameters from citizen testimonies. A retrospective analysis of EMSC database

## 2) Conference publications

### Sessions

- Peppoloni, S., Fallou, L., Dallo, I., & Mulder, F. (2022). *Seismology, geoethics and society: risk communication at the service of risk reduction*, ESC Conference 2022, [https://3eceeds.ro/wp-content/uploads/2022/02/S13\\_Seismology%5eJ-geoethics-and-society-risk-communication.pdf](https://3eceeds.ro/wp-content/uploads/2022/02/S13_Seismology%5eJ-geoethics-and-society-risk-communication.pdf)
- Dallo, I., Marti, M., Fallou, L., & Bossu, R. (2022). *How to best communicate dynamic hazard and risk information?*, EGU General Assembly 2022, <https://meetingorganizer.copernicus.org/EGU22/session/43036>
- Illingworth, S., Roop, H., Stiller-Reeve, M., Trimm, K., Fallou, L., Dallo, I., Marti, M., & Mulder, F. (2021). *Science to Action: Communication of Science and strategies to fight misinformation – Practice, Research and Reflection*, EGU General Assembly 2021.

### Presentations

- Dallo, I., Stauffacher, M., and Marti, M. (2022). *Communicating actionable and understandable event-related information on multi-hazard platforms*, EGU General Assembly 2022, hybrid, <https://doi.org/10.5194/egusphere-egu22-244>.
- Dallo, I., Mati, M., Wiemer, S., & Haslinger, F. (2022). *Evidence-based and user-centred recommendations on how to design rapid impact assessments and risk scenarios for earthquakes*, ESC Conference 2022, in-person.
- Dallo, I. (2021). *Tools and methods to explore how to best communicate event-related earthquake information in a multi-hazard context*, *Workshop Learning from Earthquakes – Tools and methods for post disaster reconnaissance missions*, virtual, [https://www.youtube.com/watch?v=nFamacZhHMI&list=PLONz\\_E1IdJZu5SaFsmzGJq\\_Kbe8YwRrcmj&index=10](https://www.youtube.com/watch?v=nFamacZhHMI&list=PLONz_E1IdJZu5SaFsmzGJq_Kbe8YwRrcmj&index=10)
- Dallo, I., Fallou, L., Corradini, M., Marti, M., Mulder, F., Dryhurst, S., McBride, S., Schneider, M., Luoni, G., & Becker, J. (2021). *Evidence-based recommendations to effectively combat misinformation*, ESC Conference 2021, virtual, <https://polybox.ethz.ch/index.php/s/o5Bvyt0BgnOZokw>
- Dallo, I. and Mati, M. (2021). *Earthquake Early Warning in countries where damaging earthquakes only occur every 50 to 150 years – the Swiss case study*, ESC Conference 2021, virtual, <https://polybox.ethz.ch/index.php/s/rD2EDAN7BA6ekKV>
- Marti, M., Valenzuela, N., Crowley, H., Danciu, L., Dallo, I., al Dabbeek, J., & Zaugg, S. (2021). *Bringing the models to the people – the communication strategy behind the launch of the first seismic risk model for Europe and the next generation seismic hazard model*, ESC Conference 2021, virtual.

- *Dallo, I. and Marti, M. (2021). How to best involve different stakeholders in the design process of products and services to communicate multi-hazard information?, EGU General Assembly 2021, virtual, <https://doi.org/10.5194/egusphere-egu21-815>.*
- *Dallo, I., Stauffacher, M., and Marti, M. (2020). Understanding public's preferences for information provided on multi-hazard warning platforms, EGU General Assembly 2020, virtual, <https://doi.org/10.5194/egusphere-egu2020-1420>.*

•

### **3) Other exploitable results/data/reports**

- CsLoc exists as a service and will be integrated in the LastQuake system
- Dallo, I. (2022). Understanding the communication of event-related earthquake information in a multi-hazard context to improve society's resilience [Doctoral dissertation]. ETH Zurich. <https://doi.org/10.3929/ethz-b-000535657>
- Dallo, I., Corradini, M., Fallou, L., & Marti, M. (2022). How to fight misinformation about earthquakes? - A Communication Guide [Application/pdf]. 24 p. <https://doi.org/10.3929/ETHZ-B-000530319> [available in English and Spanish]
- Dallo, I. & Marti, M. (2020). Multi-Gefahren-Plattformen – Präferenzen der Bevölkerung. <https://ethz.ch/content/dam/ethz/specialinterest/usys/tdlab/docs/research/multigefahrenplattform.pdf>
- Valenzuela Rodríguez, N. (2021). Die aktuelle Erdbebensituation der Schweiz visualisieren—Eine Analyse der Erdbebenkarte der MeteoSchweiz-App hinsichtlich ihrer Verständlichkeit und ihres Verbesserungspotenzials [Master Thesis, Zurich University of Applied Sciences (ZHAW)]. <https://www.polybox.ethz.ch/index.php/s/vaBmjfUr0AgaVtS>

## 1.2.6 Work package 6

### Overview

WP6 deals with diverse pilot and demonstration activities that cover a wide range of potential applications of OEF, EEW, RLA and SHM; they also cover very different scales, from building scale application to national and even Europe-wide scale.

The main objectives of WP6 are to:

- Demonstrate how the use of big data collected through innovative technologies at the building-level (e.g. SHM) can be used for critical risk mitigation services (including RLA and OELF) at the city level (Task 6.1).
- Provide clear applications to demonstrate the chain from earthquake predictability to OELF and RLA at national levels (with focus on Italy and Iceland) (Tasks 6.2, 6.3).
- Clearly integrate a large number of activities from WPs 2 to 8 by developing a user-centric dynamic risk framework for Switzerland (Task 6.4).
- Make clear steps towards the development of services for RLA, EEW and OEF at a European level (Task 6.5).

The following sections highlight the main achievements towards these objectives in each task of work package 6.

### Summary of achievements in WP6 tasks

#### Task 6.1 Pilot projects for demonstrating the use of innovative technology in buildings within OELF, RLA, performance based EEW & SHM

The main objective of this task was to demonstrate how different developments of the RISE project in the fields of operational earthquake loss forecasting (OELF), rapid loss assessment (RLA) and structural health monitoring (SHM) can work together for the dynamic assessment of seismic damage and losses. To this end, the software named Real-Time Loss Tools was developed and released as an open-source tool that the research community can use to continue to explore all the aspects of this integration and develop strategies for future scalability and operationalisation, beyond the RISE project (<https://git.gfz-potsdam.de/real-time-loss-tools/real-time-loss-tools>).

The Real-Time Loss Tools are designed to carry out a user-input series of RLAs and/or OELFs and output damage and loss results that take into account the accumulation of damage due to successive earthquake action and the dynamic variation of building occupants associated with it. This is, to our knowledge, the first publicly-available attempt to carry out such an update to the number of people present in buildings at different stages of an earthquake sequence, due to both their own health status (injury, death) and the time needed to inspect and repair buildings in different damage states. The ground motions and resulting damage for each earthquake in the sequence and/or in the input short-term seismicity forecast are calculated by recursively calling the well-established OpenQuake engine (Pagani et al. 2014; Silva et al., 2014), while any user-input external source of damage assessment (such as SHM) for any particular building in the exposure model is incorporated by the Tools to the RLAs and takes precedence (for that building) over the OpenQuake damage results. The Real-Time Loss Tools create and/or update all necessary OpenQuake input files whose content needs to change during an earthquake sequence, including

the exposure model, which keeps track of the evolution of damage and number of expected people in the buildings.

The Real-Time Loss Tools have been used within Task 6.1 for a series of proof-of-concept case studies that focused on the 2009 L’Aquila and 2016-2017 Central Italy earthquake sequences and aimed at demonstrating the overall workflow of its main components, which include a series of inputs stemming directly from the RISE project:

- Short-term seismicity forecasts for Italy: The output of the *ETAS.inlabru* model (Serafini et al., 2023; Naylor et al., 2023) developed as part of RISE Task 3.3 is input in the form of catalogues (CSV files) of 10,000 possible 24-hour realisations of seismicity.
- SHM-based fragility models and probabilities of damage for monitored buildings: The output of the method developed within RISE Task 4.4 by Reuland et al. (2023a), based on damage-sensitive features (Reuland et al., 2023b) extracted from sensor data was used.
- State-dependent fragility models for Italian structural typologies developed by Orlacchio (2022) within RISE Task 4.2, which take as a starting point the state-independent fragility models of the European Seismic Risk Model 2020 (ESRM20; Crowley et al., 2021), which were finalised in RISE Task 4.1.
- Dynamic characterisation and structural properties of a 15-storey reinforced concrete shear-wall hotel in Budva, Montenegro, studied within RISE Task 6.1 by the University of Montenegro (GF-UCG) and instrumented with four low-cost QUAKE sensors. Details on the evaluation of the seismic performance of this building can be found in Popovic and Pejovic (2023).
- Dynamic characterisation and structural properties of the 13-storey reinforced concrete shear-wall Grenoble City Hall, which has been permanently instrumented since November 2004 and studied (in the long-term and within RISE) by the University of Grenoble Alps (UGA).
- Dynamic characterisation and structural properties of a theoretical building representative of typical Swiss residential structures, studied by IBK-ETH within Task 4.4.

The concept of the Dynamic Exposure Model developed by Schorlemmer et al. (2020) within RISE Task 2.7 (Deliverable D2.13) was used for this proof of concept as well. In this model, building exposure is defined in terms of a series of individual buildings whose footprints are retrieved from OpenStreetMap (OSM) and quadtree-formulated tiles of zoom level 18 (around 100-m side in central-southern Europe) that group buildings expected to exist in the tile but not yet represented in OSM. The model itself was not used, as it was decided to focus the proof of concept on buildings well-studied within RISE that allow us to incorporate the SHM component to the proof of concept, but these do not co-exist in the same real physical location. The proof of concept was thus based on a fictitious building portfolio, which combined Task 4.2 Italian building types—aggregated into nine zoom-level 18 tiles—with the existing monitored buildings in Montenegro and France, and the idealised Swiss building—the last three represented in the exposure model with their individual footprints. As the exposure model is input to the Real-Time Loss Tools in the OpenQuake CSV format, neither the Tools themselves nor the method or workflow are limited to this particular representation of exposure.

As the new generation of seismicity forecasts developed as part of RISE Task 3.3 output large numbers of stochastic realisations of seismicity (i.e., full catalogues of possible earthquakes) instead of earthquake rates on a grid, the Real-Time Loss Tools depart from the closed-form rate-based analytical formulation of MANTIS-K (Iervolino et al., 2015) and MANTIS v2.0 (Deliverable 4.3) (see Tasks 4.2 and 6.2) and instead carry out operational earthquake loss forecasts in an event-based manner, by means of a stochastic generation of ruptures for the earthquakes in the input seismicity forecast. The case-studies run within Task 6.1 with the Real-Time Loss Tools show that computational running times for OELF with such an approach pose a challenge, and hope that the Tools may serve as a means for future interactions with the OpenQuake-engine developers, with a view to getting OELF one day implemented in OpenQuake in a manner that resolves the efficiency challenges.

The proof of concept developed and presented in Deliverable 6.1 represents what would have been calculated during the 2009 L'Aquila and 2016-2017 Central Italy earthquake sequences if a RLA and event-based OELF system of this kind had been implemented and operational at the time. The two sequences were chosen to represent a case in which most of the damage occurred in the first large shock (L'Aquila) and a case in which damage increased gradually or with different shocks in the sequence, also depending on the location (Central Italy). As these sequences did not actually affect the three monitored buildings, non-linear time-history analyses (NLTHAs) were used to simulate what their SHM sensors would have recorded (provided they were all fully functioning at the time of the earthquakes). The need for accelerograms to run these NLTHAs motivated us to select study sites where seismological stations had effectively recorded the two earthquake sequences, and led to the identification of three and four sites for the L'Aquila and Central Italy sequences, respectively, which are shown in Figure 6.1.1. The same fictitious exposure model was thus placed at these seven different locations, yielding seven different case-studies, of which three were presented in detail in the deliverable.

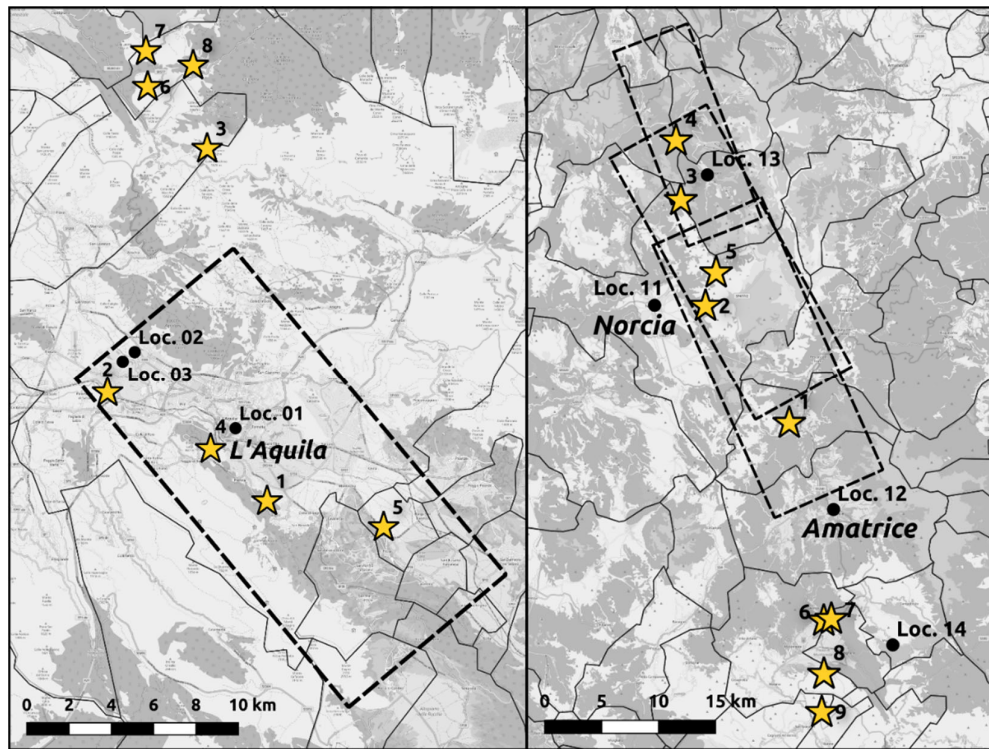


Figure 6.1.1 Earthquake epicentres (numbered stars) and exposure locations (black dots) used as case-studies for the 2009 L'Aquila (left) and 2016-2017 Central Italy (right) earthquake sequences in Tasks 6.1 and 4.6. Rupture planes of larger shocks from the Italian Accelerometric Archive (ITACA; Russo et al., 2022) shown as dashed polygons. Background: OpenStreetMap.

Deliverable 6.1, one of the main outcomes of Task 6.1, describes in detail the working of the Real-Time Loss Tools, the components of the complete integrated calculations and models, as well as all the details of the proof-of-concept case studies, which are presented in a step-by-step fashion (e.g., Figure 6.1.2, Figure 6.1.3). The deliverable also includes discussions on considerations to be made for full-scale operational implementations. All input and output files of the Real-Time Loss Tools used for the three presented case-studies have been made publicly available through a GitLab repository (<https://git.gfz-potsdam.de/real-time-loss-tools/rise-d6-1-data-files>) and an associated Zenodo publication. A short paper on the Real-Time Loss Tools has already been submitted to the 2023 SECED conference, and journal papers are now in preparation.

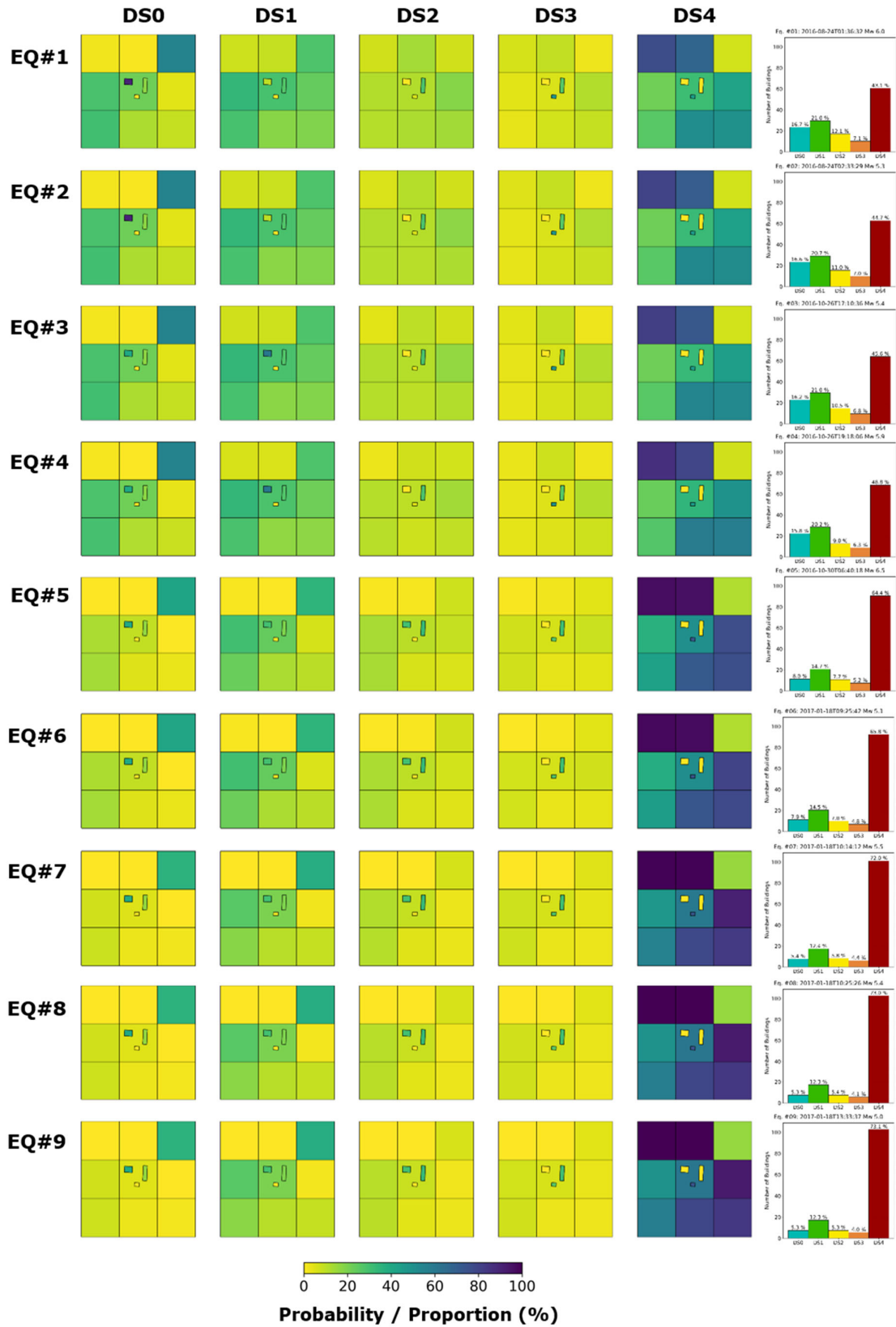


Figure 6.1.2 Expected cumulative probabilities of each damage state for each exposure tile and monitored building (left) and as an aggregate (right) obtained at location 12 after each of the nine earthquakes with magnitude 5.0+ of the 2016-2017 Central Italy sequence.

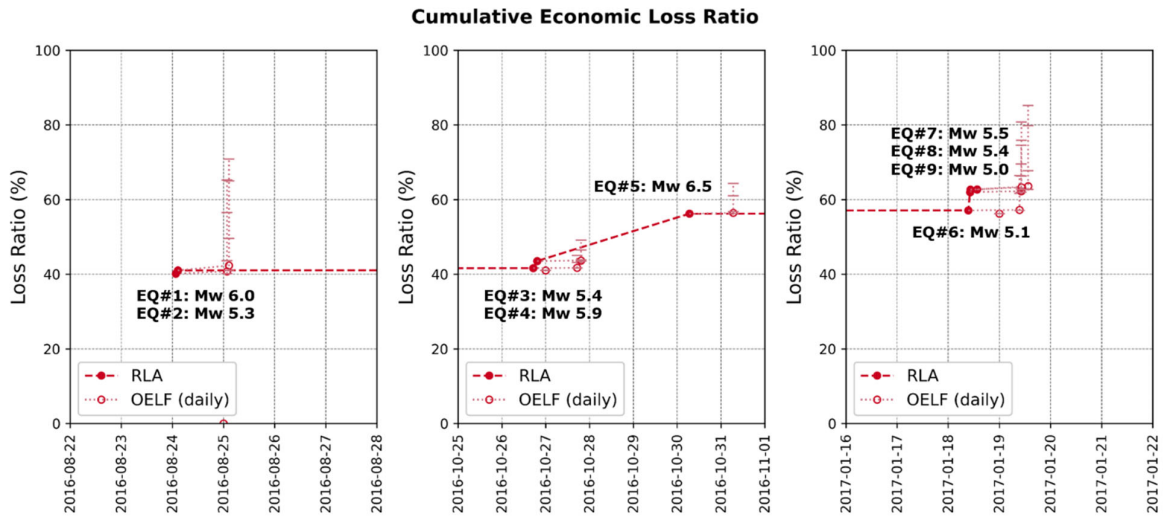


Figure 6.1.3 Cumulative economic loss ratios at location 12 after all nine shocks of Mw 5.0+ of the 2016-2017 Central Italy sequence (RLAs), and subsequent 24-hour seismicity forecasts (OELF, depicted at the end of the 24-hour periods). Vertical error bars show, in order from bottom to top, minimum, mean, 95th, 99th and 99.5th percentiles of loss ratio associated with each OELF.

The Real-Time Loss Tools have also been used to develop the case-studies used for the Multi-Criteria Decision Analysis in Task 4.6. In fact, the capability to carry out cumulative damage calculations using state-independent fragility models was added to the software to support Task 4.6 and be able to compare damage and loss results obtained using state-dependent or state-independent fragility models.

RISE developments in the front of performance-based earthquake early warning (EEW) have been described separately in Deliverable 4.6, where their application was demonstrated as well (see Task 4.5), and their associated publications (e.g., Iaccarino et al., 2021).

The difficulties faced by RISE partners to produce and deploy a large number of low-cost sensors during the project as originally planned (see Deliverable 2.5) resulted in activities that relied on the availability of large volumes of sensor data to be hindered. For this reason, the incorporation of sensor-derived data to exposure models and rapid loss assessment calculations was tackled within Task 6.1 in a more encompassing way that does not limit itself to a particular technological deployment but is based on the development of publicly-available and reproducible methods, such as those developed based on a smaller number of monitored buildings as part of Task 4.4.

Similarly, planned activities aimed at comparing the performance of low-cost sensors and force-balanced accelerometers installed in the Grenoble City Hall (Grenoble, France) and the Sapphire Building (Istanbul, Turkey) were hindered by incompatibilities that precluded the two technologies to be integrated during the project. Fortunately, the permanent instrumentation of the Sapphire Building yielded satisfactory results in the development of a performance-based EEW system for the building, as reported in Deliverable 4.6, and the 18 years of recordings from the permanent instrumentation of the Grenoble City Hall made it possible for a large number of studies to be

carried out by UGA on this building during the project. These include investigations on torsional behaviour (Guéguen et al., 2020; Guéguen and Astorga, 2021), the value of structural health monitoring in areas of weak-to-moderate seismicity (Astorga and Guéguen, 2023; Guéguen et al., 2023) and an analysis on the efficiency of intensity measures from earthquake data recorded in buildings (Ghimire et al., 2021); the comprehensive list can be found under “Summary of Exploitable Results in WP4”.

### **References cited above**

Astorga A, Guéguen P (2023) On the value of weak-to-moderate earthquake data recorded in build-ings. Submitted to Bull. Seism. Soc. Am.

Crowley H, Dabbeek J, Despotaki V, Rodrigues D, Martins L, Silva V, Romão, X, Pereira N, Weatherill G, Danciu L (2021) European Seismic Risk Model (ESRM20), EFEHR Technical Report 002, V1.0.1, 84 pp, <https://doi.org/10.7414/EUC-EFEHR-TR002-ESRM20>

Ghimire S, Guéguen P, Astorga A (2021) Analysis of the efficiency of intensity measures from real earthquake data recorded in buildings. *Soil Dynamics and Earthquake Engineering* 147:106751.

Guéguen P, Astorga A (2021) The torsional response of civil engineering structures during earthquake from an observational point of view. *Sensors* 21(2):342.

Guéguen P, Guattari F, Aubert C, Laudat T (2020) Comparing direct observation of torsion with array-derived rotation in civil engineering structures. *Sensors* 21(1):142. <https://doi.org/10.3390/s21010142>

Guéguen P, Astorga A, Langlais M (2023). Amplitude-frequency noise models for seismic building monitoring in a weak-to-moderate seismic region. Submitted to *Seism. Res. Letters*.

Iervolino I, Chioccarelli E, Giorgio M, Marzocchi W, Zuccaro G, Dolce M, Manfredi G (2015) Operational (short-term) earthquake loss forecasting in Italy. *Bulletin of the Seismological Society of America* 105:2286–2298. <https://doi.org/10.1785/0120140344>

Naylor M, Serafini F, Lindgren F, Main I (2023) Bayesian modelling of the temporal evolution of seismicity using the ETAS.inlabru R-package. *Frontiers in Applied Mathematics and Statistics*, special issue Physical and Statistical Approaches to Earthquake Modeling and Forecasting. <https://doi.org/10.3389/fams.2023.1126759>

Orlacchio M (2022) The effects of seismic sequences on seismic hazard and structural vulnerability. PhD Thesis. University of Naples Federico II, Naples, Italy.

Pagani M, Monelli D, Weatherill G, Danciu L, Crowley H, Silva V, Henshaw P, Butler L, Nastasi M, Panzeri L, Simionato M, Vigano D (2014) OpenQuake engine: An open hazard (and risk) software for the global earthquake model. *Seismological Research Letters* 85(3):692–702.

<https://doi.org/10.1785/0220130087>

Popovic N, Pejović J (2023) Seismic Performance Evaluation of Existing RC High-Rise Building In Montenegro. Proceedings of the 2nd Croatian Conference on Earthquake Engineering - 2CroCEE, Zagreb, Croatia, March 22 to 24, pp. 565-575, <https://doi.org/10.5592/CO/2CroCEE.2023.13>

Reuland Y, Khodaverdian A, Crowley H, Nievas C, Martakis P, Chatzi E (2023a) Monitoring-driven post-earthquake building damage tagging, 10th International Conference on Experimental Vibration Analysis for Civil Engineering Structures, Milan, Italy.

Reuland Y, Martakis P and Chatzi E (2023b) A Comparative Study of Damage-Sensitive Features for Rapid Data-Driven Seismic Structural Health Monitoring, Applied Sciences, 13(4): 2708, DOI: 10.3390/app13042708

Russo E, Felicetta C, D Amico M, Sgobba S, Lanzano G, Mascandola C, Pacor F, Luzi L (2022) Italian Accelerometric Archive v3.2 - Istituto Nazionale di Geofisica e Vulcanologia, Dipartimento della Protezione Civile Nazionale. doi:10.13127/itaca.3.2

Schorlemmer D, Beutin T, Cotton F, Garcia Ospina N, Hirata N, Ma KF, Nievas C, Prehn K and Wyss M (2020), Global Dynamic Exposure and the OpenBuildingMap – A big-data and crowd-sourcing approach to exposure modelling, EGU General Assembly 2020 Conference Abstracts, p. 18920, DOI: 10.5194/egusphere-egu2020-18920

Serafini F, Lindgren F and Naylor M (2023) Approximation of Bayesian Hawkes process with inlabru. Environmetrics, e2798. <https://doi.org/10.1002/env.2798>.

Silva V, Crowley H, Pagani M, Monelli D, Pinho R (2014) Development of the OpenQuake engine, the Global Earthquake Model's open-source software for seismic risk assessment. Natural Hazards 72:1409-1427. <https://doi.org/10.1007/s11069-013-0618-x>

### **Task 6.2 Demonstrating OEF and OELF at regional and national levels: Italy**

The upgraded system for OELF in Italy, MANTIS v2.0, was used to retrospectively analyse two significant seismic sequences: L'Aquila 2009 and Central Italy 2016.

The mainshock (moment magnitude,  $M$ , 6.1) of L'Aquila 2009 struck at 01:32 a.m. of the 06/04/2009 and, from January 2009 to June 2010, a sequence of twenty-four earthquakes with moment magnitude larger than 4.0 occurred, within 50 km from the mainshock epicentre. Among them, those with moment magnitude larger than 4.5 were eight (excluding the mainshock), all of them occurred after the mainshock in a short time interval ranging between 06/04/2009 and 10/04/2009.

The first significant earthquake of the Central Italy seismic sequence occurred at 1:36 on the 24/08/2016. It was characterised by  $M$  equal to 6 and it was followed by a sequence of earthquakes that, until the end of October, showed lower magnitudes. Indeed, the  $M_6$  was

considered as the mainshock of the sequence for several weeks until, at 06:40 on the 30/10/2016, a M6.5 earthquake occurred. The significant length of sequence and the occurrence of several earthquakes of significant magnitude, makes the sequence different from the one of L'Aquila and, thus, interesting for a second application of MANTIS v2.0.

The results computed with the work-in-progress formulation of MANTIS v2.0 for L'Aquila sequence are described in Chioccarelli et al. (2022) in which a comparison with the results provided by MANTIS-K (the first version of the OELF system) is also discussed. On the other hand, the final version of the system was used to compute results of the Central Italy seismic sequence as discussed in Chioccarelli et al. (2023). An example of results is provided in the following figures in which the forecasted percentage of buildings in each damage state (varying from the undamage conditions, DS0, to the complete damage, DS4) for each municipality within the epicentral area of the sequence is reported. The first figure provides results computed after the M6 earthquake of the 24/08/2016 whereas the second figure shows results computed after the 30/10/2016 M6.5 earthquake. Further details are reported in the cited deliverable.

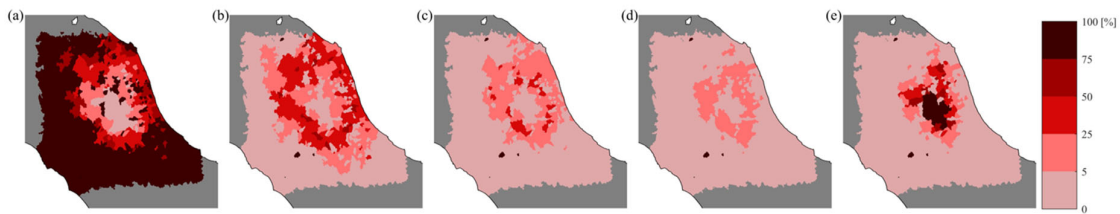


Figure 6.2.1. Expected percentage buildings per municipality in (a) DS0, (b) DS1, (c) DS2, (d) DS3, and (e) DS4: Date of forecasting 24/08/2016, at 02:00.

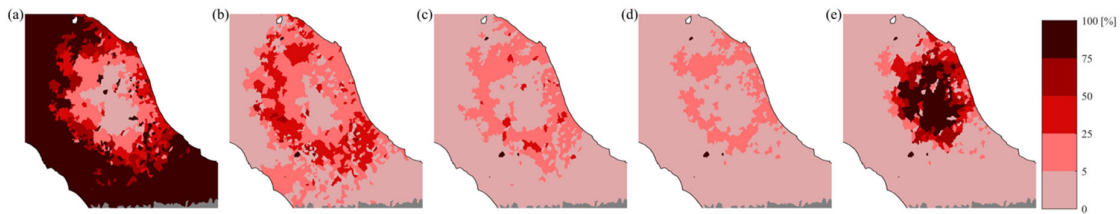


Figure 6.2.2. Expected percentage buildings per municipality in (a) DS0, (b) DS1, (c) DS2, (d) DS3, and (e) DS4: Date of forecasting 30/10/2016, at 07:00.

Figure 6.2.3 summarises the forecasted damage evolution during the whole sequence showing the percentage of buildings in each damage state for all the considered municipalities. As shown, the first forecasting provides about 80% of the buildings in the undamaged conditions: this account for the estimated damage produced by the M6 and M4.5 earthquake occurred at 01:36 and 01:37 and the forecasted damages in accordance with OEF rates released at 02:00. In the last forecast, the expected percentage of buildings in undamaged conditions are about 60% and those in complete damage conditions are less than 20%.

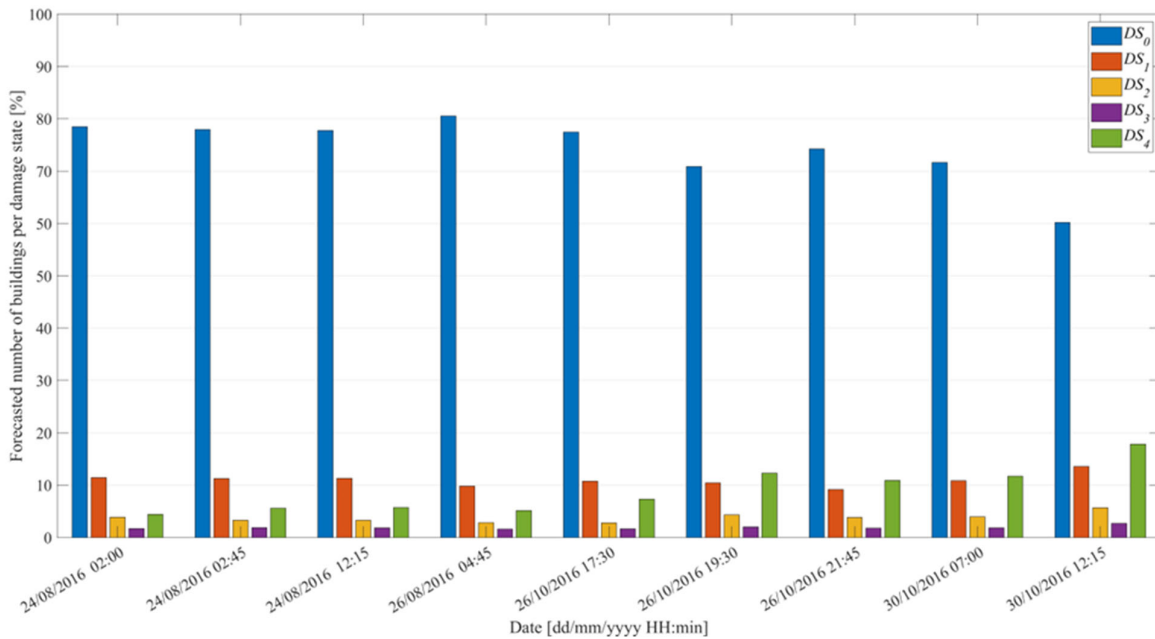


Figure 6.2.3. Expected percentage buildings in each damage state for the whole geographic area. References cited above

Chioccarelli, E., Pacifico, A., & Iervolino, I. (2022). *Operational earthquake loss forecasting for Europe, RISE Project Deliverable 4.3.*

Chioccarelli, E., Pacifico, A., & Iervolino, I. (2023). *Report on testing OEF and extending earthquake forecasts to loss forecasts in Italy, RISE Project Deliverable 6.2.*

### Task 6.3 Application of the chain from earthquake predictability to EEW and RLA in Iceland

#### Rapid Loss Assessment for Iceland (RLA)

In Deliverable D6.3, the customisation of the ESRM20 Rapid Earthquake Loss Assessment service (see Task 6.5) for application in Iceland has been documented.

A GitLab repository has been set up for running the RLA in Iceland ([https://gitlab.seismo.ethz.ch/hcrowley/RISE\\_Iceland\\_scenarios](https://gitlab.seismo.ethz.ch/hcrowley/RISE_Iceland_scenarios)). This repository has exposure (disaggregated to 30 arc second) and vulnerability models needed for RLA and the results of two ShakeMaps produced by IMO (using their upgraded Shakemap system) have been included in this repository. The two ShakeMaps correspond to two events that occurred during the RISE project:

- an earthquake of Mw 5.3 with a depth of 2.7 km (IMO) that occurred on Reykjanes peninsula, close to the town of Grindavík, on 31st July 2022 and which caused some minor damage
- an earthquake of Mw 5.0 that occurred with a depth of 3.9 km, farther east on the peninsula, ~15 km away from Reykjavík, on 2nd August 2022

The ShakeMaps for these events were very different to those produced by the European ShakeMap system, thus highlighting the need for customisation of the system, an activity that is planned in the GeoINQUIRE project.

#### **Task 6.4 Application of a User-Centric Dynamic Risk Framework for Switzerland**

The Swiss Seismological Service (SED) and the Institute of Structural Engineering (IBK) at ETH Zurich are developing a dynamic user-centered earthquake risk framework for Switzerland. This framework uses all available information to assess seismic risk at various stages of the earthquake cycle, and encourages widespread dissemination and communication of the resulting information. Earthquake risk products and services include Operational Earthquake (Loss) Forecasting, Earthquake Early Warning, Rapid Impact Assessment, Structural Health Monitoring, and Recovery and Rebuilding Efforts. Standardization of products and workflows across various applications is essential for achieving broad adoption, universal recognition, and maximum synergies. The harmonization of products into seamless solutions that access the same databases, workflows, and software is crucial in the Swiss dynamic earthquake risk framework. A user-centered approach utilizing quantitative social science tools like online surveys and focus groups is a significant innovation featured in all products and services.

##### **6.4.1 Seismic Hazard**

1000 to 1500 earthquakes are detected in Switzerland and neighboring countries every year, including 20 to 30 events that are felt by the Swiss population. The Swiss Seismic Hazard Model (SUIhaz2015; Wiemer *et al.*, 2016), which assesses the potential for ground shaking, predicts that earthquakes of magnitude  $M \geq 5$  are likely to occur every 8 to 15 years and of  $M \geq 6$  to occur every 50 to 150 years. Geographic features, such as large and deep peri-alpine lakes, steep slopes, and alluvial basins with a high water table, make Switzerland susceptible to secondary hazards, including rockfalls, landslides, lake tsunamis, and liquefaction.

##### **6.4.2 Seismic Risk**

The National Earthquake Risk Model of Switzerland (ERM-CH23; Wiemer *et al.*, 2023), which assesses the potential impact of earthquakes on both people and structures, and resulting financial losses, follows a modular structure with three decoupled components: seismic hazard, structural vulnerability, and exposure. ERM-CH23 is largely supported by high-quality local data, including a database of more than 2 million building objects and a detailed soil model. The economic damage in Switzerland caused by earthquakes over a 100-year period is estimated as CHF 11 to 44 billion for building and contents alone.

##### **6.4.3 Seismic Monitoring → RISE WP 2**

The Swiss Seismic Network counts about 220 permanent stations used to monitor the seismic activity in Switzerland, support scientific research, and assess seismic risk. A newly developed sensor concept allows the SED to deploy much larger numbers of temporary stations more rapidly and in more remote locations. Real-time data acquisition, archival, and distribution, as well as automated earthquake detection and quantification, manual earthquake review, and catalog management is mostly done with SeisComP. For advanced processing the SED has developed new

SeisComP modules, such as *scdetect* for earthquake detection from template matching and *scrtdd* for real-time double difference relocation. Also noise interferometry and machine learning approaches are evaluated and implemented.

#### **6.4.4 Operational EQ (Loss) Forecasting (OEF & OELF) → RISE WP 3 & 4**

In addition to long-term forecasts based on SUIhaz2015, the SED is working on an Epidemic-Type Aftershock Sequence (ETAS)-based earthquake forecasting model for Switzerland that takes temporal fluctuations in earthquake rates into account. The SED is currently developing OEF and OELF systems to produce automated real-time earthquake and loss forecasts for Switzerland.

#### **6.4.5 Earthquake Early Warning (EEW) → RISE WP 4 & 5**

The SED has been developing open-source software and methods for EEW for around one decade. The ETHZ-SED SeisComP EEW (ESE) system with the Virtual Seismologist and Finite-Fault Rupture Detector is used to demonstrate EEW in Switzerland. Earthquakes in areas with high station density are detected in as little as 4 to 6 seconds. Future mass notifications could be enabled through the Swiss multi-hazard *AlertSwiss* and *MeteoSwiss* platforms or cell broadcast once available.

#### **6.4.6 ShakeMaps → RISE WP 4**

The SED has been utilizing ShakeMap® in Switzerland for approximately 15 years and is a core founder and contributor to the European ShakeMap initiative. ShakeMaps are used (i) to inform the Swiss public about the severity of ground shaking and affected areas; (ii) to estimate the likelihood of earthquake-triggered mass-movements for significant events; (iii) to rapidly assess the potential damage caused by ground shaking as part of the SED RIA system.

#### **6.4.7 Rapid Impact Assessment (RIA) → RISE WP 4**

The SED RIA system estimates various types of losses (including damage, economic loss, injuries, deaths, and shelter needs) at the national, cantonal, and municipal levels. The system uses OpenQuake's scenario calculator and ShakeMaps. In the future, the system will become fully integrated and synchronized with the Swiss Seismic Network operations, and perform near-real-time calculations for every earthquake with magnitude  $M > 3.0$  within a specified radius around Switzerland.

#### **6.4.8 Structural Health Monitoring (SHM) → RISE WP 3**

Damage-sensitive features can be extracted from continuous measurements and contribute to the detection and localization of earthquake-induced damage. The IBK has developed several approaches to overcome the scarcity of real-world dynamic monitoring data of both healthy and damaged structures. Integrating monitoring data and engineering models into a robust framework will pave the way to make SHM-based real-time building tagging operational in Switzerland and elsewhere.

#### **6.4.9 Recovery and Rebuilding Efforts (RRE) → RISE WP 4**

By combining regional recovery and resilience assessment tools with the iRe-CoDeS RRE

framework developed by IBK, uncertainty in recovery trajectories can be reduced, and real-time what-if analyses can inform decision-makers on the state of the community during recovery and optimal resource deployment. The iRe-CoDeS model can be updated with early inspection information after an earthquake, providing recommendations for recovery efforts and remaining recovery time.

#### 6.4.10 Communication & Societal Perspective → RISE WP 5

As a federal agency, the SED is responsible for informing the public, authorities, and media about earthquakes in Switzerland, and to provide warnings when needed. To ensure effective communication products, it is necessary to build interdisciplinary expert groups to design and test them with relevant end-users before public release. In preparation of the ERM-CH23 release, the SED has tested various output formats for risk products with professional stakeholders of the society and the general public. To achieve successful campaigns, key factors to consider include regular communication, context, channel choice, risk communicator training, and community-based approaches

### Task 6.5 Demonstrating RLA, EEW and OEF capabilities at a European level

#### 6.5.1 Rapid Loss Assessment (RLA)

The European exposure and vulnerability models from Task 4.1 have been used in the workflow shown in Fig. 6.5.1 as part of a new European Rapid (earthquake) Loss Assessment service to produce damage and loss statistics and maps, based on ShakeMap data (i.e., grid and uncertainty xml files) that are automatically downloaded from the European ShakeMap service (see Task 4.1) using the available webservices, as documented further in Deliverable D6.5.

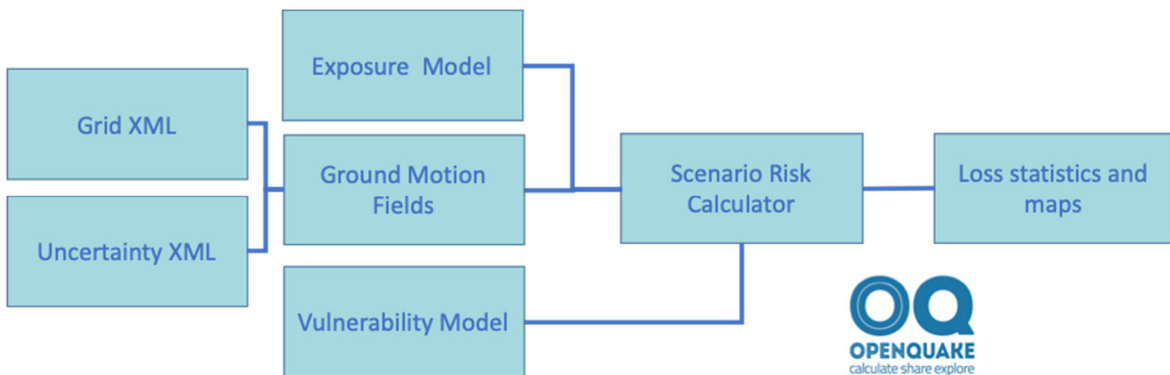


Figure 6.5.1 Scenario from ShakeMap workflow of the OpenQuake engine (Silva et al., 2014; Pagani et al., 2014; Silva and Horspool, 2019)

A first version demonstrator of the ESRM20 Rapid earthquake Loss Assessment service has been openly published on a GitLab repository ([https://gitlab.seismo.ethz.ch/hcrowley/rapid\\_loss\\_eu](https://gitlab.seismo.ethz.ch/hcrowley/rapid_loss_eu)). This demonstrator uses web services to download ShakeMaps as soon as they have been published on the European ShakeMap system, retrieves and crops the 30 arc second resolution exposure models for the countries covered by the ShakeMap grid, and launches the scenario damage and risk calculations with the OpenQuake-engine. Currently the code is set up to calculate completely damaged buildings, economic loss and fatalities, but it can be easily expanded to output other

damage states as well as injuries (using the newly developed injury models from Task 4.1). An example output of the service (in terms of the loss distribution for Turkey and Greece for the 30th October 2020 Samos/Izmir earthquake) is shown in Fig. 6.5.2. The mean, median and fractiles of loss can be extracted from these distributions.

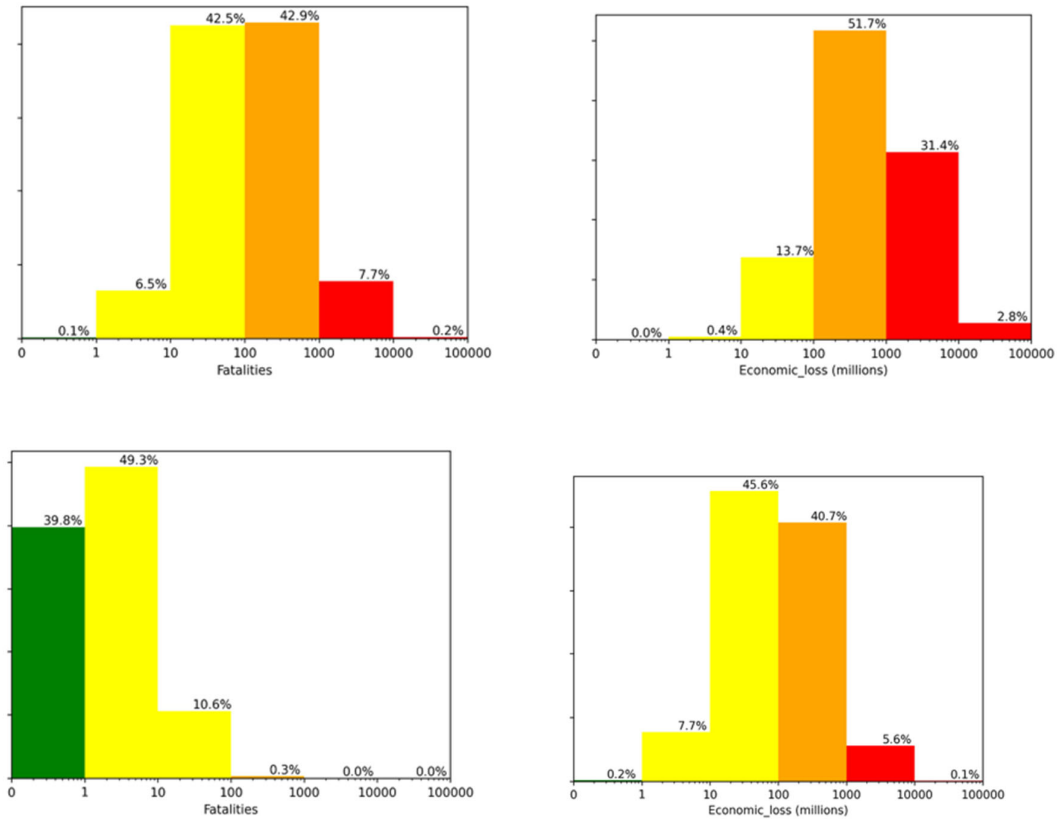


Figure 6.5.2 Example output for the 30th October 2020 Samos/Izmir earthquake. Distribution of the fatalities (left) and economic loss (right) for (top) Turkey and (bottom) Greece based on the PAGER impact scale (Wald et al., 2010)

The ReLA software provides an alert for each metric and country separately, based on the median value in the plots in Figure 6.5.2; there would thus be an orange alert for fatalities in Turkey, but yellow in Greece, and there would be an orange alert for economic loss in Turkey, but yellow in Greece.

The ESRM20 Rapid Earthquake Loss Assessment (ReLA) code has been applied to all events in the European ShakeMap archive since it was launched in 2020 (which at the time of producing this deliverable was a total of 1100 events with magnitude above 4). The results presented in Deliverable 6.5 show that the alert level would have been correctly estimated in 98.6% of the cases (and overestimated by one alert level in 1.4%).

### 6.5.2 European Crowdsourcing-based Earthquake Early Warning (EEW)

Started in 2012, Earthquake Network (EQN) is a citizen science initiative implementing the first smartphone-based earthquake early warning (EEW) system. Thanks to a smartphone app, the

devices made available by citizens are exploited to create a network for the real-time detection of earthquakes. When an earthquake is detected, an alert is sent to the smartphones with the app installed and published on social networks (Twitter and Face-book) and on Telegram channels. The aims of EQN are to possibly alert people before strong ground shaking begins and to improve people's awareness of the seismic events that are happening in their area. The developments of EQN are summarised in Deliverable 6.5.

The recent Turkish-Syrian earthquake of February 6, 2023 has been detected by the EQN system with a delay of only 11 seconds from origin time. This allowed to disseminate a rapid alert to people exposed to very damaging shaking levels. While the data analysis is still ongoing, preliminary results suggest that EQN provided a forewarning up to 25 seconds for people exposed to shaking intensities between 8.5 and 9.

### **6.5.3 European Operational Earthquake Forecasting (OEF)**

The goal of operational earthquake forecasting (OEF) is to provide reliable, up-to-date information about the likelihood of earthquakes (and potentially also their impacts in terms of ground shaking, damage and losses) in a given area. By combining the latest data and modelling techniques, the aim is to better understand the patterns and processes behind earthquakes, leading to more accurate and actionable information for decision-makers. With continued progress and refinement, these efforts can help to minimize the impact of earthquakes on communities and reduce the risks associated with seismic activity.

The feasibility of setting up a European OEF service - from rates, to ground motion to damage and losses - has been explored in the RISE project in Deliverable 6.5. Whilst such a model cannot yet be demonstrated at the European scale, in Deliverable 6.5 we provide a summary of the steps that have been taken towards achieving such a goal and the main challenges and areas of future development that are still needed, and that are planned in upcoming projects, such as GeoINQUIRE.

### **List of submitted deliverables and achieved milestones in WP6**

D6.1 Integration of RISE Innovations in the Fields of OELF, RLA and SHM

D6.2 Report on testing OEF and extending earthquake forecasts to loss forecasts in Italy

D6.3 Report on the Iceland demonstration site for earthquake predictability and RLA

D6.4 A User-Centric Dynamic Risk Framework for Switzerland

D6.5 Report on the Development of RLA, EEW and OEF at European Scale

D6.6 Framework for the assessment of economic losses in a dynamic risk context [*Note that this deliverable differs from the description in the Grant Agreement, and the activities originally foreseen for this deliverable have instead been included in D4.7: Good-practice report on risk-cost-benefit in terms of socio-economic impact*]

M37 Sensors set up and collecting data in buildings in Tokyo, Lourdes, Turkey and Valais (GFZ)

MS39: Upgraded EEW capability in Iceland operational (IMO)

MS40: Improved observational capabilities operational (IMO)

MS42: National Swiss stakeholder board established (ETH)

MS44: Operational versions for OEF, RLA and crowdsourcing based EEW capabilities at European level installed (EUCE)

## Summary of Exploitable Results in WP6

### 1) Peer reviewed publications

- Bergamo P et al. (2023). A site amplification model for Switzerland based on site-condition indicators and incorporating local response as measured at seismic stations. Submitted to Bulletin of Earthquake Engineering.
- Böse, M., A. N. Papadopoulos, L. Danciu, J. F. Clinton, & S. Wiemer (2022). Loss-based Performance Assessment and Seismic Network Optimization for Earthquake Early Warning, *Bull. Seismol. Soc. Am.* 112 (3): 1662–1677, <https://doi.org/10.1785/0120210298>.
- Bossu, R., Finazzi, F., Steed, R., Fallou, L. and Bondár, I., 2022. “Shaking in 5 Seconds!”—Performance and user appreciation assessment of the earthquake network smartphone-based public earthquake early warning system. *Seismological Research Letters*, 93(1), pp.137-148.
- Fallou, L., Finazzi, F. and Bossu, R., 2022. Efficacy and Usefulness of an Independent Public Earthquake Early Warning System: A Case Study—The Earthquake Network Initiative in Peru. *Seismological Society of America*, 93(4), pp.2410-2410.
- Finazzi, F., Bondár, I., Bossu, R. and Steed, R., 2022. A Probabilistic Framework for Modeling the Detection Capability of Smartphone Networks in Earthquake Early Warning. *Seismological Society of America*, 93(6), pp.3291-3307.
- Han, M, Mizrahi L., Wiemer S (2023). Towards Operational Earthquake Forecasting for Europe” *In preparation*.
- Massin, F., J. Clinton, and M. Böse (2021). Status of Earthquake Early Warning in Switzerland, *Front. Earth Sci.* 9, doi:10.3389/feart.2021.707654.
- Mizrahi, L., Nandan, S., Wiemer, S. Developing and Testing ETAS-Based Earthquake Forecasting Models for Switzerland. In preparation.
- Papadopoulos, A.N, M. Böse, L. Danciu, J. Clinton, and S. Wiemer (2023). Effectiveness of Earthquake Early Warning in Mitigating Seismic Risk, *Earthquake Spectra*, accepted.
- Reuland, Y., Martakis, P., & Chatzi, E. (2023). A comparative study of damage-sensitive features for rapid data-driven seismic structural-health monitoring. *Applied Sciences*. *Under Review*.
- Wiemer, S., P. Bazzurro, P. Bergamo, C. Cauzzi, I. Dallo, L. Danciu, B. Duvernay, E. Fagà, D. Fäh, C. Hammer, F. Haslinger, P. Kästli, A. Khodaverdian, P. Lestuzzi, M. Marti, Ö. Odabaşı, F. Panzera, A. Papadopoulos, V. Perron, P. Roth, N. Schmid, N. Valenzuela, & S. Zaugg (2023). Earthquake Risk Model of Switzerland ERM-CH23, DOI: <https://doi.org/10.12686/a20>.

### 2) Conference publications

- Michelini, A., Faenza, L., Cauzzi, C., Lauciani, V., Clinton, J., Kästli, P., Haslinger, F., Wiemer, S., Melis, N., Theodoulidis, N., Böse, M., Weatherill, G., Cotton, F., and Giardini, D.: ShakeMap-EU: an update on the shakemap service in Europe, EGU General Assembly 2023, Vienna, Austria, 24–28 Apr 2023, EGU23-5937, <https://doi.org/10.5194/egusphere-egu23-5937>, 2023.

- Nievas CI, Crowley H, Reuland Y, Weatherill G, Baltzopoulos G, Bayliss K, Chatzi E, Guéguen P, Naylor M, Orlacchio M, Pejovic J, Serafini F, Serdar N (2023) Exploration of state-dependent Rapid Loss Assessment and event-based Operational Earthquake Loss Forecasting incorporating Structural Health Monitoring: an open source tool. SECED 2023 Conference, 14-15 Sept, Cambridge, UK. (Submitted). (Task 6.1)
- Popovic N, Pejović J (2023) Seismic Performance Evaluation of Existing RC High-Rise Building in Montenegro. Proceedings of the 2nd Croatian Conference on Earthquake Engineering - 2CroCEE, Zagreb, Croatia, 22-24 March, pp. 565-575, <https://doi.org/10.5592/CO/2CroCEE.2023.13>

### 3) Other exploitable results/data/reports

- Open-source and publicly available Real-Time Loss Tools, developed within Task 6.1: <https://git.gfz-potsdam.de/real-time-loss-tools/real-time-loss-tools>.
- Nievas CI, Crowley H, Reuland Y, Weatherill G, Baltzopoulos G, Bayliss K, Chatzi E, Chioccarelli E, Guéguen P, Iervolino I, Marzocchi W, Naylor M, Orlacchio M, Pejovic J, Popovic N, Serafini F, Serdar N (2023) Integration of RISE innovations in the fields of OELF, RLA and SHM: input and output datasets (Version 1.0) [Data set]. Zenodo. <https://doi.org/10.5281/zenodo.7784841>. GitLab repository: <https://git.gfz-potsdam.de/real-time-loss-tools/rise-d6-1-data-files>. (Task 6.1)
- Web services for automatic download of European ShakeMap products from <https://shakemapeu.ingv.it> (Task 6.5)
- European Rapid earthquake Loss Assessment service from Task 6.5: [https://gitlab.seismo.ethz.ch/hcrowley/rapid\\_loss\\_eu](https://gitlab.seismo.ethz.ch/hcrowley/rapid_loss_eu)
- The upgraded Italian system for operational earthquake loss forecast MANTIS v2.0.

## 1.2.7 Work package 7

### Overview

WP7 addresses the need of rigorous testing and validation of all dynamic risk model components as a critical input for societies to appraise and confidently adopt models for decision-making and loss reduction. WP7 comprises the testing, model evaluation, model validation and ensemble modelling by adopting and transforming the Collaboratory for the Study of Earthquake Predictability (CSEP), a global platform for independent, reproducible and transparent testing of earthquake prediction algorithms and forecast models. The main objectives of this work package are:

- Design and implement a CSEP 2.0 platform for Europe with transformed capacity to test OEF hypotheses, models and procedures, establishing Europe as a major contributor to the global CSEP Collaboratory (→ Task 7.1).
- Leverage the global CSEP collaboration through open-source, co-designed and shared software that enables user-friendly testing of models across tectonic settings (→ Task 7.1).
- Conduct formal and independent evaluations, both pseudo-prospective and fully prospective, of RISE OEF candidate models (or model components) (→ Tasks 7.2 & 7.3).
- Develop rigorous testing approaches of other dynamic risk model components, including ground-motion forecasts, micro-zonation, exposure and loss models (→ Task 7.4).

The following sections highlight the main achievements towards these objectives in each task.

### Summary of achievements in WP7 tasks: (2-3 pages for each task)

#### Task 7.1 Developing and implementing the CSEP2.0 framework and test-centre pyCSEP Toolbox

Over the last decade, the Collaboratory of the Study of Earthquake Predictability (CSEP) has led numerous prospective earthquake forecasting experiments (see, e. g., Michael & Werner, 2018; Schorlemmer et al., 2018). These experiments are formally conducted within testing centers (Schorlemmer & Gerstenberger, 2007). Such testing centers were installed at USC, ERI, GNS, and ETH, covering a variety of testing regions, e. g. California, Japan, New Zealand, Italy, and a global experiment. They are all operated by the same CSEP software stack (Zechar et al., 2009). However, its monolithic design made it difficult for researchers to use various routines in the testing centers in their own work without replicating the entire testing center configuration on their own system. As a consequence, the CSEP group decided to fundamentally change the design paradigm of the CSEP software to address these problems. The new software stack, formerly referred to as CSEP 2.0, is designed as a Python toolbox (called pyCSEP) for easy use by modelers but also for the assembly of readily deployable fully-reproducible earthquake forecasting experiments (see MS47). pyCSEP was designed to provide vetted methods to evaluate earthquake forecasts that researchers can include directly in their research (Rhoades et al., 2011; Savran et al., 2020, 2022a, 2022b; Schorlemmer et al., 2007; Werner et al., 2011; Zechar et al., 2013). In addition, pyCSEP provides routines for working with earthquake catalogs and visualizations. As of now, pyCSEP is being used by several research groups participating in RISE and other projects.

Floating Community Experiments

With the monolithic concept of CSEP testing centres becoming obsolete through pyCSEP, a new, more participatory, version of CSEP experiments needed to be designed. A Floating Experiment represents an idealized experiment implementation organized by CSEP, where the results from the experiment are recorded and shared with the community. To operate official experiments and the authoritative results of a Floating Experiment, CSEP would operate the required hardware on-demand and publish results to a publicly available repository. This lowers the effective run-time and computational burden of the testing system and allows the experiment to be run essentially anywhere, hence the name Floating Experiment.

Floating Experiments rely heavily on Digital Object Identifiers (DOI), obtained from open data repositories (e.g. Zenodo), that ensure the immutability of the results and the prolonged experiment's reproducibility. Every experiment release (e.g. for every catalog update) has assigned a DOI version, containing all the necessary artifacts to run the experiment. Instead of storing all the results in a physical testing center, we are creating a reproducibility package (Krafczyk et al., 2021) that contains all the elements of an experiment.

An individual Floating Experiment can be as simple as downloading the package and running it with a few commands on a suitable computer. It should be provided as a "turn-key" product that can be executed with a single command by anyone with sufficient computing power (or time) to run the experiments. In practice, a Floating Experiment can be allocated in an official repository (Gitlab & Zenodo), cloned to a local machine, run, and results being committed/pushed back into the repository.

#### feCSEP Application

The feCSEP application constitutes the system architecture of a testing experiment, curating the experiment's constituent artefacts. It satisfies the current open-source scientific standards (i.e. FAIR principles) as well as CSEP philosophy. The core functionality of feCSEP is based on the previously released package pyCSEP and has the following features:

- Manifest explicitly the experiments' rules and definitions
- Perform the fundamental tasks of a testing experiment
- Allow an experiment to be run from scratch or from a previously executed state in the machine
- Provide the book-keeping of numerous forecasts and result files/databases
- Display the results comprehensively

An additional difficulty to guarantee full reproducibility is to maintain the experiment's computational environment unmodified. To address this, feCSEP allows the integration with Docker, which containerizes the computational environment of the experiment and each forecasting model.

The application can be found in: <https://git.gfz-potsdam.de/csep-group/fecsep>

#### Applications of the new CSEP 2.0 software

##### Testing the European Seismic Hazard Model 2020 (ESHM20)

The long-term forecasting components, i.e. the source-model logic-tree, of the ESHM20 are being put under constant pseudo-prospective tests, using out-of-sample data from 2014 (Figure 7.1.1). It evaluates time-independent forecasts with  $M > 4.8$  observations within an 8-year time window. The experiment is contained in a repository open to the public, which can be easily reproduced in a local machine. It is being updated on-demand, until a continuous data-feed of the EMEC catalog

is implemented. The floating experiment is available in: <https://git.gfz-potsdam.de/csep-group/fecsep-efehr20>

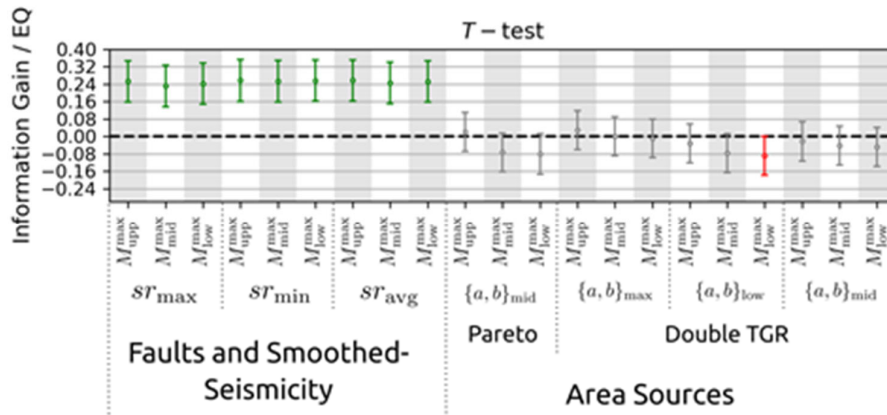


Figure 7.1.1: The results of the T-test showing the information gain of each branch compared to the previous 2013 ESHM smoothed-seismicity model. Only fault models present a significant improvement to the ESHM2013.

#### Global Earthquake Forecasting Experiment (GEFE) - Quadtree

Quadtrees are hierarchical tree structures to represent a spatial region with variable resolution, in opposition to classic gridded spaces, where each node is allowed to have either zero or four child nodes (Khawaja et al., 2023). The main goals of this experiment are to understand the dependency of the testing region definition on the evaluation results and to understand whether forecasts defined on different spatial grids can be accurately compared against one another. The experiment is designed on a global region, for magnitudes greater than 6.0 and a time-independent window of 9 years, starting from 2014. This type of experiment provides a useful working example, because Quadtree regions drastically improve the computational performance of the evaluations enabling this experiment to be reproduced on any laptop computer.

The floating experiment is available in: <https://git.gfz-potsdam.de/csep-group/gefe-quadtree/>

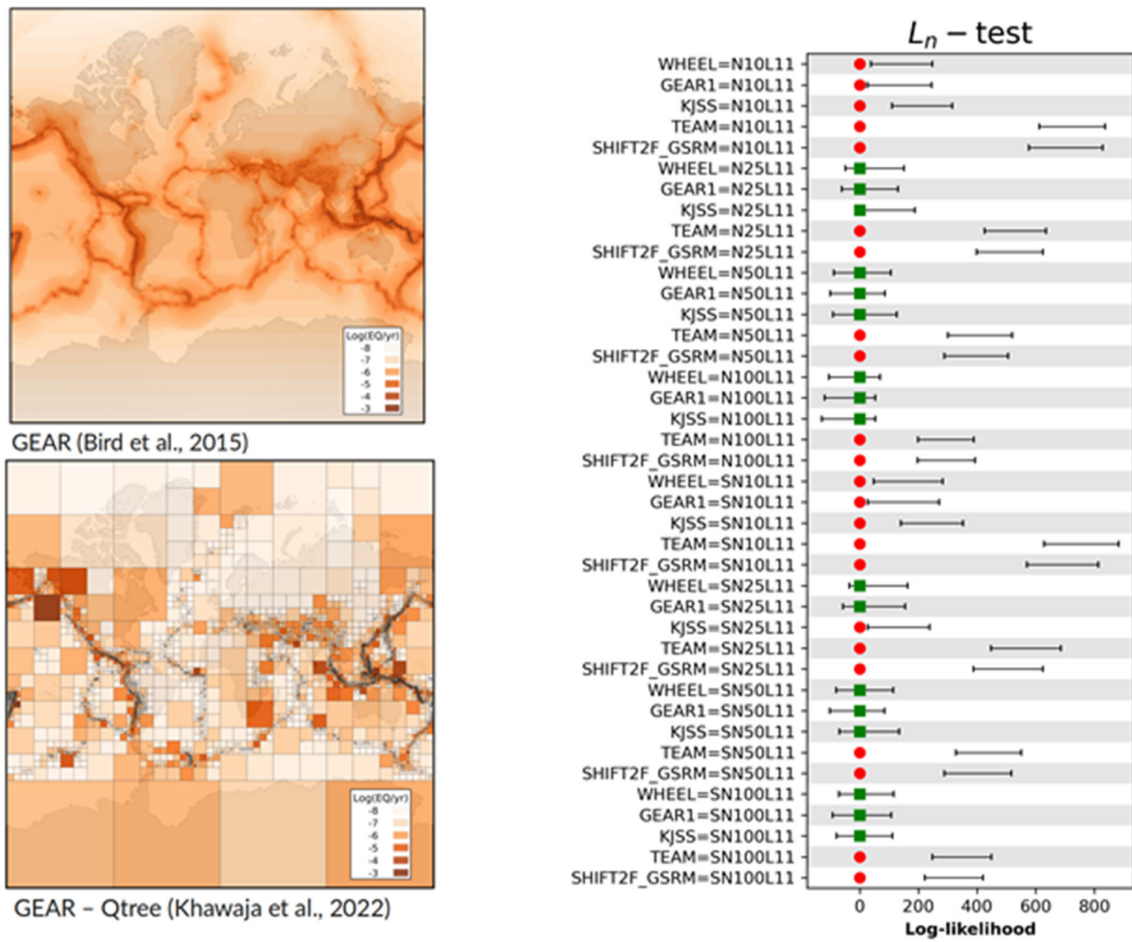


Figure 7.1.2: (left) A Quadtree model composed from a parent forecast (GEAR1, Bird et al., 2015) (right) Results of a conditional log-likelihood tests. Results show that GEAR1 outperforms other models at multiple resolutions. All the tests and figures are contained in the experiment repository.

### The 2010 Italy Forecasting Experiment

The Italy region was submitted to a forecasting experiment in 2010 for a 10-year period of observation (Schorlemmer et al., 2010). However, unlike short-term operational earthquake forecasting, the scarcity of earthquakes targeted by long-term forecasts (e.g. magnitude larger than 5.0) requires an observation frame large enough to empirically validate a forecast. RISE continues the experiment, exploiting the forecasts' time-independence, to study the regularity of testing results in time.

The floating experiment is available in: [https://git.gfz-potsdam.de/csep-group/fe\\_italy\\_ti](https://git.gfz-potsdam.de/csep-group/fe_italy_ti)

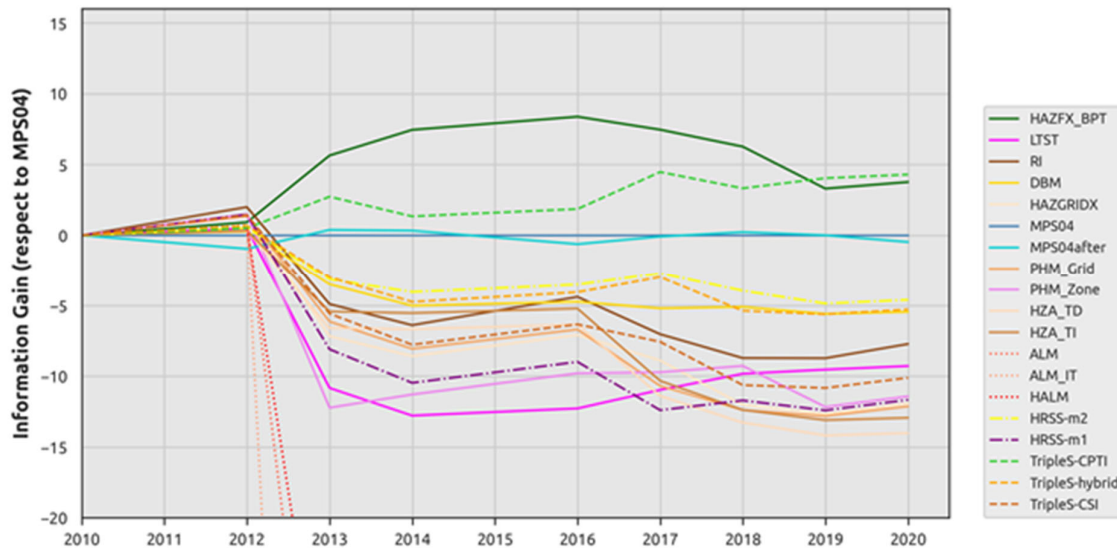


Figure 7.1.3: Information Gain (respect to the reference national model) evolution of the competing models during the Experiment. Models are colored by clustering their performance at 2015 (e.g. green are performing well, blue indifferent, red poorly). The groups' performance remains fairly constant (i.e. the clusters maintain similar ranking) until the end of the experiment, vouching for the stability of the evaluation results.

The (new) Earthquake Forecasting Experiment for Italy

This Experiment has been designed to test the performance of novel short-term (time-dependent) forecasting models for 1-day time windows. It expands the classical CSEP horse-race to inter-model and intra-model hypothesis testing. Here, the capacities of feCSEP are being explored due to the complexity arising from operating and book-keeping time-dependent forecasts. The beta-phase of the experiment, although delayed, will begin at the end of April with opening the call to modelers external to RISE. The experiment rules, competing models and the beta implementation of this Floating Experiment can be found in:

[https://git.gfz-potsdam.de/csep-group/rise\\_italy\\_experiment/experiment\\_setup](https://git.gfz-potsdam.de/csep-group/rise_italy_experiment/experiment_setup)

[https://git.gfz-potsdam.de/csep-group/rise\\_italy\\_experiment/models](https://git.gfz-potsdam.de/csep-group/rise_italy_experiment/models)

[https://git.gfz-potsdam.de/csep-group/rise\\_italy\\_experiment/experiment\\_system](https://git.gfz-potsdam.de/csep-group/rise_italy_experiment/experiment_system)

### Task 7.2. Test new physics-based, stochastic and hybrid OEF models

Goal: This task aims to evaluate newly developed physics-based, stochastic and hybrid earthquake forecast models that might be suitable for operational earthquake forecasting (OEF) in order to drive model improvement and characterise confidence in the model forecasts.

Progress / Achievements

The summaries below refer to progress and achievements since the mid-term report (delivered 31.8.2021).

Do Hybrid Models Achieve Greater Prospective Predictive Skill? [Bayona et al., 2022]:

The Regional Earthquake Likelihood Models (RELM) experiment, conducted within the Collaboratory for the Study of Earthquake Predictability (CSEP), showed that the smoothed seismicity (HKJ) model by Helmstetter et al. (2007) was the most informative time-independent earthquake model in California during the 2006–2010 evaluation period. The diversity of

competing forecast hypotheses and geophysical datasets used in RELM was suitable for combining multiple models that could provide more informative earthquake forecasts than HKJ. Thus, Rhoades et al. (2014) created multiplicative hybrid models that involve the HKJ model as a baseline and one or more conjugate models. In retrospective evaluations, some hybrid models showed significant information gains over the HKJ forecast. Bayona et al. (2022) prospectively assess the predictive skills of 16 hybrids and 6 original RELM forecasts at a 0.05 significance level, using a suite of traditional and new CSEP tests that rely on a Poisson and a binary likelihood function. In addition, they include consistency test results at a Bonferroni-adjusted significance level of 0.025 to address the problem of multiple tests. Furthermore, they compare the performance of each forecast to that of HKJ. The evaluation dataset contains 40 target events recorded within the CSEP California testing region from 1 January 2011 to 31 December 2020, including the 2016 Hawthorne earthquake swarm in southwestern Nevada and the 2019 Ridgecrest sequence. Consistency test results show that most forecasting models overestimate the number of earthquakes and struggle to explain the spatial distribution of epicenters, especially in the case of seismicity clusters. The binary likelihood function significantly reduces the sensitivity of spatial log-likelihood scores to clustering, however; most models still fail to adequately describe spatial earthquake patterns. Contrary to retrospective analyses, our prospective test results show that none of the models are significantly more informative than the HKJ benchmark forecast, which they interpret to be due to temporal instabilities in the fit that forms hybrids. These results suggest that smoothing high-resolution, small earthquake data remains a robust method for forecasting moderate-to-large earthquakes over a period of five to fifteen years in California.

Are Regionally Calibrated Seismicity Models More Informative than Global Models? Insights from Prospective Tests in California, New Zealand, and Italy [Bayona et al., 2023]:

Earthquake forecasting models express hypotheses about seismogenesis that underpin global and regional probabilistic seismic hazard assessments (PSHAs). An implicit assumption is that the comparatively higher spatiotemporal resolution datasets from which regional models are generated lead to more informative seismicity forecasts than global models, which are however calibrated on greater datasets of large earthquakes. Bayona et al. (2023) prospectively assess the ability of the Global Earthquake Activity Rate (GEAR1) model and 19 time-independent regional models to forecast M 4.95+ seismicity in California, New Zealand, and Italy from 2014 through 2021, using metrics developed by the Collaboratory for the Study of Earthquake Predictability (CSEP). Their results (Figure X) show that regional models that adaptively smooth small earthquake locations perform best in California and Italy during the evaluation period; however, GEAR1, based on global seismicity and geodesy datasets, performs surprisingly well across all testing regions, ranking first in New Zealand, second in California, and third in Italy. Furthermore, the performance of the models is highly sensitive to spatial smoothing, and the optimal smoothing likely depends on the regional tectonic setting. Acknowledging the limited prospective test data, these results provide preliminary support for using GEAR1 as a global reference M 4.95+ seismicity model that could inform eight-year regional and global PSHAs.

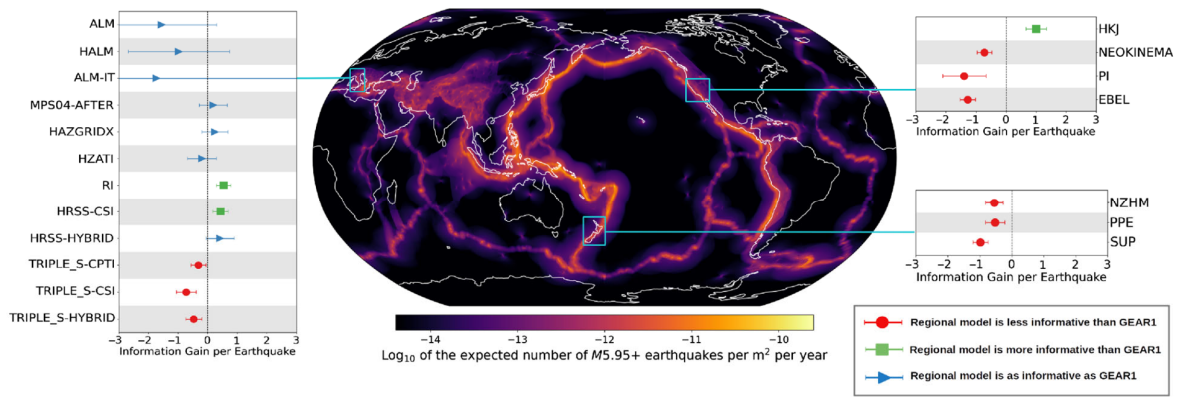


**Figure 7.2.1** [from Bayona et al., 2023]: Prospective T-test results for globally and regionally calibrated seismicity models for California, New Zealand, and Italy. We show Information Gain per Earthquake (IGPE) obtained by 19 regional models over GEAR1, along with their 95% confidence intervals shown as bars. Green squares denote regional models that can be considered statistically more informative than GEAR1, blue triangles show regional models that can be considered as informative as GEAR1, and red circles display regional models that are less informative than GEAR1. We include a global forecast map showing  $M_w5.95+$ ,  $d \leq 70\text{km}$  estimates of seismicity per square meter per year, originally provided by the GEAR1 model.

*Do Enhanced Seismicity Catalogs Improve Physics-based and Statistical Aftershock Forecasts?*  
[Mancini et al., 2022]:

Artificial intelligence methods are revolutionizing modern seismology by offering unprecedentedly rich seismic catalogs. Recent developments in short-term aftershock forecasting show that Coulomb rate-and-state (CRS) models hold the potential to achieve operational skills comparable to standard statistical Epidemic-Type Aftershock Sequence (ETAS) models, but only when the near real-time data quality allows to incorporate a more detailed representation of sources and receiver fault populations. In this framework, the high-resolution reconstructions of the seismicity patterns introduced by machine-learning-derived earthquake catalogs represent a unique opportunity to test whether they can be exploited to improve the predictive power of aftershock forecasts. Mancini et al. (2022) present a retrospective forecast experiment of the first year of the 2016-2017 Central Italy seismic cascade, where seven  $M5.4+$  earthquakes occurred between a few hours and five months after the initial  $M_w 6.0$  event, migrating over a 60-km long normal fault system. As target dataset, they employ the best available high-density machine learning catalog recently released for the sequence, which reports  $\sim 1$  million events in total ( $\sim 22,000$  with  $M \geq 2$ ). First, they develop a CRS model featuring (1) rate-and-state variables optimized on 30 years of pre-sequence regional seismicity, (2) finite fault slip models for the seven mainshocks of the sequence, (3) spatially heterogeneous receivers informed by pre-existing faults, and (4) updating receiver fault populations using focal planes gradually revealed by aftershocks. The authors then test the effect of considering stress perturbations from the  $M2+$  events. Using the same high-precision catalog, Mancini et al. produce a standard ETAS model to benchmark the stress-based counterparts. All models are developed on a 3D spatial grid with 2 km spacing; they are updated daily and seek to forecast the space-time occurrence of  $M2+$  seismicity for a total forecast horizon of one year. Mancini et al. formally rank the forecasts with the statistical scoring

metrics introduced by the CSEP and compare their performance to a generation of CRS and ETAS models previously published for the same sequence by Mancini et al. (2019), who used solely real-time data and a minimum triggering magnitude of  $M=3$ . Mancini et al. find that considering secondary triggering effects from events down to  $M=2$  slightly improves model performance. While this result highlights the importance of better seismic catalogs to model local triggering mechanisms, it also suggests that to appreciate their full potential future modelling efforts will likely have to incorporate also fine-scale rupture characterizations (e.g., smaller source fault geometries retrieved from enhanced focal mechanism catalogs) and introduce denser spatial model discretizations.

*A Prospective Test of the Seismic Gap Hypothesis [Husker et al., 2022]:*

The seismic gap hypothesis has a long and controversial history, but continues to be popular and is frequently cited in the media. In particular, the seismic gap hypothesis has been widely cited in Mexico to predict the location of future earthquakes and to assess seismic hazard, specifically in the context of the so-called 'Guerrero gap'. However, no analysis of the outcome of any predictions of the hypothesis in Mexico has been done to-date. Husker, Bayona, Werner and Santoyo are preparing a manuscript that analyzes the outcome of the formal seismic gap prediction by Nishenko and Singh (1987). The prediction has well-defined probabilities, areas and timeframes that allow for its evaluation. Those timeframes were 5 years, 10 years and 20 years after 1986. The prediction relies on the precise repeat times of characteristic earthquakes to define segments, but the catalog that the authors use relies on an imprecise definition of characteristic earthquakes. Husker et al. discuss some of their decisions in building their catalog to explain how they analyze the outcome of the prediction. They create catalogs of earthquakes based on the probabilities of earthquake occurrence for each segment. They also generate null model earthquake catalogs using the average number of earthquakes that occur in the subduction zone, and randomly distribute these along the distance of the segments. They find that null model performed better than the seismic gap hypothesis prediction. The prediction over the longest time frame of 20 years correctly predicted the outcome in only 48% of the segments compared to 91% coinciding for the null model. The gap hypothesis also greatly over predicted the total number of segments with a characteristic earthquake.  $M_s \geq 7.4$  earthquakes were predicted to occur in 6 of the 11 segments over the 20-year timeframe, but only 1 actually occurred. That lone earthquake was a  $M_w$  8.0 which occurred in a segment with a 0% chance of an earthquake in one of their models and 16% change in another. Husker et al. conclude that the gap hypothesis did not perform well at predicting earthquakes in Mexico and, in fact, its predictions were worse than predicting earthquakes by chance. There is thus no evidence to suggest earthquakes are overdue in the Guerrero gap, and therefore Husker et al. recommend taking special care in invoking the gap hypothesis to communicate earthquake hazards in Mexico.

*Does Aseismic Afterslip Control Aftershock Productivity? [Churchill et al., 2022b]*

Understanding the controls on aftershock triggering is key to skillful operational earthquake forecasting and short-term hazard assessment. Many studies suggest that aseismic afterslip plays a key role in driving aftershock sequences, often citing strong correlations in their spatio-temporal evolutions. Churchill, Werner, Fagereng and Biggs (2022a) showed that the amount of afterslip

produced after an earthquake can vary greatly, from <1% to >300% of the coseismic moment. Thus, afterslip could feasibly account for some of the spatio-temporal complexity many aftershock sequences exhibit, which coseismic Coulomb static stress change alone struggles to explain. If this link is robustly established, including afterslip in frameworks such as ETAS (which currently assumes that every earthquake triggers aftershocks in a statistically identical way) may improve their predictive capabilities.

To shed new light on the purported link between afterslip and aftershocks, Churchill, Werner, Fagereng and Biggs (2022b) examined the relationship between afterslip moment release and aftershock number. Both afterslip moment and aftershock number broadly increase with mainshock size, but can vary beyond this scaling. They examine whether relative afterslip moment (afterslip moment/mainshock moment) correlates with several key aftershock sequence characteristics, including aftershock number and cumulative moment (both absolute and relative to mainshock size), seismicity rate change,  $b$ -value, and Omori decay exponent. We select  $M_w \geq 4.5$  aftershocks for 41 tectonically varied mainshocks with available afterslip models. Against expectation, relative afterslip moment does not correlate with tested aftershock characteristics or background seismicity rate. Furthermore, adding afterslip moment to mainshock moment does not improve predictions of aftershock number. Their findings place useful empirical constraints on the link between afterslip and potentially damaging  $M_w \geq 4.5$  aftershocks and raise questions regarding the role afterslip plays in aftershock generation.

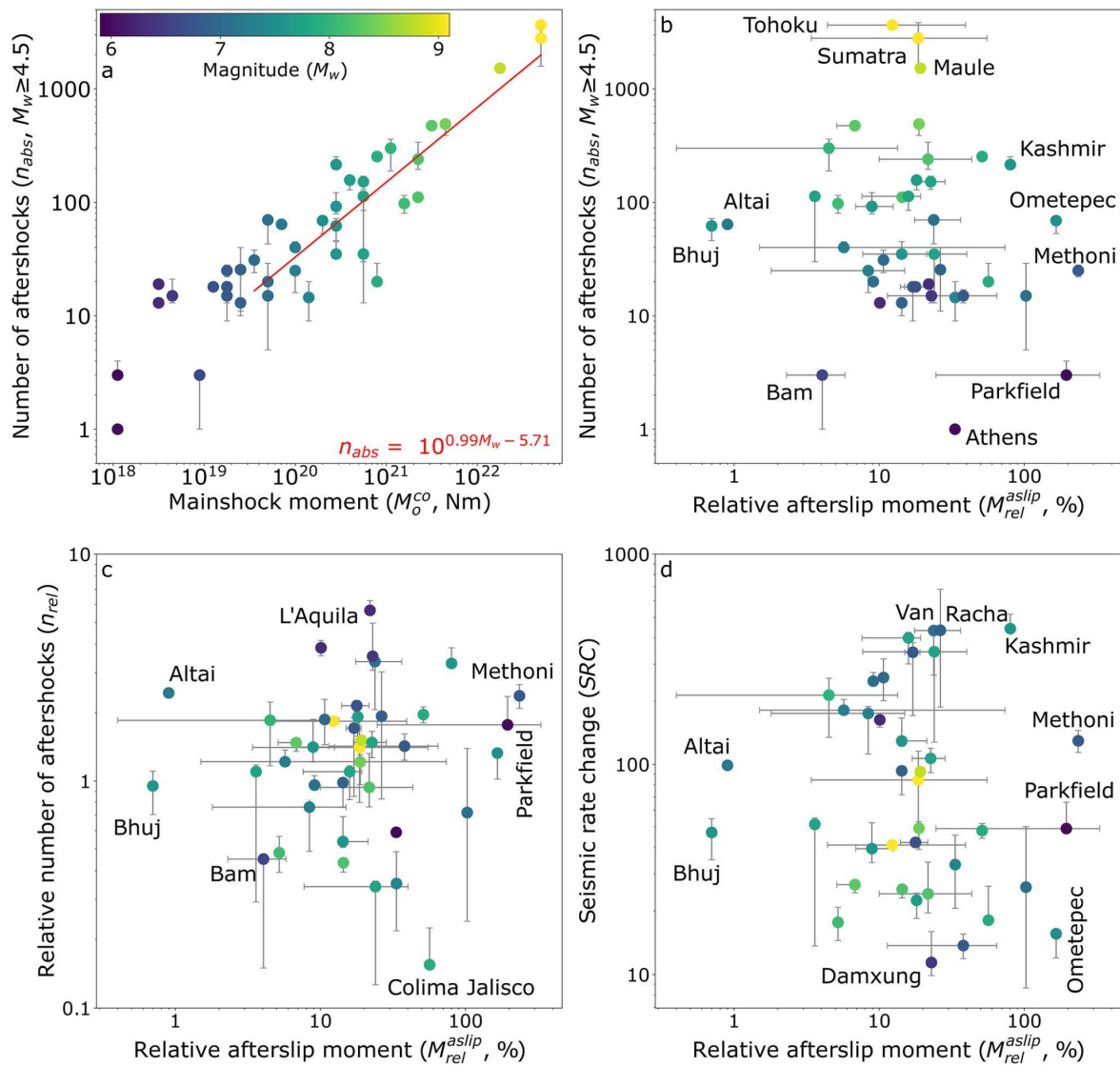


Figure 7.2.2 [from Churchill et al., 2022b]: Data showing the strong relationship between coseismic moment and aftershock number and the lack of relationships between relative afterslip moment and key aftershock sequence characteristics: (a) coseismic moment and aftershock number, (b) relative afterslip moment and aftershock number, (c) relative afterslip moment and relative aftershock number, and (d) relative afterslip moment and seismicity rate change. Circles denote median values, color denotes mainshock magnitude, gray bars in the y-direction reflect the multiple aftershock selection methods and in the x-direction, reflect multiple estimates of relative afterslip moment. Endmember mainshocks are annotated.

Retrospective forecast model for Italy using the Coulomb-based rate-and-state framework [Cheng et al., 2023, in preparation]:

During 2009-2014, the Collaboratory for the Study of Earthquake Predictability (CSEP) executed a state-wide rate-based forecast in Italy. Cheng et al. (2023) implement a retrospective study using the rate and-state framework and the Epidemic Type Aftershock Sequence (ETAS) method to forecast the spatiotemporal variation of earthquakes in a retrospective scenario. They test the hypothesis that an enhanced CRS framework involving improved source and fault characterization and model updates could improve the skill of forecasts on the Italy-wide scale for the 1-day

interval. Cheng et al. (2023) also evaluate how the state-wide CRS models perform during specific earthquake sequences, namely the 2009 L’Aquila sequence and the 2012 Emilia sequence. The result indicates that adopting the finite slip models, spatially variable receiver faults, and including stress rearrangement from secondary triggering could increase the performance of the Italy-wide CRS forecast.

### **Task 7.3. Optimizing earthquake forecasting capabilities through ensemble modelling**

An ensemble model integrates forecasts of different models (or different parametrizations of the same model) into one single ensemble forecast. The most advanced probabilistic forecasts combine a set of models that may be of different kind, ranging from entirely statistical to deterministic. Combining forecasts in a post process is meant to improve the forecasting skill over the individual forecasts. This procedure has different names in the literature and is approached through different philosophies in theory and practice. To date, ensemble models usually collapse all forecasts into one single forecast. Although different probabilistic ensemble strategies exist, the most common approach involves the weighted average.

In this task, we made two improvements over the state of art, as outlined in the following two sections.

#### Maximizing the forecasting skill of an ensemble model (*Herrmann & Marzocchi 2023*)

To build a weighted-average forecast, no common strategy exists to assign weights. Previous approaches often weighted forecasts equally or according to their individual skill. To guarantee that the ensemble is the best combination of all forecasts, weights should maximize the skill of the ensemble (and not depend on the skill of each individual model, for instance). We approach this more meaningful weighting strategy using multivariate logistic regression. We applied this strategy to the OEF system in Italy (Marzocchi et al. 2014), which provides an ensemble forecast based on a combination of ETAS\_LM, ETES\_FCM, and STEP\_LG using Score Model Averaging (SMA). Our ensemble demonstrated superior skill with statistical significance over the best individual forecast model (ETAS\_LM) as well as SMA. But to obtain a performant ensemble in our application, we had to discard the fitted logistic model and instead map its coefficients to weights (see Figure 7.3.1). Those weights then created a better-performing weighted-average ensemble of the candidate forecasts.

Additionally, we expose some level of flexibility when fitting the ensemble to emphasize different aspects of the problem. In particular, we highlight that the skill improves when exploiting this flexibility, e.g., (i) using only recent data (of the previous year) and not the entire historical data, and (ii) exchanging the observable: applying the logistic regression to target earthquakes that were obtained for a lower magnitude threshold ( $M_L \geq 2.95$ ) than the target threshold considered by the forecast models ( $M_L \geq 3.95$ )—the results for this setup are shown in the Figures 7.3.1 and 7.3.2.

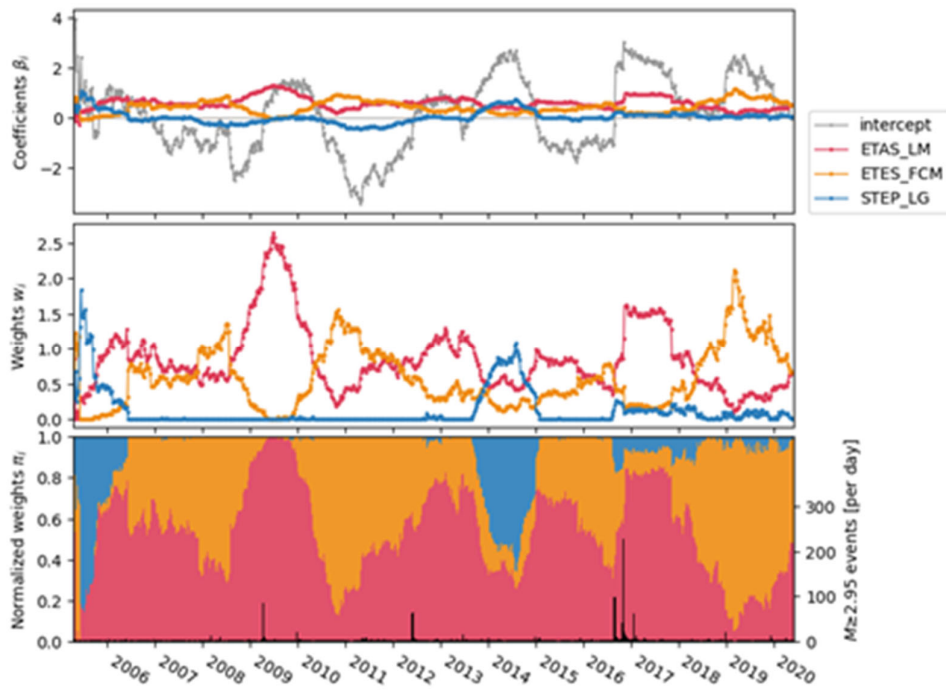


Figure 7.3.1: Applying the logistic regression over time. Top: Logistic regression coefficients (colored curves) for the three models and intercept (gray curve) after correcting for the bias due to undersampling non-target bins; Middle: Regression coefficients mapped to non-normalized weights; Bottom: Normalized weights; the black bars at the bottom axis represent the number of target earthquakes per day.

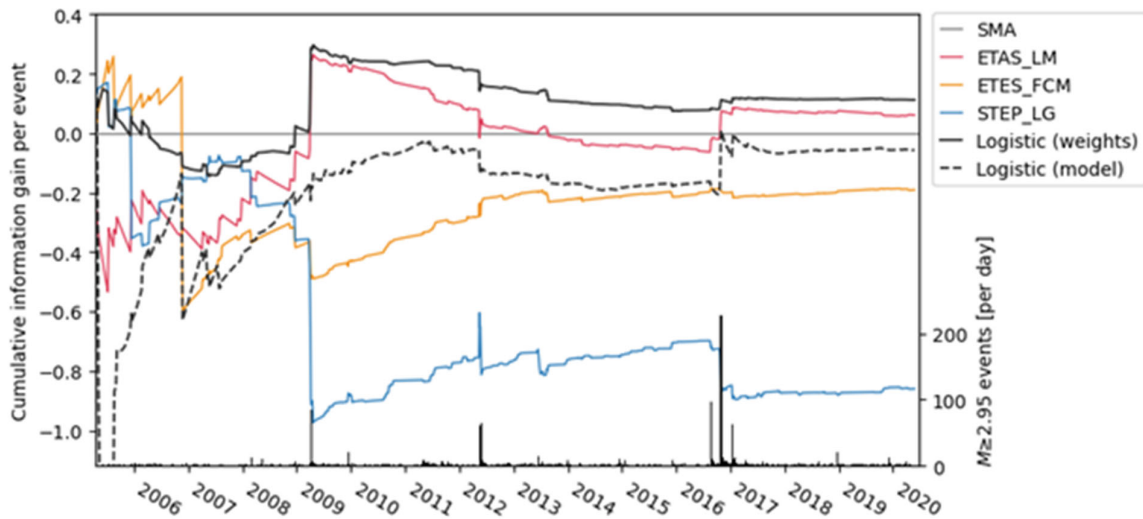


Figure 7.3.2: Evolution of the cumulative information gain per event (CumIGPE) for each of our new ensembles (black curves, see legend) and candidate model (colored curves) over the SMA ensemble (gray horizontal line). The black bars at the bottom axis represent the number of target earthquakes per day.

Numerous other modifications beyond those explored in our analysis may further increase the flexibility and skill of the ensemble. While improving the ensemble skill will require extracting more (diverse) information from the candidate forecasts, a more flexible ensemble approach will

be practical for conforming with the multipurpose and authoritative character of OEF to address different end users (i.e., with a focus on recent seismicity, overall rate, spatial skill, etc.).

Since candidate models capture the current knowledge, they ultimately limit the skill of the ensemble. Here we used only statistical models, but the ensemble would undoubtedly benefit from a pool of diverse forecast models, which should include both statistical and physics-based approaches, and models that perform exceptionally well in particular situations.

#### Ontological ensemble modeling

Collapsing the individual forecast distributions into a single ensemble distribution has some remarkable shortcomings regarding the validation of the ensemble model and due neglecting epistemic uncertainty (see Deliverable 7.3 for more details). In essence, we need a complete description of what we know and what we do not know. Therefore, we introduced ontological ensemble modeling, which is rooted in a unified probabilistic framework (Marzocchi & Jordan 2014; 2017)—it separates the different kinds of uncertainties (aleatory variability, epistemic uncertainty, and ontological error) and acknowledge the ignorance of the “true” model.

To build the ontological ensemble model, we can use the model weights that we obtained in the previous step: previously, these weights optimized the forecasting skill of the 1st moment (weighted average); now, they are used to estimate the 2<sup>nd</sup> moment (weighted variance), which reflects the dispersion of the forecasts and mimics the epistemic uncertainty.

To illustrate how the method can be applied in a real case, we created the ontological ensemble model for OEF-Italy (see Figure 7.3.3).

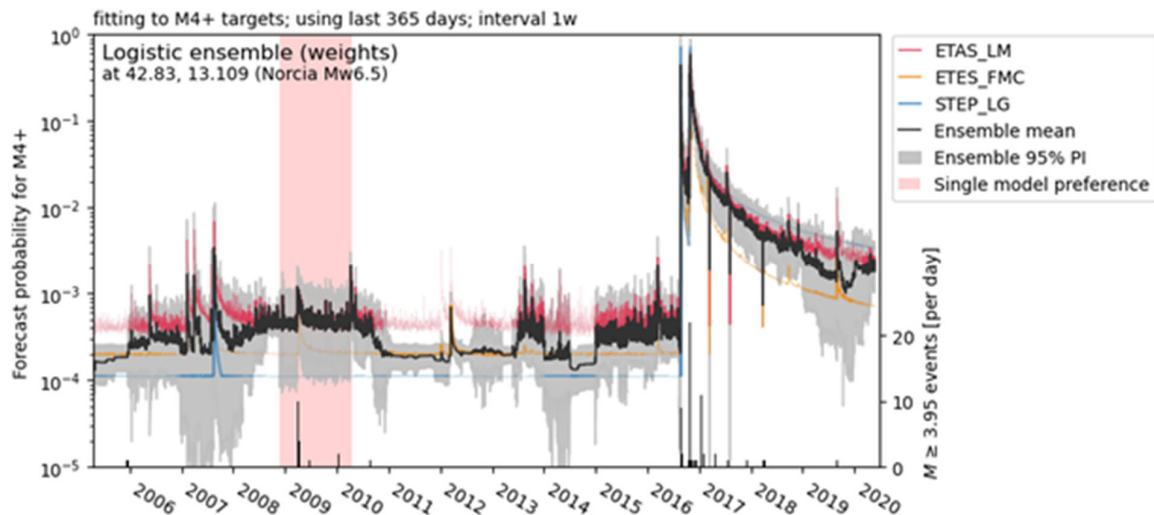


Figure 7.3.3: Ontological ensemble forecast for the spatial bin where the 2016 Norcia (central Italy) mainshock occurred. The forecast rate of the various models is indicated by the curves (see legend): each candidate model (colored curve), our weighted-average ensemble (black curve), 95% prediction interval (PI) of the ontological forecast (gray shaded band). The temporal evolution of the individual model weights in the ensemble is indicated by an opacity/transparency effect of the candidate forecast curves. The vertical red shaded band represents a time period in which a single model has all the weight (see text). At the bottom, the daily rate of target events within 50 km is displayed by vertical bars.

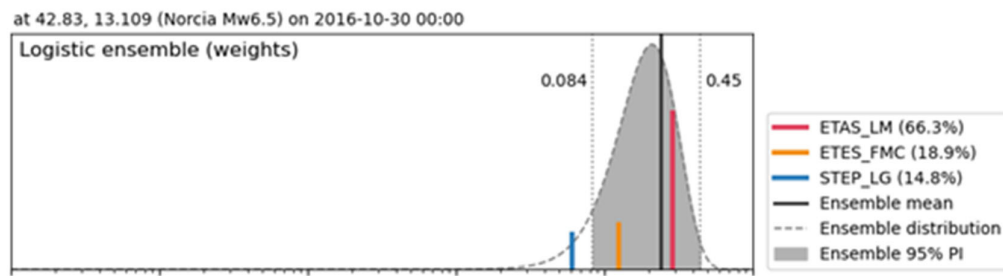


Figure 7.3.4: Ontological forecast distributions (dashed curves) corresponding to Figure 7.3.3 at midnight before the Norcia mainshock. The forecasts of individual models are shown as bars at the appropriate forecast probability with their heights corresponding to the assigned weights. The 95% prediction intervals (vertical dotted lines) are annotated with their corresponding probabilities.

The novelty is that we now also model the epistemic uncertainty of the forecast, that is, given the weights and the dispersion of the forecasts, we quantify the reliability of the ensemble as a probability distribution. The probability distribution allows scientists a more honest and versatile communication of forecast probabilities (e.g., with 95% reliability). More importantly scientifically, keeping the uncertainties separated allows validating the probabilistic model: For instance, if the true (unknown) frequency is unlikely to be a sample of the probability distribution (i.e., the ontological null hypothesis is rejected), we found an ontological error (i.e., that our models do not represent the system well).

The ontological approach clarifies that reducing the epistemic uncertainty does not necessarily require *more* models, but rather models that are more *diverse* and use different information (see previous part).

#### **Task 7.4. Formal testing of ground motion forecasts, micro-zonation, exposure and loss models**

This task has been hampered strongly by the cancelled deployment of low-cost sensors (due to the international chip crisis) in the test areas as were planned in the proposal. For the investigation of high-resolution ground-motion models (GMM), an experiment in the Valais, Switzerland, area was planned in order to cover the sedimentary basin and the mountain slopes on each side of the valley with instruments. Measurement in such an environment would have provided the necessary high-resolution recordings for the envisioned study. To compensate for that, we conducted a testing study on non-linear GMMs to investigate whether or not the concept of non-linearity is warranted by the data and we also investigated the impact of local geology on earthquake ground motions.

Likewise, due to a lack of distributed low-cost sensors in buildings in Europe, we were not able to develop the necessary testing metrics for exposure/risk testing as no measurements were available. However, to compensate for this, we have collected damage reports of the 29 December 2020 M6.4 Petrinja earthquake and the 6 February 2023 M7.8 Turkey-Syria earthquake sequence. The building-scale exposure model (→ Task 2.7) has been finished (→ Deliverable D2.13) and we provide first tests of the exposure model (in combination with the respective fragility model) against real damage assessments.

### Testing of non-linear site-amplification models

Nonlinear site effects mainly occur for large ground motion at soft soils where there are few measured observations. Predicting and modeling such effects is therefore challenging, and most nonlinear site amplification models used in ground-motion models (GMMs) are either partly or fully based on numerical simulations. To test the prediction power of nonlinear site-amplification models, Loviknes et al. (2021) developed a testing framework using observed site-amplification from the KiK-net network in Japan. For most of the KiK-net stations, the observed site response shows a large variability and little clear trend, even within stations with similar  $V_{S30}$  values. This is especially clear when the stations are grouped by  $V_{S30}$  as in Figure 7.4.1. We found that, for most stations, the simple linear site amplification model has the best performance and therefore argue that using nonlinear site-amplification models in this ground-motion range is not necessary. The study only considers nonlinear amplification models based on  $V_{S30}$  and PGA, other models using other parameters to capture non-linearity should therefore be tested in the future.

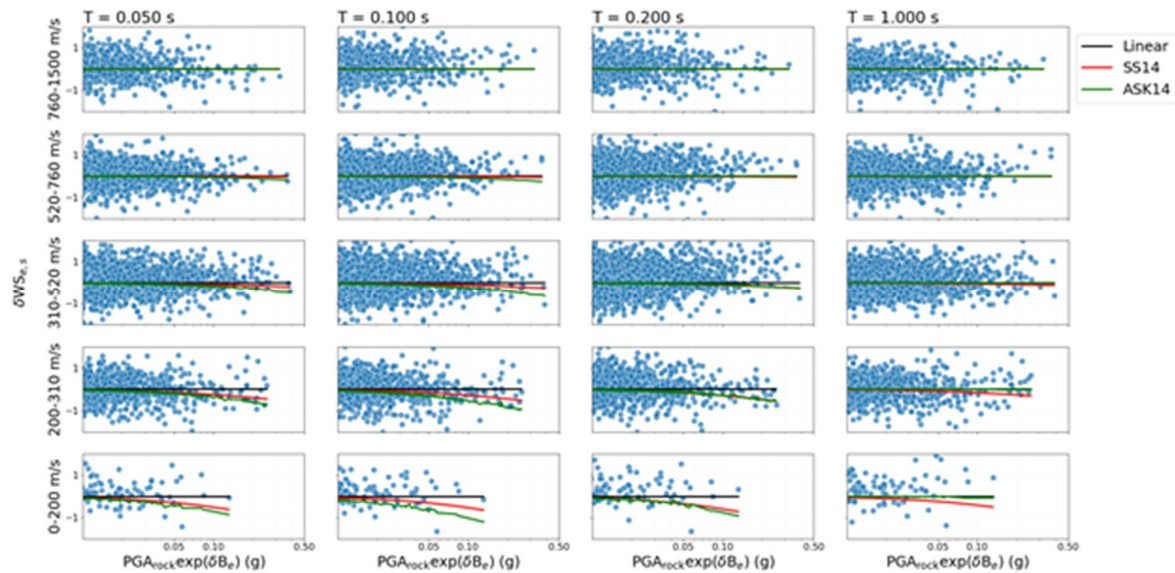


Figure 7.4.1: The KiK-net stations grouped by  $V_{S30}$  with the linear and non-linear site amplification models compared to  $\delta W_{Se,s}$  with respect to rock peak acceleration with event variability ( $PGA_{rock} \exp(\delta B_e)$ ). The non-linear models are from Seyhan and Stewart (2014) (SS14) and Abrahamson et al. (2014) (ASK14). The trend predicted by the models are not observed.

### Testing a new site proxy for site-amplification prediction models

Local geology can have a strong impact on earthquake ground shaking. This is especially true for sites with mainly loose sediments which are expected to amplify the recorded ground motion. In many, non-site-specific, applications where seismic hazard and risk assessments must be computed on large regions, this site amplification is commonly predicted using the average shear-wave velocity of the upper 30 meters of the soil column ( $V_{S30}$ ). For a single site, the velocity profile

and  $V_{S30}$  can be measured directly, but for larger areas and regions the  $V_{S30}$  must be inferred from other parameters. A much-used method to calculate  $V_{S30}$  is the model by Wald and Allen (2007) based on topographic slope from digital elevation models (DEMs). However, inferring  $V_{S30}$  based on topographic slope has several limitations, especially for basins and particular geological conditions (Lemoine et al. 2012).

We propose a geomorphological model for inferred sediment depth by Pelletier et al. (2016), as an alternative site proxy to predict ground motion site-amplification on a regional or global scale. The Pelletier et al. (2016) model use DEM and geological maps to distinguish between lowlands, uplands, hill slopes and valley bottoms. To test whether the model can be used to predict ground-motion site amplification, we compare the geomorphologically-inferred sedimentary thickness to inferred  $V_{S30}$ , topographic slope and empirical site amplification as shown in Figure 8 for frequency Hz. For each proxy we use linear regression to derive a simple site amplification model (black lines in Figure 8) and evaluate the performance of each model. The results show that the geomorphologically-inferred sedimentary thickness performs better than or equally well as the traditional and much used proxies  $V_{S30}$  inferred from topographic slope and topographic slope. We therefore argue that the inferred geomorphologically-inferred sedimentary thickness from the Pelletier et al. (2016) model is a promising new alternative to traditional inferred proxies for predicting site amplification on a regional or global level for large scale seismic hazard or risk studies.

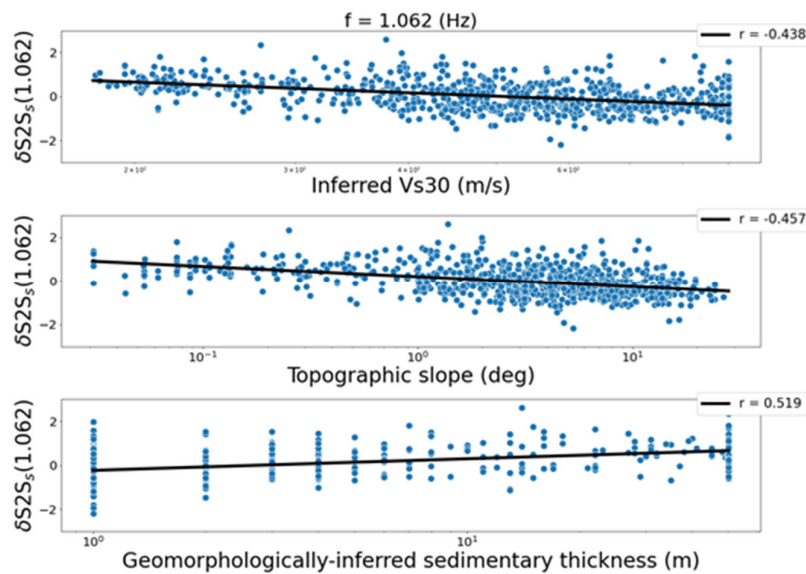


Figure 7.4.2: The linear regression (black lines) and correlation coefficient  $r$  between the empirical site amplification  $\delta S2S_s$  for frequency  $f=1.062$  Hz and the inferred  $V_{S30}$  from topographic slope (top) and topographic slope (middle) and the geomorphologically-inferred sedimentary thickness (bottom) at stations from the European Engineering Strong-Motion (ESM) dataset.

### **Preliminary Testing of Damage and Loss Assessments**

We have tested the scenario risk assessment for the Turkey 2023 and Petrinja 2020 earthquakes. For this, we have used excerpts of the Global Dynamic Exposure model ( $\rightarrow$  Deliverable D2.13)

for the affected areas. Although this deliverable was defined to only cover the model for European countries, we have extended it to many more countries, including Syria, as it was also heavily impacted by the earthquake. This was done by including the Middle East exposure model provided by the Global Earthquake Model.

To separately check for damage and loss, we have developed the loss-calculator (→ Deliverable D2.13) that aggregates damage and loss to either buildings or tiles of a grid. To compute the damage and loss of the earthquakes, we used ShakeMaps provided by the United States Geological Survey (USGS) for the Turkey and Petrinja earthquakes.

#### Turkey Earthquake

Our results show a good match between the building-specific assessment of damage and the true numbers as reported in the media. 164,000 completely or severely damaged buildings were reported (including some that collapsed during the aftershocks) and the model was able to reproduce a similar number: 96,000 completely collapsed and 38,000 extensively damaged buildings, totaling to 144,000 completely or severely damaged buildings. The difference is little more than 10% of the total number including the results of the aftershock damage. This indicates that at least the combination of exposure data and fragility functions shows an agreement with the observations. Contrary to that, the number of fatalities is computed at 8,300 and significantly lower than the recently reported more than 50,000 casualties. This points to two possible problems: either the vulnerability functions are not well calibrated or the number of people considered inside of buildings are wrongly estimated in the exposure model. Such functions or numbers are difficult to estimate and also the USGS reports with almost equal probability fatalities ranging from 1,000 to 1,000,000, indicating that our results are within the same range. Finding the true cause of this mismatch will continue after the RISE project as will the further development of the exposure model.

#### Petrinja, Croatia Earthquake

For the Petrinja earthquake the model prediction were significantly above the observed numbers. Our model predicts 31,500 collapsed and 13,500 extensively damaged buildings while only 4,200 buildings were reported as uninhabitable and approx. 8000 temporarily uninhabitable. Likewise the number of fatalities is predicted to be around 700 while only 8 people were reported dead. This mismatch requires a more in-depth study to identify the problem.

### References

- Abrahamson, N. A., Silva, W. J., and Kamai, R. (2014). "Summary of the ASK14 ground motion relation for active crustal regions". *Earthquake Spectra*, 30(3):1025–1055.
- Bird, P., Jackson, D., Kagan, Y., Kreemer, C., & Stein, R. (2015). GEAR1: A Global Earthquake Activity Rate Model Constructed from Geodetic Strain Rates and Smoothed Seismicity. *Bulletin of the Seismological Society of America*, 105(5), 2538-2554.
- Kraczyk, M. S., Shi, A., Bhaskar, A., Marinov, D., & Stodden, V. (2021). Learning from reproducing computational results: introducing three principles and the Reproduction Package. *Philosophical Transactions of the Royal Society A*, 379(2197), 20200069.

- Lemoine, A., Douglas, J., and Cotton, F. (2012); Testing the Applicability of Correlations between Topographic Slope and VS30 for Europe. *Bulletin of the Seismological Society of America*, 102 (6): 2585–2599. <https://doi.org/10.1785/0120110240>
- Michael, A. J., & Werner, M. J. (2018). Preface to the focus section on the Collaboratory for the Study of Earthquake Predictability (CSEP): New results and future directions. *Seismol. Res. Lett.*, 89(4), 1226–1228. <https://doi.org/10.1785/0220180161>
- Pelletier, J. D., Broxton, P. D., Hazenberg, P., Zeng, X., Troch, P. A., Niu, G.-Y., Williams, Z., Brunke, M. A., and Gochis, D. (2016), A gridded global data set of soil, immobile regolith, and sedimentary deposit thicknesses for regional and global land surface modeling, *J. Adv. Model. Earth Syst.*, 8, 41– 65, <https://doi.org/10.1002/2015MS000526>
- Rhoades, D. A., Schorlemmer, D., Gerstenberger, M. C., Christophersen, A., Zechar, J. D., & Imoto, M. (2011). Efficient testing of earthquake forecasting models. *Acta Geophysica*, 59(4), 728–747. <https://doi.org/10.2478/s11600-011-0013-5>
- Schorlemmer, D., & Gerstenberger, M. C. (2007). RELM testing center. *Seismol. Res. Lett.*, 78(1), 30–36. <https://doi.org/10.1785/gssrl.78.1.30>
- Schorlemmer, D., Gerstenberger, M. C., Wiemer, S., Jackson, D. D., & Rhoades, D. A. (2007). Earthquake likelihood model testing. *Seismol. Res. Lett.*, 78(1), 17–29. <https://doi.org/10.1785/gssrl.78.1.17>
- Schorlemmer, D., Christophersen, A., Rovida, A., Mele, F., Stucchi, M., & Marzocchi, W. (2010). Setting up an earthquake forecast experiment in Italy. *Annals of Geophysics*.
- Schorlemmer, D., Werner, M. J., Marzocchi, W., Jordan, T. H., Ogata, Y., Jackson, D. D., Mak, S., Rhoades, D. A., Gerstenberger, M. C., Hirata, N., Liukis, M., Maechling, P. J., Strader, A., Taroni, M., Wiemer, S., Zechar, J. D., and Zhuang, J. C. (2018). The Collaboratory for the Study of Earthquake Predictability: Achievements and Priorities, *Seismol. Res. Lett.*, 89(4), 1305-1313. <https://doi.org/10.1785/0220180053>
- Seyhan, E. and Stewart, J. P. (2014). "Semi-empirical nonlinear site amplification from NGA-West2 data and simulations." *Earthquake Spectra*, 30(3):1241–1256.
- Wald, D. J., Allen, T. I. (2007); Topographic Slope as a Proxy for Seismic Site Conditions and Amplification. *Bulletin of the Seismological Society of America*, 97 (5): 1379–1395. <https://doi.org/10.1785/0120060267>
- Werner, M. J., Helmstetter, A., Jackson, D. D., & Kagan, Y. Y. (2011). High-resolution long-term and short-term earthquake forecasts for California. *Bull. Seismol. Soc. Am.*, 101(4), 1630–1648. <https://doi.org/10.1785/0120090340>
- Zechar, J., Schorlemmer, D., Liukis, M., Yu, J., Euchner, F., Maechling, P. J., & Jordan, T. H. (2009). The Collaboratory for the Study of Earthquake Predictability perspective on computational earthquake science. *Concurrency and Computation: Practice and Experience*, 22(12), 1836–1847. <https://doi.org/10.1002/cpe.1519>
- Zechar, J., Schorlemmer, D., Werner, M. J., Gerstenberger, M. C., Rhoades, D. A., & Jordan, T. H. (2013). Regional earthquake likelihood models I: First-order results. *Bull. Seismol. Soc. Am.*, 103(2A), 787–798. <https://doi.org/10.1785/0120120186>

## 1) Peer reviewed publications

Asayesh, B. M., Zafarani, H., Hainzl, S., & Sharma, S. (2022). Effects of large aftershocks on spatial aftershock forecasts during the 2017–2019 western Iran sequence. *Geophysical Journal International*, 232(1), 147–161. <https://doi.org/10.1093/gji/ggac333>

Bayona, J. A., Savran, W. H., Rhoades, D. A., & Werner, M. J. (2022). Prospective evaluation of multiplicative hybrid earthquake forecasting models in California, *Geophys. J. Int.*, ggac018, <https://doi.org/10.1093/gji/ggac018>

Bayona, J. A., Savran, W. H., Iturrieta, P., Gerstenberger, M. C., Graham, K. M., Marzocchi, W., ... & Werner, M. J. (2023). Are Regionally Calibrated Seismicity Models More Informative than Global Models? Insights from California, New Zealand, and Italy. *The Seismic Record*, 3(2), 86–95. <https://doi.org/10.1785/0320230006>

Cheng, J., Main, I., Segou, M. & Werner, M. J. (2023, in preparation). A Coulomb/rate-state earthquake forecast model for Italy.

Churchill, R. M., Werner, M. J., Biggs, J., & Fagereng, Å. (2022a). Afterslip moment scaling and variability from a global compilation of estimates. *Journal of Geophysical Research: Solid Earth*, 127(4), e2021JB023897. <https://doi.org/10.1029/2021JB023897>

Churchill, R. M., Werner, M. J., Biggs, J., & Fagereng, Å. (2022b). Relative afterslip moment does not correlate with aftershock productivity: implications for the relationship between afterslip and aftershocks. *Geophysical Research Letters*, e2022GL101165. <https://doi.org/10.1029/2022GL101165>

Herrmann, M. & Marzocchi, W. (2023). Maximizing the forecasting skill of an ensemble model. *Geophysical Journal International*, 234(1), 73–87. <https://doi.org/10.1093/gji/ggad020>

Husker, A., Werner, M. J., Bayona, J. A., Santoyo, M., & Corona-Fernandez, R. D. (2023). A Test of the Earthquake Gap Hypothesis in Mexico: The Case of the Guerrero Gap. *Bulletin of the Seismological Society of America*, 113(1), 468–479. <https://doi.org/10.1785/0120220094>

Khawaja, M. A., Schorlemmer, D., Hainzl, S., Iturrieta, P., Savran, W. H., Bayona, J. A., & Werner, M. J. (2023). Multi-resolution grids in earthquake forecasting: The Quadtree approach. *Bulletin of the Seismological Society of America*, 113(1), 333–347. <https://doi.org/10.1785/0120220028>

Khawaja, M. A., Hainzl, S., Schorlemmer, D., Iturrieta, P., Bayona, J. A., Savran, W. H., ... & Marzocchi, W. (2023). Statistical power of spatial earthquake forecast tests. *Geophysical Journal International*, 233(3), 2053–2066. <https://doi.org/10.1093/gji/ggad030>

Khawaja, M. A., Asayesh, B. M., Hainzl, S., & Schorlemmer, D. (2023). Towards improving the testability of aftershock forecast models. *Preprint available via EGUsphere*. <https://doi.org/10.5194/egusphere-2023-309>

Loviknes, K., S. R. Kotha, F. Cotton, and D. Schorlemmer (2021). Testing Nonlinear Amplification Factors of Ground-Motion Models, *Bull. Seismol. Soc. Am.*, 111, 2121–2137. <https://10.1785/0120200386>

Mancini, Segou, Werner, Parsons, Beroza & Chiaraluce (2022): On the Use of High-Resolution and Deep-Learning Seismic Catalogs for Short-Term Earthquake Forecasts: Potential Benefits and Current Limitations, *Journal of Geophysical Research: Solid Earth* 127 (11), e2022JB025202. <https://doi.org/10.1029/2022JB025202>

Savran, W. H., Werner, M. J., Marzocchi, W., Rhoades, D. A., Jackson, D. D., Milner, K., Field, E. H., & Michael, A. J. (2020). Pseudoprospective evaluation of UCERF3-ETAS forecasts during the 2019 Ridgecrest sequence. *Bull. Seismol. Soc. Am.*, 110(4), 1799–1817. <https://doi.org/10.1785/0120200026>

Savran, W. H., Werner, M. J., Schorlemmer, D., & Maechling, P. J., (2022a). pyCSEP: A Python Toolkit For Earthquake Forecast Developers. *Journal of Open Source Software*, 7(69), 3658. <https://doi.org/10.21105/joss.03658>

Savran, W. H., Bayona, J. A., Iturrieta, P., Asim, K. M., Bao, H., Bayliss, K., Herrmann, M., Schorlemmer, D., Maechling, P. J., & Werner, M. J. (2022b). pyCSEP: A Python Toolkit for Earthquake Forecast Developers. *Seismological Research Letters* 2022, 93(5): 2858–2870. <https://doi.org/10.1785/0220220033>

## 2) Other exploitable results/data/reports

### Data (including Model Output):

Bayona, Jose A., Savran, William H., Rhoades, David A., & Werner, Maximilian J. (2021). Mainshock+aftershock M4.95+ seismicity forecasts derived from the Regional Earthquake Likelihood Models (RELM) and the multiplicative hybrid earthquake models developed by Rhoades et al. (2014) (v1.0.0) [Data set]. Zenodo. <https://doi.org/10.5281/zenodo.5141567>

Bayona, Jose A., Savran, William H., Iturrieta, Pablo, Gerstenberger, Matthew C., Marzocchi, Warner, & Werner, Maximilian J. (2022). Global and regional long-term M4.95+ seismicity forecasts undergoing prospective evaluation [Data set]. Zenodo. <https://doi.org/10.5281/zenodo.7116221>

Churchill, Robert, Werner, Maximilian, Biggs, Juliet, & Fagereng, Ake. (2022). Afterslip Model Database RC2022 (Afterslip Moment Scaling and Variability from a Global Compilation of Estimates) [Data set]. Zenodo. <https://doi.org/10.5281/zenodo.6414330>

Khawaja, M. A., Iturrieta, P., Savran, W. H., Bayona, J. A., Werner, M. J., Hainzl, S., Philip J., & Schorlemmer, D. (2022). Global Earthquake Forecast Testing Experiment on Multi-Resolution Quadtree Grids. <https://doi.org/10.5281/zenodo.6305669>

### Software / Reproducibility packages:

Bayona, J. A., Savran, W., Iturrieta, P., Gerstenberger, M., Graham, K., Marzocchi, W., Schorlemmer, D., & Werner, M. (2023, Apr 6). Reproducibility Package for Are Regionally

Calibrated Seismicity Models More Informative than Global Models? Insights from California, New Zealand, and Italy. [https://github.com/bayonato89/reproducibility\\_global\\_vs\\_regional](https://github.com/bayonato89/reproducibility_global_vs_regional)

Bayona, J. A., Savran, W. H., Rhoades, D. A., & Werner, M. (2022, Jan 18). Reproducing the prospective evaluation of multiplicative hybrid earthquake forecasting models in California. <https://github.com/bayonato89/Reproducibility-hybrids>

Herrmann, M. (2023). Ensembling forecast models with logistic regression. Python code. url: <https://gitlab.com/marcus.herrmann/ensembling-forecast-models-with-logistic-regression>; doi: [10.5281/zenodo.7477998](https://doi.org/10.5281/zenodo.7477998)

Savran, William H., Bayona, José A., Iturrieta, Pablo, Khawaja, Asim M., Bao, Han, Bayliss, Kirsty, Herrmann, Marcus, Schorlemmer, Danijel, Maechling, Philip J., & Werner, Maximilian J. (2022). Reproducibility Package for pyCSEP: A Toolkit for Earthquake Forecast Developers (v1.0.0). Zenodo. <https://doi.org/10.5281/zenodo.6626265>

The repository for codes for floating community experiments:

<https://git.gfz-potsdam.de/csep-group/fecsep>

The repository for the floating experiment of the European Seismic Hazard Model: <https://git.gfz-potsdam.de/csep-group/fecsep-efehr20>

The repository for the global floating experiment: <https://git.gfz-potsdam.de/csep-group/gefe-quadtree/>

The repository for the 2010 Italy floating experiment: [https://git.gfz-potsdam.de/csep-group/fe\\_italy\\_ti](https://git.gfz-potsdam.de/csep-group/fe_italy_ti)

The experiment rules, competing models and the beta implementation of the new Italy floating experiment:

[https://git.gfz-potsdam.de/csep-group/rise\\_italy\\_experiment/experiment\\_setup](https://git.gfz-potsdam.de/csep-group/rise_italy_experiment/experiment_setup)

[https://git.gfz-potsdam.de/csep-group/rise\\_italy\\_experiment/models](https://git.gfz-potsdam.de/csep-group/rise_italy_experiment/models)

[https://git.gfz-potsdam.de/csep-group/rise\\_italy\\_experiment/experiment\\_system](https://git.gfz-potsdam.de/csep-group/rise_italy_experiment/experiment_system)

The repository for the testing codes and the Jupyter notebook for non-linear ground models: [https://git.gfz-potsdam.de/karinalo/test\\_nl\\_siteampmodel](https://git.gfz-potsdam.de/karinalo/test_nl_siteampmodel)

<https://zenodo.org/record/6299826>

The codes for the risk testing were developed in Python and are using open-source databases, either PostGIS or Spatialite. The repository for the loss-calculator: <https://git.gfz-potsdam.de/dynamicexposure/globaldynamicexposure/loss-calculator>

The code repository to create the exposure model excerpts for the damage and loss calculation: <https://git.gfz-potsdam.de/dynamicexposure/globaldynamicexposure/exposure-share>

### **1.2.8 Work package 8**

#### **Overview**

WP8 focuses on securing the broad societal, economic, and scientific impact of RISE; an impact which is both demonstrable and long-term. This process started on day one of the project, continued throughout, and exposed all activities in RISE to an ongoing dialogue targeting stakeholder and end-user needs. WP8 adopted an interdisciplinary and multi-hazard user perspective and translated all RISE outputs and deliverables into tangible products and services; useful for and used by a wide range of stakeholders. WP8 further contained a comprehensive set of communication, dissemination, exploitation, and decision-support activities, prioritised in relation to what is needed to maximise impact.

#### **Summary of achievements in WP8 tasks:**

##### **Task 8.1: Plan for the Exploitation and Dissemination of Results (PEDR)**

PEDR stands for "Plan for Exploitation and Dissemination of Results" and is the master plan of RISE to maximise the demonstrable, long-term, socio-economic impact of the project and to achieve a measurable increase in societies' resilience to earthquakes. The PEDR enables sharing and measuring RISE outputs and deliverables through a range of exploitation, dissemination, and outreach activities targeting different stakeholders and audiences. To this end, a set of measures, metrics, and formats has been established to promote, define, and measure the success of RISE activities. Whereas the first two PEDR reports mainly focused on the quantitative evaluation of the outreach activities, the third report aimed to provide an overview of RISE's impact on the scientific, societal, technological, and economic level and derive recommendations for the last phase of the project.

For the quantitative measurements, the following metrics were considered: website users, Twitter followers, newsletter subscribers, publications, and the number of participants of stakeholder exchange. They are described in detail in the D8.1 PEDR (M3). The second PEDR (D8.2) is an updated version of D8.1, including brief descriptions of the impact of each WP with regards to science, society, technology, and economy. In the second half of the project, RISE research activities had advanced, and thus the impact on society, technology, science, and economy were also assessed qualitatively. To this end, we closely collaborated with the project WP and task leaders to investigate the overall impact of RISE regarding the four pillars science, society, technology, and economy through an online survey. We defined indicators to assess the impact for each of these four pillars, covering the four priorities to reduce disaster risk described in the Sendai Framework for Disaster Risk Reduction. Therefore, in the last PEDR update (D8.3), we provide an update of the quantitative measurements and a more detailed summary of RISE's impact on technology, science, society, and economy achieved so far (qualitative measurements).

#### **Survey**

We conducted the online survey from January 19 to February 8, 2022. In total, 19 representatives of the RISE project filled in the survey (see table 8.1). All WP leaders have filled in the survey. In addition, several task leaders answered the questionnaire to provide more details about the impact of certain assets and technologies developed in RISE.

	WP1	WP2	WP3	WP4	WP5	WP6	WP7	WP8
<b>Number of responders</b>	1	4	3	7	3	5	3	2
<b>Covered tasks</b>		2.2 2.4 2.6 2.7	3.1	4.1 4.3 4.4 4.6	5.1 5.2 5.3	6.1 6.5	7.1 7.2 7.3 7.4	8.1 8.4

Table 8.1: Overview of the number of responses per work package (WP) and the covered tasks

The survey consisted of five question blocks (QB), whereas QB1 assessed which work packages and tasks the responders represented. In QB2 to QB5, we then assessed the indicators (see figure 8.1.1) of the four pillars introduced in the section before.

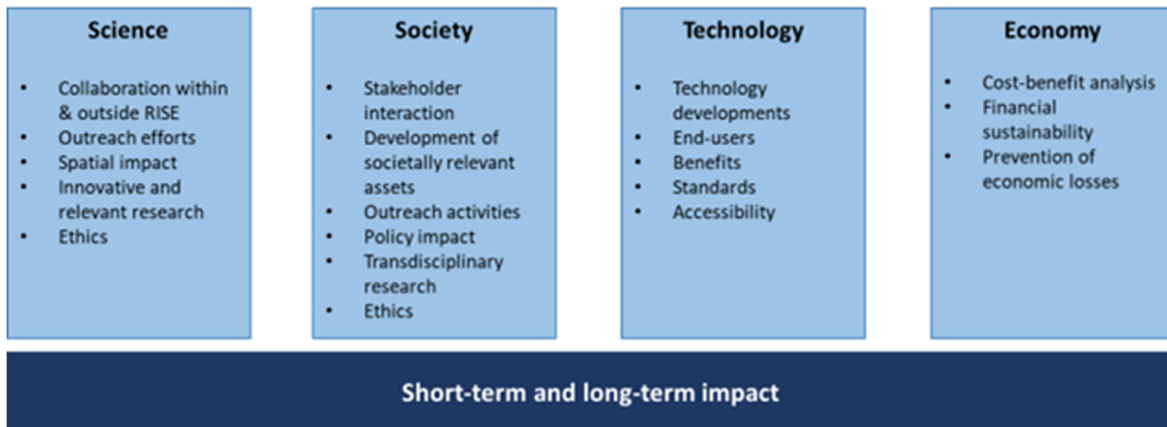
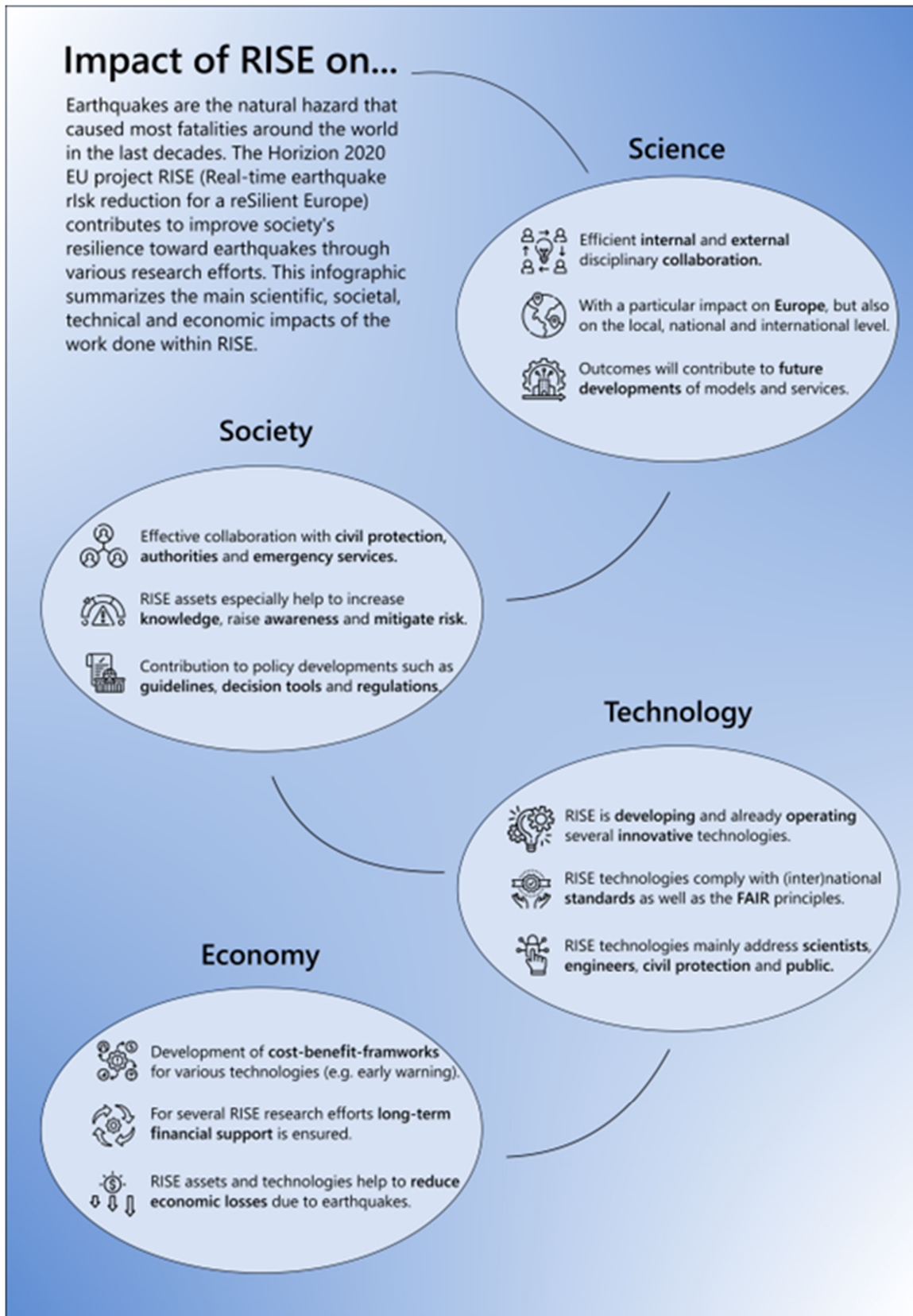


Figure 8.1.1 Overview of the indicators within each pillar to increase short- and long-term impact

### Result overview

The PEDR evaluation (D8.3) showed that the outreach platforms of RISE (e.g., website, Twitter) were increasingly used, and the RISE community efficiently shared and discussed its scientific developments and efforts at conferences and internal meetings. Further, the results of the PEDR survey illustrated that RISE interacted and was interlinked with several other European as well as national projects/initiatives, ensuring the long-term sustainability of products and services developed within RISE. The disciplinary collaboration within each WP and the community outside RISE works effectively; however, the cross-WP activities could be improved in the last project phase, which was for example successfully done for the OEF communication efforts. Further, in particular, WP5 had involved end-users already in the development process of certain products and services to ensure they meet their needs. Additionally, RISE efforts (will) contribute to preventing economic losses by facilitating rapid decision making, by increasing the efficiency of emergency intervention, by providing rapid information on building damages, and by building the basis for insurance models and the establishment of seismic building codes. Moreover, various technologies are in the development phase, and the next effort will be to test and afterwards implement them.

The following infographic shows the main impacts of the RISE efforts. Further, in D8.3 Update PEDR, the detailed results per pillar and recommendations we provided for the second phase of the RISE project to improve its impacts can be found.



## Task 8.2 Standardization of data and data access services

Data and data products are essential for reliable earthquake related services. Without data standards and standardized web services, it can be difficult to compile, analyse and compare datasets and models. Standardized formats and protocols allow for effective data exchange and interoperability, to ensure consistency and transparency, which are essential for research and development, decision-makers, and the general public.

Within the Rise Project, efforts have been focussing to support and encourage the use of open standards and community-driven standards. To ensure reliable and consistent data representation and usage, the project recommends common data formats such as Extensible Markup Language (XML), JavaScript Object Notation (JSON), comma-separated values (CSV), and binary formats (hdf5) for describing data models. These open standards are frequently used for visualising and analysing earthquake data on web-based platforms and applications. They offer a lightweight and interoperable format that can be easily parsed and rendered in a variety of mapping tools and libraries, making them a popular choice for earthquake data applications.

Among the community driven data standards which RISE promotes are QuakeML, ShakeMap and NRML. These standards are already widely used in the scientific community and have a broad ecosystem of applications built on top of them.

QuakeML is a flexible and extensible XML-based data standard used in seismology for representing and exchanging earthquake-related data. It includes definitions for a wide range of data types, including origin, magnitude, focal mechanism, station, waveform, and others. The standard is fully documented at <https://quake.ethz.ch/quakeml/>, and many seismological networks and data centres use it for data exchange and analysis. As a result, QuakeML has been widely used in RISE applications and services, including the Operational Earthquake Forecast (OEF) and Earthquake Early Warning (EEW) products. The use of QuakeML has facilitated effective collaboration and analysis of earthquake data, enabling researchers and organisations to better understand and mitigate the risks associated with earthquakes.

ShakeMap (Worden and Wald 2016) is a tool developed by the U.S. Geological Survey (USGS) for displaying maps of earthquake ground shaking and other related parameters. ShakeMap data is typically represented in XML or JSON and contains information such as ground motion values, intensity measurements, and uncertainty estimates. ShakeMap data is frequently used for rapid evaluation of earthquake impacts, including estimations of intensity of ground shaking, potential damage, and casualties.

Risk Markup Language for Natural Hazards (NRML) is a standard XML-based data format used to represent earthquake hazard and risk information, including seismogenic sources, exposure, vulnerability, and loss models. NRML (<https://docs.openquake.org/oq-engine/1.4/schema.html>) is maintained and developed by Global Earthquake Model - Foundation, provides a standard format

for describing earthquake hazard and risk models, allowing for interoperability and comparison of different risk assessment tools and methodologies. NRML is used as a default data format to disseminate the results of the European seismic hazard models at [hazard.efehr.org](http://hazard.efehr.org).

Data Access Services: Data access services (APIs) provide standardised interfaces for accessing data from different sources or systems. The main hazard and risk services use standard communication protocols (HTTP) and leverage appropriate pre-existing standards like [Open Geospatial Consortium \(OGC\)](#) standards for location information, or above-mentioned standards like QuakeML, NRML, JSON and others where appropriate.

For technical documentation and (automatic) generation of service clients, we provide service documentation in WADL (web application description language) format: [WADL, machine readable](#), and [WADL html extraction, human readable](#) or [OpenAPI](#) documentations.

### WADL documentation: Share-Services

Documentation of the web services to discover and deliver pre-calculated Data to evaluate earthquake hazard in Europe.

#### Summary

Resource	Method	Description
<a href="http://apocsvr.share-eu.org:8080/share/map">http://apocsvr.share-eu.org:8080/share/map</a>	GET (getMapModel)	Model: provide an index of all hazard models that are defined for a specific point of interest
	GET (getMapImt)	Intensity measurement type: Provide all intensity measurement types (IMT) for which a specified model provides hazard information
	GET (getMapPoe)	Poe and timespan: Provide probability of exceedance and investigation timespan's with maps available, given model ID and intensity measurement types (IMT) for which a specified model provides hazard information
	GET (getMapSoil)	Site class: Provide site class with maps available, given model ID, IMT, POE, time span for which a specified model provides hazard information
	GET (getMapAggreg)	Aggregation: Provide aggregation types with maps available, given model ID, IMT, POE, time span, site class for which a specified model provides hazard information
	GET (getMapId)	Map id: Provide the map identity, and the layer reference for the web map service, of the hazard map for given model ID, IMT, POE, time span, site class and aggregation type.
<a href="http://apocsvr.share-eu.org:8080/share/curve">http://apocsvr.share-eu.org:8080/share/curve</a>	GET (getCurveModels)	Models: provide an index of all hazard models that are defined for a specific point of interest
	GET (getCurveImt)	IMT's: Provide all intensity measurement types (IMT) for which a specified model provides hazard curves information
	GET (getCurveSoil)	Site class: Provide site class with curves available, given model ID, IMT, POE, time span for which a specified model provides hazard information
	GET (getCurveAggreg)	Aggregation: Provide aggregation types with curves available, given model ID, IMT, POE, time span, site class for which a specified model provides hazard information
<a href="http://apocsvr.share-eu.org:8080/share/spectra">http://apocsvr.share-eu.org:8080/share/spectra</a>	GET (getCurveNrmf)	Curve data (nrmf): Provide the Curve in the Nrmf Format for given model ID, IMT, site class and aggregation type.
	GET (getSpectraModel)	Models: provide an index of all hazard spectras that are defined for a specific point of interest
	GET (getSpectraImt)	IMT's: Provide all intensity measurement types (IMT) for which a specified model provides hazard information
	GET (getSpectraPoe)	Poe and Timespan: Provide probability of exceedance and investigation timespan's with maps available, given model ID and intensity measurement types (IMT) for which a specified model provides hazard information
	GET (getSpectraSoil)	Site class: Provide site class with maps available, given model ID, IMT, POE, time span for which a specified model provides hazard information
	GET (getSpectraAggreg)	Aggregation: Provide aggregation types with maps available, given model ID, IMT, POE, time span, site class for which a specified model provides hazard information
<a href="http://apocsvr.share-eu.org:8080/share/design-spectra/design_spectra_elastic_ec">http://apocsvr.share-eu.org:8080/share/design-spectra/design_spectra_elastic_ec</a>	GET (getSpectra)	Spectra Data: Provide the data for the selected hazard spectrum
	GET (getDesignSpectra)	Design Spectra: Get the data of the elastic design spectra EC8. (Values need to be checked for correctness!)

#### Grammars

[./documents/nrml/nrml.xsd](#)

Figure 8.2.1. example of an WADL documentation for EFEHR's web-services at [hazard.efehr.org](http://hazard.efehr.org)

Data Governance: All services are developed with open-source libraries, and the distributed data follow the FAIR principles (findability, accessibility, interoperability, and reuse). The principles emphasise machine-actionability (i.e., the ability of computational systems to find, access, interoperate, and reuse data without human intervention). Furthermore, all existing hazard and risk web-services are compliant with the EPOS DCAT-AP standard for machine discovery (<https://github.com/epos-eu/EPOS-DCAT-AP>) since 2019. For all web services and data we are also working on adhering to the EPOS metadata format, ensuring that DOIs can be assigned to all products as well as CC BY SA v4.0 (<https://creativecommons.org/licenses/by-sa/4.0>) open data licences, in order to meet the requirements of the EPOS Data Policy. All datasets have DOIs identifiers and full respective metadata sets.

Data governance is a crucial aspect of the RISE project, and all its services are built using open-source libraries that follow the FAIR principles, which ensure findability, accessibility, interoperability, and reuse of distributed data. These principles prioritise machine-actionability,

which means that computational systems can find, access, interoperate, and reuse data without human intervention. To ensure compliance with the EPOS DCAT-AP (<https://github.com/epos-eu/EPOS-DCAT-AP>) standard for machine discovery, all existing hazard and risk web-services have adhered to this standard since 2019. Additionally, the RISE project is working on adhering to the EPOS metadata format for all web services and data. This format ensures that DOIs can be assigned to all products and that they comply with CC BY SA v4.0 (<https://creativecommons.org/licenses/by-sa/4.0>) open data licences to meet the requirements of the EPOS Data Policy. All datasets have DOIs identifiers and full metadata sets.

Open standards and open-source data management tools are considered vital components in the development and implementation of dynamic risk services within the RISE project. These open standards are freely available and accessible to everyone, allowing for easy integration with other systems and applications. Furthermore, using community-driven data formats such as QuakeML, NRML, and ShakeMap, which are developed by the scientific community (e.g., seismologists, engineers), facilitates the development of web services that provide quick access to information and aid in effective decision-making, emergency response, and risk mitigation in earthquake-prone areas.

Standardised data formats not only facilitate the development of web services but also ensure interoperability, data integration, and the exchange of information between various stakeholders. This is necessary in earthquake-related services, where timely communication and collaboration among stakeholders can be crucial in preventing loss of life and property. Recent devastating earthquakes in Turkey served as a prime example, as recordings of significant motion were made publicly available on the websites of AFAD (<https://en.afad.gov.tr>) and EIDA/ORFEUS (<https://www.orfeus-eu.org/data/eida>). In addition, available resources included ShakeMap, earthquake catalogues (aftershocks, instrumental), active faults, and ESHM20 hazard results. All these materials and information enabled and supported not only the general public information or the scientific commission but also provided important information for rescue missions and recovery planning.

Overall, earthquake-related data standards and web services aim to enhance communication and collaboration among stakeholders, ensuring that earthquake data can be shared and analysed rapidly and precisely. They are the foundation of the existing operational earthquake risk services and provide standardised methods for representing earthquake data, products, and services.

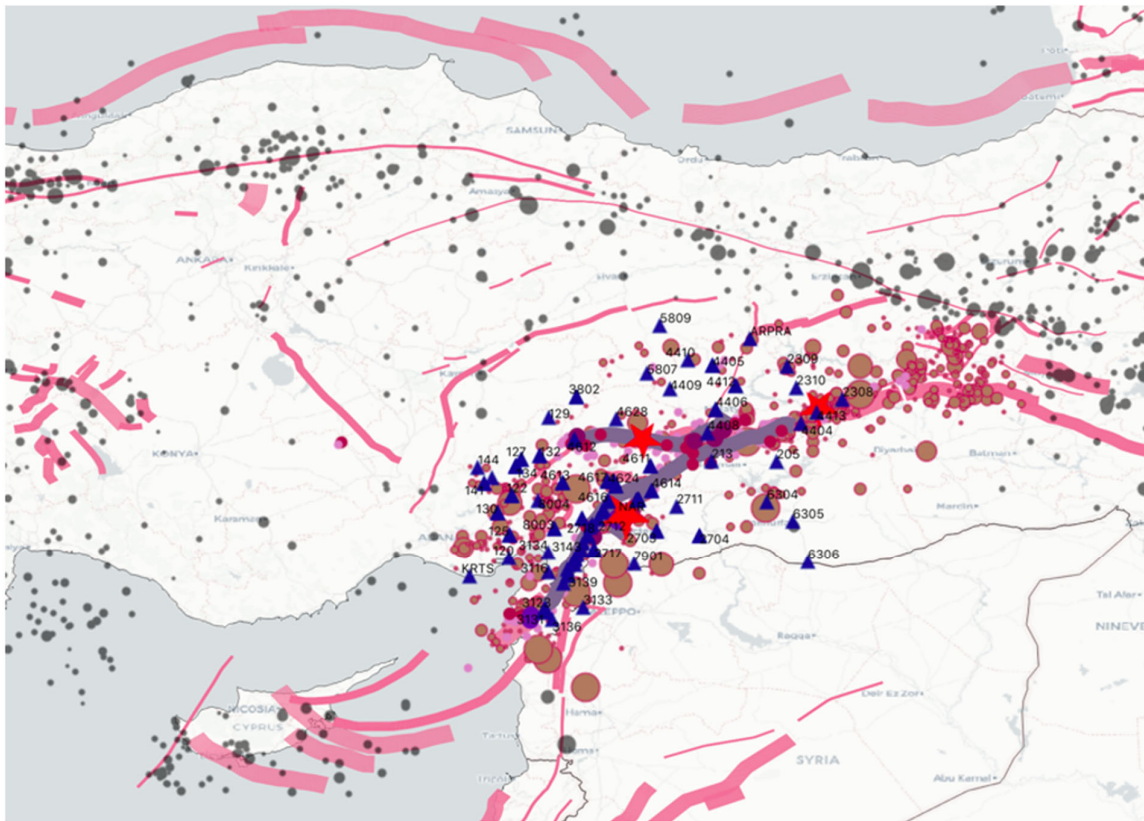


Figure 8.2.2. Example of multiple datasets i.e., active shallow faults (light red lines), earthquake catalogue (grey circle), aftershocks (brown circles), seismic stations (blue triangles), and the two mainshocks of the two M7+ earthquakes that occurred on February 6th, 2023. All datasets are openly available and distributed with open standards (csv, json, shapefiles)

### Task 8.3 RISE operational services and applications

As data, models, and computing resources grow, dynamic and operational earthquake risk services become increasingly important for evaluating and mitigating earthquake risks. A valuable resource for the community is the web-based platform of the European Facilities of the Earthquake Hazard and Risk ([www.efehr.org](http://www.efehr.org)), which provides information on earthquake hazard and risk. This platform provides access to the fully cross-border harmonised seismic hazard (Danciu et al 2021) and risk models (Crowley et al 2021), both started within the SERA project and finalised within the RISE project.

Furthermore, it is important to note that the availability of both the seismic hazard and risk models, including their main input datasets (i.e., earthquake catalogues, active faults, seismogenic sources models, ground motion models, site-amplification, exposure and vulnerability models) on the EFEHR's web-platform, is a significant milestone for the RISE Projects, as many of these components have been updated and/or directly used in the development of the RISE operational services.

Researchers, Earth scientists, practitioners, civil protection authorities, and the general public can access real-time earthquake data, products, and services also via the European Mediterranean

Seismological Centre, EMSC’s web-portal: <https://www.emsc-csem.org/>. Additionally, ORFEUS (Observatories & Research Facilities for European Seismology), collects, maintains and manages the distribution of earthquake recordings across the European-Mediterranean region. As a component of ORFEUS (Observatories & Research Facilities for European Seismology), EIDA (European Integrated Data Archive infrastructure, <https://www.orfeus-eu.org/data/eida/>) offers seismic waveform data from European archives for study and development. These services and data provider pillars are vital in supporting the community for earthquake research and development topics and initiatives such as the European Plate Observing System (EPOS) infrastructure (Haslinger et al 2022).

In this context, operational services have been developed and prototyped within the RISE project: earthquake early warning (EEW), operational earthquake forecast (OEF) and rapid loss assessment (RLA). These systems are currently installed and operated as demonstrators at ETH Zurich, and the background information of these systems has been detailed in various deliverables (i.e., D8.3, D8.4).

Web Services allow for simple, documented and standardised access to data from these services. Either (web) platforms and visualisations built on top of these Webservice in RISE, or ad hoc systems using the same web services can be used to look at the results and communicate them efficiently.

It is also important to be able to guarantee availability of those services. Therefore, a resilient and dependable server infrastructure as implemented in other parts of the project are also crucial in EEW, OEF and RLA. Geographical server redundancy, database replication, automatic failovers, monitoring and 24/7 support are required for all operational services at ETH.

In the aftermath of the February 2023 earthquakes in Turkey, for instance, the number of unique visitors and the number of pages accessed increased by a factor of ten as given in Figure xx.

Therefore, it is crucial that these web-services remain accessible and operational. Redundant servers safeguard the system's functionality in the event of hardware or network failures. Load balancing can guarantee availability in the event of high numbers of simultaneous requests to services or web platforms.

All databases of the operational services are duplicated in different virtual machines, to maintain data integrity and service continuity in the event of a database failure. Each operational service has a web-portal to disseminate data and results. The web portals are customised to make earthquake data, products, and services easy to access, visualise, analyse, and share. Examples of such web-portals updated within Rise Project, include [hazard.efehr.org](http://hazard.efehr.org) and [risk.efehr.org](http://risk.efehr.org), which are part of the European Facilities for Earthquake Hazard and Risk (EFEHR) web services.

It is worth noting that integrating RISE services, whether as demonstrators or operational services, would benefit the entire community. As a result, a roadmap to integrate these services

into the EFEHR Consortium's seismic hazard and risk services is required. The topic is expected to be addressed at the EFEHR General Assembly in October 2023. The Rapid Loss Assessment and the Operational Earthquake Forecast are expected to be integrated into European operational services within the next year.

Last but not least, that within the RISE project, the hazard and risk services of EFEHR's, i.e., [hazard.efehr.org](http://hazard.efehr.org) and [risk.efehr.org](http://risk.efehr.org), were integrated with the recently released web-platform (<https://www.ics-c.epos-eu.org/>) of EPOS (European Plate Observing System, [www.epos-eu.org](http://www.epos-eu.org)). In the long term, these existing European web-platforms should support access to data and products, which in turn will improve earthquake knowledge, preparation, and mitigation (Haslinger et al 2022).

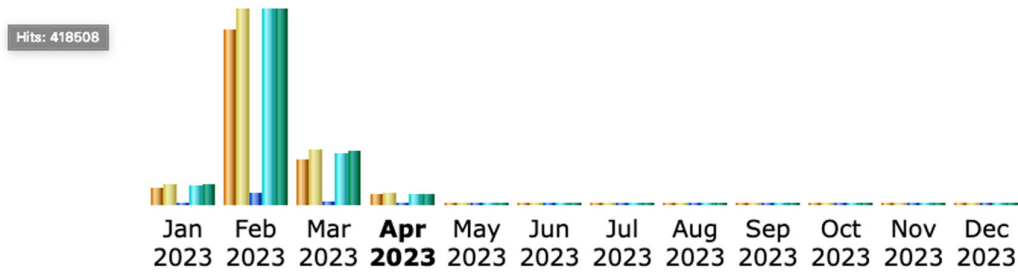
### **References:**

Haslinger F, Basili R, Bossu R, Cauzzi C, Cotton F, Crowley H, Custódio S, Danciu L, Locati M, Michelini A, Molinari I. Coordinated and interoperable seismological data and product services in Europe: the EPOS thematic core service for seismology. *Annals of Geophysics*. 2022;65(2).

Worden, C.B. and D.J. Wald (2016). ShakeMap Manual Online: technical manual, user's guide, and software guide, U. S. Geological Survey. [cbworden.github.io/shakemap](http://cbworden.github.io/shakemap). DOI: 10.5066/F7D21VPQ.

### **Task 8.4 RISE external communication, good practice series, and training**

A number of communication tools were used targeting different internal and external audiences, such as the project website, newsletters, social media (e.g. Twitter), good practice reports or training workshops. Some of these communication tools were already set up at the beginning of the project (project website, newsletter, Twitter account), and others were continuously compiled during the project development and when results were achieved (e.g., good practice, conference presentations). In particular, much effort went into preparing communication activities for the launch of the European Seismic Hazard and Risk Models (ESHM20 and ESRM20). To this end, we defined a communication strategy, developed various communication products, tested them with end users focusing on their design preferences, correct interpretation of the information provided, and information needs, and adapted the products based on the end-user testing to ensure high quality and user-oriented products. Such testing was also carried out for the newly developed rapid impact assessments (RIA), earthquake risk scenarios, and earthquake risk map of Switzerland.



Month	Unique visitors	Number of visits	Pages	Hits	Bandwidth
Jan 2023	3,140	3,982	11,260	152,757	14.38 GB
Feb 2023	32,377	36,309	97,987	1,610,247	136.86 GB
Mar 2023	8,394	10,345	27,783	418,508	36.65 GB
<b>Apr 2023</b>	1,749	2,066	5,240	82,170	6.34 GB

Figure 8.4.1. Stats of the EFEHR webpage (www.efehr.org) in the aftermath of the Earthquakes in Turkey, February 2023.

**Website**

The RISE project website was launched in September 2019 by WP8 (Figure 8.4.2). The website was used for sharing relevant project information, project news and newsletters, good practices reports, and all RISE publications and conference contributions. Further, the website promoted visibility and transparency towards stakeholders. The full content of the website is accessible on [www.rise-eu.org](http://www.rise-eu.org). The website was regularly updated by WP8. The number of website visitors had risen steadily since the project started as shown in the table in chapter “Summary of Exploitable Results in WP8”. Whereas around 420 people visited the RISE website every month in 2020, the number of website visitors per month increased to 665 people on average every month in 2021. In 2022, the RISE website registered even more than 700 website visitors every month on average.



About ▾ Dynamic Risk Activities ▾ Dissemination ▾ News & Events ▾



Activities



Good Practices



Publications



Deliverables



Subscribe to our newsletter

### RISE in brief

Earthquakes are the deadliest natural hazard. Developing tools and measures to reduce future human and economic losses is the aim of RISE. RISE stands for **Real-time earthquake risk reduction for a resilient Europe** and is a three-year project financed by the Horizon 2020 programme of the European Commission. It started in September 2019 and will end in May 2023. RISE is coordinated by ETH Zurich, it brings together 19 organisations from across Europe and five international partners.



[Learn more >>](#)

[→ Read more about RISE](#)

### News

2023-03-16  
**Earthquake forecast communication: 13 good practice guidelines**

Perhaps the most important, but also the most difficult questions that seismologists are asked: "What is the chance of a damaging earthquake happening in this area, and if it does, what are its likely effects?" This is the basis for operational earthquake forecasting (OEF) and operational earthquake loss forecasting (OELF). The answers will always have a lot of uncertainty because earthquakes cannot be predicted. However, we can sometimes tell that they are more likely in certain areas due to movements that have been detected in the earth's crust. Forecasts like this require careful, precise, honest and unambiguous communication - sometimes to people with little or no grounding in the geological principles underlying the information. They are not warnings, and they are not giving people a 'message' - telling them to do or not do something - they are more complex to communicate than that. How to best deal with this challenge? 13 best practice tips can guide you in communicating OEF.

### Twitter

 Follow us on Twitter [@research\\_rise!](#)

---

#### Upcoming events

**23-28 April 2023**  
[EGU General Assembly 2023](#)  
Vienna (Austria) & Online

---

**25-26 May 2023**  
RISE Final Meeting  
Lugano, Switzerland

---

**11-20 July 2023**  
[IUGG General Assembly](#)  
Berlin (Germany)

Figure 8.4.2. Snapshot from the RISE website (11/04/2023)

### Twitter

On the RISE Twitter account (@research\_RISE), the RISE communications team regularly share project updates, RISE publications, interesting news, open work positions, and anything else that could be of interest for our Twitter followers. So far, we have posted about 64 tweets ourselves and retweeted more than 240 tweets from others (e.g., project, project partners, conferences). As can be seen in Figure 8.4.3 and in the chapter "summary of exploitable results of WP8", the number of Twitter followers has increased significantly and counts currently 439 followers (as of March 30, 2023).

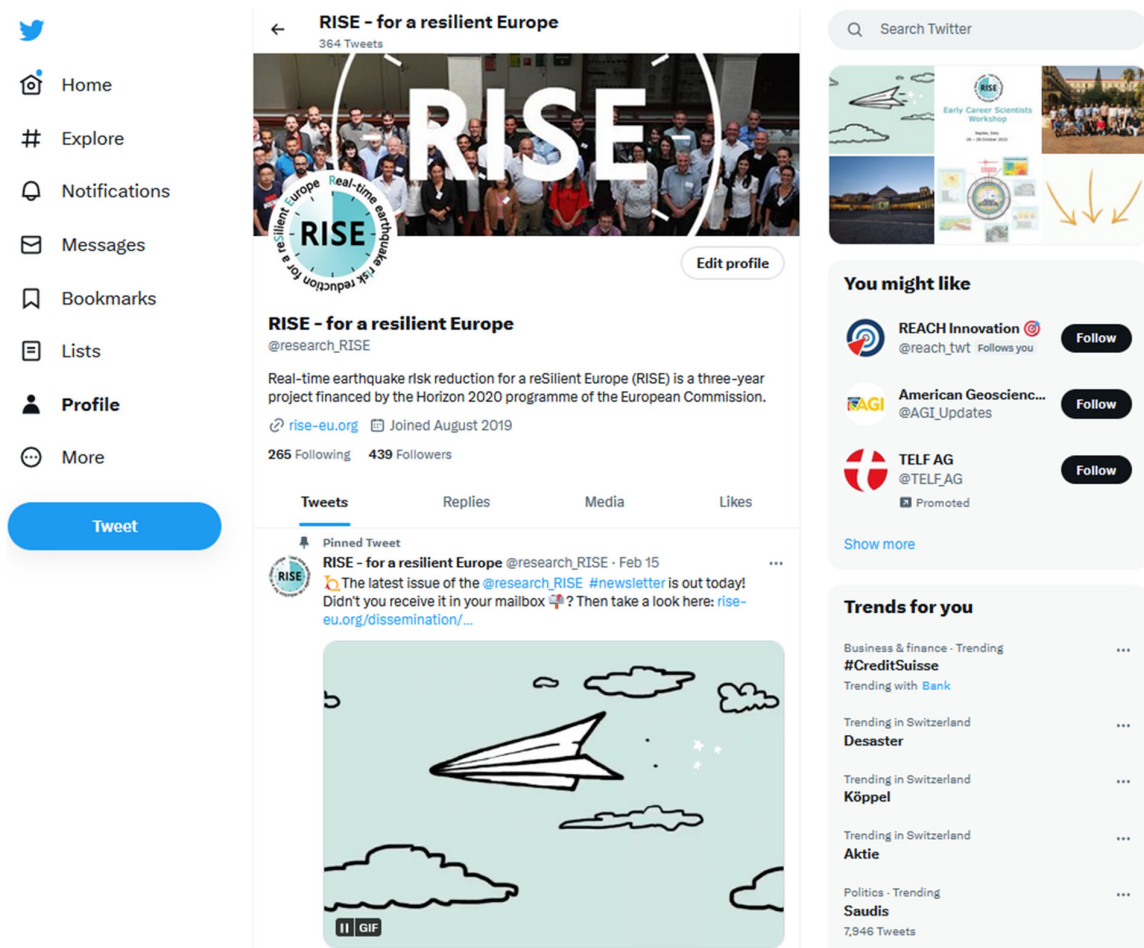


Figure 8.4.3. Snapshot of the RISE twitter profile (20/03/2023)

### External newsletters

RISE external newsletters targeted all interested stakeholders and aimed at communicating project updates and progress. They covered information on WPs, meetings, calendar, and any miscellaneous topic that the RISE community wanted to share with the public. Each issue included a closer look at a specific topic of RISE research and provided an overview of all RISE activities and achievements. The external newsletter was published once a year during the RISE project. So far, four external newsletters have been sent to the registered audience and published on the RISE website:

- [Newsletter #1 March 2020: Welcome to RISE](#)
- [Newsletter #2 October 2020: One Year of RISE](#)
- [Newsletter #3 October 2021: Half-time of RISE](#)
- [Newsletter #4 February 2023: Ris\(e\)ing numbers](#)

### Good practice series

Establishing good practices is an important legacy of RISE. They are based on RISE activities and developments. Therefore, we documented good practices and made them openly accessible through the RISE website. All good practice compilations start with a description of the topic and the respective field. Then, they provide insights into current developments and future paths. The

RISE good practices link to specific reports and publications for further reading. Currently, information on the following documentations on good practices are available:

- [European rapid earthquake loss assessment](#)
- [How can we fight earthquake misinformation?](#)
- [New developments of physics- and statistics-based earthquake forecasting](#)
- [Earthquake forecast communication](#)

The good practices series will be completed with a last report on risk-cost-benefit in terms of socio-economic impact. This will be published on the RISE website by the end of the project (May 2023).

### Training workshops

In order to improve the collaboration within the RISE community (see 8.3 PEDR update) in the second half of the project, two special training workshops were conducted.

#### Transdisciplinarity workshop, online

In a workshop led by Prof Dr Michael Stauffacher (ETH), ten scientists from the RISE project stepped out of their usual hiking track (specific research focus) and tried to grasp the environment around it (social relevance); see Figure 8.4.4. Prof. Dr. Michael Stauffacher, transdisciplinarity-expert at the TdLab at ETH Zurich, guided the participants through ten steps, allowing them to reflect on the different societal and interdisciplinary dimensions of their research projects (see <https://doi.org/10.14512/gaia.26.1.10>).

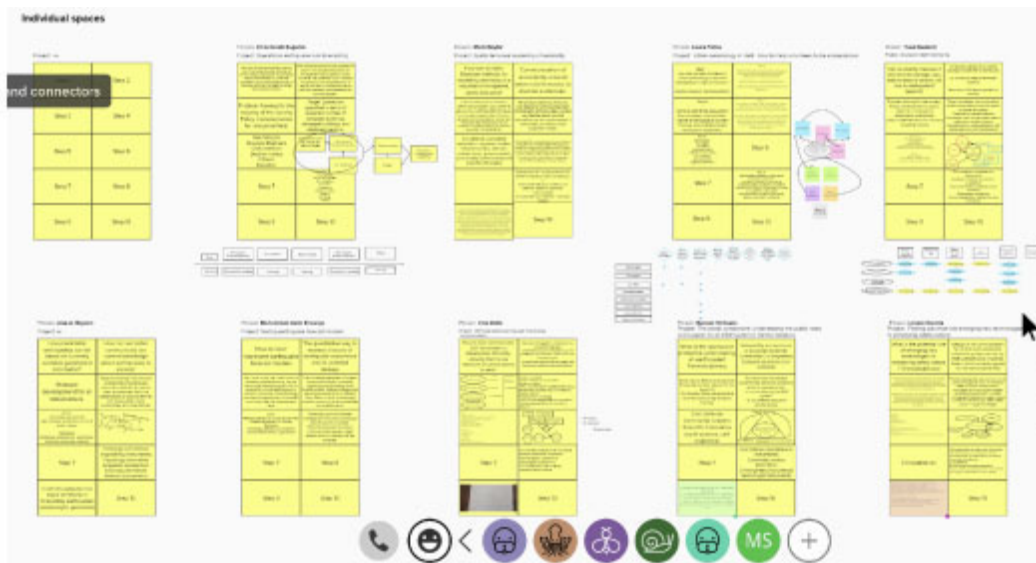


Figure 8.4.4. Overview of the participants' outcomes applying the ten steps on how to render one's research societally relevant.

#### Early Career Scientist workshop, Naples (Italy)

From October 26-28, 2022, a workshop was organised by and for Early Career Scientists (ECS) of RISE with the purpose of exchanging ideas about ongoing and future research projects,

interacting, giving context to their work, and getting to know each other better (Figure 8.4.5). Senior scientists were also welcomed, especially on the last day when the ECSs presented their reflections and ideas. The workshop took place in Naples, Italy.

The main theme was: “Bringing research to practical applications that increase society’s earthquake resilience.”, which was explored in four focus topics:

- Transdisciplinary research: integrate knowledge across academic disciplines and with non-academic stakeholders
- Open Science: making scientific research transparent, collaborative, and accessible;
- Ethical implications: consider the ethical standards and their impact of people’s lives;
- Dynamic risk: appreciate the variability of seismic risk (time, location, and context).

The ECS learned that the four topics are strongly connected and affect all of them. For example, dynamic risk services/products like operational earthquake forecasting (OEF) or rapid impact assessments (RIA) are only possible if the underlying data are openly available and continuously updated. In this regard, standardisation is key to ensure that the same data can be used for various (dynamic risk) services/products simultaneously (e.g., rapid earthquake information for OEF and RIA), making them more sustainable.

The many new insights gained at this workshop are documented in an opinion paper (preprint):

<https://doi.org/10.5281/zenodo.7708552>



*Figure 8.4.5. Participants of the RISE Early Career Scientist Workshop in Naples, 26-28 October 2022.*

### **Release of the European Seismic Hazard and Risk Models**

After the scientific release of the European Seismic Hazard (ESHM20, Danciu et al. 2021) and Risk Models (ESRM20, Crowley et al., 2021) in December 2021, both models were presented to the public in April 2022. The communications team of the Swiss Seismological Service (SED) at ETH Zurich (members of the RISE communications team) were responsible for the planning and creation of the outreach activities. For the release, a re-designed website for EFEHR (European

Facilities for Earthquake Hazard and Risk) was launched, providing much background information about earthquake hazard and risk in Europe ([www.efehr.org](http://www.efehr.org)). In addition, posters, flyers, an explainer video and factsheets in different European languages are available. Some of these products were tested before their release (e.g. risk map viewer, risk poster). Based on the results, we then adapted the different products to tailor them to the end-users' needs, ensuring high-quality products (see next chapter). In preparation for the public release of the model, we also established a network with outreach specialists of project partners and beyond as well as experts across Europe. They all supported the release of the models and shared the information within their community. This approach was considered successful in reaching more people in various European countries and increasing media outreach across Europe. Since these models have also been funded by the RISE project, RISE was acknowledged on products and publications released about the models (e.g., poster, flyer, website). This gives the RISE project additional visibility all over Europe, also in a longer term.

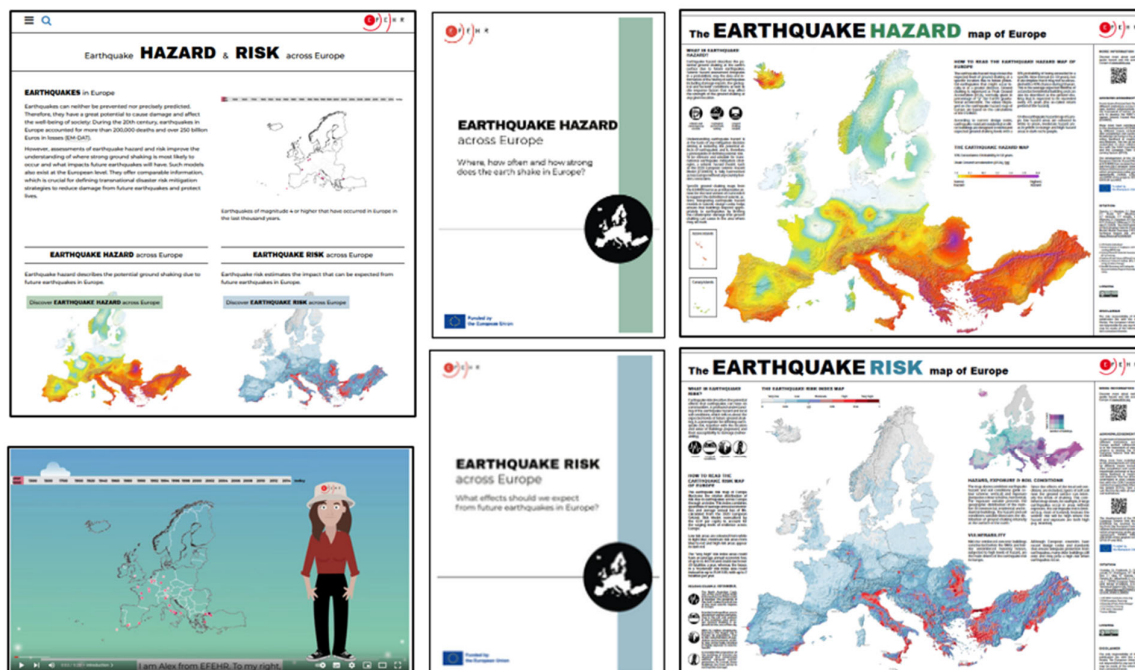


Figure 8.4.6. Collection of outreach materials about earthquake hazard and risk in Europe, all available on the EFHR website ([www.efehr.org](http://www.efehr.org)) and with RISE acknowledgement.

## Risk communication products - Testing efforts

### The European seismic risk communication products

We tested two main products of the first European seismic risk model: the risk map viewer<sup>4</sup> and the risk poster including the risk map. For the risk map viewer, we conducted an interactive online survey with 17 professional users, where participants explored the online map viewer and answered interpretation, design perception, and preference questions. For the risk map and poster, we conducted an online survey with students at various universities (N=83). Thereby, we conducted a between-subjects experiment to assess which map and poster version is correctly understood, perceived as useful, and preferred. In Figure 8.4.7 the final version is presented.

<sup>4</sup> <https://maps.eu-risk.eucentre.it/map/european-seismic-risk-index-viewer/#4/52.64/5.05> [13.03.2023]

The main results regarding the **risk map viewer** are:

- Overall, the web viewer was overall rated as easy to navigate, attractive, clear, informative, and useful.
- Information preferences: direct and indirect economic losses, number of casualties, fatalities and people in need of help, damages on physical assets, hazard and exposure data, fragility and vulnerability models, social vulnerability indicators, building stock information, and uncertainties associated with the models.
- Map preferences: map of average annual loss, combined risk results of the economic losses and fatalities, gridded map (e.g., 1km x 1km), indication of the capital cities in each country, and selectable layers (e.g., population density, significant earthquakes, active faults).
- Three primary purposes of the risk model: i) to give estimates of risk levels at various return periods of the mapped economic exposure; ii) to provide an overall view of seismic risk in Europe allowing to compare seismic risk in different EU countries; and iii) to guide the development of public/private risk mitigation strategies.

The main results for the **risk map and poster**:

- The risk map and poster were overall rated as useful, trustworthy, reliable, understandable, and clearly structured.
- The legend should have a clear title to indicate that an index is displayed on the map (e.g., earthquake risk index map).
- The main insights regarding the risk map are that: i) hill shades are preferred; ii) when smoothing than combined with hill shades; iii) qualitative labels should be combined with numerical values; iv) the indication of the capitals in every country helps for geographical orientation; and v) circles should be used for marking the location of cities to avoid covering the colour.
- The main insights regarding the risk poster are that: i) a list of factors driving high risk levels is wished; ii) a clear indication of which losses are combined is needed; iii) the components of seismic risk should be explained; iv) a reading example facilitates the interpretation of the visual information; and v) it should be stated if the model can be used for commercial purposes or not.

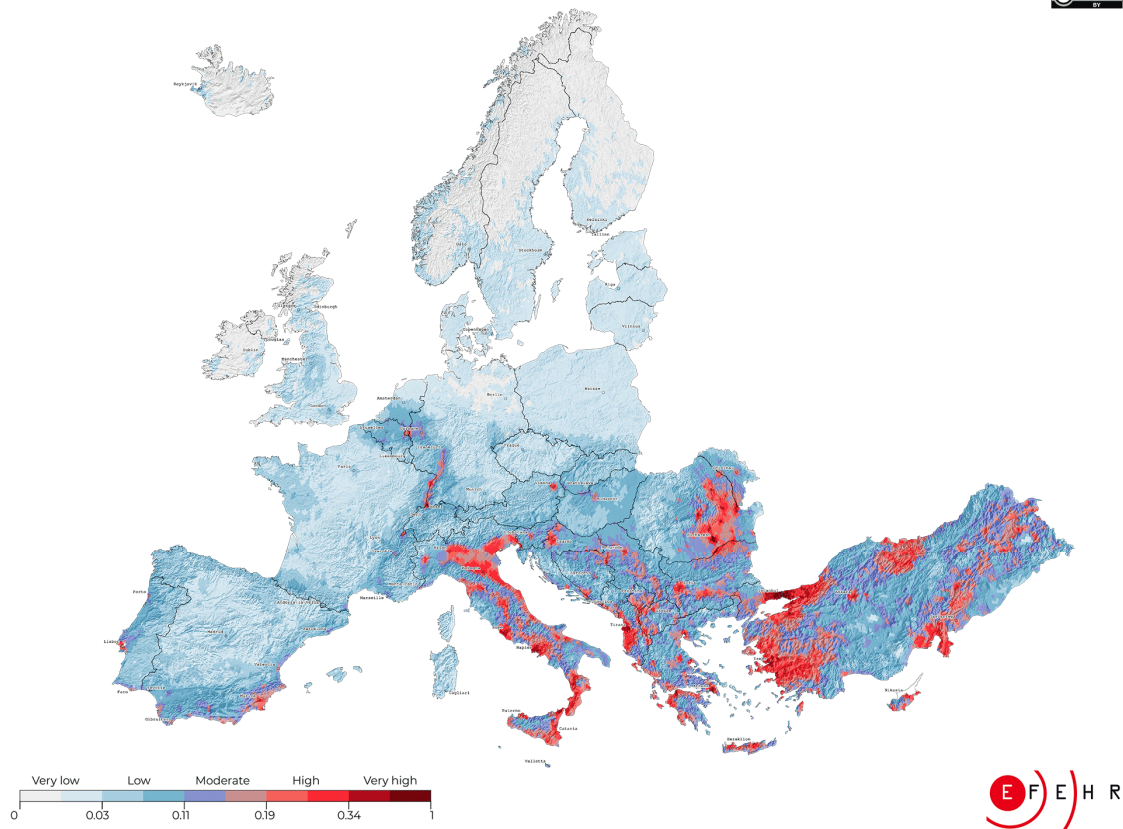


Figure 8.4.7: The first European seismic risk map. Other communication products of the European seismic risk model are available here: <http://www.efehr.org/explore/Downloads-information-material/>

To ensure that the results of the testing were incorporated into the actual design process of the products, it was part of the overall communication strategy. This communication strategy defined the vision and principles, the target audiences, communication goals, key messages, and products (e.g., flyer, poster, web content). Further, through regular meetings of the core team, steering committee, and feedback group the testing results were reflected with scientists from different disciplines to ensure the data is correctly displayed and people's information needs addressed based on the latest research findings.

A publication is in preparation for the [Special Issue Harmonized seismic hazard and risk assessment in Europe](#) in *Natural Hazards and Earth System Sciences*.

### The Swiss seismic risk communication products

Marti, M., Dallo, I., Roth, P., Papadopoulos, A. N., & Zaugg, S. (2023). Illustrating the impact of earthquakes: Evidence-based and user-centered recommendations on how to design earthquake scenarios and rapid impact assessments. *International Journal of Disaster Risk Reduction*, 103674. <https://doi.org/10.1016/j.ijdrr.2023.10367>

We tested two main products of the first detailed earthquake risk model for Switzerland, namely the rapid impact assessments (RIA), scenarios (Figure 8.4.8), and risk map. For the design of the two products we benefited from our expertise gained for the development of the European products. For the RIA testing, we conducted interviews with international experts on risk models (n=7), workshops with Swiss professional, societal stakeholders (n=150), and a survey with the Swiss general public (n=580). For the risk map, we conducted a Swiss public survey with a between-subjects experiment to identify the best performing map-legend version (n=593).

The main results regarding the **rapid impact assessments and scenarios** are:

- Uncertainty visualisations should be as simple as possible; in our study the basic icon visualisation was best understood and preferred.
- People prefer the following information on the leaflet: indication of the federal hazard level, map depicting the impacts, basic information about the event, what to do (regionally), and the probability of aftershocks.
- People's social factors influence their preferences, perceived usefulness, interpretation skills, and intention to take protective actions. To name an example, participants with earthquake insurance perceived the products as significantly more useful.
- Professionals and the public struggle with similar issues when it comes to interpreting more complex diagrams and figures.
- Indicating a range is sufficient to ensure that people understand that the estimates are linked to uncertainties.



Earthquake scenario

## Earthquake in the vicinity of Zürich (ZH)

<b>Overview</b>	<b>Magnitude 6.0 [Mw]</b>	<b>Danger level</b>	5																	
	<p>In this scenario, an earthquake has occurred in the canton of Zurich (ZH), with the epicentre located approximately 10 km northeast of Zurich (ZH). This earthquake would be felt across Switzerland. An earthquake of this magnitude would be expected to cause moderate to heavy damage within a wide radius of the epicentre. On statistical average, an earthquake with a magnitude of 6 is to be expected within a 50 km radius of this epicentre every 1210 years.</p>		<table border="1"> <tr><td>Local time</td><td>-</td></tr> <tr><td>Date</td><td>-</td></tr> <tr><td>Hypocentral depth [km]</td><td>8</td></tr> <tr><td>Magnitude [Mw]</td><td>6.0</td></tr> <tr><td>Assessment</td><td>automatic</td></tr> <tr><td>Swiss coordinates</td><td>2°688'037 / 1°256'734</td></tr> <tr><td>Additional data</td><td><a href="#">Link</a></td></tr> </table>	Local time	-	Date	-	Hypocentral depth [km]	8	Magnitude [Mw]	6.0	Assessment	automatic	Swiss coordinates	2°688'037 / 1°256'734	Additional data	<a href="#">Link</a>			
Local time	-																			
Date	-																			
Hypocentral depth [km]	8																			
Magnitude [Mw]	6.0																			
Assessment	automatic																			
Swiss coordinates	2°688'037 / 1°256'734																			
Additional data	<a href="#">Link</a>																			
<b>National</b>	<b>Estimated effects</b> The estimated impacts are described in intensities. The intensity describes the strength of an earthquake based on the extent of the impact and the subjective perception of a person.	<b>Number of fatalities in Switzerland</b> The number of fatalities is very likely to fall within the coloured range.																		
		<b>Number of people seeking protection in Switzerland</b> The number of people seeking protection is very likely to fall within the coloured range.																		
	<table border="1"> <thead> <tr> <th>Intensity</th> <th>II</th> <th>III</th> <th>IV</th> <th>V</th> <th>VI</th> <th>VII</th> <th>VIII</th> <th>IX</th> </tr> </thead> <tbody> <tr> <td>Impact</td> <td>scarcely felt</td> <td>weak</td> <td>largely observed</td> <td>strong</td> <td>slightly damaging</td> <td>damaging</td> <td>heavily damaging</td> <td>destructive</td> </tr> </tbody> </table>	Intensity	II	III	IV	V	VI	VII	VIII	IX	Impact	scarcely felt	weak	largely observed	strong	slightly damaging	damaging	heavily damaging	destructive	<b>Cost of damage to buildings in Switzerland</b> The cost of damage to buildings is very likely to fall within the coloured range.
Intensity	II	III	IV	V	VI	VII	VIII	IX												
Impact	scarcely felt	weak	largely observed	strong	slightly damaging	damaging	heavily damaging	destructive												
<b>Cantonal</b>	<b>Number of injured people</b> The number of injured people per canton and in the Principality of Liechtenstein is very likely to fall within the coloured range.	<b>Extent of building damage</b> The extent of moderate to very heavy damage to buildings per canton and in the Principality of Liechtenstein is very likely to fall within the coloured range. The percentage corresponds to the average proportion of damaged buildings per canton.																		

All information is provided without warranty and is subject to change.

With the support of: **Federal Office for the Environment FOE**  
**Federal Office for Civil Protection POC**

What should you do after an earthquake? See [www.seismo.ethz.ch/de/earthquakes/what-to-do/](http://www.seismo.ethz.ch/de/earthquakes/what-to-do/)  
More information is available at [www.seismo.ethz.ch](http://www.seismo.ethz.ch) and <https://lege.naz.ch/eld2/login>

Figure 8.4.8: Exemplary final scenario of the Swiss earthquake risk model. Further scenarios and communication products can be downloaded here: <http://seismo.ethz.ch/en/knowledge/earthquake-country-switzerland/earthquake-scenarios/>

The detailed results of the risk map study are still confidential but will be published by the end of the year. In case of any questions, please contact [irina.dallo@sed.ethz.ch](mailto:irina.dallo@sed.ethz.ch).

**List of submitted deliverables and achieved milestones in WP8**

- D8.1 Update PEDR (month 3)
- D8.2 Update PEDR (month 12)
- D8.3 Update PEDR (month 24)
- D8.8 EU RLA service operational
- D8.10 External Newsletter released (month 6)
- D8.11 External Newsletter released (month 18)
- D8.12 External Newsletter released (month 36)
- MS22: OEF output format for testing
- MS56: Community agreement on requirements and technical baseline for dynamic risk service standardisation
- MS59: RISE web page fully operational
- MS60: 15th publication related to RISE submitted
- MS61: 3rd best practise report online
- MS62: First Training workshop conducted

**Summary of Exploitable Results in WP8**

**Number of website visitors**

The following figure 8.4.9 shows the number of unique website visitors per month. Since the start of the RISE project, this number has steadily risen.



Figure 8.4.9. Number of website visitors per month

Table 8.4.9 indicates for each year the total number of website visitors and the average number of people visiting the RISE website every month.

Year	Average per month	Total number
2020	424	5,093

<b>2021</b>	665	7,979
<b>2022</b>	717	8,600

Table 8.4.10. Monthly average of website visitors and total number per year.

**Number of Twitter follower**

On Twitter, RISE has gained more and more visibility. Regular tweeting activity has increased the number of followers. As by March 2023, the account counts more than 430 followers.

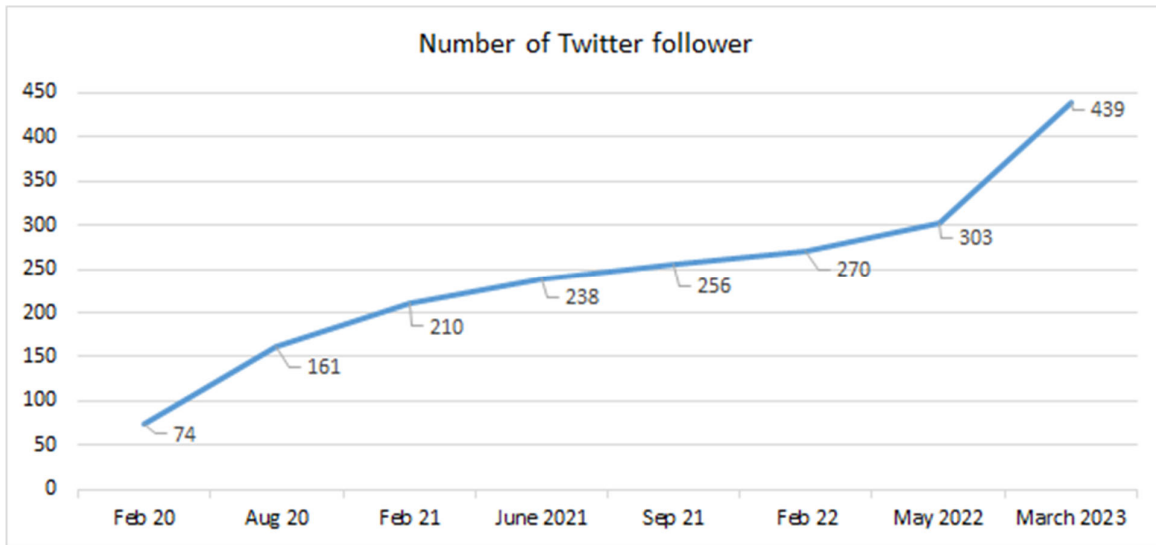


Figure 8.4.11. Statistics on the number of Twitter followers.